THE CALCULATION OF CONVECTIVE AND CONDENSATION HEAT TRANSFER COEFFICIENT TO SURFACES HELD IN AN ACOUSTIC FIELD OR SUBJECTED TO MECHANICAL OSCILLATIONS

By

J. C. DENT

THESIS SUBMITTED FOR THE DEGREE OF DOCTOR OF PHILOSOPHY OF LOUGHBOROUGH UNIVERSITY OF TECHNOLOGY

1969

Synopsis

The work described in this thesis falls into five parts. Four of these parts deal with the extension of the Danckwerts-Mickley surface renewal concept for turbulent mixing, to the problem of calculating the convective and condensation heat transfer coefficients from surfaces which are in mechanical oscillation, or are maintained in an acoustic field. The fifth part discusses experiments carried out by the author on the condensation of steam at atmospheric pressure on a horizontal tube subjected to mechanical oscillations in the vertical plane. A perturbation analysis of the problem has also been carried out and compared with experiment.

The four parts dealing with the Danckwerts-Mickley surface renewal concept are under the following headings.

(1) The effects of combustion driven acoustic oscillation on the forced convective heat transfer in turbulent flow through a cylindrical gas air burner.

(2) The effects of mechanical oscillation in a transverse plane, on free convection from a vertical heated plate in air.

(3) The effects of mechanical and acoustic oscillation on free convection from heated horizontal cylinders in air.

(4) The effects of lateral mechanical oscillation on condensation heat transfer on a vertical tube.

The use of the Danckwerts-Mickley model in (1) above has been justified through the observations of Kline and others on the structure of turbulent boundary layers, and the observations of Male and others on the effects of combustion oscillation on gas flow in the region of a wall. Further preference for the surface renewal model over the more usual Von-Karman-Martinelli analogy for calculating the average heat transfer is the fact that quantitative empirical information on velocity distributions are not required.

The use of the Danckwerts-Mickley model in (2) and (3) above, has been based on the observations of Locke and Trotter on the structure of turbulent free convective boundary layers, and on the observations of

Eckert and others, of the processes of instability and transition to turbulence of the laminar free convective boundary layer.

In the extension of the Danckwerts-Mickley model in (4) above, use has been made of the observations of Portalski and Brooke-Benjamin on the instability and transition of thin liquid films down inclined and vertical surfaces.

The general philosophy in using the Danckwerts-Mickley renewal concept in this thesis has been phenomenalogical rather than mathematical. That is, from observed experimental facts concerning the behaviour of boundary layer flows, and flow behaviour in the presence of mechanical or acoustic oscillations, a mixing mechanism is postulated in conjunction with the results of the Danckwerts-Mickley renewal concept, the adequacy of the postulate is then tested by observation of the gross effects of mixing on the average heat transfer at the heat transfer surface. In these comparisons, use is made of the available experimental data in the heat transfer literature.

Agreement between the calculated ratio of average heat transfer coefficients in the presence and absence of oscillation h_v/h_o using the methods outlined above, and available experimental data is generally good, within the limitations of the mixing model and experimental error.

Comparisons have also been made in one case (3) with the asymptotic solutions of Richardson, and it is found that the methods developed in this thesis show better agreement with a wider range of experimental data than the solutions of Richardson.

Much of the work outlined here has been published or is in press. A list of these publications are given below. Copies of these papers are also grouped together in Appendix (VIII) at the end of the thesis.

Publications by the Author

(1) The Calculation of Heat Transfer Coefficient for Combustion Driven Transverse Oscillations in a Gas-Air Burner.
A. I. Ch. E. Jour. 13, 1114 (1967)

(2) Heat Transfer from a Vertical Transversely Vibrating Plane Surface to Air by Free Convection.
Int. Jour. Heat and Mass Transfer 11, 605 (1968)

(3) The Effect of Vibration on Condensation Heat Transfer to a Horizontal Tube.
Proc. I. Mech. E. (In Press)

(4) The Calculation of Heat Transfer Coefficient for Condensation of Steam on a Vibrating Vertical Tube.
Int. Jour. Heat and Mass Transfer (In Press)

(5) The Effect of Acoustic and Mechanical Oscillation on Free Convection from Heated Cylinders in Air.
Chem. Eng. Science (In Press)

Acknowledgements

The author is indebted to Professor B. Downs, Head of the Mechanical Engineering Department at Loughborough University of Technology, for permission to conduct this work in his Department and for his encouragement through the facilities and time which he made available for its execution.

The author would also like to express his indebtedness to the following people for their assistance during this project.

Mr. J. R. Mitchell, his colleague, for his assistance in programming the work in section (16.0) for the digital computer.

Mr. J. R. Baggaley who constructed the experimental equipment for the condensation studies and painstakingly ran off the experimental results.

Mrs. M. Hubbard and Miss M. Tivey for typing the manuscript.

Mr. K. Topley for his assistance with photographic services.

Mr. T. Middleton for construction of electronic equipment.

Mr. E. Schofield for his assistance with experiments.

Thanks are also due to Mr. H. Russell, Chief Technician, in the Department of Mechanical Engineering and those of his staff who have not been mentioned, for their help generally.

The author would like to express his thanks to Mr. H. C. Lowe of the Staffordshire College of Technology who kindly provided a copy of his Masters thesis which has been most useful in the provision of accurate experimental data.

Finally, the author would like to express his deep appreciation of the interest and encouragement of Mr. H. W. M. Kropholler, Senior Lecturer in the Department of Chemical Engineering, during the progress of this work.

----------oOo----------

Notation

a	=	Amplitude of Oscillation ft.
A	=	Surface Area ft^2
C	=	Acoustic Velocity ft/sec.
C_p	=	Thermal Capacity Chu/lbm ^oC = Btu/lbm ^oF
D	=	Diameter ft
f	=	Frequency c/s
g	=	Acceleration due to gravity. 32.2 ft/sec^2
g_c	=	Gravitational constant 32.2 $\frac{lbm}{lb_f}$ $\frac{ft}{sec^2}$
G_R	=	Grashof Number - Dimensionless
h	=	Heat Transfer Coefficient Btu/hr ft^2 ^oF
J_n	=	nth Order Bessel Function of the 1st kind
k	=	Thermal Conductivity Btu/hr ft ^oF
$\mathcal{l}$	=	Length ft
L	=	Length ft
m	=	Mass flow rate lbm/sec.
M	=	Mach Number - Dimensionless
n	=	Normal Co-ordinate - ft
P	=	Pressure - lb_f/ft^2
P_R	=	Prandtl Number - Dimensionless
Q	=	Heat Transfer Rate - Btu/hr
r	=	Radius - ft
R	=	Radius, or Resistance ft or ohms
Re	=	Reynolds Number - Dimensionless
s	=	Characteristic length of Duct ft
S	=	Mixing Coefficient - 1/hr
t	=	Time - hours
u	=	velocity parallel to surface ft/sec
U	=	Free Stream Velocity ft/sec
v	=	velocity normal to surface ft/sec
$\bar{V}$	=	Free Stream velocity ft/sec
α	=	Thermal Diffusivity; or Temperature Coefficient of Resistance ft^2/hr or $/^oC$
δ	=	Boundary Layer, condensate film thickness - ft
Δ	=	Difference
ρ	=	Density or Resistivity lbm/ft^3 or ohm.cm.
ϵ	=	Perturbation Parameter - Dimensionless
λ	=	Characteristic Length - ft
μ	=	Absolute Viscosity lbm/ft hr

Notation

ν	=	Kinematic Viscosity ft^2/hr
θ	=	Temperature ^oF or ^oC
ϕ	=	Angular Position - degrees
ω	=	Circular frequency rads/sec
τ	=	Shear Stress lb_f/ft^2

Other notation and suffices defined in text.

List of Contents

List of Contents

List of Contents

List of Contents

List of Contents

1.0. Introduction

In the study of convective transport processes our concern is in the transfer of heat, mass or momentum due to the motion of a fluid. This motion may be caused by an external agency (Forced Convection) such as a pump, fan or stirrer, or it may result from buoyancy forces set up by thermal gradients within the fluid (Free or Natural Convection). In some instances fluid motion may result from the combined effects of these two convective modes. Convection can be further classified depending on whether the flow regime is laminar or turbulent.

In laminar flow the transport across adjacent fluid layers takes place on a molecular scale, whereas in turbulent motion, because of random mixing of the fluid, transport across adjacent fluid layers takes place predominantly on a macroscopic scale. Because the transport coefficients for the macroscopic process are much larger than those for the molecular process, turbulent transport processes are more effective than laminar ones. Since convective transport depends on the motion of the fluid it can be seen that forced convective transport is generally more effective than free convective transport for a given fluid medium.

If the region in the vicinity of a fluid - solid interface is considered, the effect of viscosity of the fluid is to reduce the velocity of the flow progressively to zero at the solid or wall surface. The region over which the velocity decreases from its free stream value to zero at the wall is termed the boundary layer. In the case of a turbulent flow, the turbulent mixing motion is progressively damped out in the boundary layer, and at the wall a predominantly laminar sub-layer is considered to exist. This progressive diminishing in the flow velocity and turbulent mixing as the wall is approached from the free stream, results in less effective transport between the bulk of the fluid and the wall.

1.1 Convective Heat transfer from gases and methods for increasing it.

Because of differences in fluid properties between gases and liquids characterised by the Prandtl number, it is known that Forced and Free convective heat transfer coefficients for gases are amongst the lowest for these two modes of convective transport, provided similarity of the fluid motion is preserved through the Reynolds or Grashof numbers. This being so, it is often found that

the gas side heat transfer coefficient is the factor controlling the overall heat transfer rate in a particular process. It is of importance therefore to find ways by which the gas side convective heat transfer coefficient may be increased.

Methods for improving the convective heat transfer coefficient for gases, usually employ some means of causing more efficient thermal transport across the boundary layer, such as the use of turbulence promoters in the form of spiral elements for tube flow or roughened or grooved surfaces, which, provided the surface roughness elements protrude through the laminar sub-layer cause increased turbulence and heat transfer. A further method is the seeding of the transfer gas with fine particles of high thermal capacity which are thought to carry out a shearing and penetration of the sub-layer thereby causing improved thermal transfer with the wall.

Other methods employ oscillations in the flow or the superposition of an acoustic oscillation in the fluid medium to promote either earlier transition to turbulence in a laminar boundary layer, or greater mixing in a turbulent one.

Finally methods may be employed which cause the heat transfer surface to oscillate relative to the fluid, and in this way set up greater mixing in the fluid.

This thesis is concerned with the effects of acoustic and mechanical oscillations on convective heat transfer. The subsequent sections will therefore be devoted to the survey of the relevant literature on the subject, and calculation methods for predicting heat transfer under conditions of acoustic or mechanical oscillation will be presented.

2.0 THE EFFECT OF ACOUSTIC OSCILLATIONS ON FORCED CONVECTIVE HEAT TRANSFER FROM GASES IN CYLINDERS

2.1. Acoustic Oscillation of a Gas in a Cylindrical Cavity in the absence of Bulk flow of the Gas and Heat Transfer with the Cylinder walls.

Under the above conditions, resonant acoustic oscillations of a gas within a rigid cylindrical cavity occur because the frequency of the driving oscillation corresponds to one of the acoustic modes of resonance for the chamber.

Figure 2-1 illustrates schematically the three principal acoustic modes of oscillation that can occur in a cylindrical cavity, assuming standing wave conditions.

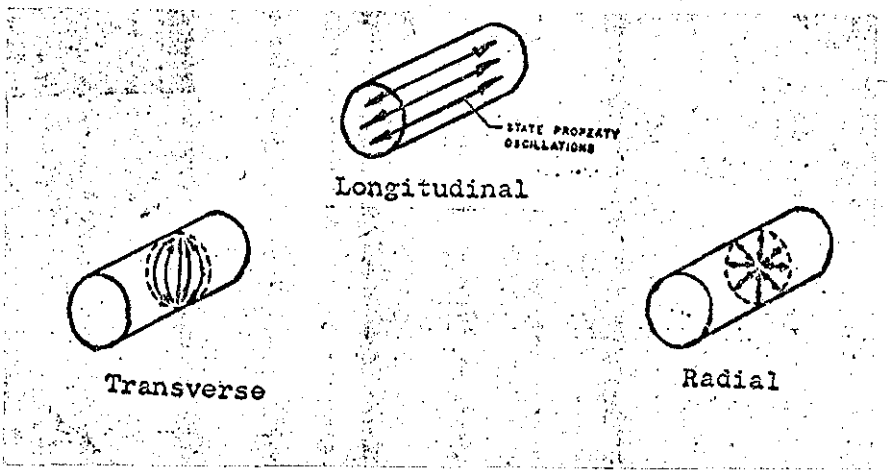

Principal Acoustic Modes of Oscillation for Standing Wave Conditions in a Cylindrical Cavity. Fig. 2-1

The resonant frequency of the acoustic oscillation for a cylindrical cavity can be obtained from the solution of the three dimensional wave equation for the perturbation of the cavity pressure due to acoustic oscillation. This yields a general expression for the acoustic frequency in terms of the wave numbers for each particular mode. In this way the frequency of combination modes of oscillation can be determined. From Morse (Bibliography 1), the general frequency equation for a cylindrical cavity of radius R and length L is

$$f_{m,\,n,\,q} = \frac{\bar{V}_{sonic}}{2} \left[\left(\frac{\alpha_{m\,n}}{R} \right)^2 + \left(\frac{q}{L} \right)^2 \right]^{1/2} \qquad 2.1.1.$$

where $f_{m,\,n,\,q}$ is the acoustic frequency depending on the wave numbers m, n, q for the pure radial, tangential and longitudinal modes respectively. $\bar{V}_{sonic}$ is the sonic velocity for the gas in the cavity

based on the assumption of an ideal gas. The constant $\alpha_{m,n}$ is the value of the argument of J_n such that

$$\frac{d}{dr}\left[J_n\left(\pi\alpha_{m,n}\cdot\frac{r}{R}\right)\right]_{r=R} = 0. \qquad 2.1.2.$$

Since J_n is an oscillating function of its argument, the sequence of m's and n's yield a doubly infinite set of frequencies.

The dependence of the acoustic mode on the wave number is shown below. The value of the constant $\alpha_{m,n}$ is also given for various values of m and n.

Dependence of Acoustic Mode on Wave No.

Wave No.			Type of Mode
m	n	q	
m	o	o	Pure Radial
o	n	o	Pure Tangential
o	o	q	Pure Longitudinal
combination of two or three wave no's.			Combination Modes

Value of $\alpha_{m,n}$

n \ m	0	1	2	3	4
0	0.000	1.220	2.233	3.238	4.241
1	0.586	1.697	2.714	3.725	4.731
2	0.972	2.135	3.173	4.192	5.204
3	1.337	2.551	3.612	4.643	5.662
4	1.693	2.955	4.037	5.082	6.110

2.2 Methods of Producing Acoustic Excitation of a gas in a Cylinder

There are two basic methods of producing acoustic excitation of the gas in the cylindrical system. The first of these uses an electrical driver - Loudspeaker - which is fitted to one end of the cylinder, and fed with oscillations of the appropriate frequency and power level through an oscillator and amplifier.

The second method that can be used employs the amplification of acoustic pressure pulses because of heat addition at the peaks of the pressure pulses. This phenomenon was first studied by Lord Rayleigh, he found that if heat was periodically added to and abstracted from a mass of gas oscillating in a cylinder, the effect produced depended on the phase relationship between the oscillations in the gas pressure and the heat transfer. Pressure oscillations were amplified when

heat was either added to the gas when the pressure amplitude was at a maximum, or removed from the gas when the pressure amplitude was a minimum.

The Rayleigh mechanism for the amplification of pressure oscillations due to heat release has been observed in Ramjet and Rocket combustion systems - which can be considered as cylindrical cavities, because of the partial closure due to the propelling nozzle. In these systems the pressure oscillation is set up because of irregularities in the burning of the fuel, vortex shedding from flame holders etc., the pressure rises caused by the oscillation increase the temperature of the combustion gases and therefore increase the chemical reaction rate and heat release which in turn cause the pressure to rise. Under these circumstances an unstable situation exists and it has been found in practice that with these conditions of operation a combustion system using high energy fuels could be destroyed within seconds. With lower energy fuels however, the thermal driving of the oscillation is not so intense and the result is the establishing of an acoustic oscillation in the chamber.

It has been found (Bibliography 2, 3 4) in the study of Ramjet and Rocket combustion systems that heat release due to combustion near the walls of the combustion chamber produce transverse modes of oscillation, whereas heat release at the centre of the combustion chamber produces radial modes of gas oscillation. It has been found that for cylindrical combustion chambers with $\frac{L}{D} < 1.0$ longitudinal modes are not present; with $\frac{L}{D} > 1.0$ weak longitudinal modes begin to appear. These observations are in accordance with Morse (Bibliography 1) concerning cylindrical cavities in general.

From experimental observation on rocket and ramjet systems it has been found that the frequencies for the various resonant modes of oscillation are in agreement with 2.1.1., irrespective of whether the oscillatory wave system was of the standing or travelling type. This agreement also indicates that the frequencies can be predicted in the cylindrical cavity with accuracy irrespective of the bulk flow of the gas and heat transfer to the chamber walls.

In commercial boiler plant where low energy fuels are used with moderate rates of heat release, the possibility exists of exploiting the observed increase in convective heat transfer from the combustion

gases due to their oscillatory motion. The concern in this thesis is with the second method of exciting acoustic oscillation in gases in a cylinder, because of the possibility of practical application. However, the literature concerned with electrically driven systems by means of loudspeakers will also be reviewed.

2.3. Forced Convection heat transfer in cylindrical tubes with acoustic oscillations imposed on the flow by electrical drivers

A recent survey of the effects of oscillations on heat and mass transfer carried out by Rao (1), shows that the bulk of the work covered by the above heading, was carried out by Jackson and his co-workers at the Georgia Institute of Technology (2, 3, 4, 5). Other work in the area is that of Lemlich and Hwu (6). It should be pointed out that the above heading does not include work involving the effects of large pressure pulsations in the flow.

Jackson et al (2) conducted preliminary experiments to determine the effects of acoustic oscillation and combined free and forced convection on heat transfer coefficient in a 3.75 inch I.D. vertical isothermal tube 5ft long. The acoustic waves were propagated in the same direction as the air flow which was from the lower end of the tube. Results were obtained at a constant frequency of 520 c/s and a Reynolds number of 2300. The effect of sound pressure level on average heat transfer coefficient was negligible up to 118 db. but free convection effects were significant. Beyond 118 db. acoustic effects become significant and heat transfer coefficient rose approximately linearly with sound pressure level to 129 db. which was the limit of the test. At this condition the average heat transfer coefficient was 40% greater than that with no oscillations. The whole series of tests were run for $G_R P_R D/L = 1.2 \times 10^5$. Because of the limited nature of the experiment with regard to frequency and Reynolds number, no conclusions can be drawn other than the linear variation of heat transfer coefficient with sound pressure level for constant Reynolds number and frequency.

Jackson, Purdy and Oliver (3) experimented with a horizontal 3.89 in. I.D. heated isothermal tube 10 ft long. Reynolds number for the air flow varied from 2040 to 11,600 under conditions of simultaneous development of velocity and temperature profiles. Sound pressure levels from zero to 162.5 db were propagated in the direction opposite to the air flow with resonant frequencies of approximately 171, 221 and 356 c/s. The variation of sound pressure level with axial position was determined with a microphone mounted on a probe which was traversed along the centre line of the tube. This was merely to give the flow pattern in the tube. Heat transfer runs were conducted with the microphone mounted in the inlet plenum chamber.

It was found that the effect of acoustic oscillation was to produce a periodic effect on local heat transfer coefficient, with maxima occuring at pressure nodes. The maximum increase in the average heat

transfer coefficient at 163.5 db being approximately 20% for a Reynolds number of 2100 and frequency of 221 and 13% for a Reynolds number of 11,600 and frequency of 216 c/s. For these two conditions it was found that oscillations had no effect until the sound pressure level exceeded a value of 152 and 153.5 db respectively. Both local and average values of heat transfer coefficient increased with increasing sound pressure level above the critical value. Little effect of frequency was observed on the values of heat transfer coefficient.

In a later paper Purdy, Jackson and Gorton (4) analysed the laminar flow results obtained in their earlier experiments (3), and formulated a perturbation solution for a two dimensional duct flow. From this analysis the flow pattern shown in figure 2-2 with a standing quarter wavelength vortex system at the wall was obtained. Flow visualisation studies confirmed the results shown in figure (2-2) as regards position of the vortex system.

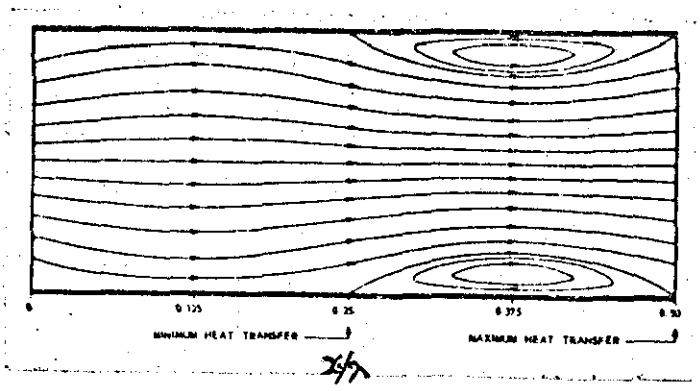

Fig. 2-2 Standing Quarter Wavelength Vortex System Ref. (4)

The main conclusions of these two studies (3), (4) were:-

1. The character of the periodic variation in local heat transfer was different for laminar and turbulent main flows, (this was further clarified in a later paper (5)).
2. From the analysis for the laminar flow condition it was found that the size of vortices produced were a function of the ratio of Acoustic Mach Number to the square of Flow Mach Number which reduces to $\frac{1}{M_o}\left[\frac{a\omega}{V_o}\right]$. Thus for a given set of flow

conditions M_o and $\bar{V}_o$ are constants, hence vortex size is proportional to $(a\omega)$

3. From experiments under laminar flow conditions it was found that the periodic variation in heat transfer coefficient had maxima at positions where the mainstream and the vortex flow impinged on the wall - this later result being obtained from the perturbation analysis - at this point there was a pressure node. Minima in local heat transfer coefficient occurred at positions where the main stream and vortex flow separated from the wall. (see figure 2-2).

Jackson and Purdy (5) extended their earlier results (3) by increasing the upper limit of Reynolds Number to 200,000, though in this paper results are only quoted up to a Reynolds Number of 49,690. In this paper the authors developed an empirical method for the computation of local variations in heat transfer coefficient along the tube. The method consisted of using available correlations for forced convection heat transfer with developing flow; and modifying this by the superposition of an instantaneous velocity which represented the effects of oscillations. An interesting feature of this paper was experimental evidence to show that when the maximum particle velocity due to oscillation was greater than the mean flow velocity; then the flow would be of a vortex type similar to that shown in figure 2-2, this was found to be the case for laminar and turbulent flows with Reynolds number up to about 30,000. At higher Reynolds number the vortex flow did not exist. The main conclusions drawn by the author's were:-

1. Resonant acoustic oscillations decreased the local heat transfer coefficient for turbulent flows where vortex cells did not exist i.e. Reynolds number greater than 30,000.
2. Local heat transfer maxima occurred at approximately half wavelengths and multiples of this, if vortex cells existed i.e. Reynolds Number less than 30,000.
3. Local heat transfer minima points occurred at approximately half wavelengths and multiples of this if the flow velocity was greater than the maximum particle velocity due to oscillation.
4. The sound pressure level below which acoustic oscillations had no effect on heat transfer varied with flow Reynolds number.

The variations of local effects discussed above are shown in figures 2-3, 2-4 and 2-5 below. It should be noted that Free convection effects are of importance for the lowest Reynolds number case.

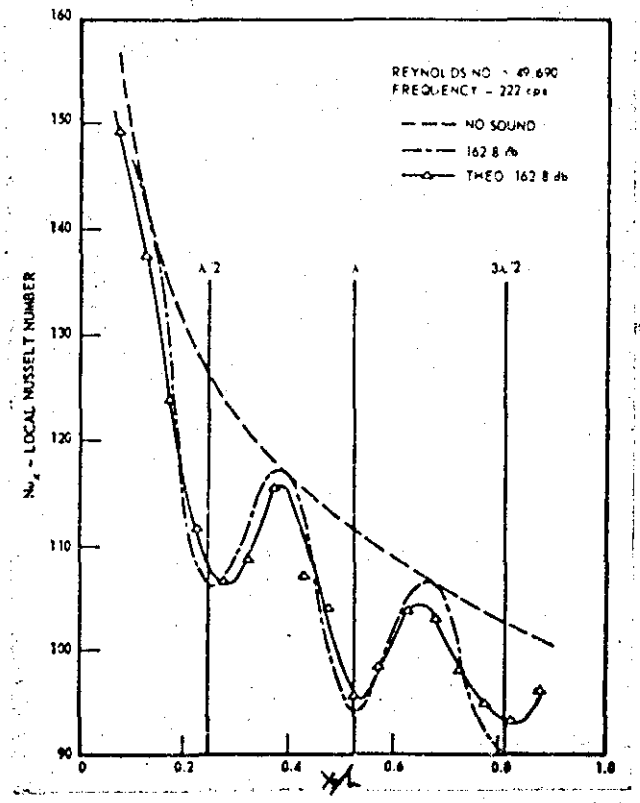

2-3 Decrease in Local Heat Transfer with Oscillation Ref. (5).

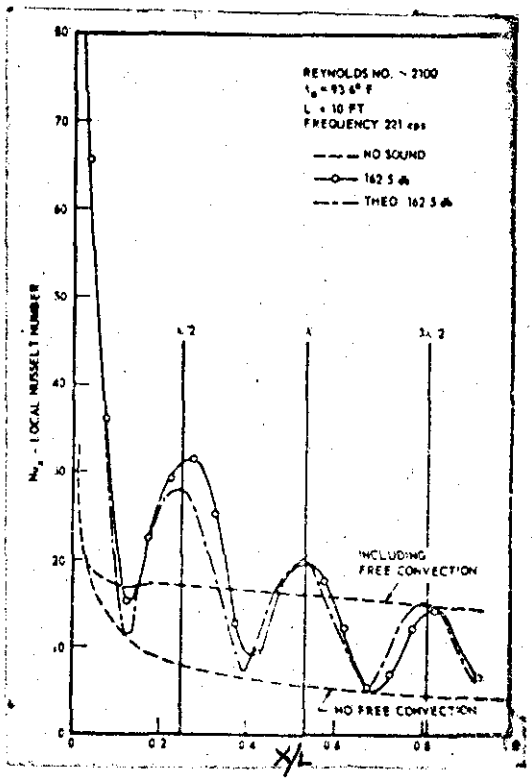

2-4 Effect of Free Convection on Local Heat Transfer Ref. (5).

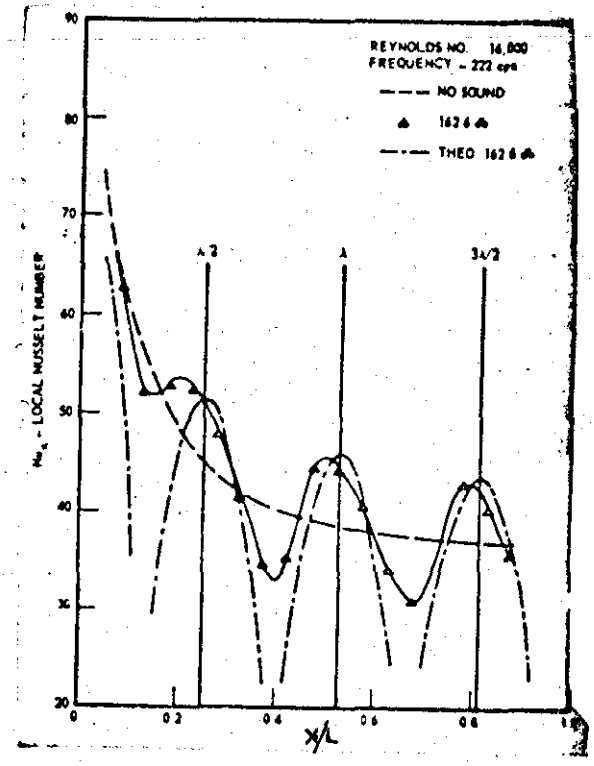

2-5 Comparison Between Experiment & Theory Ref. (5).

Lemlich and Hwu (6) in their experiments used a horizontal 0.745 I.D. heated isothermal tube through which air was passed. A calming section 65 ins. long and thermally isolated from the 25 in. test length ensured a fully developed velocity profile at entry to the heat transfer section. The acoustic driver propagated a wave in the same direction as the air flow. Tests were conducted with standing resonant waves at frequencies of approximately 198, 256 and 322 c/s. The sound pressure level was measured by traversing a total head tube of $\frac{1}{8}$" Dia. axially along the bottom of the heated section, the pressure being recorded on an inclined manometer. The Reynolds number for the tests varied from 565 to 5950. The authors obtained correlations for their data alone for the laminar flow region - Reynolds Number below 1500 and for the turbulent region Reynolds number greater than 2500. No flow visualisation studies were carried out. These experiments showed that for a constant average sound pressure level through the tube, the average heat transfer coefficient increased with increasing frequency. Evidence of earlier transition to turbulence was shown by the large increases in heat transfer with oscillation when flow Reynolds Numbers were of the order of 1500 to 2100.

The main conclusions of the authors are:-

1. Greater improvements in average heat transfer are to be obtained with laminar rather than turbulent main flows.
2. Results qualitatively agree with conclusions of Jackson et al. except for the frequency effect on heat transfer, however, the authors attribute these differences to the differing methods of measuring sound pressure level and the fact that Jackson et al. did not use the average sound pressure level in the tube in their calculations, but the value measured in the plenum chamber at entrance to the flow section.
3. One of the effects of the oscillations is to act as a turbulence trigger.

Some ideas of quantitative agreement between the results of Jackson et al (3) and Lemlich and Hwu can be obtained by considering the results common to both investigations. At a Reynolds number of approximately 2100, from Jackson et al (3) we see that for an increase in the sound pressure level from 152 db to 162.5 db. with frequency at 221 c/s the increase in average convective heat transfer coefficient is about 20%.

Now S.P.L. (db) = $20 \log_{10} \left[\frac{P}{P_o} \right]_{r.m.s.}$ where P_o is a reference pressure level of 0.0002 dyne/cm^2. Therefore the ratio

$$\frac{P_{162.5\ db}}{P_{152\ db}} = 3.35$$

From Lemlich and Hwu (6) for a Reynolds number of 2080 and frequency of 256 c/sec. The average acoustic pressure below which the heat transfer coefficient shows no appreciable effect is about 1.0 lbf/ft^2 for an increase in average pressure to about 3.0 the average heat transfer coefficient increases by approximately 35%. In the transition regime therefore qualitative agreement exists between the experiments of Jackson et al and Lemlich and Hwu.

Summary

From the foregoing work the following appear as the main facts.

1. Two basic flow regimes.
   (a) Vortex flow
   (b) Non Vortex turbulent flow.

   Vortex flow obtained with laminar conditions, and turbulent conditions up to a flow Reynolds number of 30,000.

   Non Vortex turbulent flow obtained with Reynolds number greater than 30,000. For this condition it appears that effect of oscillation is to reduce the average heat transfer coefficient, however, the evidence does not appear to be strong enough to consider this as general.

   Vortex flow generally produces an increase in the average heat transfer coefficient.
2. For a given set of conditions with vortex flow, the vortex size is directly proportional to sound intensity level.
3. Increased heat transfer at points of greater mixing at wall, similarly reduced heat transfer at points of reduced mixing when flow is away from wall. (see fig. 2-2).
4. Difference in the methods of measuring sound pressure level make quantitative comparisons between results of the two different groups of workers difficult. Ideally acoustic pressure on the boundary layer is required; this would be achieved by mounting the microphone flush with the tube wall.

2.4. Forced Convective heat transfer in cylindrical burners with combustion driven acoustic oscillations of the chamber gas

Of the early work in this field (pre world war two) that of Reynst (7) is worthy of note. Reynst had conceived the idea of utilising the combustion driven oscillation in a fanless boiler plant, where the induction and scavenging action was performed by the pressure oscillations due to acoustic resonance. A further advantage of this method of furnace design was its use with pulverised fuels, where a high relative velocity between furnace gas and fuel particle is necessary for greater combustion efficiency. The bulk of Reynst's work (7) is concerned with the aerodynamic and acoustic principles associated with these devices and their actual design. While he realised that improved heat transfer resulted from the oscillatory motion of the combustion gases, no specific study was concerned with the heat transfer processes involved.

In the post war period the bulk of the work on combustion driven acoustic oscillations has been carried out in the aero-space industry. Much of this work has been directed at understanding the aerothermochemistry of the phenomenon, and establishing design principles which avoided the occurrence of combustion driven acoustic oscillations, becuase of their damaging effects to the combustion chamber. Of the vast literature on the subject, the number of papers dealing directly with heat transfer aspects and flow visualisation studies are very few. To get the heat transfer and gas motion of the problem in perspective the papers of Male, Kerslake and Tischler (8) and Kreig (9) who carried out flow visualisation on rocket motors will be studied, the authors of reference (8) also obtained heat transfer coefficient data. Finally the experiments of Zartman (10) will be discussed.

Male, Kerslake and Tischler (8) carried out their study on a 4 in. I.D. cylindrical rocket engine of 23 in. length, terminated by a converging diverging nozzle. A transparent section extending 5½ ins. from the burner plate enabled high speed photographic studies to be carried out in this region. Simultaneous recording of the combustion process from a top and side view enabled a three dimensional picture to be constructed. Heat transfer rate was estimated from the depth of erosion in the combustion chamber - depth of erosion being proportional to heat transfer rate for a given running time.

Two basic modes of oscillation were obtained a 1000 c/s longitudinal mode and a 6000 c/s tangential mode of the spinning variety. Observations showed that the longitudinal mode was shock fronted whereas there was no

evidence of the tangential mode being shock fronted, the pressure fluctuations recorded were very large (peak to peak variations from 2 to 4 times the mean combustion chamber pressure) and therefore outside the scope of acoustics. Erosion measurements showed that heat transfer rates with the longitudinal mode were twice those of normal combustion whereas the tangential mode rates of heat transfer were six times those of normal combustion. The authors concluded that these changes were probably due to macroscopic transfer of the chamber gas to the wall, brought about by increased turbulence, or reduction in boundary layer thickness.

Kreig (9) in his study used a 15 ins. diameter rocket motor operating at mean pressures of about 330 lbf/in^2. Flow visualisation using techniques similar to those of Male et al (8) were carried out. The results of one of these visualisation studies across an axial element of the chamber is shown in figure (2-6). This was carried out for a tangential oscillation mode frequency of 1750 c/s. The figure shows clearly the motion of the gas towards the wall, which was also observed by Male et al.

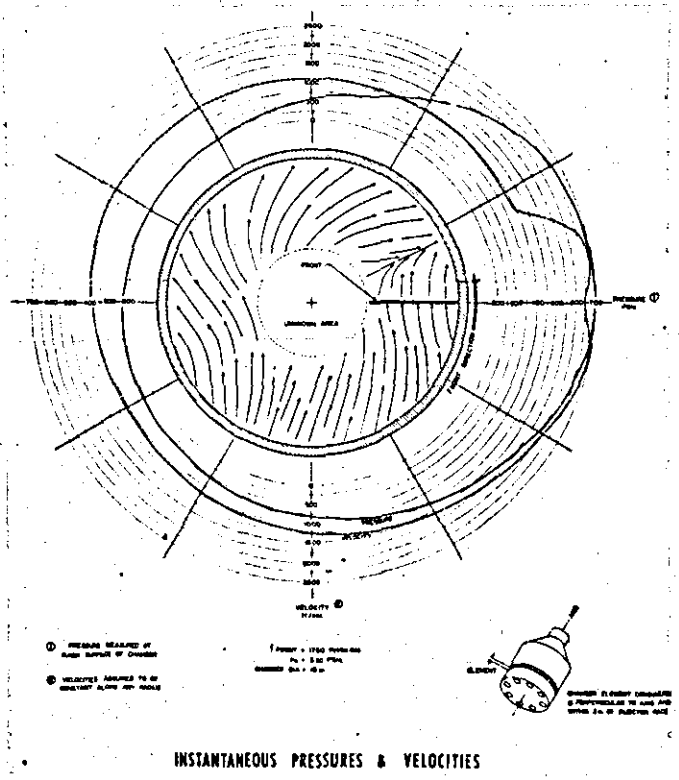

Fig. 2-6 Instantaneous Pressures and Velocities across an axial element of a rocket motor. Kreig Ref. (9)

Zartman (10) conducted experiments on a 5 inch I.D. Propane-Air burner, in which the effects of longitudinal and transverse modes of oscillation on heat transfer to the chamber wall could be studied separately. The pressure levels were recorded on a microphone mounted flush with the chamber wall and were well within the limits of acoustics. Heat transfer measurements were made at five locations along the length of the combustion chamber downstream of the flame holder, these measurements were made by means of thermocouples located in the tube wall. Gas temperature was obtained by means of the Sodium line reversal method at locations along the length of the chamber. Tests were conducted to determine the distance in which fully developed heat transfer results could be attained. This was found to be between 12 and 14 inches down stream of the flameholder depending on the type of flameholder (blockage) used in the experiments. Flow Reynolds numbers were varied from 35,000 to 48,000. Frequency of oscillations was varied from approximately 350 to 4,000 c/s and sound pressure levels from 130 to 158 db. were recorded.

The main observations of this study were

1. Up to a sound pressure level of 130 db no noticeable effects of acoustic oscillation on heat transfer rate was observed.
2. Above 130 db heat transfer coefficient increased linearly with increasing sound pressure level (see fig. 2-7).
3. The effect of oscillation on heat transfer coefficient was found to be independent of frequency - i.e. whether mode was longitudinal or transverse (350 or 4000 c/s).
4. Similarity in the temperature profiles and relative invariance of the combustion efficiency suggested that the fluid dynamics rather than the combustion process controlled the heat flux rates.
5. The effect of shortening the burning length was to increase the intensity of oscillation and therefore cause further increase in heat transfer.

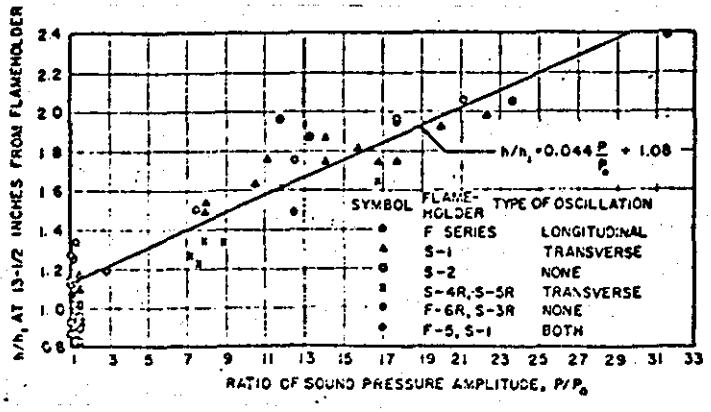

2-7 Effect of Combustion Driven Acoustic Oscillation on Heat Transfer Ref. (10)

2.5. Overall Discussion

Zartman's flow and acoustic data lie in the region classified by Jackson et al as the non vortex flow, turbulent main flow condition. (i.e. Re $>$ 30,000).

However, the heat transfer data of Zartman shows a contrary trend to that of Jackson et al - increasing heat transfer coefficient in the presence of sound.

It is clear that the flow situation in the region of the wall which controls the convective heat transfer process is different for the two situations. In the electrically driven system, the acoustic streaming vortex motion is destroyed by the main flow when Re $>$ 30,000. In the combustion driven acoustic oscillation problem, the combustion heat release drives the weak pressure oscillations present due to cavity resonance, the increase in the resulting pressure oscillation causes a modification to the bulk flow, and,as has been observed, greater mixing in the boundary layer.

However, Zartman's experiments and those of Jackson et al both show that there is no effect of acoustic frequency on the rate of heat transfer.

From what has been said above, it is apparent that any method developed for the computation of the heat transfer coefficient in the presence of combustion driven acoustic oscillation will be unsuitable for electrically driven systems.

3.0 THE DANCKWERTS-MICKLEY MODEL FOR TURBULENT HEAT EXCHANGE

And Its Application To Problems Of Forced Convective Heat Transfer In The Presence Of Combustion Driven Acoustic Oscillations In Tubular Chambers.

The Selection of a Model for Turbulent Heat Exchange between a Gas and Wall Surface in the Presence of Acoustic Oscillation

3.1. The Classical Approach to the Problem of Turbulent Flow with Heat Transfer.

The classical approach to the study of laminar fluid motion is through the Navier Stokes equations. However, Prandtl showed (11) that, from order of magnitude considerations, the complex Navier Stokes equations could be reduced to the simpler boundary layer equations.

For the steady laminar incompressible two dimensional boundary layer flow over a flat plate at zero incidence, the boundary layer and continuity equations are (11)

$$u\frac{\partial u}{\partial x} + v\frac{\partial u}{\partial y} = \nu\frac{\partial^2 u}{\partial y^2} \qquad \text{——— 3.1.1.}$$

$$\frac{\partial u}{\partial x} + \frac{\partial v}{\partial y} = o \qquad \text{——— 3.1.2.}$$

with boundary conditions.

At $y = o$; $u = v = o$ ——— 3.1.3.

$y = \infty$; $u = U_\infty$ the free stream velocity

At $x = o$; $u = U_\infty$

A corresponding order of magnitude consideration of the general energy equation (11) for the laminar forced convective transfer of heat from the heated fluid to the cooler plate of the above hydrodynamic problem yields in the absence of kinetic heating effects.

$$u\frac{\partial \theta}{\partial x} + v\frac{\partial \theta}{\partial y} = \alpha\frac{\partial^2 \theta}{\partial y^2} \qquad \text{——— 3.1.4.}$$

In the study of turbulent fluid motion, the approach to the problem is to assume after Reynolds (11), that the turbulent fluid motion can be separated into a mean motion and a fluctuating or eddy motion. If the three time averaged components of the fluid motion are given by $\bar{u}$; $\bar{v}$ and $\bar{w}$ and the fluctuating

components are given by u^1 ; v^1 and w^1, then the instantaneous values of the three components of motion are

$$u = \bar{u} + u^1 \; ; \quad v = \bar{v} + v^1 \quad \text{and} \quad w = \bar{w} + w^1$$

Similarly, fluid properties such as pressure (p), temperature (θ) and density (ρ) at any instant can be handled in the same way so that

$$p = \bar{p} + p^1 \; ; \quad \theta = \bar{\theta} + \theta^1 \quad \text{and} \quad \rho = \bar{\rho} + \rho^1$$

The time averaging is considered to be carried out at a fixed point in space and to be taken over a sufficiently long period of time for them to be independent of time.

e.g. $$\bar{u} = \frac{1}{\tau}\int_t^{t+\tau} u.dt. \qquad \text{——————3.1.5.}$$

By this definition, we see that the time average of the fluctuating quantities would be zero, so that $\overline{u^1} = o$; $\overline{v^1} = o$ etc.

The mean fluid motion must satisfy the Navier-Stokes equations and the continuity equation, reference (11). The fluctuating velocity components u^1; v^1 and w^1 influence the mean motion $\bar{u}$; $\bar{v}$; and $\bar{w}$ in such a way that the mean motion exhibits an apparent increase in its resistance to deformation. The fluctuations v^1 and w^1 normal to the bulk flow in the x direction give rise to shear stresses in the fluid $-\rho\overline{u^1v^1}$ and $-\rho\overline{u^1w^1}$ while the u^1 fluctuation gives rise to a normal stress $-\rho\overline{u^{1^2}}$. Therefore, the Navier-Stokes equations take on an extra set of stress terms - The Reynolds Stresses - which account for the turbulent fluctuations in the flow.

For the steady two dimensional incompressible turbulent flow over a plate at zero incidence, the Prandtl boundary layer equation and continuity equation from order of magnitude considerations are from reference (11).

$$\bar{u}\frac{\partial \bar{u}}{\partial x} + \bar{v}\frac{\partial \bar{u}}{\partial y} = \frac{\partial}{\partial y}\left\{\left[\nu + E_m\right]\frac{\partial \bar{u}}{\partial y}\right\} \qquad \text{——————3.1.6.}$$

$$\frac{\partial \bar{u}}{\partial x} + \frac{\partial \bar{v}}{\partial y} = o \qquad \text{——————3.1.7.}$$

where E_m is the eddy momentum transport coefficient and is equal to

$$\frac{\overline{u^1 v^1}}{\frac{\partial \bar{u}}{\partial y}}$$

the boundary conditions on 3.1.6. and 3.1.7. are the same as for 3.1.1. and 3.1.2.

For the forced convective turbulent heat transfer for the above hydrodynamic situation, the thermal boundary layer equation is:-

$$\bar{u} \frac{\partial \bar{\theta}}{\partial x} + \bar{v} \frac{\partial \bar{\theta}}{\partial y} = \frac{\partial}{\partial y}\left\{\left[\alpha + E_H\right] \frac{\partial \bar{\theta}}{\partial y}\right\} \qquad \text{3.1.8.}$$

The boundary conditions on temperature are:-

$$\begin{aligned} &\text{at } y = o ; \quad \bar{\theta} = \theta o \\ &\text{at } y \to \infty ; \quad \bar{\theta} \quad \theta\infty \\ &\text{at } x = o ; \quad \bar{\theta} = \theta\infty \end{aligned} \qquad \text{3.1.9.}$$

E_H is the eddy heat transport coefficient and is equal to $\dfrac{\overline{v^1 \theta^1}}{\frac{\partial \bar{\theta}}{\partial y}}$

The evaluation of the local or average heat transfer rate to the plate surface necessitates the solution of 3.1.6., 3.1.7. and 3.1.8. along with appropriate boundary conditions 3.1.3. and 3.1.9.

For the case of fully developed flow on a semi-infinite plate - (very long in the x direction). The velocity and temperature gradient which are of importance are those in the y direction. This can be shown from an order of magnitude consideration as follows.

It is assumed that x is the order of magnitude of a length L which is $\gg 1$, and that $\bar{u}$ is of the same order. Further y is of the order of magnitude of the boundary layer thickness δ which is $\ll L$ and we assume $\bar{v}$ is of the order of δ

Then $\bar{u} \frac{\partial \bar{u}}{\partial x}$ ——— $o(L)$

$\bar{v} \frac{\partial \bar{u}}{\partial y}$ ——— $o(L)$

$$\frac{\partial}{\partial y}\left[(\nu + E_M)\frac{\partial \bar{u}}{\partial y}\right] \quad \text{———} \quad \frac{o(L)}{o(\delta^2)}$$

Since $\frac{o(L)}{o(\delta^2)} \gg o(L)$ only the term of $\frac{o(L)}{o(\delta^2)}$ need be retained in equation 3.1.6. which reduces to

$$\frac{d}{dy}\left[(\nu + E_M)\frac{d\bar{u}}{dy}\right] = 0$$

$$(\nu + E_M)\frac{d\bar{u}}{dy} = C_1 = \frac{\tau_o g_c}{\rho} \qquad \text{———3.1.10.}$$

By similar reasoning, equation 3.1.8. reduces to

$$(\alpha + E_H)\frac{d\bar{\theta}}{dy} = C_2 = \frac{Q}{A\rho C_p} \qquad \text{———3.1.11.}$$

The simplest solution of equations 3.1.10. and 3.1.11. for average or local heat transfer coefficient, which is also compatible with experiment over a reasonable range of Prandtl numbers (suitable to cover the range of investigation here) is that using the Von-Karman-Martinelli analogy between momentum and heat transfer. (12)

The analogy assumes a definite relationship to exist between E_M and E_H, in its simplest form, it is assumed that $E_M = E_H$. The Von-Karman-Martinelli method further assumes that the boundary layer is made up of three distinct regions.

Nearest the wall, a laminar sublayer is considered to exist in which the momentum and heat transfer are achieved on a molecular scale, (i.e. E_M and E_H are zero). This region is considered to exist over the range $0 < y^+ < 5$ where $y^+ = \left[y\frac{v^*}{\nu}\right]$ is the non dimensional distance from the wall surface, and v^* is the so called friction velocity and is equal to $\left[\frac{\tau_o g_c}{\rho}\right]^{1/2}$

Adjacent to the sublayer is a buffer region in which molecular and macroscopic eddy transfer are considered to be of equal importance (ν; E_M; α and E_H all of equal importance). This region is considered to extend over $5 < y^+ < 30$.

Finally, a fully developed turbulent core region is considered beyond $y^+ = 30$. In this region, the effects of molecular transport are

considered small in relation to the macroscopic eddy transfer ($\nu \ll E_M$; $\alpha \ll E_H$).

The method for calculating heat transfer coefficient is semi-empirical in that, to solve equations 3.1.10. and 3.1.11., the velocity $\bar{u}$ as a function of y^+ must be known, in the usual boundary layer notation, this is:-

$$u^+ = f(y^+)$$

where $u^+ = \dfrac{\bar{u}}{\left[g_c \tau_{o/p}\right]^{1/2}}$

and, secondly, the relationship between E_M and E_H and u^+ and y^+ must be known. These two items of information are obtained from experimental observation. For the case of steady incompressible pipe flow or flow over a flat surface this information is readily available.

In the problems under study here the main flow is affected by oscillation and the wall shear stress is increased. Therefore, any attempt at calculating the heat transfer coefficient using the Von-Karman-martinelli analogy would necessitate two sets of empirical information.

An alternative approach to the problem of calculating heat transfer coefficient between a wall surface and a fluid, in the presence of oscillation, is by the use of a Surface Renewal Model.(13) This type of model has found wide application in Chemical Engineering in the design of stirred reactors and fluidised beds, where, because the flow path is so complex, no attempt is made at defining this, but the average heat transfer is computed from determining the averaged effect of fluid mixing on it.

3.2. The Danckwerts-Mickley Surface Renewal Model

The concept of the surface renewal model was first put forward by Higbie (14). However, this model made no allowance for the randomness of the mixing motion. Danckwerts (13) is generally credited with being the first to develop a renewal model which allowed for the randomness of the mixing process. A similar model to that of Danckwerts was put forward by Mickley (15) to account for effect of mixing on heat transfer in a fluidized bed.

The physical model of Danckwerts and Mickley for the transfer of heat between a turbulent fluid motion and a wall surface is considered as follows:- Macroscopic "lumps" of fluid from the turbulent bulk or core of the fluid move randomly and at high frequency to the wall surface, exchange heat with it in a transient manner before being displaced by fresh fluid from the bulk region.

In figure (3-1) one such lump is considered. The lump is at the temperature of the bulk fluid $\theta\infty$, which is assumed to be greater than that of the surface θo.

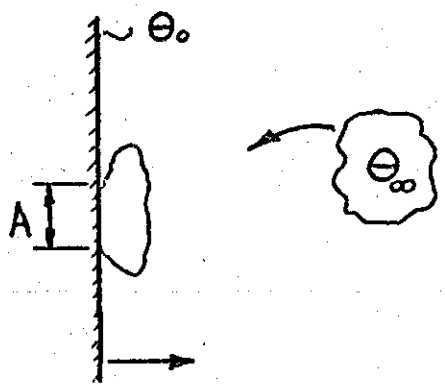

FIGURE 3.1.

Transfer of a fluid lump to the wall surface.

Because of turbulent motion in the fluid, this lump is brought into contact with the boundary surface. This contact is transitory, therefore unsteady conduction between the fluid "lump" and the surface takes place over a very short period of time. Because of the short contact time between the fluid and the surface, heat may be considered to have been transferred from a semi-infinite fluid mass at $\theta\infty$ which has been subjected to a step change in temperature to θo.

Mathematically this involves solution of the one dimensional unsteady state heat conduction equation with suitable boundary conditions.

$$\text{i.e. } \frac{1}{\alpha}\frac{\partial \theta}{\partial t} = \frac{\partial^2 \theta}{\partial y^2} \qquad \text{——————3.2.1.}$$

$$t = 0;\ \theta = \theta\infty$$
$$t > 0;\ \theta = \theta o \text{ at } y = o \qquad \text{——————3.2.2.}$$
$$\theta = \theta\infty \text{ at } y = \infty$$

Remembering that $\theta\infty$ and θo are independent of t, the solution of equation 3.2.1. with boundary conditions 3.2.2. can be found in most texts on heat transfer. e.g. (16).

The instantaneous heat flow at y = o from reference (16) is

$$Qi = \frac{k\,A\,(\theta\infty - \theta o)}{\left[\pi \alpha t\right]^{1/2}} \qquad \text{——————3.2.2.}$$

The local instantaneous heat transfer coefficient is

$$h_i = \frac{Qi}{A(\theta\infty - \theta o)} = \left[\frac{k \rho C_p}{\pi t}\right]^{1/2} \qquad \text{——————3.2.3.}$$

The object now is the relation of t in equation 3.2.3. to the random mixing of the fluid.

Danckwerts and Mickley consider the motion of the fluid continually replacing the older fluid lumps at the surface with fresh lumps from the fluid bulk - (the lumps at the surface are older in the sense that they have been in contact with the surface for a finite time).

Because of the assumed steady flow conditions and the fact that the turbulent process is completely random, the rate of renewal of fluid lumps at the surface is a constant dependent only on the fluid mechanics and geometry of the particular situation, hence no correlation exists between the age of a fluid lump and its replacement - i.e. no preferential replacement of any particular age group. Therefore, the fractional rate of replacement or renewal of lumps belonging to any "age" group is defined by S per unit area.

If a fractional surface area-age distribution function ϕ_t is defined, then, at time t, the area covered by lumps of age t will be A ϕ_t. In the time interval dt, there will be a decrease in the fractional surface area covered because of displacement of some fluid lumps into the bulk fluid. This decrease of the fractional surface area with respect to time must be equal to the fractional rate of renewal of the surface from the bulk region. This may be expressed mathematically as

$$-\frac{d\phi_t}{dt} \cdot A = S\,\phi_t\,A \qquad \text{——————} \quad 3.2.4.$$

Hence $\log_e \phi_t = -St + \text{CONSTANT}$ —————— 3.2.5.

or $\phi_t = (\text{CONSTANT})\,e^{-St}$ —————— 3.2.6.

From the definition of ϕ_t, we know that $\int_o^\infty \phi_t.dt = 1$

Therefore $\int_o^\infty \phi_t.dt = \left[-\frac{(\text{CONSTANT})}{S}\,e^{-St}\right]_o^\infty = 1$ ——3.2.7.

and hence the CONSTANT from integration 3.2.5. is equal to S.

$$\therefore\ \phi_t = S\,e^{-St} \qquad \text{——————} \quad 3.2.8.$$

The local heat transfer coefficient at any point x on the surface will be due to lumps of all ages and will be given by

$$h_x = \int_o^\infty h_i\,\phi_t.dt \qquad \text{——————} \quad 3.2.9.$$

substituting for h_i and ϕ_t from 3.2.3. and 3.2.8. respectively.

$$h_x = S\left[\frac{k\rho C_p}{\pi}\right]^{1/2}\int_o^\infty t^{-\frac{1}{2}}.\,e^{-St}\,.\,dt \qquad \text{——————} \quad 3.2.10.$$

the integral $\int_o^\infty t^{-\frac{1}{2}}\,.\,e^{-St}\,dt = \left[\frac{\pi}{S}\right]^{1/2}$ Dwight (17)

Therefore $h_x = \left[k\rho C_p S\right]^{1/2}$ —————— 3.2.11.

The average coefficient over the whole surface Ao is

$$h_o = \frac{1}{A_o}\int_{A_o} h_x\,.\,dA \qquad \text{——————} \quad 3.2.12.$$

$$\therefore \quad h_o = \left[k \rho C_p\right]^{\frac{1}{2}} \frac{1}{Ao} \int_{Ao} \cdot \; S^{\frac{1}{2}} \cdot dA \qquad \text{——————3.2.13.}$$

Defining the area mean renewal coefficient over the area Ao as

$$So^{\frac{1}{2}} = \frac{1}{Ao} \int_{Ao} \cdot \; S^{\frac{1}{2}} \cdot dA \qquad \text{——————3.2.14.}$$

The average heat transfer coefficient over the surface is then

$$ho = \left[k \rho C_p \; So\right]^{\frac{1}{2}} \qquad \text{——————3.2.15.}$$

3.3. Assessment of the Assumptions in the Danckwerts-Mickley Model in the light of Experiments

The general concept of surface renewal - lumps of bulk fluid penetrating to the wall surface is consistent with the observations of Fage and Townend (18), Harratty (19), Bakewell and Lumley (20), Sherwood et al (21) and Kline et al (22). All these workers have studied the structure of the forced convective boundary layer on a flat surface. Locke and Trotter (23) from their study of the structure of the turbulent free convective boundary layer conclude that the assumption of a laminar sublayer is not valid. Therefore, adequate experimental evidence backs up the concept of renewal in the wall region.

The assumption of a constant renewal rate S per unit area is consistent with continuity since if for assumed steady state conditions of flow, the time averaged rate of fluid arrivals and departures from the surface must be the same. This is in no way different to the traditional approach to turbulent boundary layer problems discussed in section 3.1. where it is assumed that the time average of the fluctuating components is equal to zero, for example

$$\overline{v^1} = \frac{1}{\tau} \int_t^{t+\tau} v^1 dt = 0$$

The assumption of constant renewal rate S is also consistent with the detailed observations of the boundary layer by Kline et al (22). These studies have shown that in the region of the wall, relatively large elements of low velocity fluid are violently ejected into the bulk flow where they break up and follow a pattern of decaying turbulence, the reason for this ejection is thought to be due to instability in the region of the boundary layer close to the wall. Highly energetic fluid from the turbulent bulk fluid moves towards the wall surface to replace the ejected elements. It is thought that the energy supplied by these elements contribute to the ejection of the slower elements from the wall region.

Ruckenstein (24) in a study of the renewal model, states that the model due to Danckwerts considers the wall fluid elements to be static during contact, and if the wall fluid elements are in motion then consideration must be given to their deformation. Ruckenstein then presents a model which considers the bulk motion of the fluid bringing elements into contact with the wall surface, which then move in laminar flow over a short distance before moving into the bulk region. From this model, Ruckenstein concludes that for heat transfer at high Prandtl number Pr the Nusselt number Nu as a function of the Reynolds number Re and Pr for pipe flow is

$$Nu \propto (Re)^{0.9} (Pr)^{1/3} \qquad \text{3.3.1.}$$

Equation 3.3.1. is in good agreement with experimental data for heat transfer at high Pr. (i.e. Pr $>$ 20) from the correlation of Kays (12). That this is so can be seen from the fact that at high Pr the thermal boundary layer is extremely thin, and the major part of the thermal gradient is confined to the viscous region near the wall. This in no way invalidates Danckwerts' model. Danckwerts (13), (25) does not specifically mention that renewal elements at the wall are static. But, he does state that the renewal or mixing coefficient S is a function of the fluid mechanics and geometry of the system under study. If sufficient is known about the flow situation or can reasonably be assumed about it, the possibility exists of defining the form of S analytically. This is, in effect, what Ruckenstein has done by confining attention to high Pr systems.

Toor and Marchello (26) in the application of the Danckwerts renewal model to the problem of heat transfer in turbulent pipe flow show that S_o is given by

$$S_o \propto \frac{\bar{U}}{D} \; Re^{0.8} \qquad \text{——————} 3.3.2.$$

where $\bar{U}$ is the mean flow velocity of the fluid through the pipe.

In the problems under study here, concern is focussed on the mixing motion in the region of the wall. The friction velocity $v^* = \left[\frac{g_c \tau_o}{\rho}\right]^{1/2}$ is a measure of the intensity of turbulent eddying and of the momentum transfer due to this in the region of the wall. Because of the proportionality of v^* with the mean flow velocity $\bar{U}$, its use would give a better representation in 3.3.2. than $\bar{U}$.

Hence $$S_o \propto \frac{v^*}{D} \; Re^{0.8} \qquad \text{——————} 3.3.3.$$

$$\therefore \quad h_o \propto \left[k \rho C_p \; \frac{v^*}{D} \; Re^{0.8}\right]^{1/2} \qquad \text{——————} 3.3.4.$$

For turbulent pipe flow with $Re \leq 100{,}000$, v^* can be obtained from reference (11) in the form

$$v^* = (0.0396)^{\frac{1}{2}} \; \frac{\bar{U}^{\frac{7}{8}} \nu^{\frac{1}{8}}}{D^{\frac{1}{8}}} \qquad \text{——————} 3.3.5.$$

or $$v^* \propto \frac{\bar{U}^{\frac{7}{8}} D^{\frac{7}{8}}}{\nu^{\frac{7}{8}}} \cdot \frac{\nu}{D} \qquad \text{——————} 3.3.5.$$

$$\therefore \quad \frac{h_o D}{k} \propto \left[\frac{\nu}{\alpha}\right]^{\frac{1}{2}} \left[Re\right]^{0.838} \qquad \text{——————} 3.3.6.$$

or $$\frac{h_o D}{k} = C_1 \left[Re\right]^{0.838} \left[P_R\right]^{0.5} \qquad \text{——————} 3.3.7.$$

C_1 is a constant to be determined from experimental results.

The McAdam correlation for fully developed turbulent pipe flow (27) is:

$$\frac{h_o D}{k} = 0.023 \; Re^{0.8} \; P_R^{0.4} \qquad \text{——————} 3.3.8.$$

3.3.8. is valid in the range $10,000 \leq Re \leq 120,000$

$$0.7 \leq P_R \leq 120$$

The results from 3.3.7. and 3.3.8. are shown in figure 3.2. for $P_R = 0.73$ and $C_1 = 0.0162$. Agreement of these results is to within 6%, a slight devergence occuring at high Re.

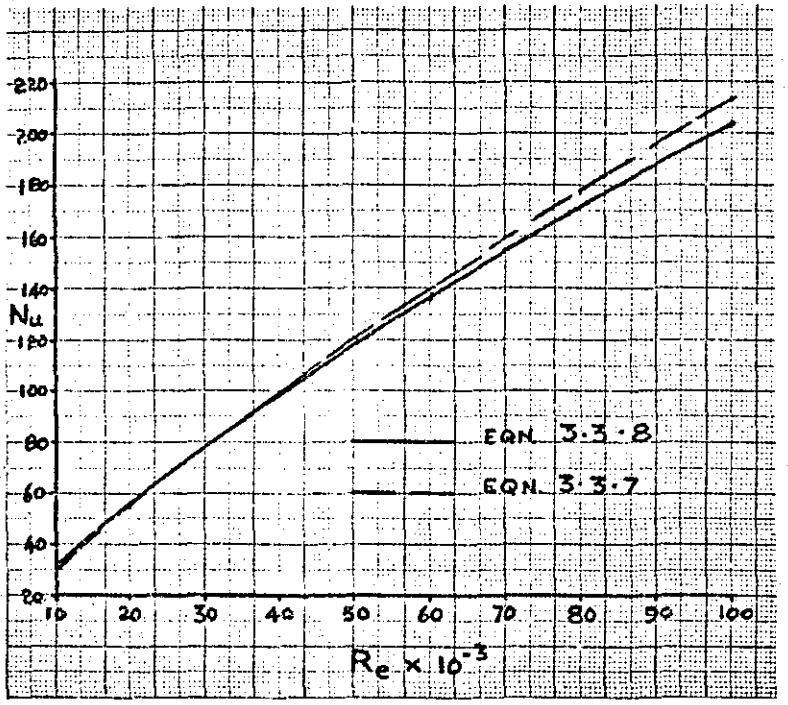

FIGURE 3.2. Comparison between equation 3.3.7. and the McAdams correlation equation 3.3.8.

Having established that the Danckwerts model can be applied to problems of turbulent heat transfer in pipes with an accuracy acceptable for most practical purposes, the next section will indicate how the method can be extended to turbulent pipe flow with superimposed combustion driven acoustic oscillation.

3.4. Application of the Danckwerts-Mickley Model for Heat Transfer in Fully Developed Turbulent Pipe Flow in the Presence of Combustion Driven Acoustic Oscillation.

From the earlier discussion of the photographic studies of Male et al (8) and Krieg (9), it was seen that the effect of oscillation was to cause greater mixing in the region of the wall. The problem here is to relate this increased mixing motion with recorded acoustic data.

From the discussions immediately preceeding this section, it was noted that Kline et al (22) postulated that the mixing action in the region of the wall was caused by energy supply from the bulk region fluid lumps. It was further noted in the last section that v^*, the friction velocity, was important in characterising the intensity of the turbulent eddying (mixing) in the vicinity of the wall. Therefore $\frac{\rho v^{*2}}{g_c}$ should be of the order of magnitude of the energy supply postulated by Kline et al, because the highly energetic v^1 fluctuations give rise to a large momentum flux which is equal to the opposing shear stress at the wall τ_o, and we know that $\frac{\rho v^{*2}}{g_c} = \tau_o$.

If from the experimental evidence of Male et al and Krieg, it is considered that the effect of the combustion driven acoustic oscillation is to supplement the turbulent mixing motion in the wall region due to the bulk flow.

Then, if the acoustic pressure is measured or can be calculated along the wall surface, the average energy density in the acoustic wave is:- (from Morse Bibliography (1))

$$\frac{I}{C} = \frac{\rho u^2_{max}}{2 g_c} \qquad \text{3.4.1.}$$

Details of the derivation of 3.4.1. are to be found in Appendix I(a).

In terms of r.m.s. quantities, for an acoustic wave of sinusoidal form, equation 3.4.1. may be written as

$$\frac{I}{C} = \frac{\rho}{g_c} \left[a_{r.m.s.}\, \omega \right]^2 \qquad \text{3.4.2.}$$

From the consideration that acoustic energy is supplementing the turbulent mixing motion in the wall region, and the hypothesis of Kline et al, we have

$$\text{Total energy in wall region} = \frac{\rho}{g_c}\left[a_{r.m.s.}\,\omega\right]^2 + \frac{\rho v^{*2}}{g_c} \qquad 3.4.3.$$

$$= \frac{\rho}{g_c}\left[(a_{r.m.s.}\omega)^2 + v^{*2}\right] \qquad 3.4.4.$$

A modified friction velocity v^{**} is now defined so that

$$v^{**} = \left[(a_{r.m.s.}\omega)^2 + v^{*2}\right]^{\frac{1}{2}} \qquad 3.4.5.$$

Now the mixing coefficient for a turbulent bulk flow in the presence of combustion driven acoustic oscillation S_v, by analogy with equation 3.3.3. for S_o will be

$$S_v \propto \frac{v^{**}}{D}\, Re^{0.8} \qquad 3.4.6.$$

Therefore the average heat transfer coefficient h_v in the presence of combustion driven oscillations will be

$$h_v \propto \left[k\,\rho\,C_p\,\frac{v^{**}}{D}\,Re^{0.8}\right]^{\frac{1}{2}} \qquad 3.4.7.$$

From equations 3.3.4. and 3.4.7. one obtains the ratio

$$\frac{h_v}{h_o} = \left[\frac{v^{**}}{v^*}\right]^{\frac{1}{2}} = \left[1 + \left(\frac{a_{r.m.s.}\,\omega}{v^*}\right)^2\right]^{\frac{1}{4}} \qquad 3.4.8.$$

The constants of proportionality in equations 3.3.4. and 3.4.7. must be the same and hence cancel out when 3.4.7. and 3.3.4. are ratioed. If this were not so, h_v would not tend to h_o as $(a_{r.m.s.}\omega)$ became small compared with V^*, which is observed experimentally.

3.5. Comparison and Discussion of Results predicted by Equation 3.4.8. with the Experiments of Zartman.

The experimental data of Zartman (10) for a burning length of $17\frac{1}{2}$ ins. was used for comparison with equation 3.4.8. The reasons for this were:

(1) Zartman observed that the effects of chemical reaction due to combustion were effectively complete with the $17\frac{1}{2}$ in. burning length.

(2) The turbulent flow at this length was fully developed.

(3) The microphone used by Zartman for recording pressure was located just upstream of the flame holder. In this position, the sound pressure level recorded would have been approximately the same as that at the $17\frac{1}{2}$ in. position.

The justification for the last statement is based on studies of transverse mode combustion driven acoustic oscillations in a 6 in. burner tube carried out by the N. A. C. A. Lewis Laboratory (28). In this study the position of the flameholder was changed and the effect of this was noted on the pressure variation along the wall of the chamber. The results of this study are shown in figure 3.3.

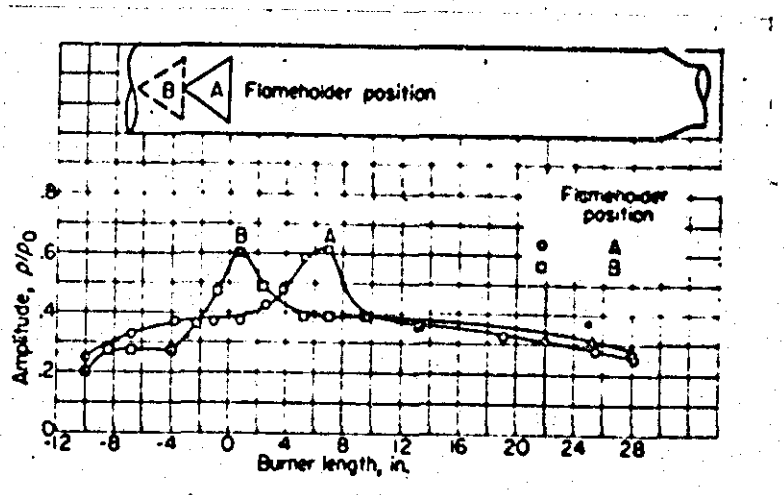

FIGURE 3.3. Variation of Acoustic Pressure along Combustion Chamber Wall. (Reference 28)

It will be noted that with the microphone placed at a point just upstream of the flame holder baffle, the acoustic pressure at that point is approximately the same as that about 17-18 ins. downstream of the baffle.

The evaluation of v^* in equation 3.4.8. can be carried out by using the expression for v^* for fully developed turbulent pipe flow, from Schlichting (11), this is

$$v^* = (0.0396)^{\frac{1}{2}} \bar{U}^{\frac{7}{8}} \left[\frac{\nu}{D}\right]^{\frac{1}{8}} \qquad \text{3.5.1.}$$

From Morse (Bibliography 1) $(a_{r.m.s.}\omega)$ can be related to the sound pressure level; this derivation is shown in Appendix I(b).

Hence

$$(a_{r.m.s.}\omega) = \frac{P_{r.m.s.}\ g_c}{\rho c} \qquad \text{3.5.2.}$$

$P_{r.m.s.}$ is obtained from the definition of the (S.P.L.) db. scale relative to a reference pressure level Po.

Where $\text{(S.P.L.) db.} = 20 \log_{10} \left[\frac{P}{Po}\right]_{r.m.s.}$ 3.5.3.

All properties were evaluated on an average molal basis at the mean of the gas and wall temperatures at the same location at which heat transfer measurements were made.

A sample calculation for Zartman's data run number 20 is carried through in detail in Appendix II.

The comparison between Zartman's data and equation 3.4.8. is shown in figure 3.4. below.

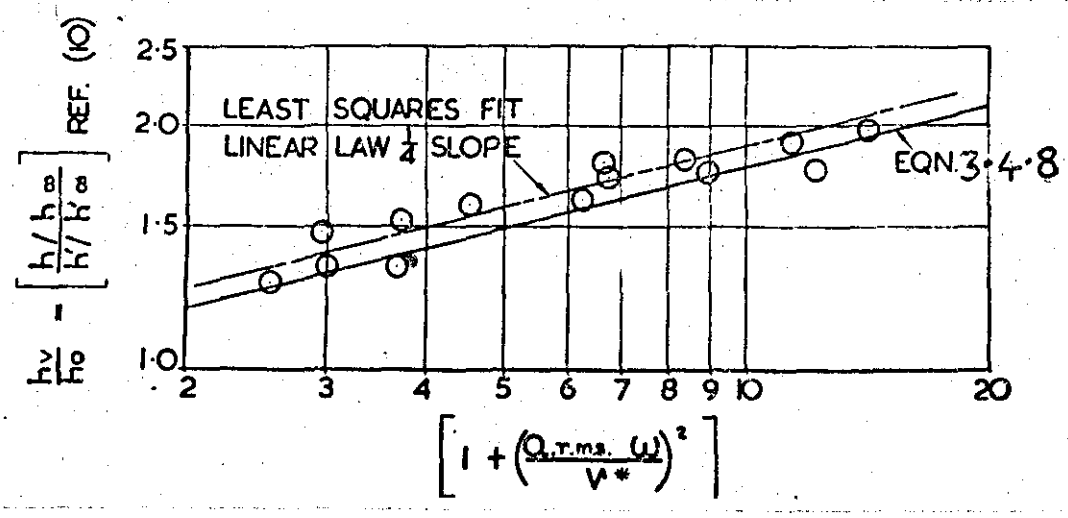

FIGURE 3.4. Comparison between Equation 3.4.8. and the Experimental Data of Zartman. (Reference 10)

Discussion

From figure 3.4. it is seen that equation 3.4.8. is a good representation of the experimental data points. The experimental data points are consistently above their predicted positions. This is most probably due to the assumption of sound pressure level being equal at the recording point and that at 17½ ins. from the baffle, the results in figure 3.4. indicate that the recorded S.P.L. is slightly higher than at the 17½ in. position.

The consistency of the data relative to equation 3.4.8. indicates that the postulated model for mixing and heat transfer in the presence of combustion driven acoustic oscillations is a reasonable one. However, the validity of equation 3.4.8. is expected to break down as the acoustic pressure waves steepen into shock fronts. The model is expected to hold for weak shock fronts - finite pressure waves - provided that in this case the pressure ratio across the shock is not large. The criterion for acceptable pressure ratio

across the shock is that the wave propagation speed, ν, should not differ appreciably from that of the sonic velocity in the undisturbed gas C^1. Bannister (29) obtained the following relation between wave propagation speed, sonic velocity in the undisturbed gas and the pressure ratio P/p^1 across the finite wave.

$$\nu = C^1 \left[\left(\frac{k+1}{k-1} \right) \left(\frac{P}{p^1} \right)^{\frac{k-1}{2k}} - \frac{2}{k-1} \right] \qquad 3.5.4.$$

p^1 is the pressure in the undisturbed gas. Note that when $P/p^1 \approx 1$ as in acoustics then $\nu \approx C^1$.

The method discussed here does not enable the prediction of the critical sound pressure level, below which the effect of acoustic oscillation on heat transfer is negligible. However, the low increases in heat transfer predicted by equation 3.4.8. in the region of the observed critical sound pressure level, would fall within the range of experimental error with normal combustion systems.

Conclusions

Using the Danckwerts-Mickley model for heat transfer in fully developed turbulent pipe flow, and interpreting the surface renewal or mixing coefficient S in the light of the observations and hypotheses of Kline et al, Male et al and Krieg, concerning the wall exchange process, a suitable model has been set up for the calculation of heat transfer coefficient in the presence of combustion driven acoustic oscillation in a cylindrical gas air burner. This model shows good agreement with the experimental observations of Zartman.

4.0. THE EFFECTS OF TRANSVERSE MECHANICAL OSCILLATIONS OF HEATED VERTICAL PLANE SURFACES IN FREE CONVECTION IN AIR.

4.1. Survey of Literature

The literature surveyed in this section is that associated with transverse mechanical oscillations of plane surfaces, because, this mode of oscillation is usually found in practice on large panel and box structures.

The open published literature on this subject is limited to three papers. The first by Shine (30) who conducted an experimental investigation on the effects of transverse mechanical oscillations on free convective heat transfer from an eight inch vertical plate. The second and third are those of Blankenship and Clark (31) (32) who carried out a combined analytical and experimental study of free convection from a heated vertical transversely vibrating plate to air.

Shine (30) used a plate eight inches tall by ten inches wide. Instrumentation for flow visualisation and temperature measurement included a Mach-Zender interferometer and an optical system for phase discrimination, by which the dependence of heat transfer coefficient on the position of the plate in its oscillation cycle could be observed. Heat transfer coefficients were determined at constant heat flux, for wall temperatures ranging from 131° to 279°F. The amplitude and frequency of oscillation of the plate varied from 0 to 0.61 ins. and 11 to 315 c/s. respectively.

It was observed that below a certain critical oscillation intensity - where intensity is the product of amplitude and frequency - there was no effect of oscillation on the boundary layer flow or on the heat transfer coefficient. At a critical intensity instability was observed in the form of a wave motion in the outer region of the boundary layer. The instability was observed to increase with increasing oscillation intensity above the critical. The heat transfer coefficient was observed to increase with oscillation intensity greater than the critical, the maximum increase being about 40% above the value for the oscillation free case.

Indifference curves were plotted, these consisted of plots of oscillation frequency versus amplitude at the critical condition. Curves were plotted for two differing criteria for the critical condition, in the first case the data was plotted on the basis of the first observation of wave motion in the boundary layer, in the second case the data was plotted on the observation of the first increase in heat transfer coefficient above the oscillation free value. Both these methods yielded a critical intensity of oscillation of approximately

1.0 ins c/s.

No observable relationship between heat transfer coefficient and position of the plate in its oscillation cycle was noticed.

The only data presented in any detail for computational purposes were those for the maximum plate temperature of approximately 279°F ($Gr_L \approx 60 \times 10^6$). see figure (4-1)

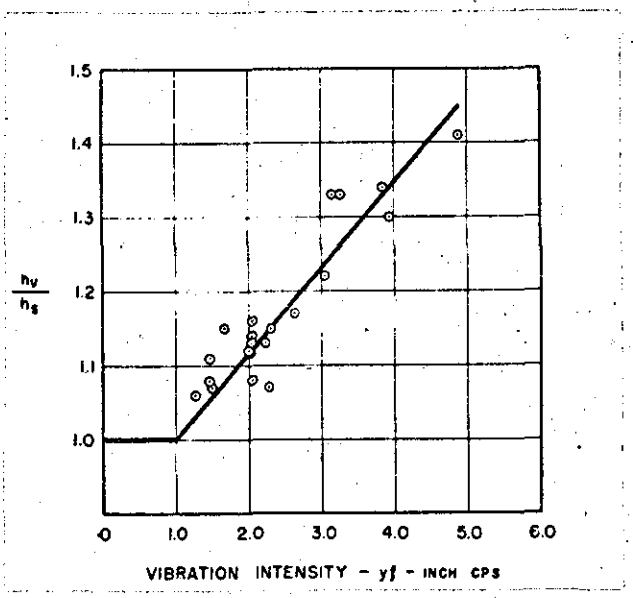

Fig. 4-1 Variation in Heat Transfer Coefficient with Intensity of Oscillation Shine Ref. (30).

Blankenship and Clark (31) carried out a theoretical analysis of the above problem utilising a perturbation solution. The results of this analysis indicated an infinitesimal decrease in the heat transfer coefficient in the presence of oscillation. In an experimental investigation Blankenship and Clark (32) used a six inch square, heated plate which was maintained at temperatures such that the Grashof number varied between 8×10^6 and 21×10^6. The vibration Reynolds number defined as $(a\omega L/\nu)$ was varied between zero and about 8000. Flow visualisation studies were carried out by means of smoke filaments being introduced into the boundary layer. Heat transfer data was recorded at constant heat flux. Their results are shown in figure (4-2)

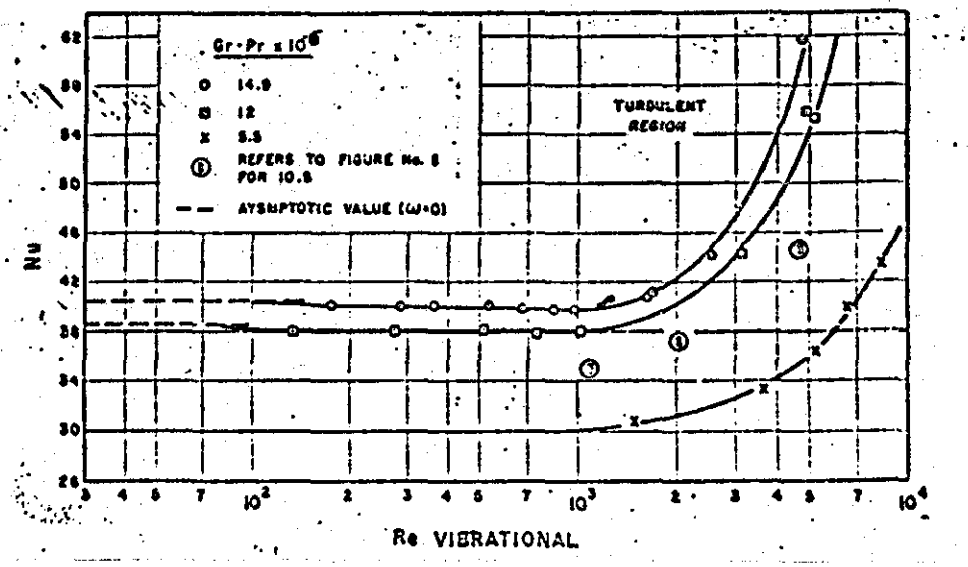

Fig. 4-2 Variation of Nusselt Number with Vibration Reynolds Number Blankenship & Clark Ref. (32)

The authors of this study observed that for intensities of oscillation below a critical value the heat transfer coefficient decreased by a negligible amount from the oscillation free case the flow maintaining its laminar character, this was in accord with the perturbation solution. Above the critical intensity the heat transfer coefficient was observed to increase rapidly with intensity. Flow visualisation studies indicated a transition to turbulence when oscillation intensity was greater than the critical. It was noted that the instability originated in the outer region of the boundary layer and was propagated towards the surface. Instability was always observed to occur at the top of the plate. Smoke studies were used to experimentally determine the conditions under which transition occurred and from this an indifference curve was plotted. The authors noted the difficulty in ascertaining transition from heat transfer data alone. The increased heat transfer coefficient for intensities of oscillation greater than the critical were attributed to the turbulence and greater mixing observed in the boundary layer.

The findings of both groups of workers appear to be substantially the same, the very important point being the cause of earlier transition to turbulent flow brought about by the transverse oscillation of the plate surface.

Because of the evidence of earlier transition to turbulence of the laminar free convective boundary layer on a transversely vibrating plane

surface, it was decided to survey the literature on experimental investigations of transition of laminar free convective boundary layers on vertical surfaces, with the object of setting up a suitable physical model for the mixing coefficient, so that use of the Danckwerts-Mickley model could be extended to problems of vibration induced transition.

5.0 SURVEY OF LITERATURE ON TRANSITION TO TURBULENCE OF FREE CONVECTION BOUNDARY LAYERS ON VERTICAL SURFACES

5.1. Survey of Literature

Early analytical studies of the stability of laminar forced convective flows indicated that the form of the velocity profile had a strong effect on the stability of the flow. Instability was associated with points of inflexion in the laminar boundary layer velocity profile. The laminar free convective boundary layer velocity profile shown in figure (5-1) below has such a point of inflexion in the outer region of the boundary layer, the velocity at this point is $0.683 \cdot \overline{V}_{max.}$ (Ref.33)

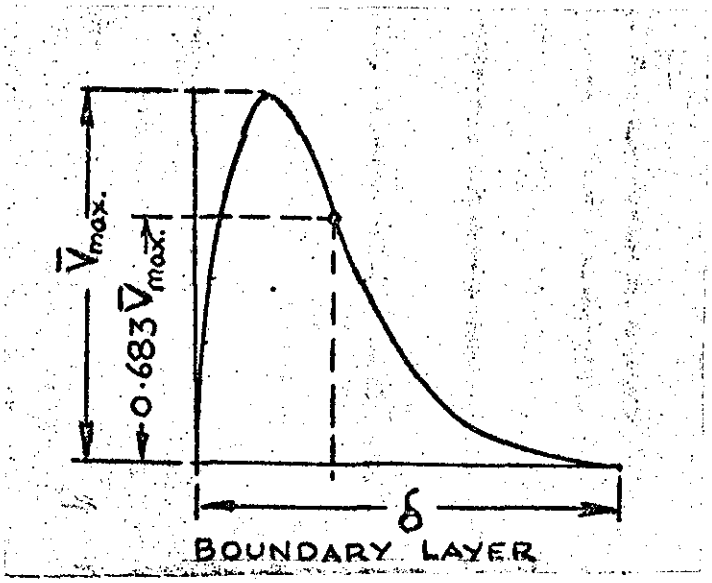

Fig. 5-1 Laminar Free Convective Boundary Layer Velocity Profile

Eckert and Soehnghen (33) conducted the first experiments to investigate the stability of the laminar free convective boundary layer on a vertical heated plate in air. The flow in the boundary layer was visualised by means of a Mach-Zender interferometer. The height of the plate was 36 ins and its temperature was maintained at 15 to 40°F above ambient before allowing it to cool slowly in air.

At a distance of 15 to 20 ins. from the leading edge occasional waves were observed in the outer region of the boundary layer; the occurrence of these waves indicated the boundary layer flow had started to become unstable. The wave length (λ) of these fluctuations was determined as $\lambda = 3.1\delta$ where δ is the boundary layer thickness defined in figure (5-1) above. The wave velocity corresponded closely to that in the laminar boundary layer at the point of inflexion. This is one of the conditions for instability used in the mathematical theory(11). It was observed that the disturbance within the boundary layer which started out with just one wave increased in duration as it travelled down stream by building more waves behind it. At the same time the amplitude of the waves increased in their downstream path until they began to roll up

in the direction opposite to the flow. The velocity and temperature profiles were observed to maintain their laminar character, however, the average heat transfer coefficient was noted to be about 25% higher than for laminar flow. This being attributed to turbulent bursts.

To study transition near the fully developed turbulent region, Eckert and Soehnghen used an enclosed electrically heated plate 36 ins. high at a temperature approximately 50°F above the ambient gas which was Freon. Turbulence fluctuations at high frequency were observed (with magnification) right up to the wall in agreement with forced turbulent flows. The scale of turbulence decreased towards the wall surface, in the inner region of the boundary layer the scale appeared approximately the same as those observed in forced convective flows.

A later combined analytical and experimental study of the problem of laminar free convection boundary layer stability was carried out by Szewczyk (34). His experiments were conducted in water with a heated plate 60 ins. high maintained at a temperature of about 74°F. Flow visualisation was carried out by means of dye injection in the water.

The experimental observations revealed a double row vortex system. Near the wall the dye streak was observed to roll up in a manner similar to that with forced convective flow i.e. inwards towards the wall. Whereas the dye streaks near the outer point of inflexion rolled outwards in the manner observed by Eckert and Soehnghen. The following conclusions were drawn by the author with regard to the experimental observations.

1. The instability due to the outer critical layer - in the region of the point of inflexion - is predominant and sets in first, well in advance of the onset of instability due to the inner layer near the wall.
2. The outer layer vortices completely control the behaviour of the flow development and impress their effect onto the more stable inner layer near the surface, provoking its instability.

The two papers discussed above show clearly that the instability originates in the region of the outer critical layer and is propagated towards the wall surface. These observations agree closely with those of Blankenship and Clark (32), however the critical Grashof number of Eckert's experiment was approximately 4×10^8 compared with Blankenship and Clark's values of Grashof number of about 1.5×10^7.

In the discussion of combustion driven acoustic oscillations a model for the mixing coefficient was postulated from experimental flow visualisation and the resulting expressions for heat transfer tested

against experiment. A similar method is to be developed in the following section utilising the experimental heat transfer measurements of Shine and Blankenship and Clark to test the postulated mixing mechanism.

6.0 APPLICATION OF THE DANCKWERTS-MICKLEY MODEL FOR THE COMPUTATION OF THE HEAT TRANSFER COEFFICIENT FOR PLANE SURFACES IN FREE CONVECTION IN AIR UNDERGOING TRANSVERSE OSCILLATION

6.0. Application of the Danckwerts-Mickley Model to Free Convection from a Plane Surface in Transverse Oscillation

From the foregoing discussion of the literature on plane surfaces in air in free convection undergoing transverse oscillation, and of the instability and transition of laminar free convective boundary layers on vertical surfaces, it is apparent that the outer critical layer in the region of the point of inflexion of the laminar velocity profile is significant. From the earlier discussion in connection with the heat transfer in the presence of combustion driven oscillations, it was found that the postulated mechanism of vibration energy supplementing the friction energy in the turbulent boundary layer, to cause better mixing, gave results which were in accord with experiment. The problem under discussion here is the prediction of the heat transfer coefficient for a plane surface in free convection in air undergoing transverse oscillation with an intensity greater than the critical. It is expected therefore that the mixing coefficient in the presence of oscillations S_v, will have the form

$$S_v \propto \frac{V_v}{L} \quad G_{R_v}{}^{n} \qquad 6.0.1.$$

where V_v is a representative velocity, G_{R_v} is the Grashof number under oscillating conditions; and L is a characteristic length. Here it is assumed that the oscillation energy supplements the energy of the fluid in the critical layer to promote instability and transition to turbulence. Recall the hypothesis of Kline et al (22) in section 3.3. concerning energy supply to the viscous wall region causing instability in the flow in that region.

$$\text{Hence} \quad V_v = \left[(0.683\ V_{max})^2 + (a_{r.m.s.}\omega)^2 \right]^{\frac{1}{2}} \qquad 6.0.2.$$

If it is assumed that, at the point of transition, oscillation does not supplement the energy of the boundary layer in any way, then $V_v = 0.683\ V_{max}$. It is also known that at the point of transition $h_v = h_o$. Therefore from equation 3.2.15, 6.0.1. and 6.0.2. and the above argument

$$\frac{h_v}{h_o} = \left[1 + 2.14 \left(\frac{a_{r.m.s}\,\omega}{V_{max}} \right)^2 \right]^{\frac{1}{4}} \qquad 6.0.3.$$

V_{max} is the maximum velocity in the boundary layer and is evaluated at the top of the plate because transition is first observed at that point. From Schlicting (11) V_{max} may be expressed in terms of the Grashof number and the length of the plate as

$$\frac{\bar{V}_{max}}{x=L} = 0.55 \cdot \frac{G_{R_v}^{\frac{1}{2}} \nu}{L} \qquad 6.0.4.$$

From equations (6.0.3.) and (6.0.4.) and defining a vibration Reynolds number $(a_{r.m.s.} \omega L/\nu)$ = Re vib

$$\frac{h_v}{h_o} = \left[1 + \frac{7.09 \ Re^2_{vib}}{G_{R_v}} \right]^{\frac{1}{4}} \qquad 6.0.5.$$

Equation (6.0.5.) has been derived under the assumption that the temperature difference between the wall surface and the air are identical for oscillatory and non oscillatory conditions. The experimental data of Shine (30) and Blankenship and Clark (32) were obtained under constant heat flux conditions. Therefore equation (6.0.5.) must be corrected for temperature difference before a comparison is made with the experimental data. Under constant heat flux conditions the temperature difference between the surface and air falls with the increasing heat transfer coefficient due to oscillation; therefore equation (6.0.5) is modified to

$$\frac{h_v}{ho} = \left[1 + \frac{7.09 \ Re^2_{vib}}{G_{R_v}} \right]^{\frac{1}{4}} \cdot \left[\frac{G_{R_v}}{G_{R_o}} \right]^{\frac{1}{4}} \qquad 6.0.6.$$

The comparison between equation (6.0.6.) and the experimental data of Shine and Blankenship and Clark is shown in figure (6-1). All properties were evaluated at the mean of the surface and air temperatures.

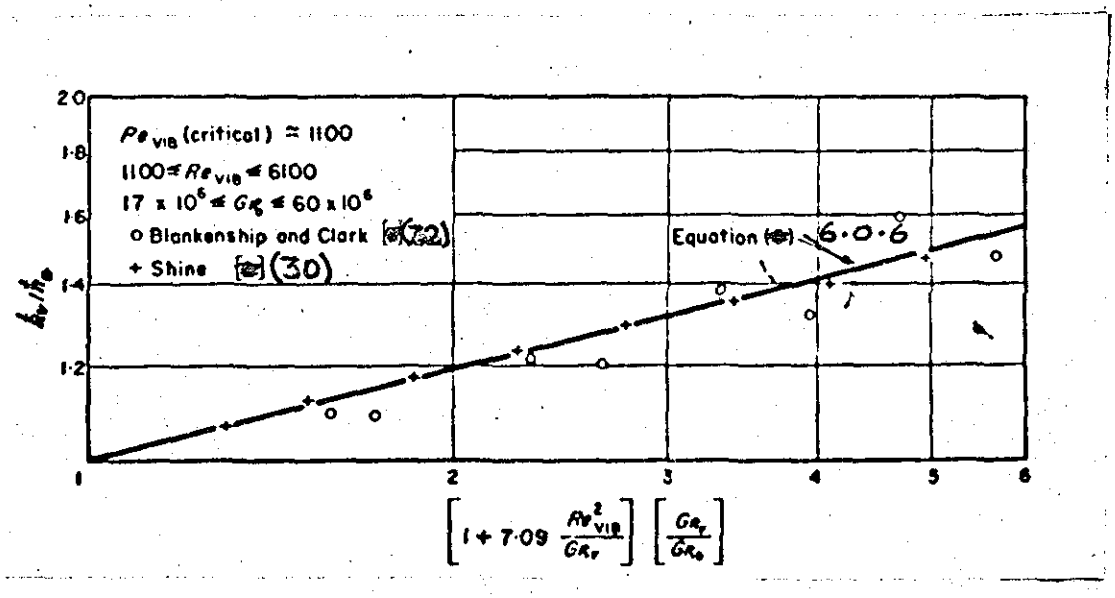

Fig. 6-1 Comparison between Equation 6.0.6 and Data of Ref. (30), (32)

Discussion

From figure (6-1) agreement is seen to exist between prediction and experimental results, though the range of Grashof number is seen to be somewhat limited.

The lower limit of validity of equation (6.0.6.) will depend on the Grashof number in the absence of oscillation and on the critical vibration Reynolds number. The variation of Re^2_{vib}/GR_o with GR_o from the experimental observations of Shine and Blankenship and Clark is shown plotted in figure (6-2).

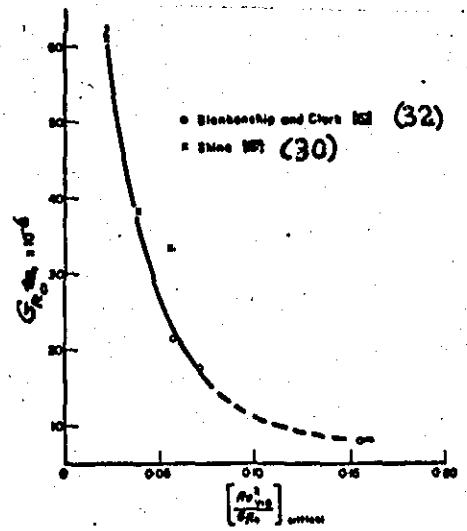

Fig. 6-2 Lower Limit of $\left[\frac{Re^2_{vib}}{GR}\right]$ critical

The upper limit of validity of equation 6.0.6. would occur when vibration forced convection controls. The usual practice in problems of mixed forced and free convection (Kreith 35) is to assume that forced convection controls when the contribution of free convection is less than 10% of the total heat transfer. In the problem under study here it is assumed that forced convection prevails when the heat transfer coefficient due to free convection at the centre of the vertical plate is 10% of the combined total heat transfer coefficient due to forced and free convection at the same point.

For free convection, the local coefficient of heat transfer at the centre of the plate $h_{L/2}$, from Kreith (35) is

$$h_{L/2} \propto 0.214 \cdot G_{R_o}^{\frac{1}{4}} \qquad 6.0.7.$$

For vibration forced convection, assuming laminar flow conditions h_s at the staghation point at the centre of the plate, from Eckert (36) is

$$h_s \propto \left[\frac{a\omega L}{\nu}\right]^{\frac{1}{2}} \qquad 6.0.8.$$

Now, for forced convection to control

$$h_{L/2} = 0.1(h_{L/2} + h_s)$$

$$\therefore \quad \frac{h_s}{h_{L/2}} = 9.0 = \left[\frac{a\omega L}{\nu}\right]^{\frac{1}{2}} \Big/ 0.214 \; G_{R_o}^{\frac{1}{4}}$$

Hence $$\left[\frac{(a_{r.m.s.}\,\omega L)^{\frac{1}{2}}}{G_{R_o}^{\frac{1}{4}}}\right]^4 = (9 \times 0.214)^4 \times 0.5 = \frac{Re^2_{VIB}}{G_{R_o}}$$

$$\therefore \quad \frac{Re^2_{VIB}}{G_{R_o}} \approx 7 \qquad 6.0.9.$$

The range of experimental data, taken by Shine and Blankenship and Clark, did not permit verification of equation 6.0.9.

However, Lowe (37) has conducted experiments with a horizontal cylinder in free convection in air carrying out large amplitude oscillations in a horizontal plane. These experiments on average showed that forced convection occurred when. $\frac{Re^2_{VIB}}{G_{R_o}} \approx 80.$

Using arguments similar to those above for the flat plate but working with the horizontal cylinder geometry, the local free convection heat transfer coefficient at 90° from the bottom of the cylinder according to Hermann (38) is.

$$h_{90^o} \propto 0.39 \, (G_{R_D})^{\frac{1}{4}} \qquad 6.0.10.$$

The stagnation point heat transfer at 90° on the cylinder will correspond to that for the flat plate as given by equation 6.0.8. Therefore, for forced convective conditions to prevail,

$$\frac{Re^2_{VIB}}{G_{R_D}} \approx 76 \qquad 6.0.11.$$

In view of the simplifying assumptions, including the neglect of turbulence, the agreement between 6.0.11. and Lowe's data is adequate. Hence the estimate obtained through 6.0.9. for vibrational induced forced convection would appear reasonable.

The method of defining the mixing coefficient used here would not be expected to hold for $G_{R_o} \geq 1.5 \times 10^8$ as under these conditions a turbulent boundary layer would exist on the stationary plate. In this case, a method similar to that used for combustion driven oscillations would be applicable.

Conclusions

The Danckwerts-Mickley model has been extended to account for vibrational induced turbulence in a free convective boundary layer over a vertical laterally vibrating plane surface. From the experimental observations of Eckert and Soehnghen, Szewezyk, Blankenship and Clark, and Shine, a model for the mixing coefficient S was developed which considered the vibrational energy of the plate to supplement the kinetic energy of the fluid in the outer critical region of the laminar velocity profile, thereby causing transition to turbulence and increased fluid mixing.

Agreement of the developed model with the experimental data of Shine and Blankenship and Clark is good.

7.0 THE EFFECTS OF TRANSVERSE ACOUSTIC AND MECHANICAL OSCILLATIONS ON FREE CONVECTIVE HEAT TRANSFER FROM HEATED CYLINDERS TO AIR.

7.0. The Problem

The transverse oscillation of a circular cylinder in still air, or maintaining a stationary cylinder in a transverse acoustic field, causes a steady isothermal streaming motion of the fluid to be set up about the body, termed Isothermal Streaming. The streaming motion has been shown by Westervelt (39) to be identical for both types of oscillation provided that for the acoustic oscillation the diameter is small compared with the wavelength of sound. This streaming motion results from the interaction between viscous forces and forces resulting from the Reynolds stresses set up by the oscillations in the fluid medium.

In free convection from a heated stationary cylinder to a quiescent fluid medium, the convection flow is dependent on the interaction of buoyancy and viscous forces within the fluid.

The problem under study here would therefore involve an interaction between the forces resulting in Isothermal Streaming and those associated with Free Convection.

7.1. Isothermal Streaming

Schlichting (11) published the first mathematical solution to the problem of isothermal streaming around a circular cylinder, which was in a transverse mode of oscillation in the horizontal plane. Working on the assumption that the amplitude to diameter ratio was much smaller than unity, and that the Reynolds number of the streaming flow $a^2\omega/\nu$ was small, Schlichting used a method of successive approximation to solve the boundary layer equations for the flow. His solution predicted two regions of streaming in each quadrant. In a thin layer - the D.C. boundary layer $\delta_{D.C.}$ or inner layer - next to the cylinder, the streaming motion is along the horizontal diameter towards the cylinder, and away from it along the vertical diameter. In the outer region the streaming flow is towards the cylinder along the vertical diameter, and away from it along the horizontal diameter. This outer vortex system in the absence of confining walls extends to infinity. Schlichting carried out experiments to verify his theory. These experiments confirmed the theory qualitatively and showed that in the presence of the confining walls of the apparatus the outer vortex system is finite in size. The results of Schlichting's theory and experiments are shown in figures (7-1) and (7-2) respectively.

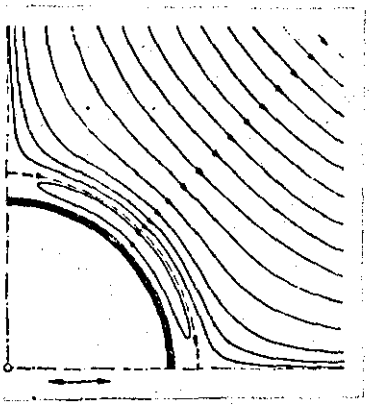

Fig. 7-1 Isothermal Streaming about an Oscillating Cylinder Ref. (11)

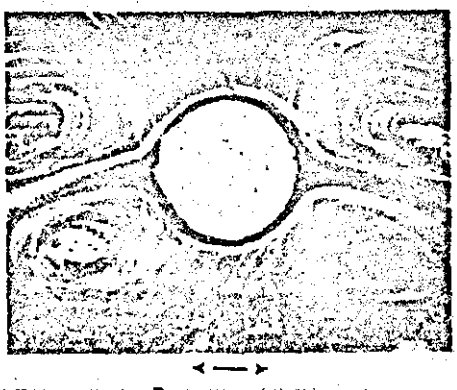

Fig. 7-2 Experimental Study of Ref. (11) Indicating Streaming

Schlichting's analysis gives the following result for the steady streaming flow in the outer region.

$$\bar{V}\ (x,\ y) = 4\ \frac{a^2\omega}{R}\ \sin\left(\frac{x}{R}\right) \cdot \cos\left(\frac{x}{R}\right)\left[\zeta\right] \qquad 7.1.1.$$

where $$\zeta = -\frac{3}{4} + \frac{1}{4}\exp-\left[2\eta\right] + 2\sin\eta\ \exp-\left[\eta\right]$$

$$+\frac{1}{2}\cos\eta\ \exp-\left[\eta\right] - \frac{1}{2}\exp-\left[\eta\right]\left[\cos\eta - \sin\eta\right] \qquad 7.1.2.$$

where $$\eta = y\cdot\sqrt{\frac{\omega}{2\nu}}$$

West (40) oscillated a cylinder of 0.077 cms diameter in air and water. He found that for low frequencies (3-4 c/s) streaming flow was very weak. With increase of amplitude or frequency the streaming flow increased. At a frequency of 550 c/s and amplitude $<$ 0.04 cms, the circulation around the cylinder was as shown in figure (7-3). However, an increase of amplitude to 0.045 cms. caused the streaming pattern to change to that shown in figure (7-4), with the inner region shrinking to the vicinity of the wall of the cylinder, around it was a vigorous circulation in the opposite sense. Further increase in the amplitude of oscillation caused the inner layer to become even smaller. Similar results were obtained by West for the case of a stationary

cylinder with acoustic oscillations set up in the fluid by use of a Kundt's tube arrangement.

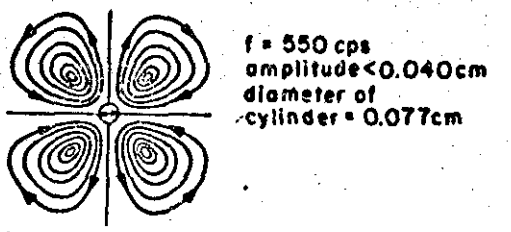

Streaming around a vibrating cylinder (after West)

Fig. 7-3

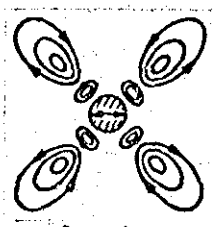

Streaming around a vibrating cylinder (after West)

Fig. 7-4

Holtsmark et al (41) conducted an extensive theoretical and experimental investigation of the problem of streaming past a cylinder which was located in an acoustic field. Their investigation involved the solutions of the Navier- Stokes equations for the flow, under the assumption that the cylinder diameter was small in comparison with the half wavelength of sound. The results obtained by these workers also predicted an inner and outer streaming flow, but the inner region thickness - $\delta_{D.C.}$ - was found to be dependent on the cylinder diameter and thicker than the D.C. layer predicted by Schlichting's theory, which showed $\delta_{D.C.}$ to be independent of diameter. Fig. (7-5) shows these results along with those from experiment.

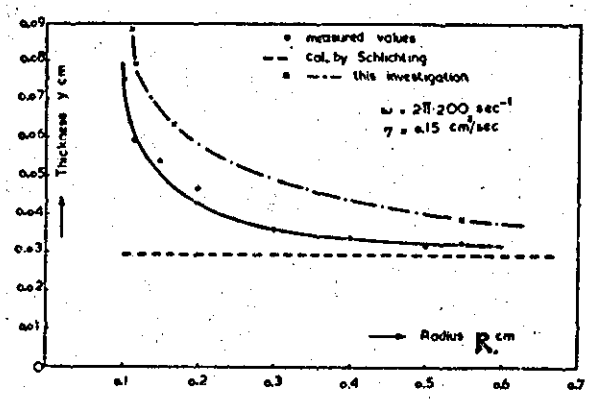

Experimental and theoretical values of the thickness of the inner vortex system. Velocity amplitude U_0=8 cm/sec, frequency 200 cps and kinematic viscosity η=0.15 cm²/sec (air temp. 20°C).

Fig 7-5 Ref. (41)

It will be noted that as the cylinder diameter increases the value of $\delta_{D.C.}$ from experiment and Schlichting's theory approach each other closely.

Raney et al (42) in a combined theoretical and experimental study showed the dependence of $\delta_{D.C.}$ on the so called A.C. or acoustic boundary layer thickness $\delta_{A.C.}$ (The A.C. boundary layer thickness arises in the study of unsteady boundary layer problems, it is defined as $\delta_{A.C.} = \left[\nu/\omega\right]^{1/2}$ The experimental plot of $\delta_{D.C.}/R$ versus $R/\delta_{A.C.}$ is shown in figure (7-6), which is valid for $a/R \leq 0.5$. Under these conditions $\delta_{D.C.}$ is independent of a/R. At higher values of a/R the inner streaming motion shrinks (as observed by West). It was found that the region $5 \leq R/\delta_{A.C.} \leq 12$ was a transition regime from inner streaming in the D.C. layer to outer streaming.

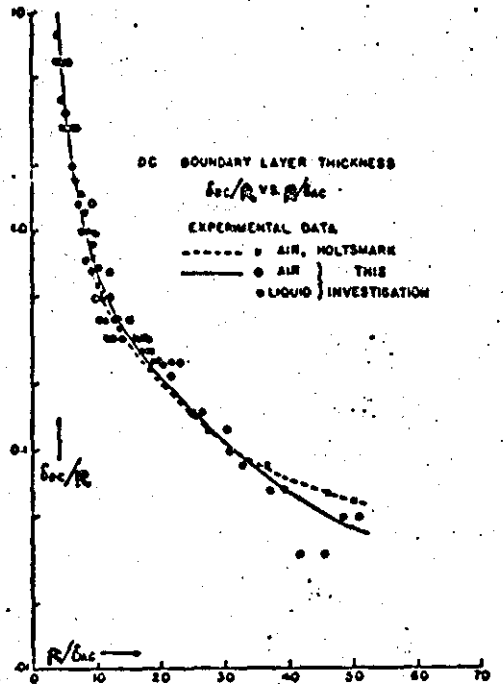

Experimental curves showing the existence of a universal curve for the *DC* boundary-layer thickness.

Fig. 7-6 Ref. (42)

From the foregoing discussion it is seen that West's results for oscillations with amplitude $<$ 0.04 cm at 550 c/s is a case of predominantly inner streaming. Increasing the amplitude so that $a/R > 0.5$ caused a shrinkage of the inner streaming motion and a prominent outer streaming flow. Schlichting's results fall in the outer streaming category.

Stuart (43) in a mathematical study of the problem pointed out that Schlichting's theory was valid only for low streaming Reynolds numbers. He suggested that when the streaming Reynolds number is large an outer boundary layer is formed over the D.C. layer. In this layer the outer streaming velocity gradually reduces to zero at the edge furthermost from the cylinder. This layer of thickness δ_o has the magnitude $\frac{D}{a} \cdot \delta_{A.C.}$, since the D.C. layer is thinner than $\delta_{A.C.}$; and $\delta_o \gg \delta_{D.C.}$ but $\delta_o < D$. Stuart's analysis was based on the assumption of small a/D and small diameter to wavelength ratio. The theory was considered to be in qualitative agreement with Schlichting's experiments.

Summary

1. Acoustic and Mechanical oscillation produce the same streaming flow provided the cylinder diameter is small compared with the wavelength of sound, and $\frac{a}{D} < .3$ Stuart (43).
2. Oscillation produces streaming in two regions a D.C. region near the cylinder surface and counter rotating outer streaming further away from the cylinder.
3. For $a/R \leq 0.5$ small diameter cylinders - such as wires give a predominantly inner streaming flow, as diameter increases shift from inner to outer streaming flow, inner streaming flow shrinks towards cylinder surface.
4. Shrinkage of inner D.C. layer produces vigorous chaotic motion near the wall region - which has been likened by some to turbulence.
5. For $a/R \geq 0.5$ flow is predominately outer streaming.

7.2. Free Convection from a heated horizontal cylinder to air

The first theoretical study of this problem was that of Hermann (38) who studied the problem of free convection from horizontal cylinders to diatomic gases. Hermann applied boundary layer theory to the solution of the problem to obtain an expression for the average heat transfer coefficient. Expressions were also obtained for local details such as the temperature distribution and the velocity distribution at any azimuthal position. Hermann also carried out an extensive comparison of the theoretical results with experiment, the agreement being good. The validity of the boundary layer analysis was estimated by Hermann to hold for Grashof Number between 10^4 and 10^8.

The universal velocity profile for the cylindrical geometry is similar to that for the flat plate case discussed earlier, with the point of inflexion in the outer region of the boundary layer occurring at $0.683\ \bar{V}_{max}$. Hermann obtained the following expression for $\bar{V}_{max}$ based on Grashof number evaluated with the cylinder diameter.

$$\bar{V}_{max} = \frac{0.725}{\sqrt{2}} f(x)g(x) \frac{G_R^{\frac{1}{2}} \nu}{D} \qquad 7.2.1.$$

where $f(x)g(x)$ is the product of two azimuthal functions and is shown plotted in figure (7-7). Zero being the lower and 180° the upper stagnation points on the cylinder.

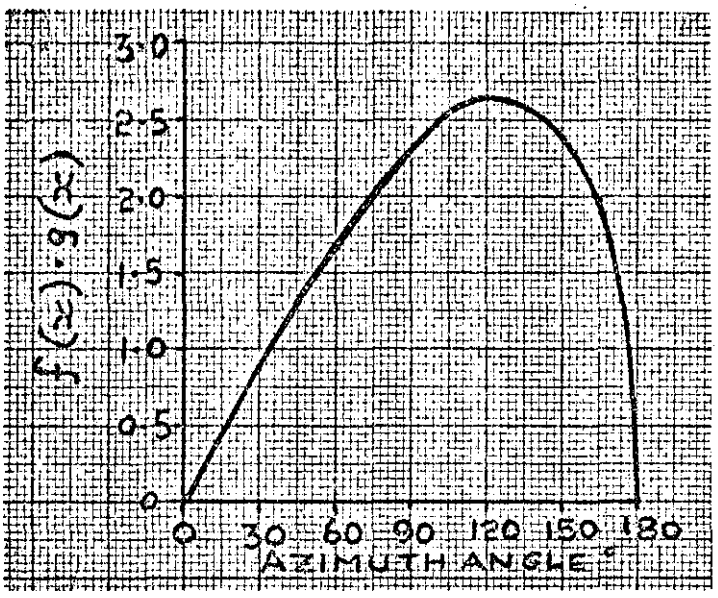

Fig. 7-7 f(x)g(x) versus angular position Hermann Ref. (38)

7.3. Free Convection from heated horizontal cylinders in air in the presence of acoustic or mechanical oscillation

In this section only those papers relating to free convection from cylinders in air will be discussed. The problem of heat transfer from wires will not be discussed - i.e. problems where the inner streaming is of importance.

Kubanskii (44) appears to have been the first investigator to study the effects of acoustic oscillation on free convection from heated horizontal cylinders in air. In his experimental study, he arranged for the sound field to be parallel to the axis of the cylinder which was 2.4 cm in diameter. In a subsequent theoretical study of this problem Kubanskii made the assumption that the effect of sound and natural convection upon the Nusselt number were additive, good agreement was obtained between theory and experiment. Kubanskii verified the validity of his assumption by a flow visualisation study which showed that the free convective flow field was distorted by the acoustic streaming flow.

Fand and Kaye (45) carried out an extensive experimental investigation of the influence of transverse acoustic oscillations upon free convection from a horizontal $\frac{3}{4}$ ins. diameter cylinder in air. The sound field was in a horizontal plane, and the acoustic system tuned to produce a stationary field, the cylinder was located at a velocity antinode. The range of experimental variables covered were:

$1100 \leq f \leq 6120$ c/s; $\quad 0 \leq \Delta\theta \leq 250^{\circ}F$

$0 \leq$ S.P.L. ≤ 151 db;

The experimental data showed that a critical sound pressure level existed below which the influence of sound was negligible, and above which the rate of heat transfer was increased by sound (Critical S.P.L. $\approx$ 140 db). The data also showed that for sound waves with the ratio, half wavelength to cylinder diameter ≥ 6.0 the heat transfer coefficient was a function of the temperature difference between the cylinder and the air, and of the intensity of oscillation, where the intensity of oscillation is defined as the product of amplitude and frequency (a f). Their experimental results are shown in figure (7-8) for cases where the ratio half wavelength to diameter ≥ 6.0. The form of the curves shown are typical for all frequencies. It should be noted that extrapolated data to 400°F are shown in this figure.

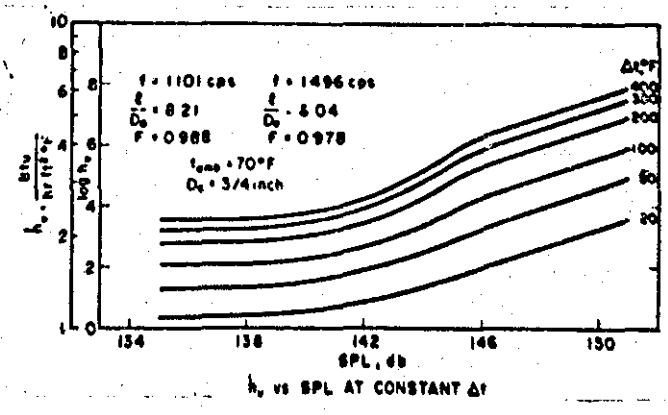

Fig. 7-8 The Influence of Sound on Free Convection Heat Transfer From a Horizontal Cylinder Fand and Kaye Ref. (45).

In order to gain an insight into the physical mechanism of which caused the rate of heat transfer to increase in the presence of sound Fand and Kaye (46) performed flow visualisation studies, using smoke as the indicating medium. These tests were carried out with $20 \leq \Delta\theta \leq 250^{\circ}F$; $1100 \leq f \leq 4872$ C/s; $0 \leq$ S.P.L. ≤ 151 db. Working with constant frequencies and increasing the sound intensity, a critical sound intensity was noted at which a streaming motion began to develop, this established itself at a higher intensity, and consisted of the periodic growth and collapse of two vortices centred in the two quadrants above the cylinder. The growth and collapse

of the vortices alternated between each quadrant, the sense of rotation of the vortices being towards the cylinder along the vertical diameter and away from it along the horizontal diameter. Further increases in intensity caused the vortices to increase in size, but the basic character of the flow remained unaltered. It was found that with the ratio of half wavelength to diameter of cylinder $\geq$ 6.0 the development and size of the vortices were independent of frequency of oscillation, for this ratio less than six and a constant oscillation intensity, it was found that the vortices decreased in size with increase in frequency.

The phenomenon of alternate growth and collapse of vortices was termed "Thermo-acoustic Streaming" by the Authors.

For the half wavelength to diameter ratio $\geq$ 6.0 Fand and Kaye found that the oscillation, intensity for fully developed thermo-acoustic streaming was $af = 0.71$ ft/sec (or S.P.L. = 146 db). For $af \geq 0.71$ ft/sec $\Delta\theta \leq 400^{\circ}F$. Fand and Kaye found the heat transfer coefficient to have the form

$$h_v = 0.722 \left[\Delta\theta \ (af)^2 F \right]^{1/3} \qquad 7.3.1.$$

where F is a geometrical weighting factor, such that the product $(af)^2F$ is proportional to the mean kinetic energy density in the standing wave averaged over the diameter of the test cylinder, for large values of half wavelength to diameter ratio $F \rightarrow 1.0$.

Fand et al (47) carried out a further experimental test for conditions under which equation (7.3.1.) was valid; to determine the variation of local heat transfer coefficient about the cylinder. Results were obtained for only a single set of conditions which were:- $\Delta\theta = 169^{\circ}F$; $f = 1500$ c/s; S.P.L. = 146 db. the results of this test are shown in figure (7-9)

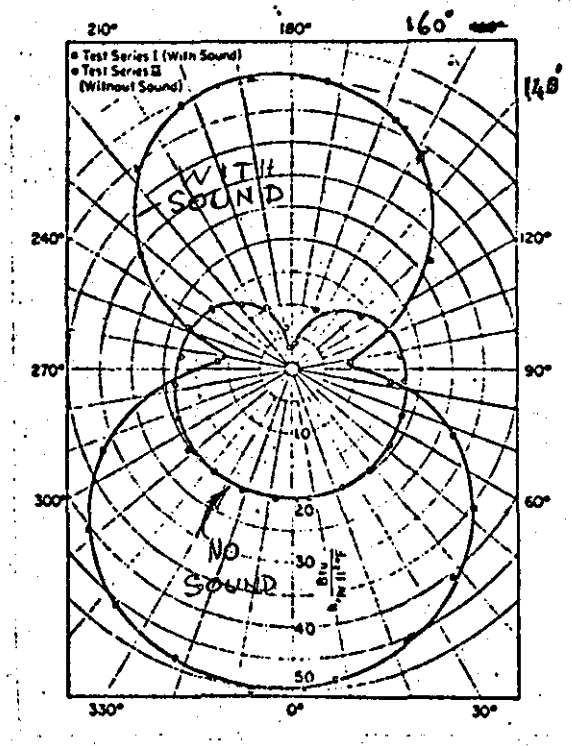

Fig. 7-9 Local Heat Transfer Coefficient Around a Heated Horizontal Cylinder with and without Oscillation. Fand et al Ref. (47)

Figure (7-9) shows that the effect of acoustic oscillation with "thermoacoustic streaming" is to produce large increases on both upper and lower surfaces of the cylinder. Free convective results in absence of acoustic oscillation are shown for the sake of comparison. The increases on the upper surface are attributed to "thermoacoustic streaming" while that on the lower surface is attributed to changes in the laminar boundary layer temperature profile because of unsteadiness induced in the boundary layer.

Fand and Peebles ((48)) have shown by an experiment conducted with a $\frac{7}{8}$ ins. diameter heated horizontal cylinder subjected to mechanical oscillations in a horizontal plane, that equation (7.3.1.) is valid over a wide range of frequency. The results of these tests are shown in figure (7-10).

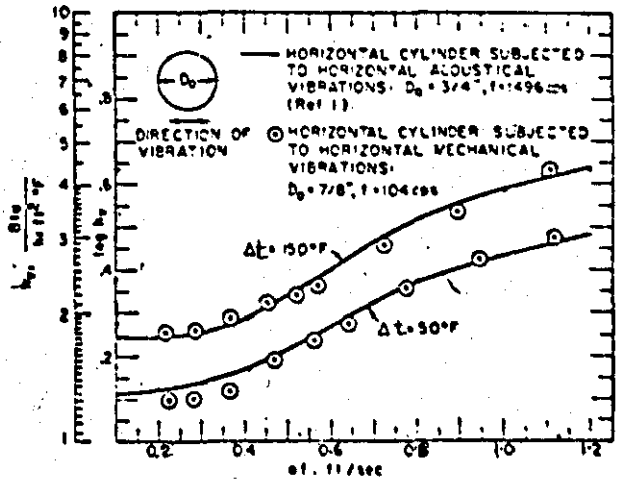

Fig. 7-10 Comparison of the Effects of Mechanical and Acoustic oscillations in a Horizontal Plane on Free Convective Heat Transfer from Cylinders Ref.(48).

Flow visualisation studies carried out for this series of tests, revealed a flow field closely resembling thermoacoustic streaming. These tests showed that with the effect of free convection superimposed on that of streaming; the flow field and average heat transfer for mechanical oscillations and acoustic oscillations in which the halfwavelength to diameter ratio $\geq$ 6.0 are the same in either case.

The same apparatus as above was used by Fand and Kaye (49) to study the effects of mechanical oscillations in the vertical plane on free convection to air. The range of experimental variables covered in these tests were: $54 \leq f \leq 225$ c/s. $25 \leq \Delta\theta \leq 185^{\circ}F$; $0 \leq a \leq 0.16$ ins; $0 \leq af \leq 1.22$ft/sec.

These experiments revealed that intensity and temperature difference were the two controlling variables. For intensities of vibration less than 0.3 ft/sec, the influence of oscillation was negligible. Above this "critical" intensity the effect of oscillation was to increase the average heat transfer coefficient significantly. Experimental results are shown in figure (7-11)

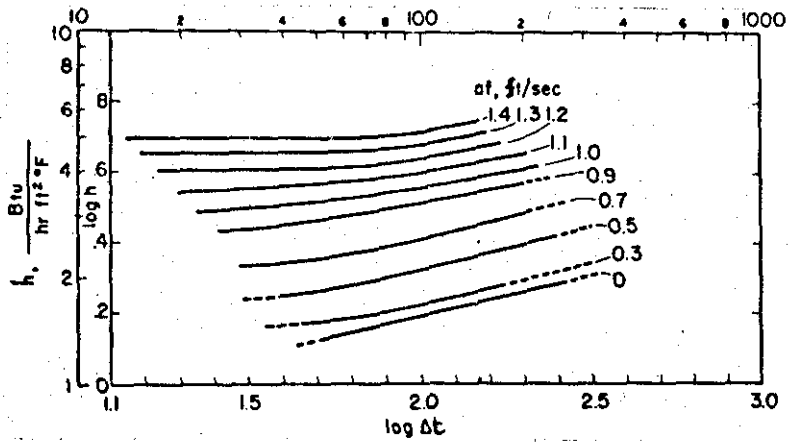

Fig. 7-11 Effect of Mechanical Oscillations in the Vertical Plane on free Convection from a Cylinder Ref. (49).

Flow visualisation indicated that the flow mechanism which caused the increases in average heat transfer coefficient was vibrationally induced turbulence. However, the authors are not explicit in discussing the development of the turbulence with increasing intensity of oscillation above the critical intensity. This type of flow was considered to differ radically from "thermoacoustic streaming". In the experimental region defined by $\Delta\theta \geq 100^{\circ}F$ and $af \geq 0.9$ ft/sec the following empirical equation was developed for the heat transfer coefficient.

$$h_v = 0.847 \cdot \left[\frac{\Delta\theta}{D}\right]^{0.2} af \qquad (7.3.2.)$$

It was suggested that the vibration intensity af = 0.9 ft/sec corresponded to fully developed turbulent flow in the neighbourhood of the cylinder.

Westervelt (50) put forward a suggestion that the effect of acoustic oscillation on heat transfer was mainly the result of modification of the D.C. layer, which occurs when the amplitude of acoustic oscillation exceeds in magnitude $\delta_{A.C.}$ Westervelt argued that the collapse of the inner layer and the vigorous and chaotic motion close to the wall region causes the increase in the observed heat transfer. By using $\frac{a}{\delta_{A.C.}} \approx 1$ as the criterion for the increase in heat transfer, Westervelt was able to obtain an expression for critical acoustic intensity as a function of frequency. This expression predicted values of critical intensity close to those obtained by Fand and Kaye (45) in their experiments.

Lowe (37) in his thesis reviewed the work of Fand and his co-workers, and extended the range of experiments with mechanical oscillations by working in the frequency range of 27 to 54 c/s. with horizontal oscillations and at 29 and 46.8 c/s with vertical oscillations. These experiments were conducted with a 5/8 in. diameter cylinder with vibration amplitude varying from 0-0.325 ins. for both directions of oscillation and temperature differences in the range. $20 \leq \Delta\theta \leq 200^{o}F$. An interesting feature of this work was that the author obtained a correlation for his data in terms of $\frac{a}{\delta_{A.C.}}$ shown in figure (7-12). Lowe found that the effect of oscillation in either plane on heat transfer was negligible when $\frac{a}{\delta_{A.C.}} \lesssim 10.0$. His results also displayed an effect of frequency on the heat transfer coefficient. The low frequencies producing larger values of heat transfer coefficient for the same value of Vibration Reynolds number, (where Vibration Reynolds number is equal to $\frac{4a\,f\,D}{\nu}$ which for constant temperature difference is proportional to the intensity of oscillation).

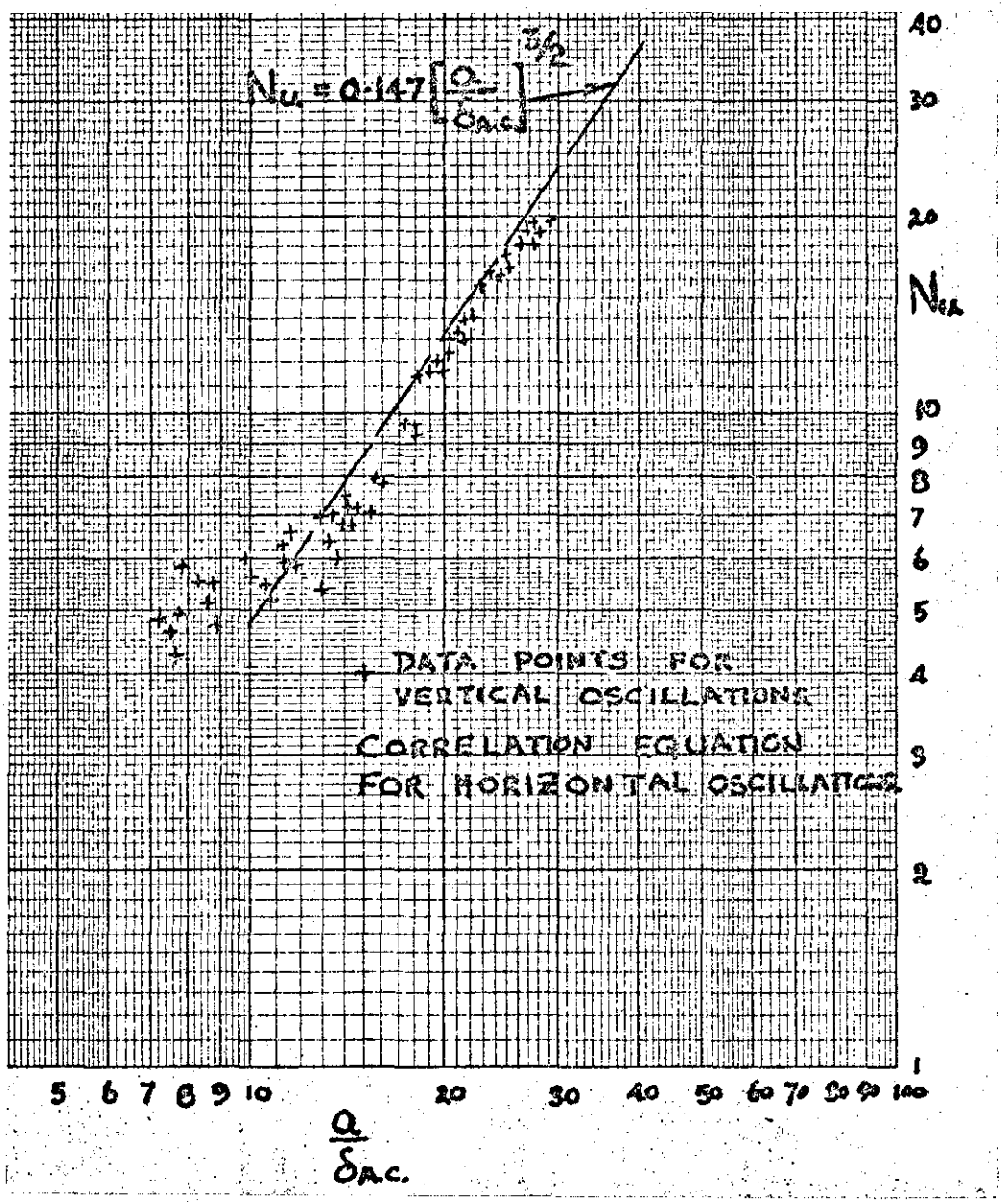

Fig. 7-12 The Effect of Mechanical Oscillation in the Vertical and Horizontal Plane on Free Convection from a Cylinder. Ref (37).

Heat transfer rates with horizontal oscillations were slightly higher than those with vertical oscillation at the same conditions of temperature difference and oscillation intensity.

For horizontal oscillations a smoke study revealed a "thermoacoustic streaming" system as with the experiments of Fand and Kaye. The smoke study with vertical oscillations revealed

"vibration induced turbulence". Instability in the flow was first observed at the top of the cylinder at the critical oscillation intensity corresponding to $\frac{a}{\delta_{A.C.}} = 10$. With further increase of oscillation intensity the instability developed to turbulence which moved upstream towards the bottom of the cylinder, until at high intensities of oscillation a fully turbulent field surrounded the oscillating cylinder. For values of $\frac{a}{\delta_{A.C.}}$ just below the critical value of 10; a slight decrease of the average heat transfer coefficient compared with that for free convection was noted, this amounted to about 3 - 4 %.

For $a/\delta_{A.C.} > 16$ the author obtained the correlation

$$N_{u_v} = 0.146 \left[\frac{a}{\delta_{A.C.}}\right]^{3/2} \qquad 7.3.3.$$

In the region where oscillation and free convective effects are both significant - in the range $12 \leq a/\delta_{A.C.} \leq 16$,

Lowe obtained the correlation .

$$\frac{h_v}{h_o} = 0.31 \frac{\left[a/\delta_{A.C.}\right]^{3/2}}{(G_R \; P_R)^{\frac{1}{4}}} \qquad 7.3.4.$$

Richardson (51) correlated the work of Fand and Kaye (45) in the frequency range $1100 \leq f \leq 3378$ c/s with $50 \leq \Delta\theta \leq 150^{\circ}F$. The results were correlated in terms of a Reynolds number based on the streaming velocity and the cylinder diameter, a correction on the Nusselt number was incorporated to allow for low Grashof number. The correlation had the form

$$N_c = \frac{N_u}{G_R^{\frac{1}{4}}\left[1 + 1.62\, G_R^{-\frac{1}{4}}\right]} = 0.372 \cdot \left[1 + B\,\frac{R_e^2}{G_R}\right]^{\frac{1}{4}} \qquad 7.3.5.$$

where B is a function of G_R and f

The final correlation had the form

$$N_c = 0.372 \left[1 + 29\, G\, (a\, f)^4\right]^{\frac{1}{4}} \qquad 7.3.6$$

where $G = \left[1 + (49)^{10}\,(1 - F)^{10}\right]^{1/10}$ where F is the weighting factor defined by Fand and Kaye (45).

In a later paper Lee and Richardson (52) discussed some experiments with free convection from a heated $\frac{3}{4}$ ins. dia. horizontal cylinder located at a velocity antinode of a transverse standing sound field in the horizontal plane. These experiments were conducted at 672 and 645 c/s and $\Delta\theta \approx 100^{\circ}F$. The object was to obtain information at frequencies between the 104 and 1101 c/s data of Fand and his co-workers. Lee and Richardson correlated their data with that of Fand and Peebles (48) for 104 c/s mechanical oscillations, using a correlation equation of the same form as equation (7.3.5.). Flow visualisation studies with a modified Schlieren system showed that before the critical intensity was reached an appreciable change in local effects occurred. These cancelled each other out so as to give approximately constant values of average heat transfer coefficient. Their results showed that above 135 db sound intensity the convective plume above the cylinder was split and moved progressively down towards the horizontal diameter with increasing intensity. It was this elimination of the regions of reduced heat transfer at the top of the cylinder that contributed to increases in heat transfer along with increases noted because of changes in the boundary layer over the lower portion of the cylinder, which were discussed by Fand and Kaye (46). The authors suggested that the modification of the flow pattern is qualitatively consistent with a superposition of the acoustic streaming field and that due to free convection.

Richardson (53) described some exploratory experiments conducted with free convection from a heated 1.83 ins. diameter horizontal cylinder located in a standing sound field in the vertical plane. Flow visualisation was conducted with a modified Schlieren system. The main conclusions of this paper are:-

(1) Local changes in heat transfer were observed that were about 5 times the average heat transfer; these local changes occurred at sound intensities below those at which any changes in average heat transfer were noted. The nett effect of these local changes was to cancel each other out and leave no change in the average heat transfer.

(2) When local effects developed initially, they had the opposite directions at the same azimuthal positions for vertical and horizontal acoustic propagation.

(3) With sufficiently intense vertical sound fields, the boundary layer on the bottom of the cylinder thickens, becomes unstable and finally bubbles up repeatedly into the top convective plume. The initial thickening of the boundary layer causes a decrease in the average heat transfer coefficient of about 3 - 20%.

(4) The distribution of initial local effects is qualitatively consistent with the superposition of isothermal acoustic streaming on the free convective flow.

The interesting observation here is the drop in average heat transfer coefficient prior to the bubbling motion. This is in accord with Lowe's observations. With the smoke visualisation used by Lowe the bubbling motion into the convective plume appeared as an instability at the top of the cylinder.

Richardson (54) carried out an extensive classification and theoretical study of the problem of acoustic and mechanical oscillations on free convection from a heated horizontal cylinder. Figure (7-13) is the classification according to Richardson for experiments with air; the area covered by Lowe's experiments have been included in this diagram. This classification could be made from the work of Raney et al (42).

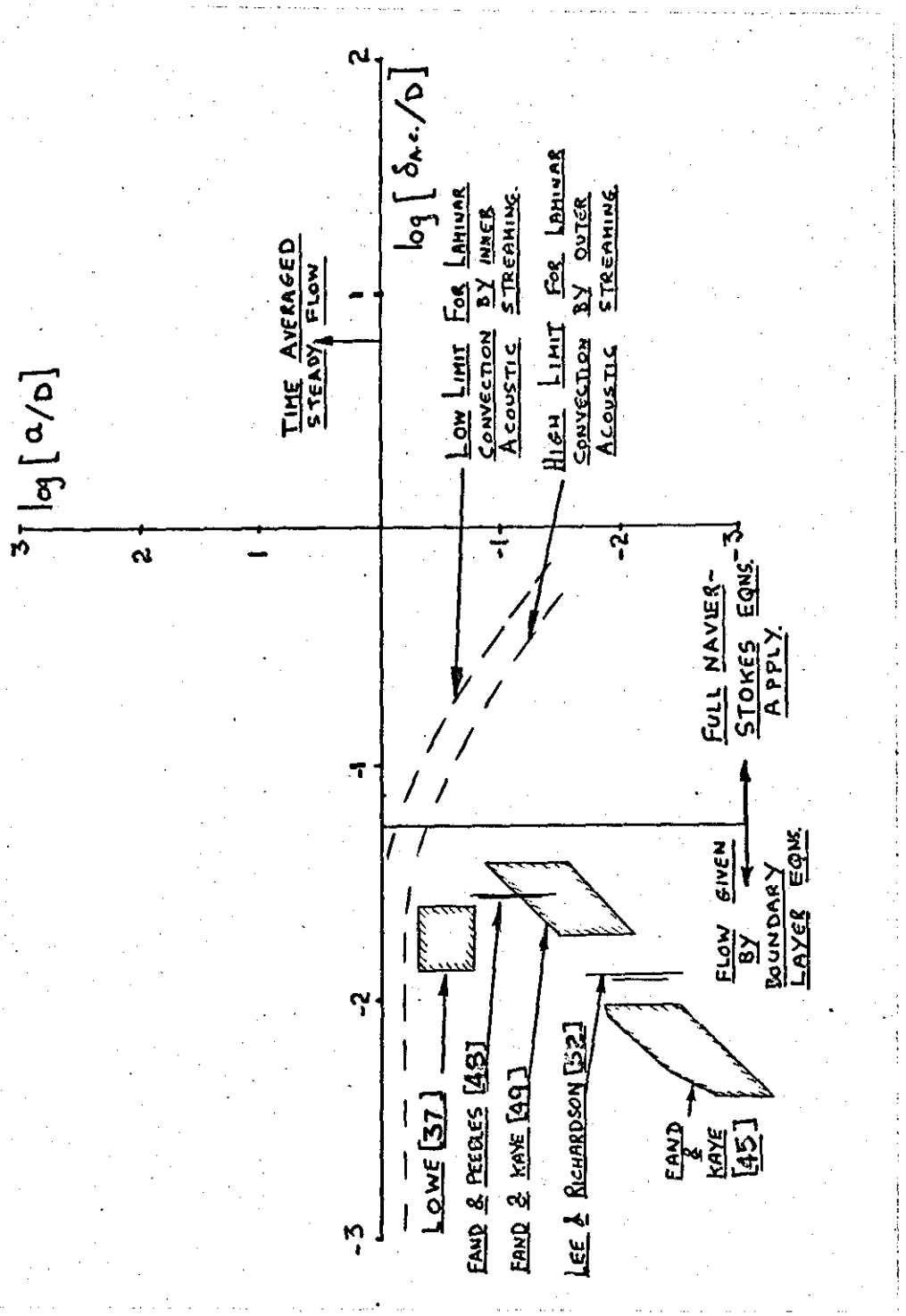

Fig. 7-13 Classification of Work on Free Convection in the Presence of Oscillation. Richardson Ref. (54).

The theoretical study carried out by Richardson involved obtaining asymptotic solutions to the problem of free convection from cylinders in the presence of transverse oscillations as the Grashof Number $G_R \rightarrow 0$.

The outer streaming flow case will be considered here since it is the problem under study. Richardson considered two cases of outer streaming. The first with small streaming Reynolds number; utilised the results of Schlichting's (11) boundary layer analysis to describe the velocity field when $G_R \rightarrow 0$. The second case was that for large streaming Reynolds numbers, which utilised Stuarts analysis (43) to describe the velocity field as $G_R \rightarrow 0$. To account for thermal transport Richardson considered the two further asymptotic solutions as Prandtl number $P_R \rightarrow 0$ and $P_R \rightarrow \infty$; from order of magnitude considerations from the Energy Equation and the Navier - Stokes equations it may be shown that the ratio of the thermal boundary layer thickness δ_T to the hydrodynamic boundary layer thickness is equal to $1/P_R^{\frac{1}{2}}$, it is expected that a similar relationship between the hydrodynamic boundary layer and thermal boundary layer exists in streaming flow. The characteristic hydrodynamic boundary layer thickness in an unsteady flow is $\delta_{A.C.}$ hence

$$\delta_T = \frac{\delta_{A.C.}}{P_R^{\frac{1}{2}}} \qquad 7.3.7.$$

In the limit as $P_R \rightarrow 0$ we see that $\delta_T \gg \delta_{A.C.}$ the above equation (7.3.7.) is valid for the case of small streaming Reynolds number, therefore Schlichting's results from boundary layer analysis hold. Using techniques appropriate to $P_R = 0$ for the conduction thickness k/h and Schlichting's results for the flow field, Richardson obtained an expression for the local heat transfer coefficient which gave a "figure of eight" distribution (recall figure (7-9)). This figure of eight is rotated through $\pi/2$ when the direction of oscillation is changed from the horizontal to the vertical plane. The average coefficient of heat transfer for either plane of oscillation was found to be

$$\frac{Nu}{Re_s^{\frac{1}{2}} P_R^{\frac{1}{2}}} = 1.76 \qquad 7.3.8.$$

where Re_s is the streaming Reynolds number $\frac{a^2\omega}{\nu}$ The analysis for outer streaming for $P_R \rightarrow 0$ neglects all details of the D.C. boundary layer. However, as the streaming Reynolds number increases and h increases the conduction thickness is reduced, and more resistance to thermal transport is offered by the D.C. layer. Richardson corrected for this effect by considering the thermal resistances of the D.C. layer and the conduction thickness to be in series. He found that for cases where P_R is small - as for air - the correction factor would be small.

For the case of outer streaming at large Reynolds numbers Richardson used the results of Stuart for the velocity field to obtain the following expression as the upper limit for heat transfer when the streaming Reynolds number is large and $P_R = 0.72$

$$Nu \quad R \left[1 + 0.95 \cdot \frac{a}{D}\right] \Big/ R_{osc} \left[\frac{3\nu}{\omega}\right]^{\frac{1}{2}} P_R^{\frac{1}{2}} = 0.484 \qquad 7.3.9.$$

where $R_{osc} = \frac{a\,\omega\,D}{\sqrt{2}\,\nu}$

Re-arranging (7.3.9.) in terms of the streaming Reynolds number Re_s.

$$\frac{Nu \left[1 + 0.95 \cdot \frac{a}{D}\right]}{Re_s^{\frac{1}{2}} \cdot P_R^{\frac{1}{2}}} = 1.185 \qquad 7.3.10.$$

Richardson compared the available experimental results with prediction; this was carried out by plotting the left hand side of equations (7.3.8.) and (7.3.9.) against G_R/Re^2_{osc} and extrapolating to a zero value of G_R/Re^2_{osc}, to see if the intercept on the ordinate corresponded to the numerical value on the right hand side of these equations. Good agreement was found for the low streaming Reynolds number case, but for the large Reynolds number case the experimental data extrapolated about 30 - 40% below the value of 0.484 predicted by equation (7.3.9.), for oscillation frequencies of the order of 50 c/s.

To account for the effects of combined free convection and streaming Richardson assumed a simple superposition to exist as a first order initial influence effect, however, comparison with experiment did not show close agreement. The analysis showed that at small values of the parameter $\epsilon = 4\,Re_s/G_R^{\frac{1}{2}}$ the heat transfer is a linear function of ϵ. The final topic of importance here which was discussed by Richardson concered separation.

He found separation for the horizontal oscillation case to first occur around 135°; this was obtained by matching the velocities from the acoustic field with those for the convective field at the same distance from the cylinder. The result of 135° has been observed to be in approximate agreement with experiment. For the case of vertical oscillation it was concluded that a recirculating flow between 0° and 45° occurred this was deduced from experimental results.

Summary

An important feature of the work surveyed is the complementary nature of the results with acoustic and mechanical oscillation, for either plane of oscillation.

The results of Fand and Kaye (45) and Lee and Richardson (52) with horizontal acoustic oscillations and those of Fand and Peebles (48) and Lowe (37) with horizontal mechanical oscillations all displayed the same basic flow mechanism above the critical intensity. Fand and Kaye's (45) experiments with acoustic oscillation with the half wavelength to diameter ratio ≤ 6 show a strong effect of frequency (or wavelength). The effect of frequency was also noted in the low frequency oscillations of Lowe.

The visual observations of Richardson (53) and Lowe (37) for acoustic and mechanical oscillations in the vertical plane, show again the results being complementary as for the horizontal oscillations; more important, the results show that beyond the critical condition turbulence develops on the upper half of the cylinder. If it is recalled that for horizontal oscillations the large disturbance to flow was initiated on the upper half of the cylinder, the possibility exists of setting up a common analysis to calculate average heat transfer from a cylinder in the presence of oscillation. Further strength to this argument is given by Lowe's observations that there was little difference in the average heat transfer coefficients when the plane of oscillation was either vertical or horizontal.

7.4. Discussion

In attempting the problem of predicting the heat transfer from a heated cylinder in free convection in the presence of acoustic or mechanical oscillation, where the plane of oscillation is either horizontal or vertical, and the intensity such that conditions of fully developed turbulence or vortex streaming exist. A common analysis cannot be made by trying to specify local conditions of the

temperature and flow fields and by integrating these obtain the desired average effect. This fails because the details of the flow vary for each case - other than for the asymptotic case as $G_R \rightarrow 0$ discussed by Richardson (54).

An analysis of local conditions for each plane of oscillation could be attempted; but, as pointed out by Richardson (54), it is unlikely that a satisfactory analysis can be made, other than in the initial influence case.

Here the approach to be adopted is semi-empirical, in that from observed facts certain parameters will be chosen to characterise the flow, such as certain velocities and lengths. A mixing mechanism will be postulated and, from this, an expression for average heat transfer set up. The hypothesis will then be tested against experiments discussed in this section.

8.0 APPLICATION OF THE DANCKWERTS MICKLEY MODEL FOR THE COMPUTATION OF HEAT TRANSFER COEFFICIENT FOR HORIZONTAL CYLINDERS IN FREE CONVECTION IN AIR IN THE PRESENCE OF ACOUSTIC OR MECHANICAL OSCILLATIONS

8.1. The Mixing Model

The experimental observations of Fand and his co-workers (45-49) on free convection from heated horizontal cylinders in air, which are subjected to mechanical or acoustic oscillation in a horizontal plane, show that, provided the ratio half wavelength to cylinder diameter $\frac{\lambda}{2D} \geq 6.0$ for acoustic waves, the average heat transfer coefficient and basic flow pattern - vortex growth and collapse - are dependent only on the intensity of the oscillation for a given temperature difference between the cylinder and air. The basic flow pattern was further corroborated by the experiments of Lowe (37).

For the case of free convection in air from heated horizontal cylinders, subjected to mechanical or acoustic oscillation in a vertical plane, the observations of Richardson (53) and Lowe (37) for average heat transfer coefficient and flow field are similar. Richardson's experiments were carried out in an acoustic field with $\frac{\lambda}{2D} \geq 6.0$. The flow instability observed by Richardson and Lowe originated in the wake region on top of the cylinder. Lowe observed that the disturbance moved upstream with increase in oscillation intensity, and finally developed to turbulence about the cylinder. Lowe (37) also found that, despite the differing flow fields, there was little difference in the average heat transfer coefficient for oscillation in either horizontal or vertical plane. It was seen from the literature survey in the previous section, that it was the destruction of the region of low heat transfer coefficient on the top of the cylinder that was the major contributor to the increased average heat transfer coefficient. Because for both horizontal and vertical modes of oscillation, the increased mixing in the region of the upper surface of the cylinder causes increased heat transfer, and because Lowe's results for average heat transfer show little dependence on the plane of oscillation, the possibility exists of setting up a common method to calculate the average heat transfer coefficient for either plane of oscillation. Further support to this is given by the conclusions of Lee and Richardson (52) and Richardson (53) drawn from flow visualisation. They conclude that, for horizontal and vertical modes of oscillation, the flow

field is qualitatively consistent with a superposition of the streaming and convective flows about the cylinder.

In attempting a common method of calculating the heat transfer coefficient, an analysis cannot be made by specifying local conditions of flow, and, by integrating these, obtain an averaged effect. This is so because local conditions are different for each plane of oscillation. However, a semi-empirical approach can be adopted whereby, from observed data, variables can be chosen which characterise the flow and mixing behaviour in the boundary layer. A mixing mechanism can be postulated to account for increased mixing in the boundary layer due to oscillation, and from this the average heat transfer coefficient calculated and checked against experiment.

In the problem under study here, the mixing is induced by the streaming flow interacting with the laminar free convective flow field, to produce transition type of instability.

In section 5.0. it was found that transition instability in the laminar free convective boundary layer originated in the region of the outer point of inflexion in the laminar velocity profile. It would appear reasonable therefore to expect the instability arising from the interaction of the streaming and free convective flow fields to occur in this region.

It was pointed out earlier that the greater part of the increased mixing and heat transfer due to oscillation occured on the upper surface of the cylinder. From Hermann's analysis (38) of the laminar free convective flow of gases over a horizontal cylinder, it is known that decceleration of the flow commences at a point approximately 135^{o} from the lower stagnation point on the cylinder. The tendency to separation and vortex formation in the deccelerating flow over a cylinder, and the instability in the outer critical layer discussed above, make the choice of the point of interaction between the streaming and the free convective flow, at the outer inflexion point in the laminar velocity profile, 135^{o} from the lower stagnation point, appear quite reasonable.

Because of the observed interaction between the streaming and free convective fields, it is assumed that the energy of the streaming flow supplements the energy of the free convective flow in the critical region of the laminar velocity profile.

Hence

$$\frac{V_v^2}{2\,g_c} = \frac{1}{2\,g_c}\left[V^2_{\text{INFLEXION}} + V^2_{\text{STREAMING}} \right]_{@135^\circ} \qquad 8.1.1.$$

From Hermann (38)

$$V_{\substack{\text{INFLEXION} \\ @\ 135^\circ}} = \frac{0.345\,\nu\,G_R^{\frac{1}{2}}}{D} \qquad 8.1.2.$$

The streaming velocity $V_{STREAMING}$ is evaluated from equation 7.1.1., the value of η being that corresponding to the outer critical layer of the laminar velocity profile. At this value of η, the value of $V_{STREAMING}$ is similar to that at $\eta \to \infty$, which is

$$V_{STREAMING}\,(x) = -\,3\,\frac{a^2\omega}{R}\,\sin\,\frac{x}{R}\,\cos\,\frac{x}{R} \qquad 8.1.3.$$

For $\frac{x}{R}$ corresponding to 135°

$$V_{\substack{STREAMING \\ @\ 135^\circ}} = \pm\ 3\,\frac{a^2\omega}{D} \qquad 8.1.4.$$

The positive sign indicates direction of fluid motion for a horizontal mode of oscillation and the negative sign, fluid motion for a vertical oscillation mode.

Making appropriate substitutions from 8.1.2. and 8.1.4. in 8.1.1. results in

$$V_v = \left[0.119\left(\frac{\nu G_R^{\frac{1}{2}}}{D}\right)^2 + 9\left(\frac{a^2\omega}{D}\right)^2 \right]^{\frac{1}{2}} \qquad 8.1.5.$$

In the presence of oscillation and free convection, where there has been a transition to vortex growth and collapse, or turbulence in the fluid flow, the mixing coefficient S_v might be expected to have the form

$$S_v \propto \frac{V_v}{\Gamma}\,G_R^{\,m} \qquad 8.1.6.$$

Therefore

$$hv \propto \left[\frac{k \ Cp \ GR^m}{\Gamma}\right]^{\frac{1}{2}} \left[0.119\left(\frac{\nu GR^{\frac{1}{2}}}{D}\right)^2 + 9\left(\frac{a^2\omega}{D}\right)^2\right]^{\frac{1}{4}} \qquad 8.1.7.$$

At the critical intensity of oscillation, when the average heat transfer coefficient is first beginning to increase, the effect of the streaming flow on the mixing coefficient, and therefore on average heat transfer coefficient, is negligible. Therefore

$$S_{CRITICAL} \propto \frac{GR^m}{\Gamma_{CRITICAL}} \left[0.119\left(\frac{GR^{\frac{1}{2}}\nu}{D}\right)^2\right]^{\frac{1}{2}} \qquad 8.1.8.$$

Hence

$$\frac{hv}{h_{CRITICAL}} = \left[\frac{\Gamma_{CRITICAL}}{\Gamma}\right]^{\frac{1}{2}} \left[1 + \frac{75.5 \ Re_s^2}{GR}\right]^{\frac{1}{4}} \qquad 8.1.9.$$

In the study of unsteady laminar boundary layer flows (11), the region in the boundary layer over which unsteady effects are of importance is found to be $\left[\frac{\nu}{\omega}\right]^{\frac{1}{2}}$. In the study of turbulence (55), $\left[\frac{\nu}{\omega}\right]^{\frac{1}{2}}$ is found to be proportional to the scale of turbulence. Therefore, putting $\Gamma \propto \left[\frac{\nu}{\omega}\right]^{\frac{1}{2}}$ relates the scale of the mixing motion due to the oscillation with the frequency.

In the case of mechanical oscillation of the heated cylinder (frequencies < acoustic frequencies), in which the intensity of oscillation is such that a fully developed vortex system or turbulent mixing is created about the cylinder, it is expected that an increase in the scale of the mixing process will be present when compared with acoustic oscillations for which $\frac{\lambda}{2D} \geq 6.0$.

If it is assumed that, at the critical condition for both mechanical and acoustic oscillation, the scale of mixing is the same (provided $\frac{\lambda}{2D} \geq 6.0$) then evaluation of $\Gamma_{CRITICAL}$ at $\frac{\lambda}{2D} = 6.0$ for an ambient temperature of 70°F and D = ¾ in. yields $\Gamma_{CRITICAL} \propto \left[\frac{\nu}{1496}\right]^{\frac{1}{2}}$.

Therefore

$$\left[\frac{\Gamma_{CRITICAL}}{\Gamma}\right]^{\frac{1}{2}} = \left[\frac{f}{1496}\right]^{\frac{1}{4}}$$

For acoustic oscillation for which $\frac{\lambda}{2D} \gg 6.0$, the effects of frequency on vortex size was negligible, (Fand and Kaye (46)), therefore the effect of scale of mixing on $\frac{hv}{h_{CRITICAL}}$ will be negligible, hence for acoustic oscillation.

$$\frac{hv}{h_{CRITICAL}} = \left[1 + \frac{75.5\ Re^2_s}{G_R}\right]^{1/4} \qquad 8.1.10.$$

For mechanical oscillation where scale of mixing is of importance.

$$\frac{hv}{h_{CRITICAL}} = \left[\frac{f}{1496}\right]^{\frac{1}{4}} \left[1 + \frac{75.5\ Re^2_s}{G_R}\right]^{\frac{1}{4}} \qquad 8.1.11.$$

Numerically $h_{CRITICAL} \approx h_o$ the heat transfer coefficient in the absence of oscillation. Therefore, $\frac{hv}{h_{CRITICAL}}$ from equations 8.1.10. and 8.1.11. can be plotted against $\frac{hv}{ho}$ from experiment.

Before a comparison between equations 8.1.10. and 8.1.11. and experimental data is carried out, it would be desirable to establish the conditions of validity of these two equations. The method put forward here considers a superposition of the energy in the streaming flow with that of the critical layer in the laminar boundary layer. The distabilising effect of the hot wall surface has not been accounted for. Hermann (38) has found experimentally that the point of transition to turbulence of a laminar free convective boundary layer on a horizontal cylinder moves upstream with increase in Grashof number, these results are shown in Figure 8.1. below.

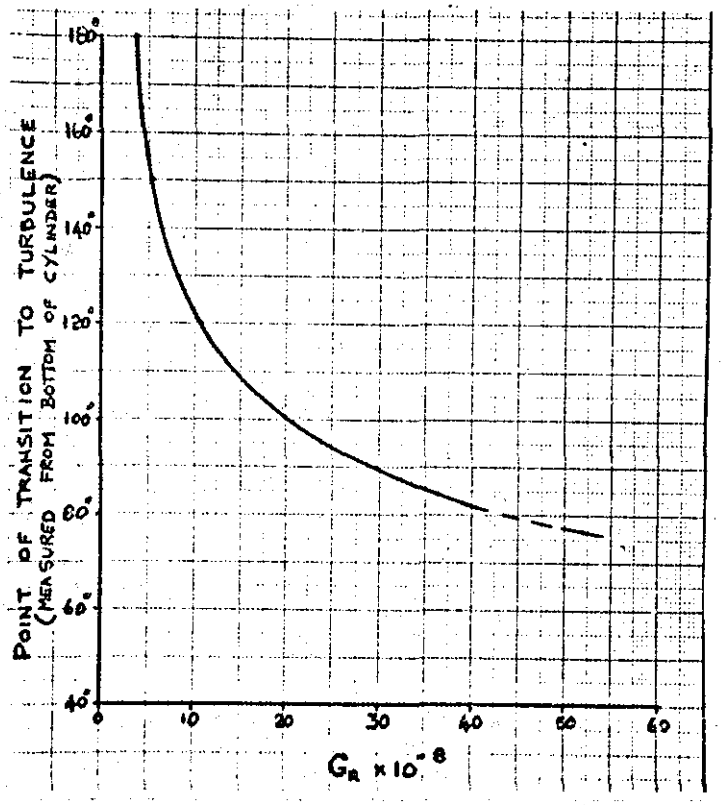

FIGURE 8.1. Variation of point of transition on a heated horizontal cylinder in air with Grashof number (Hermann (38)).

It is expected, therefore, that the method developed here would be valid for cases in which the temperature difference between the wall surface and air is small. Therefore, comparison with the experimental data of references (45), (48), (49) and (37) have been considered at the lowest temperature differences at which heat transfer data was obtained.

From Lowe's experimental data (37), it is clear that an upper limit to the validity of equations 8.1.10. and 8.1.11. occurs when oscillation induced forced convection prevails. This will occur when $\frac{Re^2_s}{G_R} \gtrsim 10$. The lower limit of validity would be at conditions of oscillation which first produce a fully developed condition of turbulence or vortex growth and collapse about the cylinder. From the data of references (45), (49) and (37), this has been established in Figure 8.2.

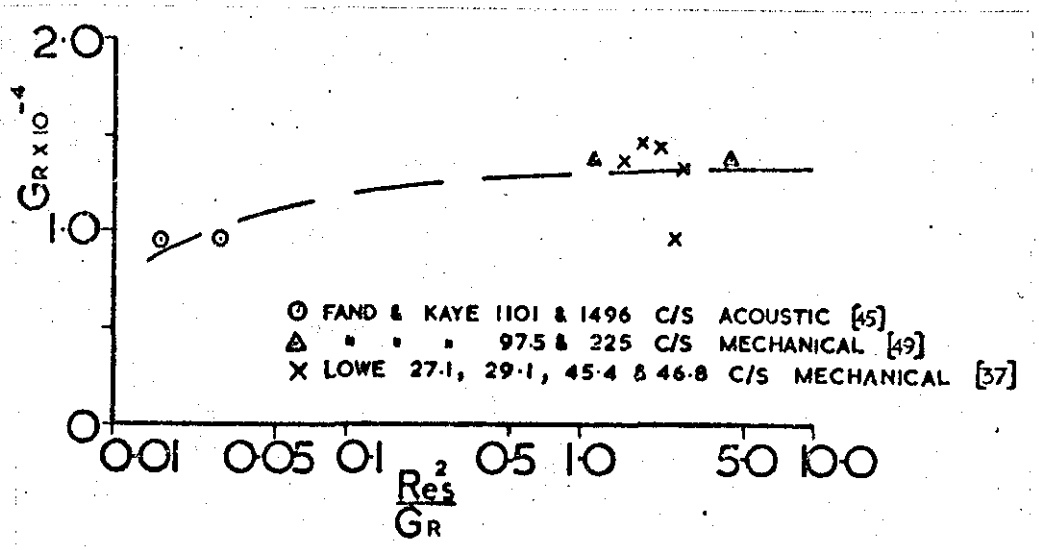

FIGURE 8.2. Conditions for fully developed vortex flow or turbulence.

8.2. Comparison with Experiment and Discussion

A plot of $\frac{hv}{ho}$ from the experimental data of references (45), (48), (49) and (37) is shown against $\frac{hv}{h_{CRITICAL}}$ from equation 8.1.10. and 8.1.11. in Figure 8.3. below. It will be seen that the calculated results are in agreement with experimental data, provided $\Delta\theta \lesssim 50^{\circ}F$ and $\frac{Re^2_s}{G_R} \lesssim 10$.

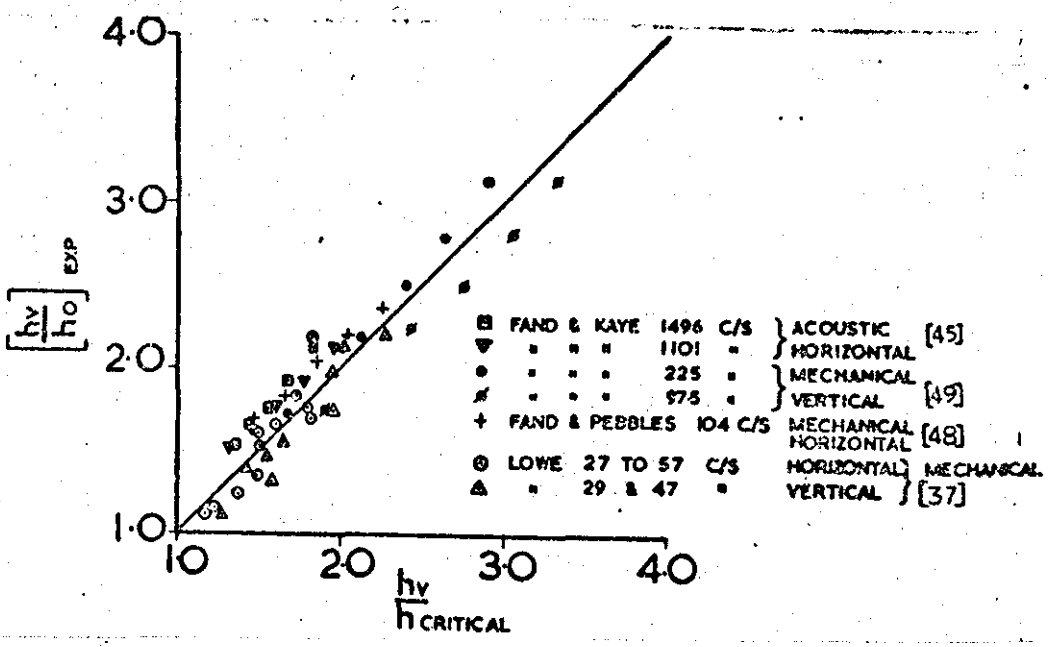

FIGURE 8.3. Comparison between equations 8.1.10. and 8.1.11. and experiment.

From the discussion in section 8.1. it was seen that equations 8.1.10. and 8.1.11. would be valid for cases where the temperature difference is small. The comparison with experimental data showed that this temperature difference was $\lesssim 50^{\circ}F$. It is of interest to compare equations 8.1.10. and 8.1.11. with the results of Richardon's asymptotic analysis obtained for $G_R \rightarrow 0$, which was discussed in section 7.0.

For the case of large streaming Reynolds numbers, Richardson (54),with the aid of Stuart's analysis (43), obtained the following expression relating Nusselt, Reynolds and Prandtl numbers and the ratios a/D and (γ/ω).

$$\frac{Nu\ R \left[1 + 1.66 \left(\frac{a}{D}\right) P_R^{\frac{1}{2}} \right]}{Rosc\ P_R^{\frac{1}{2}} \left[\frac{3\gamma}{\omega}\right]^{\frac{1}{2}}} = 0.484 \qquad 8.2.1.$$

Large Streaming Reynolds Number experimental data was plotted as function of the L.H.S. of 8.2.1. and $\frac{G_R}{Ros^2c}$ by Richardson, this plot is shown in Figure 8.4.

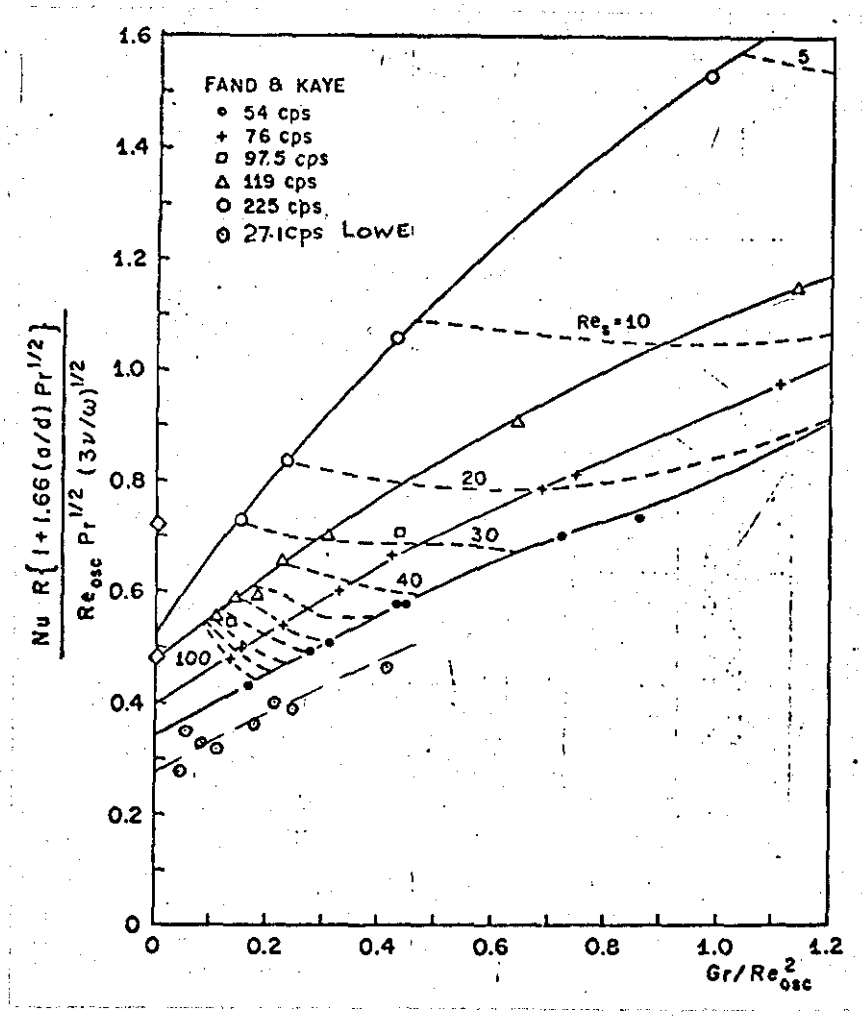

FIGURE 8.4. Comparison between experimental data and asymptotic solution of Richardson (54) for large Streaming Reynolds Numbers.

It will be seen from Figure 8.4. that only the high frequency mechanical oscillation data of Fand and Kaye at frequencies of 119 and 225 C/s converge on to the asymptotic solution of Richardson. The variation between Richardson's solution and the experimental data will be seen to increase as the frequency becomes smaller. The 27.1 C/s frequency data of Lowe has been plotted by the author on Richardson's co-ordinates to emphasise this point.

Stuart's analysis on which Richardson's solution was based is valid up to $\left(\frac{a}{D}\right) \approx 0.3$, assuming $P_R = 0.73$ for air and recasting 8.2.1. in terms of the streaming Reynolds number $\frac{a^2\omega}{\nu}$, remembering that $Re_{osc} = \frac{a_{rms}\,\omega\,D}{\nu}$ results in

$$Nu = 0.713\ Re_s^{\frac{1}{2}} \qquad 8.2.2.$$

8.2.2. is a limiting case of Richardson's analysis for $\frac{a}{D} \approx 0.3$. As pointed out earlier, Richardson's theory does not agree closely with the low frequency oscillation data. This means that the 0.713 multiplier in equation 8.2.2. will not in fact be a constant, but will vary with frequency. From the intercept of the various experimental curves in Figure 8.4., the constants for a given frequency can be substituted in 8.2.1. for the value of 0.484 and the following values obtained for the given frequencies, these constants will replace 0.713 in 8.2.2.

f C/s.	225	119	97.5	76	54	27.1
INTERCEPT ON FIG. 8.4.	0.52	0.484	0.45	0.40	0.34	0.270
MULTIPLIER FOR EQUATION 8.2.2. to replace 0.713.	0.763	0.713	0.662	0.590	0.501	0.398

Now, from equation 8.1.11., we see that as G_R becomes small,

$$\frac{Nu_V}{N_{CRITICAL}} = \left[\frac{f}{1496}\right]^{\frac{1}{4}} \cdot \frac{2.95\ Re_s^{\frac{1}{2}}}{G_R^{\frac{1}{4}}} \qquad 8.2.3.$$

For free convective flows over horizontal cylinders at low values of G_R, Eckert and Drake (56) recommend for gases

$$Nu_o = 0.40\ G_R^{\frac{1}{4}} \qquad 8.2.4.$$

Now $Nu_o \propto N_{CRITICAL}$. Hence from 8.2.3. and 8.2.4. we have

$$Nu_v = 1.18\left[\frac{f}{1496}\right]^{\frac{1}{4}} \cdot Re_s^{\frac{1}{2}} \qquad 8.2.5.$$

For the frequency range 27.1 to 225 C/s discussed above, the Multiplying constant for equation 8.2.5. for each frequency will be

f C/s.	225	119	97.5	76	54	27.1
MULTIPLIER IN 8.25 to replace $1.18\left[\frac{f}{1496}\right]^{\frac{1}{4}}$	0.736	0.630	0.600	0.560	0.515	0.433

It will be seen that over the whole frequency range from 27.1 C/s to 225 C/s, equation 8.2.5. is in agreement with the asymptotic values of the experimental data to within 15%, and is in fact a better representation of the asymptotic behaviour as $G_R \rightarrow 0$ than Richardson's analysis.

For the case of low streaming Reynolds Numbers, Richardson obtained the asymptotic solution.

$$\frac{Nu\ R\left[1 + 1.66\left(\frac{a}{D}\right) P_R^{\frac{1}{2}}\right]}{Rosc\ P_R^{\frac{1}{2}}\left[\frac{3\nu}{\omega}\right]^{\frac{1}{2}}} = 0.718 \qquad 8.2.6.$$

The results of this analysis were compared by Richardson with experimental data, this is shown in Figure 8.5.

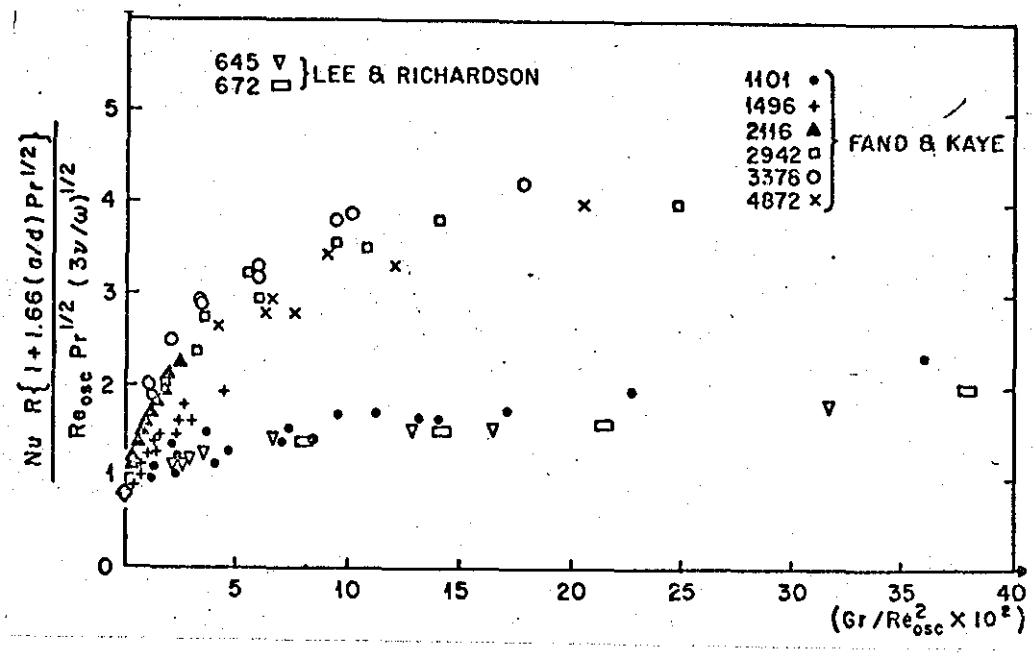

FIGURE 8.5. Comparison between experimental data and asymptotic solution of Richardson (54) for small streaming Reynolds numbers.

Now for the case of low streaming Reynolds numbers and $P_R = 0.73$ for gases, the term $\left[1 + 1.66\left(\frac{a}{D}\right) P_R^{\frac{1}{2}}\right] \approx 1$, hence 8.2.6. can be recast in terms of the streaming Reynolds number Re_S, so that, for $P_R = 0.73$, we have

$$Nu = 1.5\ Re_S^{\frac{1}{2}} \qquad 8.2.7.$$

(Recall equation 7.3.8.)

Now for the case when G_R is small, 8.1.10. can be re-written as

$$\frac{Nu_V}{N_{CRITICAL}} = \frac{2.95\ Re_S^{\frac{1}{2}}}{G_R^{\frac{1}{4}}} \qquad 8.2.8.$$

As before, $N_{CRITICAL} \approx Nu_o = 0.40\ G_R^{\frac{1}{4}}$

$$\therefore \quad Nu_V = 1.18\ Re_S^{\frac{1}{2}} \qquad 8.2.9.$$

There is a 27% variation in the value of Re_S predicted by 8.2.9. and 8.2.7. due to Richardson. However, a closer look at Richardson's comparison of his asymptotic solution with experimental data (figure 8-5) will show that, because of the large scale used, it is difficult to assess the accuracy of his comparison. To assess this, the present author has replotted the data of Fand and Kaye (45) for low $\Delta\theta$ (i.e. low G_R) for frequencies of 2116; 1496 and 1100 C/s. on a much larger scale. This plot is shown in Figure 8.6. Also shown on this Figure is the result from 8.2.9., this will yield a constant 27% smaller than the 0.718 constant of Richardson. (i.e. 0.565).

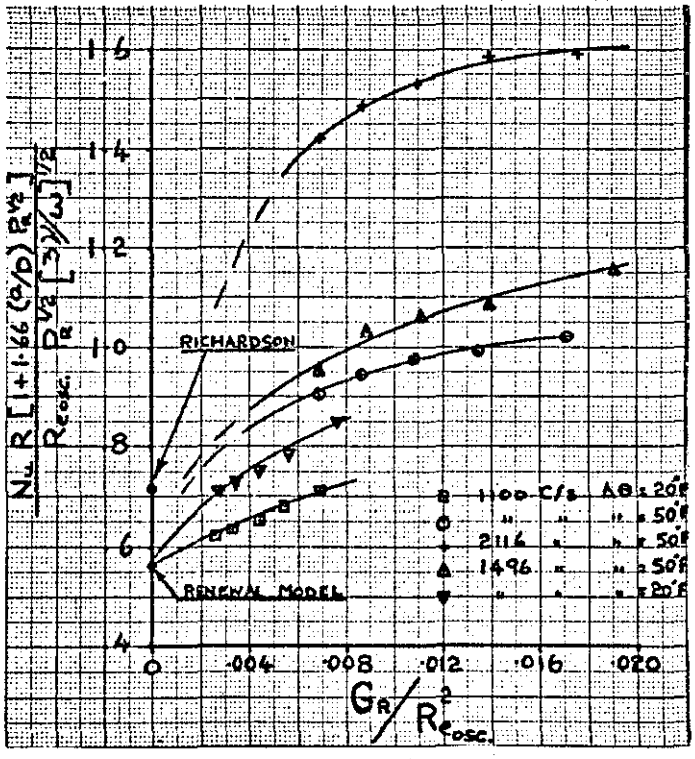

FIGURE 8.6. Replot of data of Fand and Kaye (45) in the Region $\frac{G_R}{Re_{osc}} \rightarrow 0$.

From the replotting of data in Figure 8.6. using a larger scale, it is seen that the experimental data shows a trend towards the 0.565 constant predicted through equation 8.2.9. rather than the value 0.718 predicted by Richardson's analysis.

Conclusion

By considering the steady streaming flow set up by acoustic or mechanical oscillations to interact at the outer critical layer of the laminar velocity profile and so cause greater mixing, the Danckwerts-Mickley model has been used to compute the average heat transfer coefficient in the presence of oscillations, provided the temperature difference between the surface and air $\lesssim 50^{\circ}F$ and that $\frac{Re_s^2}{G_R} \gtrsim 10$

It has been shown that the method developed here gives closer agreement with experiment for the average heat transfer coefficient, as $G_R \rightarrow 0$, than the asymptotic solutions of Richardson (54).

9.0 CONDENSATION HEAT TRANSFER ON VERTICAL SURFACES AND HORIZONTAL TUBES

9.1. Condensation Processes

When a saturated vapour comes in contact with a surface at a lower temperature, condensation occurs, the condensate flowing downwards off the surface under the action of gravity. There are two distinctly different kinds of condensation process, and the type found in any particular situation depends primarily upon the behaviour of the condensate on the cooled surface. If the condensate wets the surface and forms a liquid film over it the process is called Filmwise Condensation. If on the other hand the condensate does not wet the surface, it collects in growing droplets on the cooled surface. These large droplets coalesce and roll off the surface under the action of gravity. This type of condensation is known as Dropwise condensation.

In the case of Filmwise Condensation under normal conditions and in the absence of non-condensable gases mixed with the vapour, a continuous ~~flow~~ film of liquid is formed over the surface which flows downwards under the action of gravity. Unless the velocity of the vapour is very high, or the liquid film over the surface is very thick, the motion of the condensate film is usually laminar, and heat is transferred from the vapour-liquid interface to the surface merely by conduction. The rate of heat transfer depends, therefore, primarily on the thickness of the condensate film, which in turn depends on the rate at which vapour is condensed and the rate of removal of the condensate. On a vertical surface the film thickness increases continuously from the top to the bottom of the surface. On a horizontal tube the local component of the gravitational force along the surface causing the liquid flow is reduced, and the film becomes thicker, this effect is particularly noticeable on the underside of the tube surface.

In Dropwise-Condensation only a part of the surface is covered with condensate droplets. Nucleation sites for the formation of droplets are thought to be small surface indentations, on which minute droplets may or may not establish themselves, depending on whether the droplet radius is greater or less than a critical value established from the Kelvin Helmoltz equation. The droplet grows because of condensation on it, this condensation releases the enthalpy of vapourisation at the droplet surface, from where heat is conducted through the droplet to the tube or wall surface. The continuing growth of neighbouring drops cause these to coalesce, until they are

swept from the surface under the action of gravity, and the process of droplet growth repeated at the free nucleation sites.

Jakob (57) noted that the rate of drainage of condensate from a surface was more rapid with dropwise condensation than with the filmwise mode. He also noted that the ratio of surface volume of drops to film was large. These factors contribute to the fact that heat transfer coefficients as observed with dropwise condensation are usually an order of magnitude larger than those obtained with the filmwise mode. Because of the difficulty in maintaining dropwise condensation over very long periods with chemical promoters, it is usually the practice in equipment design, where condensation processes are involved, to assume that filmwise condensation conditions apply, though in fact a mixed mode often prevails.

In the following survey only that literature pertinent to filmwise condensation will be considered.

9.2. The Nusselt Theory for Laminar Filmwise Condensation on Vertical Flat Plates and Horizontal Cylinders

Theoretical relations for calculating the heat transfer coefficients for filmwise condensation of pure vapours on vertical flat plates and horizontal tubes were first obtained by Nusselt in 1916. These solutions are derived in almost all books on heat transfer e.g. Jakob (57). Because certain aspects of Nusselt's classical theory are to be used here, this theory and its comparison with experimental observation will be discussed.

In considering the condensation of a pure vapour by the laminar filmwise mode, on a vertical flat plate, Nusselt made the following assumptions. Constant vapour and surface temperatures; negligible vapour velocity. Heat transfer across the liquid film is solely by conduction, the interfacial shear stress between liquid and vapour was negligible. By setting up a force balance on an element of the liquid film which involved equating the gravitational forces on the element to the resisting viscous shear forces, and utilising the assumption of conduction across the film . Nusselt obtained the following expressions for; local thickness of the liquid film δ_x; local velocity u(y) of the liquid in the film, at any station x down the plate and y in the film; and average condensation heat transfer coefficient h for the plate.

$$\delta_x = \left[\frac{4\mu_{kx}\,(\theta_v - \theta_s)}{g\,h_{fg}\,\rho^2}\right]^{\frac{1}{4}} \qquad 9.2.1.$$

$$u(y) = \frac{g\delta_x^2}{\nu}\left(\left[\frac{y}{\delta_x}\right] - \tfrac{1}{2}\left[\frac{y}{\delta_x}\right]^2\right) \qquad 9.2.2.$$

$$h = 0.943\left[\frac{\rho^2\, g\, h_{fg}\, k^3}{\mu_L\,(\theta_v - \theta_s)}\right]^{\frac{1}{4}} \qquad 9.2.3.$$

Utilising the same assumptions and general analysis Nusselt obtained theoretical results for filmwise condensation on a horizontal tube. Since this part of Nusselt's theory is to be utilised extensively in later discussions it will be rederived here in more detail than is generally found in the literature.

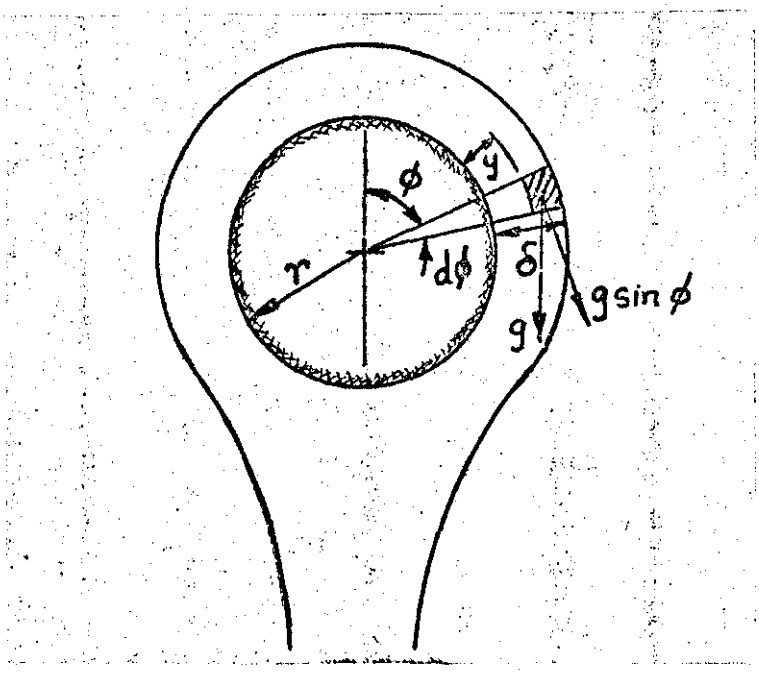

Fig. 9-1 Model of Condensate film on a Horizontal Tube

Considering the element of fluid film shown in figure (9-1), and equating viscous forces to gravitational forces on the element results in the following mathematical expression.

$$\frac{\mu}{g_c}\,\frac{du}{dy}\cdot(r + y)\,d\phi = (r + y)\,d\phi\,(\delta - y)\,\frac{\rho\, g\, \sin\phi}{g_c} \qquad 9.2.4.$$

$$\frac{du}{dy} = \frac{g \sin \phi}{\nu} \left[\delta - y \right] \qquad 9.2.5.$$

$$\text{and } u = \frac{g \sin \phi}{\nu} \delta^2 \left[\left(\frac{y}{\delta} \right) - \tfrac{1}{2} \left(\frac{y}{\delta} \right)^2 \right] + C \qquad 9.2.6.$$

at $y = 0$, $u = 0$ $\therefore$ $C = 0$.

Mean velocity of condensate at ϕ is

$$\bar{u} = \frac{1}{\delta} \cdot \int_0^{\delta} u \cdot dy \qquad 9.2.7.$$

$$\bar{u} = \frac{\delta^2 g \sin \phi}{3 \nu} \qquad 9.2.8.$$

Heat transfer over the arc length $r.d\phi$ by conduction is equal to heat release by condensation, expressed mathematically this is

$$\frac{k\,(r.d\phi).1}{\delta} \left[\theta_v - \theta_s \right] = \rho h_{fg} \, d \left[\bar{u} . \delta . 1 \right] \qquad 9.2.9.$$

Substituting for $\bar{u}$ from (9.2.8.) in (9.2.9.) and rearranging

$$\frac{3 \nu k r}{g \rho h_{fg}} \cdot (\theta_v - \theta_s) \cdot d\phi = \delta \, d \left[\delta^3 \sin \phi \right] \qquad 9.2.10.$$

For a given set of operating conditions and geometry θ_v, θ_s and r are fixed hence $\frac{3 \nu k r}{g \rho h_{fg}} \left[\theta_v - \theta_s \right]$ is a constant B say.

$$\therefore \quad B \, d\phi = \delta \, d \left[\delta^3 \sin \phi \right] \qquad 9.2.11.$$

Now $\delta \, d \left[\delta^3 \sin \phi \right] = \delta^4 \cos \phi . d\phi + 3 \delta^3 \sin \phi . d\delta$

$$= \delta^4 \cos \phi . d\phi + \tfrac{3}{4} d (\delta^4) \sin \phi \qquad 9.2.12.$$

$$\text{Putting } \frac{\delta^4}{B} = Y \quad \text{then} \quad \frac{d(\delta^4)}{B} = dY \qquad 9.2.13.$$

From (9.2.11.); (9.2.12) and (9.2.13)

$$\frac{dY}{d\phi} \sin \phi + \frac{4}{3} Y \cos \phi - \frac{4}{3} = 0 \qquad 9.2.14.$$

The solution of the above linear differential equation (9.2.14.) is shown in appendix (III) and is:-

$$Y = \frac{1}{\sin^{4/3}\phi} \left[\frac{4}{3} \int \sin^{1/3} \phi . d\phi + C \right] \qquad 9.2.15.$$

at $\phi = 0$, $\frac{dY}{d\phi} = 0.$

$\therefore$ from (9.2.14) $Y = 1$

and from (9.2.15) since $\phi \approx \sin \phi$ for small angles.

$$\frac{1}{\sin^{4/3}\phi} \frac{4}{3} \int \sin^{1/3} \phi . d\phi = 1. \quad \text{Therefore } C = 0$$

$$Y = \frac{4/3}{\sin^{4/3}\phi} \cdot \int_0^{\phi} \sin^{1/3} \phi . d\phi \qquad 9.2.16.$$

Equation (9.2.16) was evaluated by graphical methods by Nusselt and is tabulated in Jakob (57) and in appendix (IV) from this the local variation of δ with azimuth ϕ, can be obtained and hence local and average values of the heat transfer coefficient can be calculated.

The variation of the film thickness δ and heat transfer coefficient ϕ are shown in figure 9-2. This information was computed by Nusselt for the condensation of steam at 100°C on a surface at 90°C; the tube diameter being 2.6 cm.

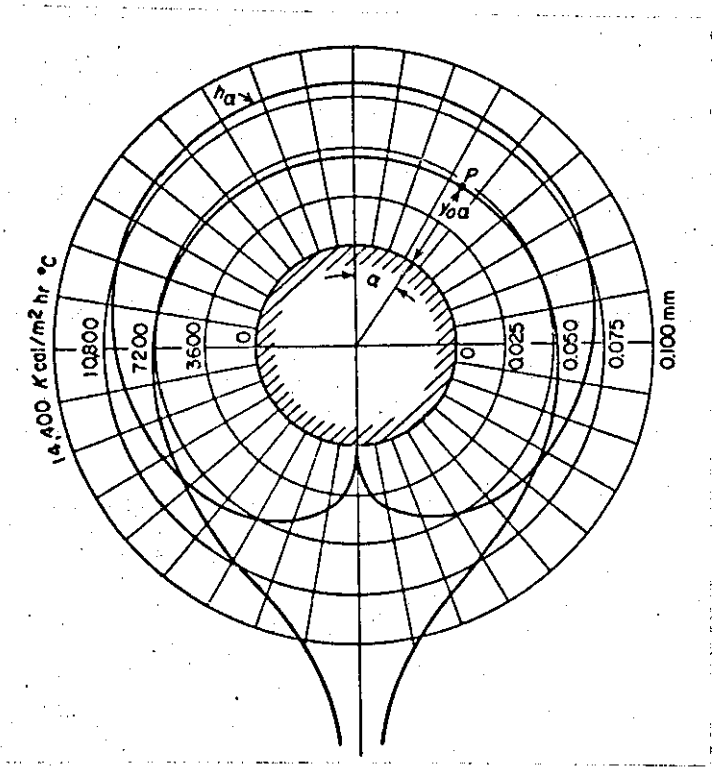

Fig. 9-2 Local Condensate film thickness and Heat Transfer Coefficient around a Horizontal tube computed by Nusselt - Jakob Ref.(57)

The average condensation heat transfer coefficient for a horizontal tube of Diameter D was determined by Nusselt to be:-

$$h = 0.725 \left[\frac{\rho^2 \, g \, h_{fg} \, k^3}{\mu D \, (\theta_v - \theta_s)} \right]^{\frac{1}{4}} \qquad 9.2.17.$$

9.3. The use of Reynolds number for the liquid film

Equation (9.2.3.) was derived on the assumption that the liquid film was laminar. However, as the rate of condensation increases and the height of the surface over which condensation is occurring is large, the condensate film at the lower end of the surface becomes turbulent. Colburn (1934) (see McAdams (27) for derivation) recast (9.2.3.) in a form which gave the average heat transfer coefficient for the vertical surface as a function of liquid film properties and a Reynolds number for the film $Re_f = \frac{4G}{\mu}$ where G is the rate of condensation per unit wetted perimeter. This enables the average heat transfer coefficient of (9.2.3.) to be expressed as

$$h = 1.46 \left[\frac{\rho^2 k^3 g}{\mu^2} \right]^{1/3} Re_f^{-1/3} \qquad 9.3.1.$$

The critical Re_f above which the film has been observed to become turbulent is about 1200, McAdams (27).

Equations (9.2.3) and (9.3.1) will be valid for condensation on vertical tubes also, provided these are of adequate diameter, (i.e. not capillary tubes).

9.4. Comparison of Theory with Experiment

Since Nusselt's theory for laminar filmwise condensation was put forward, numerous workers have carried out experimental investigations with vertical plates and tubes and horizontal tubes, and various condensing vapours, to test the validity of equations (9.2.3.) and (9.2.17.)

In the cases where the theoretical assumptions have been satisfied it has been shown experimentally that the average condensation heat transfer coefficient is proportional to $(\theta_v - \theta_s)^{-\frac{1}{4}}$ and $(\text{Length})^{-\frac{1}{4}}$ for laminar flow conditions. However, the average values of the heat transfer coefficient show considerable deviation with respect to Nusselt's predictions. For the case of the vertical surface, McAdams (27) tabulates the results of several workers studying condensation of steam on vertical plates and tubes, ranging in length from 0.39 to 12 ft with $(\theta_v - \theta_s)$ ranging from 5° - 83°F. The average coefficient of heat transfer ranged from 1.1 to 1.5 of the value predicted by (9.2.3.).

For the case of the horizontal tube McAdams (27) quotes an average result for the condensation heat transfer coefficient of steam at atmospheric pressure which is 1.23 times the value predicted by Nusselts theory (9.2.17). The tube diameters in these experiments ranged from 0.675 ins. to 2.0 ins.; with $\theta_v - \theta_s$ covering the range 2° - 43°F. In the comparisons between Nusselt's theory and experiment made by McAdams, all the liquid properties were evaluated at the mean of the vapour saturation temperature and average surface temperature with the latent enthalpy being evaluated at the saturation temperature.

Numerous workers have tried to account for the variation observed between experiment and Nusselt's theory. Bromley et al (58) carried out a combined theoretical and experimental investigation to determine the effect of non uniformity of surface temperature on the condensation heat transfer coefficient on horizontal tubes. These workers were particularly interested in the effect of the low thermal conductivity of condenser tubes made from stainless steel. Their investigation

showed results that were in close agreement with Nusselt's theory for the horizontal tube. It is expected that similar results would be obtained for the vertical tube case. McAdams (27) gives a correction factor for use with equation (9.2.3.) for condensation on vertical tubes, which is based on the ratio of the overall temperature difference at the bottom of the tube to that at the top of the tube. For $\theta_{overall\ bottom}/\theta_{overall\ top}$ of 0.5 the correction to (9.2.3.) is 0.96 whereas for this ratio equal to 2.0 the correction is 1.06.

Peck and Reddie (59) considered the effects of Inertia Forces in the liquid film (which were neglected by Nusselt), in obtaining a semi-empirical correction to Nusselt's theory for the horizontal tube case. They obtained $h/h_{Nusselt}$ varying from 0.7 to 1.3 from an empirical analysis.

Bromley (60) obtained a correction to Nusselt's theory to account for the effects of finite thermal capacity of the condensate and its contribution to the sensible heat transfer through the condensate film. The effect of the finite heat capacity is to increase the temperature gradient at the tube wall and therefore increase the heat transfer. Bromley et al obtained the following correction.

$$\frac{h}{h_{Nusselt}} = \left[1 + 0.4\ \frac{C_p\ (\theta_v - \theta_s)}{h_{f_g}}\right]^{\frac{1}{2}} \qquad 9.4.1.$$

For the condensation of steam $\frac{C_p\ (\theta_v - \theta_s)}{h_{f_g}}$ is very small because of the large values of h_{f_g}, therefore in the case of steam the contribution from this source is very small.

More recent theoretical studies have considered the laminar filmwise condensation problem as a problem in laminar boundary layer theory. Sparrow and Gregg (61) considered the problem of filmwise condensation on a vertical surface. In their solution the authors considered the effects of inertia and thermal capacity of the condensate film, but considered the interfacial shear stress between the liquid film and the vapour to be zero. Their results show that for values of the liquid Prandtl number ≥ 1 and $Cp\ (\theta_v - \theta_s)/h_{f_g} \leq 0.4$ the effects of inertia are negligible and therefore Nusselt's theory

is applicable. In a later study Koh et al (62) considered the same problem as Sparrow and Gregg (61) but with the further refinement of including the interfacial shear stress between the liquid and vapour as a boundary condition. By considering the interfacial shear stress, the motion of the liquid film is allowed to induce motion in the vapour, in the course of this process the liquid film looses momentum. So for a given condensate film thickness; the average condensate velocity will be lower when interfacial shear is permitted. Since the heat transfer is roughly proportional to the mass flow times the enthalpy of vapourisation, it is expected that the heat transfer will decrease. However from their computations the authors show that for $P_R \geq 1.0$ the interfacial shear stress is of little importance. The authors results are shown in figure (9-3) where it will be

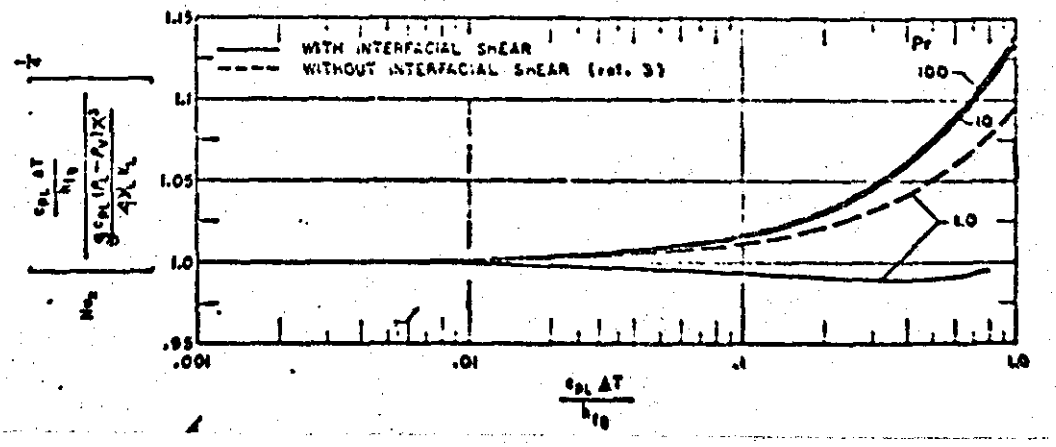

Fig. 9-3 Effect of Interfacial Shear Stress on Condensation Heat Transfer on a Vertical Plate. Ref. (62).

noted that for the small values of $C_p(\theta_v - \theta_s)/h_{fg}$ obtained with steam the results for local heat transfer coefficient agree closely with those of Nusselt's theory. Chen (63) in a later paper considered the same problem as Koh et al (62). Using a different analytical approach, he obtained results in agreement with those of Koh et al.

Sparrow and Gregg (64) also carried out an analysis for laminar filmwise condensation heat transfer on a horizontal cylinder using boundary layer theory. In this analysis the effect of interfacial shear stress was neglected. The results obtained by the authors are shown in figure (9-4) where it will be noted again that for low

values of $C_p \frac{(\theta_v - \theta_s)}{h_{fg}}$ there is close agreement with Nuselt's theory.

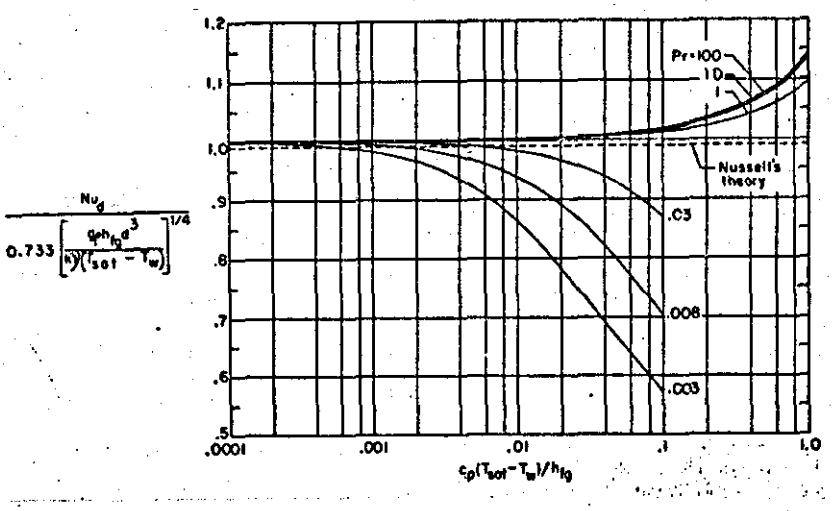

Fig. 9-4 Heat Transfer Results for Laminar filmwise condensation on a horizontal Cylinder Ref. (64).

From the foregoing survey on condensation of pure vapours on vertical plates or tubes and on horizontal tubes, two points emerge clearly.

1. For the condensation of vapours such as steam which have very high enthalpy of vapourisation, the parameter $C_p(\theta_v - \theta_s)/h_{fg}$ is small. Theoretical results from boundary layer analysis show that Nusselt's theory is adequate for theoretical prediction of condensation heat transfer coefficient.
2. Effects of non uniform surface temperature, thermal capacity of the condensate film, inertia of the liquid film and interfacial shear, collectively contribute little to modifying the results predicted by Nusselts theory for fluids with $P_R \geq 1.0$ and low $C_p(\theta_v - \theta_s)/h_{fg}$.

Peck and Reddie's empirical corrections (59) for inertia effects in the liquid film, would in the light of the discussions on boundary layer analysis of condensation heat transfer, appear to be excessive. Their method attributes all the variation between Nusselt's theory and experiment to the effects of inertia in the liquid film.

Grigull (65) considers that the deviation between experiment and Nusselt's theory is due mainly to the effects of ripple formation in the liquid film, and the possibility of mixed (filmwise and

dropwise) modes of condensation.

The formation of ripples has been observed by Dukler and Berglin (66) in the study of thin liquid films on an unheated vertical surface. Ripples were observed to occur in the liquid film at a film Reynolds number of about 8.0. Transition to turbulence was observed at a film Reynolds number of about 1400. The authors found that in the laminar region considered to be that with film Reynolds number < 1400; the average film thickness as measured, agreed closely with that of a theory developed by Nusselt (see Jakob (57)) for the prediction of film thickness, for flow of a liquid down unheated surfaces. (The assumptions and developments in this theory are similar to those of Nusselt's condensation theory).

Kapitsa developed a theoretical analysis for ripple motion of the liquid film based on the Navier Stokes equations, which also considered the effects of surface tension forces at the fluid gas interface. This theory is extensively discussed in Portalski's thesis (67). Portalski has shown (68) that the formation of ripples sets up a circulatory vortex motion in the troughs of the ripples, as shown in figure (9-5) and postulates that this mechanism causes greater mixing motion, and therefore accounts for the higher heat transfer and mass transfer coefficients that have been observed in the presence of ripple motion of the film.

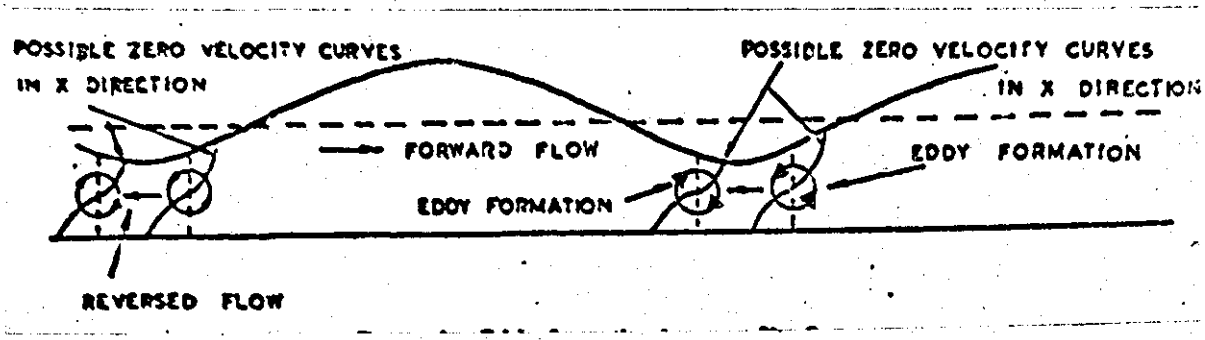

Fig. 9-5 Eddy Formation in wavy film flow Portalski (68)

Portalski (69); (70) also observed that a transition from the "pseudo-laminar" flow with rippling motion , to a "pseudo-turbulent" motion of the film occurs at a film Reynolds number of about 400. In

the "pseudo-turbulent" mode of flow; the ripple formation has a random motion as compared with that in the pseudo-laminar case. Portalski (70) also concluded that Nusselts parabolic velocity profile was suitable for use up to the point of transition to "pseudo-turbulent" motion.

Kapitsa's theory (67) results in an average film thickness which is 8% smaller than that predicted by Nusselt (57). Therefore, it is quite likely that the reduction in thickness of the liquid film, plus the inner vortex motion in the film is accounting for the increased heat transfer results as compared with Nusselt's theory for filmwise condensation. It should be recalled here that rather a similar observation was made by Eckert and Soehnghen (33) in their investigation of transition of the laminar free convective boundary layer on a vertical plate. Wave motion was observed in the outer part of the boundary layer; though the character of the boundary layer as a whole was laminar; the average coefficients of heat transfer observed were some 25% greater than those expected for laminar flow. It is likely that Grigull's comment on ripple motion is correct.

As to the effect of mixed condensation this is also likely to be a contributory cause to the increased heat transfer results, since only small patches of dropwise condensation can contribute a substantial increase in the observed heat transfer coefficient. Furthermore to the maintain pure filmwise condensation on a surface is difficult for long periods.

While the foregoing discussion accounts for experimental heat transfer coefficients which have been observed to be in excess of those predicted by Nusselt theory; another explanation has to be sought for those results which have been observed to be below the Nusselt theory.

It has been known McAdams (27) that small traces of non-condensable gases which might be present in the vapour; due to poor de-aeration of the boiler feed water, or leakage into the condenser when the latter is operating at subatmospheric pressures causes a reduction in the condensation heat transfer coefficient. The reason for this is that as condensation takes place on the surface, a higher concentration of air which is mixed with the vapour, is found in the vicinity of the surface, with the result that the partial pressure of the vapour is reduced. At a distance from the surface, the vapour concentration is greater, therefore mass transfer or difusion of the

vapour through the air to the condensing surface occurs. The mass transfer process is now the rate controlling process, and the rate of condensation will be dependent on it. This is so because the rate controlling process is one of difusion through a gas which is a slower process when compared with difusion (conduction) through a liquid. Therefore the condensation rate and heat transfer coefficient will be reduced when non-condensable gases are present with the vapour. Experiments by Hampson (71) on the effects of non-condensable gases on the condensation of steam by either the filmwise or dropwise mode, on horizontal or vertical tubes, showed that the heat transfer coefficient for filmwise condensation was reduced to 75% of that calculated from Nusselt's theory for filmwise condensation, when as little as 0.2% by mass of non-condensables was present in the steam.

It may be reasonably concluded that the main causes for deviation between experiment and Nusselt's theory for filmwise condensation have been accounted for.

In this thesis no discussion of turbulent filmwise condensation is to be given; since this mode of condensation has been observed only at the bottom of long vertical tubes - greater than about 8 ft. in length - McAdams (27). Whereas the concern here is with tubes of about half this length, with low vapour velocities along the tube length so that the contribution from shear effects to transition will be small. Vapour velocities of up to approximately 6 ft/sec have been found by Kutateladze (72) to have little effect on the laminar filmwise coefficient of heat transfer, when the vapour and condensate flow are in the same direction.

Summary

For the filmwise condensation of steam on short vertical surfaces or tubes or on horizontal tubes Nusselt's theory is adequate for computing the heat transfer coefficient from a theoretical standpoint. Provided precautions can be taken to exclude air and other non-condensables from the system and care taken to obtain pure filmwise condensation. It is expected that experimental results would be of the order of 20% greater than that predicted by Nusselts theory. It appears almost certain that to account for the increased heat transfer theoretically; the effects of ripple motion must be taken into account including the inner vortex motion which was found to exist by Portalski (68), however to account for ripple motion of the

film involves the loss of the use of the very simple expressions of Nusselt's theory. The possibility therefore exists of using Nusselt's simple theory in any analysis, and correcting for its defects empirically.

10.0 THE EFFECT OF MECHANICAL OSCILLATIONS OF THE CONDENSING SURFACE ON CONDENSATION HEAT TRANSFER COEFFICIENT.

Introduction

10.1. It has long been known that tube vibration is present in the underslung power plant condenser. The usual practice has been to minimise any transverse vibration of the tubes to reduce the possibility of fatigue failure. However, from a heat transfer standpoint it is interesting to investigate the effect of transverse oscillations of the condenser tube on the condensation heat transfer rate. In this section a survey of any relevant literature on the topic of surface oscillation effects on condensation heat transfer will be made.

10.2. Survey of literature on the Effects of Mechanical Oscillation of the condenser surface on condensation heat transfer

Work was carried out at the South West Research Institute, by Raben et al (73) under a grant from the U.S. Department of Interior,* on oscillatory effects on heat transfer and scale formation on tube surfaces.

The object of the research program was to demonstrate the feasibility of using vibrational energy to improve the economy of saline-water evaporator systems. Improvements sought through transverse tube oscillations were; The increased water side convective heat transfer coefficient. The increased steamside film condensation heat transfer coefficient, with the possible promotion of dropwise condensation. The reduction of scale formation on the outside of tubes.

The apparatus and methods used for the transverse oscillation of the condenser tube for the waterside and condensation studies will be discussed at some length, as this review will be of use when discussing later the apparatus used for the experiments carried out at the Loughborough University of Technology by the author.

10.3. Water Side Heat Transfer Study

The test section consisted of a 1 in. O.D. x .035 in wall vertical stainless steel tube 48 ins. long. The test section was heated electrically through a 5 KVA transformer with input control which enabled the output current to be varied from 0 - 500 amps.

* I am indebted to the U.S. Department of the Interior, Washington D.C., for providing me with a copy of Report No. 49. (Ref.(73)).

The electrical energy input to the test section was through two aluminium strips attached to the tube at locations 48 ins. apart. An electro-magnetic vibrator was connected through a "tuning bar" to the centre of the test section. Rubber hoses provided flexible input and output water connections to the test section. Sixteen thermocouples were mounted in groups of four around the tube at locations 3 ins. and 6 ins. on either side of the centre of the test section. Inlet and outlet water temperature were also recorded on thermocouples. The experiments covered a range of Reynolds number from 1,117 to 24,000 with and without oscillation. The frequency of oscillation was varied from 17 to 144 c/s with amplitude varying from 0.375 ins. down to 0.009 ins. Tests were conducted with the temperature difference between the wall and water of from 15° to 30°F. It was found that tests without oscillation gave results which agreed well with standard correlations for pipe flow with the exception of results at a flow Reynolds number of 1,117 which showed the presence of strong free convective effects.

The tests with oscillation did not reveal any significant increase in the heat transfer coefficient, over values obtained in the absence of oscillation. A maximum increase of 4% was observed, the increase being independent of flow Reynolds number.

10.4. Steam Condensation Study

A schematic diagram of the apparatus used and the method of tube support are shown in figure (10-1) and (10-2).

The test tube was of aluminium 1 in. O.D. with 0.049 ins. wall thickness and was 41 ins. long. The tube was installed in a 3 ins. I.D. pyrex tube 38 ins. long with a central T section as shown in figure 10-1. The aluminium tube passed through end flanges on the pyrex tube; the seal between the aluminium tube and the flange being made by means of an "O" ring seal. This enabled the aluminium tube to expand freely, and to oscillate in a transverse direction as a pivot ended beam. The aluminium tube was connected to the vibrator, through a driving rod attached to it as shown in figure 10-2. Suitable precautions being taken to seal the moving joint at the outlet from the "T" section.

Tests were carried out with a constant inlet steam flow rate at atmospheric pressure which was sufficient to allow for an uncondensed flow from the exhaust. Water rate was kept constant and at the highest rate possible, but a temperature controller

Fig. 10-1 Schematic Arrangement of Condensation Rig of Raben et al Ref. (73)

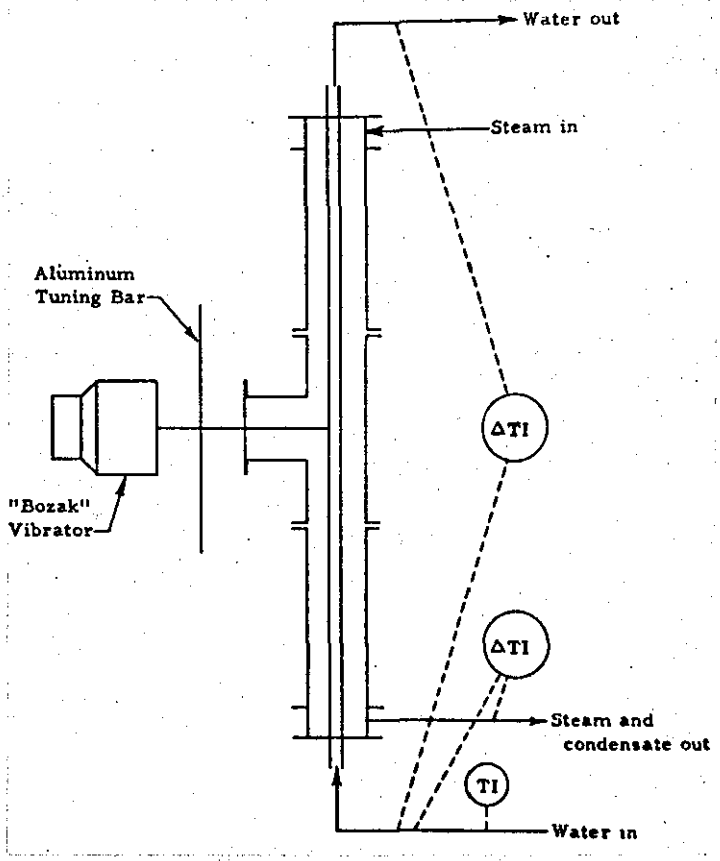

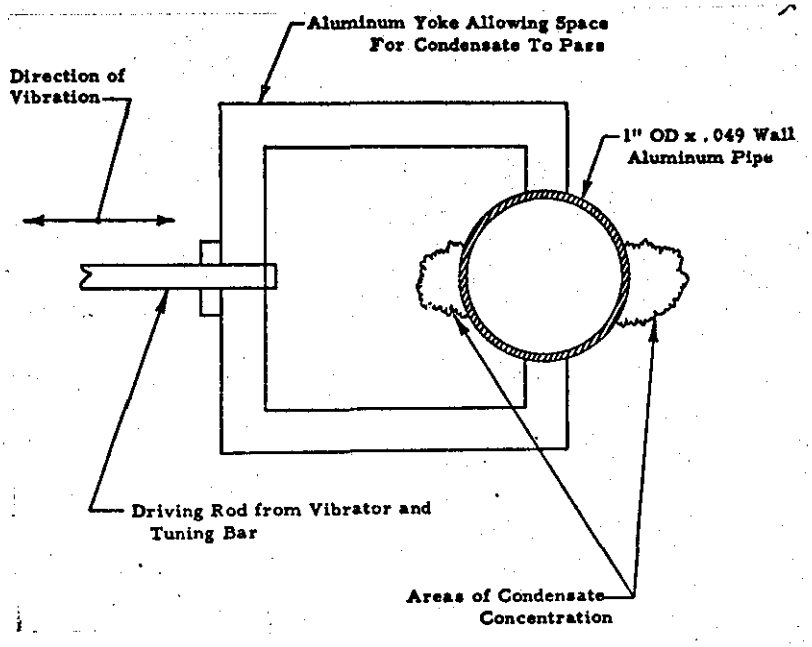

Fig. 10-2 Method of Connecting Vibrator to Condenser tube and Condensate Accumulation (73)

enabled the inlet water temperature to be maintained constant at values of 120°; 150° and 180°F.

Experimental data were obtained with and without oscillation of the aluminium tube. The frequency range of the oscillations used was from 22.5 c/s to 98 c/s. with a maximum amplitude of 0.5 ins. obtained at the resonant frequency of 38 c/s. For the three inlet temperatures used above; the approximate overall steam-water temperature differences were 90°; 60° and 30°F. respectively.

The steam side coefficient was obtained from the overall heat transfer coefficient. The overall heat transfer coefficient consisting of the inverse of the sum of the water side; tube wall and condensation film resistances. The tube wall resistance was determined from the properties and measurements of the aluminium tube. The average water side resistance was determined from an empirical relationship which accounted for the $(L/_D)$ ratio of the tube. From accurate measurements of the water side temperature rise and water flow rate the total heat transfer and average bulk temperature of the water were obtained. Accurate measurements were also made of the steam temperature. From this information the average condensation heat transfer coefficient was computed. The estimated error on the cnndensation heat transfer coefficient was considered to be about $\pm$ 4%.

The authors obtained a correlation for the ratio of average coefficients of heat transfer of the form.

$$\frac{h_v}{h_o} = 0.714 \left[a\, f^{1.2} \right]^{0.205} \qquad 10.4.1.$$

which is valid for $af^{1.2} > 4.0$. The amplitude a used in equation (10.4.1.) is the maximum amplitude measured at the centre of the tube.

The authors observations of the nature of the condensate film under conditions of oscillation is of interest. It was noted that the condensate film was swept back and forth on the tube towards the two stagnation points. (see figure 10-2). Very little condensate was observed to be thrown free of the tube.

A few tests were also conducted with non-condensable gas introduced with the inlet steam, and as was to be expected the improvement in condensation heat transfer coefficient was reduced.

10% air in the steam causing a 37% reduction of the heat transfer coefficient, with maximum amplitude oscillation of 0.5 in. This value still being about 10% greater than the condensation heat transfer coefficient in the absence of oscillation and non condensable gases.

10.5 Condensation on a tube with longitudinal oscillation of the tube

Haughey (74) conducted an experimental investigation into the effects of longitudinal oscillation of a condenser tube on the condensation heat transfer coefficient. The tests were conducted with ethanol vapour condensing on a 0.905 ins. O.D. tube, oscillating with amplitude up to 0.059 ins. and frequencies up to 140 c/s. Film Reynolds numbers varied from 30 - 50 based on laminar flow conditions. A maximum increase of 20% was observed on both condensation and water side heat transfer coefficients. The increased condensation heat transfer coefficient was attributed to the formation of standing waves occurring in the condensate film, which were thought to cause better convective mixing. These waves were in the form of equi-spaced ridges around the circumference of the tube. They were spaced about 0.18 in. apart, the spacing being independent of intensity of oscillation.

An indifference curve of amplitude versus frequency was plotted on the basis of first observation of wave formation. It was found that the critical intensity for wave formation agreed with that obtained by Shine (30) in his experiments with free convection i.e. $af \approx 1.0$ in. c/s. It was noted that the indifference curve based on first increase of heat transfer gave a result for critical intensity which was slightly less than that based on wave formation.

Condensate drainage was observed to take place predominantly from the wave ridges.

The author obtained the following correlation for his experimental data within $\pm$ 5%

$$\frac{h_v}{h_o} = 1 + 0.0018\, af \qquad 10.5.1.$$

10.6. Summary

From the foregoing discussion on mechanical oscillation of condenser surfaces, and its effect on the condensation heat transfer coefficient. The important observation was the fact that the

liquid film on the surface of the tube is not ruptured in any way but greater mixing in the film does take place. For the case of transverse oscillation of vertical tubes as studied by Raben et al the oscillation of the tube causes the film to move in the manner shown in figure (10-3) below, There is a strong possibility of

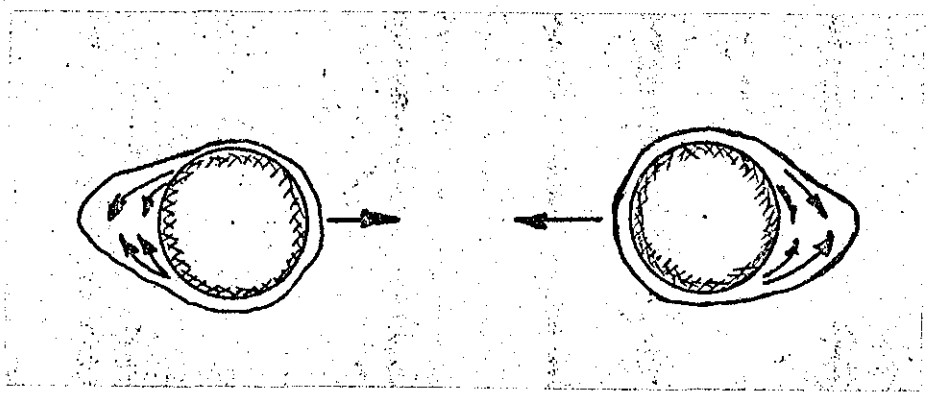

Fig. 10-3 Movement of Condensate film on a transversely oscillating Vertical tube.

vortex motion in the region of accumulated condensate, this vortex motion could if sufficiently strong cause turbulence in the film. This vortex motion along with the reduced film thickness on the forward stagnation point of the cylinder accounts for the increase in the observed heat transfer. A similar mechanism was postulated by Haughey for the increased heat transfer with longitudinal oscillation.

Raben et al and Haughey found from empirical correlation that the ratio h_v/h_o was a function of the amplitude and frequency of oscillation only. These correlations do not allow for any contribution to improved heat transfer from the motion of the film under gravity forces. In the case of Haughey's results with a horizontal tube of 0.905 ins. diameter this could possibly be justified but in the case of Raben et al who were working with a 38 in. long vertical tube the contribution of the film motion due to gravity forces could be quite significant particularly at low intensities of oscillation.

Because of evidence of the strong convective effect causing increases in the condensation heat transfer coefficient, with the possibility of promoting turbulence in the film - this is particularly so in the experiments of Raben et al. It would appear quite feasible that the Danckwerts-Mickley model could be effectively

applied here to predict the increase in the heat transfer coefficient due to oscillation. The problem is as before to set up a suitable model for the mixing in the condensate film, so that the mixing coefficient S can be defined.

In the next section, the application of the Danckwerts-Mickley Model for condensation on a vertical transversely oscillating tube will be discussed.

11.0 APPLICATION OF THE DANCKWERTS-MICKLEY MODEL FOR THE COMPUTATION OF THE CONDENSATION HEAT TRANSFER COEFFICIENT ON A VERTICAL TRANSVERSELY OSCILLATING TUBE

11.1. The Mixing Model

In the study of the stability of liquid films falling over vertical or inclined surfaces.

Portalski (69) and Brooke-Benjamin (75) have found that instability is initiated at the outer edge of the film where the velocity is a maximum. Atkinson and Caruthers (76) determined the velocity profile for film flow over an unheated surface and found it to be parabolic which is in accordance with Nusselt's theory.

In the discussion of vibration induced transition to turbulence of the laminar free convective boundary layer on a vertical surface, it was found that the mixing coefficient S could be suitably described if the vibration energy of the surface could be considered to supplement the energy of the fluid in the outer critical layer, in the region of the point of inflexion of the laminar velocity profile.

If the same assumption is used here, i.e. vibration energy of the surface supplementing the energy of the liquid film at its outer edge, to promote greater mixing, then, the mixing coefficient Sv will be given by

$$Sv \propto \frac{Vv}{\Gamma} \qquad Re_f^{\,n} \qquad 11.1.1.$$

where Γ is a scale of mixing, and

$$Vv = \left[\left(\frac{a_o\,\omega}{\pi}\right)^2 + U_{MAX}^2\right]^{1/2} \qquad 11.1.2.$$

U_{MAX} in 11.1.2. is the velocity at the outer edge of the parabolic velocity profile, and is evaluated at the point of transition to psuedo-turbulent motion i.e. when $Re_f \approx 400$. $\left(\frac{a_o\,\omega}{\pi}\right)^2$ is proportional to the mean kinetic energy of the vibrating tube, assuming a sinusoidal flexure (Ref. 77) for the pivot ended tube. (See Appendix V for derivation).

Under critical conditions of vibration when the heat transfer coefficient for the tube is just beginning to increase, the mixing coefficient will be proportional to $\frac{V_{CRITICAL}}{\Gamma}$, there

being no change in the order of magnitude of the scale of mixing which is proportional to the film thickness.

Therefore $$\frac{h_v}{h_{CRITICAL}} = \left[\frac{V_v}{V_{CRITICAL}}\right]^{1/2} \qquad 11.1.3.$$

At the critical condition, it is assumed that vibration does not supplement mixing, so that under these conditions $V_{CRITICAL} \approx u_{MAX}$.

Hence $$\frac{h_v}{h_{CRITICAL}} = \left[1 + \left(\frac{a_o\ \omega}{u_{MAX}}\right)^2\right]^{\frac{1}{4}} \qquad 11.1.4.$$

For the parabolic velocity distribution in the condensate film which is valid to the point of transition to pseudo-turbulent flow (70), Nusselt's theory (57) gives:-

$$u_{MAX} = \frac{\rho g \delta^2}{2\mu} \qquad 11.1.5.$$

and $$\delta = \left[\frac{4\ k\ \mu\ x\ (\theta_{SAT} - \theta_w)}{g \rho^2\ h_{fg}}\right]^{1/4}. \qquad 11.1.6.$$

Therefore $$u_{MAX}^2 = g\frac{k\ x\ (\theta_{SAT} - \theta_w)}{\mu\ h_{fg}} \qquad 11.1.7.$$

From equations 11.1.4. and 11.1.7.

$$\frac{h_v}{h_{CRITICAL}} = \left[1 + \frac{\left(\frac{a_o\ \omega}{\pi}\right)^2}{\frac{g\ k\ x\ (\theta_{SAT} - \theta_w)}{\mu\ h_{fg}}}\right]^{\frac{1}{4}} \qquad 11.1.8.$$

Now $$G = \int_o^{\delta} \rho\ u.d\ y \qquad 11.1.9.$$

From Nusselt's theory,

$$u = \frac{g\delta^2}{\nu}\left[\left(\frac{y}{\delta}\right) - \frac{1}{2}\left(\frac{y}{\delta}\right)^2\right] \qquad 11.1.10.$$

Therefore $$G = \frac{\rho^2\ g\ \delta^3}{3\mu} \qquad 11.1.11.$$

From equations 11.1.6. and 11.1.11., Re_f can be written as

$$Re_f = \frac{4}{3}\left[\frac{4\,k\,x\,(\theta_{SAT} - \theta_w)\,\rho^{2/3}\,g^{1/3}}{\mu^{5/3}\,h_{fg}}\right]^{\frac{3}{4}} \qquad 11.1.12.$$

11.2. Comparison with Experiment

From the data for each test run tabulated in reference (73) the value of x for which $Re_f = 400$ was evaluated from equation 11.1.12., all physical properties of the condensate being evaluated at the film temperature with the exception of enthalpy of vapourisation, this was evaluated at the saturation temperature. The value of x obtained in this way was used in equation 11.1.8. The comparison between $\frac{hv}{h_{CRITICAL}}$ from equation 11.1.8. and $\frac{hv}{ho}$ obtained experimentally in reference (73) are shown in Figure 11.1. (It should be noted that $h_{CRITICAL} \approx ho$.)

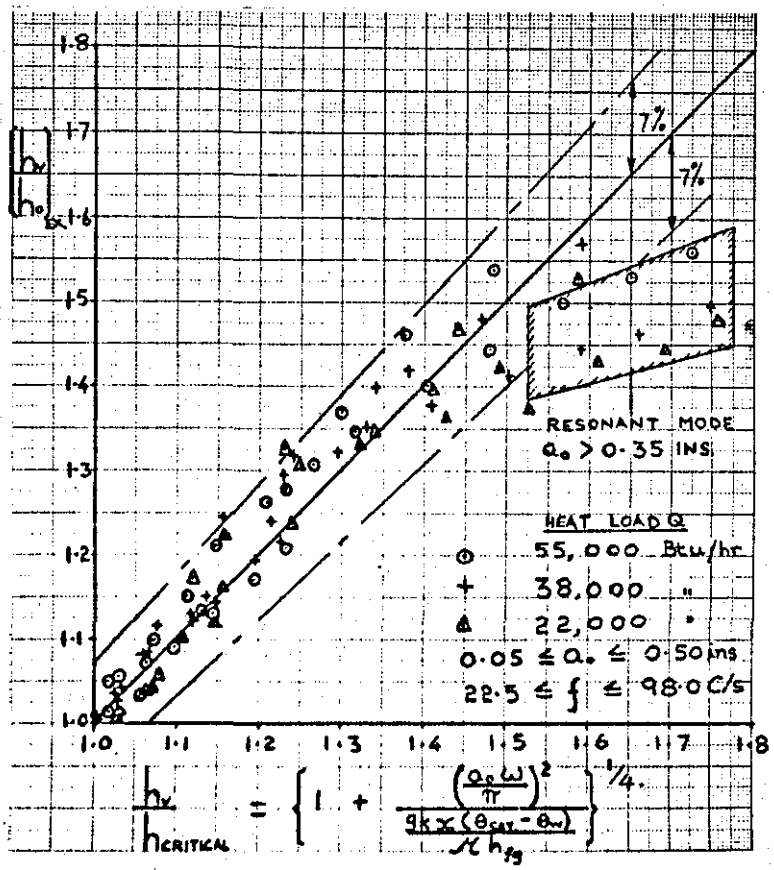

FIGURE 11.1. Comparison between 11.1.8. and data of reference (73).

Remembering that the static tube tests of reference (73) resulted in heat transfer coefficients which were about 10% in excess of those predicted by Nusselt's theory, (57), it is estimated that the error introduced by use of Nusselt's theory in equation 11.1.8. for calculation of U_{MAX} will result in an error of about 5% in comparison with the experimental data for $\left[\frac{hv}{ho}\right]$.

In the comparison of the experimental data of reference (73) with equation 11.1.8., it will be seen that the resonant mode vibration at 38 C/s with amplitudes $>$ 0.35 ins. are not in as close agreement with equation 11.1.8. as the other data. The reasons for this are thought to be:-

(1) The mixing model put forward considered only the energy associated with the tube vibration and the liquid film to characterise the process. At large amplitudes of vibration, adhesion forces in the liquid film will be of greater significance in inhibiting the lateral motion of the liquid film, thus, the simple model would overpredict mixing and heat transfer in these situations.

(2) The possibility exists that at large amplitudes of vibration ($a_o > 0.3$ ins.). There is a departure from the assumption of the tube behaving as a pivot ended beam, and the tendency to vibrate as a built-in beam. This will reduce the energy of vibration (77) and again the specified mixing model would cause an overprediction of the heat transfer coefficient.

For most situations that might arise in engineering practice, a_o is likely to be less than 0.3 ins. because of the possibility of tube failure due to metal fatigue over long periods of operation. Therefore, the method discussed here for computing condensation heat transfer coefficient in the presence of transverse vibration of vertical condenser tubes would appear adequate.

Conclusions

Using the observations of Portalski and Brooke-Benjamin concerning the instability of liquid films, it has been possible to define the mixing coefficient S in the Danckwerts-Mickley model in a similar way to that for free convection from a laterally vibrating plane surface in air.

Comparison of the calculated heat transfer coefficient ratio using the Danckwerts-Mickley model is found to be in reasonable agreement with the experimental data of Raben et al, provided the amplitude of oscillation is less than 0.3 ins.

12.0 CONDENSATION HEAT TRANSFER ON A HORIZONTAL TUBE IN THE PRESENCE OF MECHANICAL OSCILLATIONS IN A VERTICAL PLANE

12.1. Proposed Study

In the literature survey conducted in section 10.2. to determine what work had been undertaken on the effects of mechanical oscillations on condensation heat transfer, it was found that no work has been carried out on condensation heat transfer on horizontal tubes in the presence of mechanical oscillations in the vertical plane. It was also pointed out in section 10.1., that this mode of oscillation was the most common in the normal underslung power plant steam condenser. It is proposed therefore to investigate the effect of mechanical oscillations in a vertical plane, of a horizontal steam condenser tube, and determine its effects on the condensation heat transfer rate. It is proposed that this study include an exploratory experimental investigation followed by a theoretical analysis to confirm the experimental findings.

12.2. Methods for producing Mechanical oscillation and method adopted

There are two basic methods which can be used to produce large amplitude mechanical oscillations utilising the electromagnetic vibrator as a driver. The simplest of these is to couple the system to be oscillated directly to the electro-magnetic vibrator. The vibrator is fed from an oscillator through a power amplifier with the appropriate frequency of oscillation, the amplitude of oscillation being controlled by the output from the power amplifier. This method suffers from the disadvantage that at high frequencies of oscillation the bulk of the useful force output of the vibrator is utilised in accelerating the moving parts of the vibrator, hence the maximum amplitudes that can be obtained in this way at high frequencies are limited.

The second method employs the use of the double beam as shown in figure 12-1.

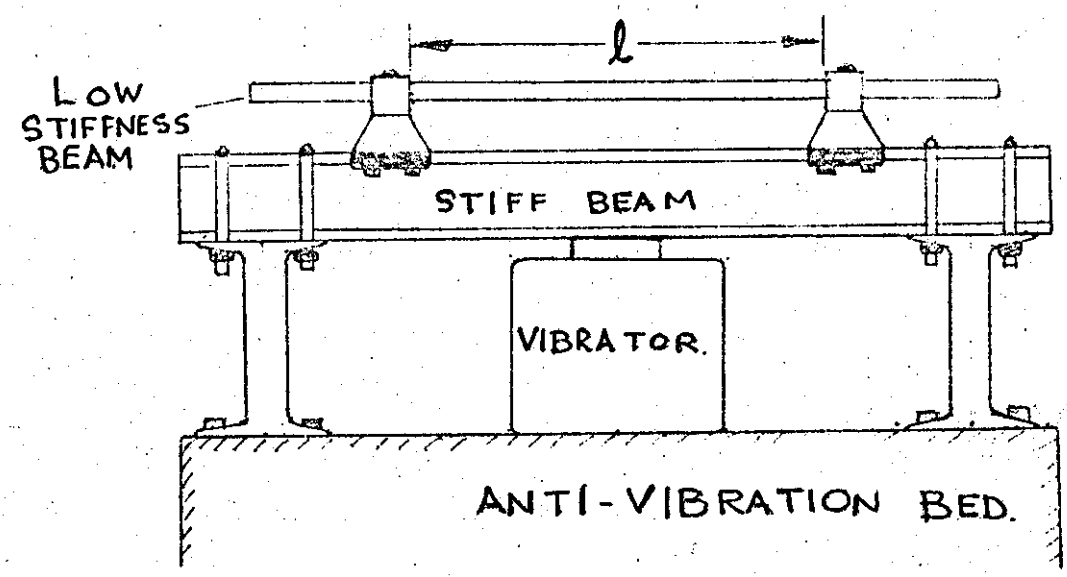

Fig. 12-1 The Double Beam Method of Producing large Amplitude Mechanical Oscillations.

The vibration force from the electro-magnetic vibrator is fed at low amplitude - (hence the bulk of the useful force output from the vibrator is available) - through the stiff beam to the supports of a beam of much smaller stiffness. The large vibration forces available cause the low stiffness beam to oscillate with large amplitudes at its fundamental frequency. The fundamental frequency of oscillation of the beam of low stiffness can be altered by adjusting the length l between the supports. The vibrator is once again fed through an oscillator and power amplifier, the input frequency corresponding to the fundamental frequency of the beam of low stiffness. The fundamental frequency for the low stiffness beam can be readily calculated from vibration theory.

To utilise the double beam method just discussed, it is necessary to couple the mid point of the low stiffness beam to the tube to be oscillated by means of a yoke system. It is not possible to use the tube as the low stiffness beam, as this would produce an unwieldy and expensive condensation chamber.

For reasons to be discussed later the test tube chosen was copper. This tube was approximately 13 ins. long by 0.830 in. outside diameter with 0.040 in wall thickness; the tube was terminated by copper flanges and support lugs and the whole mounted through insulating Paxolin strips onto a T made from $\frac{5}{8}$ in. stainless steel

tubing (see section (13) for details of tube and mounting). The total mass of the tube and T assembly was $4\frac{1}{4}$ lbs.

It was decided to carry out an initial investigation into tne double beam method for obtaining large amplitudes of oscillation of the test cylinder discussed above.

For the stiff beam a 4" x 4" x $\frac{5}{8}$" I beam 4 ft long was used. The vibrator was a Type VP 5 made by Derritron Vibrators Ltd. with associated oscillator and power amplifier. This vibrator was capable of producing a vibration force of 40 lbf. the frequency range of the vibrator was 10 to 16,000 c/s. The maximum amplitude possible was $\pm$ 0.25 ins. For the low stiffness beams a series of steel rods of varying diameters were used. The T section of the tube assembly being attached to low stiffness rods by means of knife edged phospher bronze bushes of suitable diameter.

The tube was mounted in an available condenser shell with the vertical leg of the T passing through a phosphor bronze bush in the bottom of the shell. The condenser shell itself was mounted on the vibration bed by means of Dexion angle strip (see section (13) for details). In this way the tube was free to move up and down but was constrained from any side ways motion. Tests conducted in the frequency range 20-60 c/s were not successful, because of the low fatigue life of the low stiffness rods, and the large mass of the tube assembly. Since nothing could be done to effectively reduce the mass of the tube assembly it was decided to carry out the investigation with the simpler of the two methods discussed earlier by connecting the vertical leg of the T to the vibrator with a suitable link - a $\frac{3}{8}$" steel rod. With this arrangement the following results of maximum amplitude with frequency were obtained.

Maximum amplitude a ins.	0.17	0.077	0.035	0.025	0.02
frequency c/s	20	40	60	80	100

Having determined how the test tube was to be oscillated, the next point that needs to be determined is the method of evaluating the condensation heat transfer coefficient.

12.3. Survey of Methods for measuring condensation heat transfer Coefficient

In this section various methods of determining the condensation heat transfer coefficient will be examined. What is required is a method based on direct measurement, where the accuracy of the final

results can be assessed. Methods utilising empirical correlations should be avoided because of the uncertainty in the accuracy of these. The method used by Raben et al (73) could not be used here for this reason, furthermore with the short length of tubing used here with hose connections at inlet and outlet, there would be difficulty in finding existing correlations for water side heat transfer data which would adequately cover this situation.

A method that has found wide use in the past has been the "Wilson Plot" method, which is discussed below.

The heat transfer from the condensing vapour to the water at average temperature $\bar{\theta}_\omega$ is

$$Q = U_o A_o \quad (\theta_v - \bar{\theta}_\omega) \qquad 12.3.1.$$

and

$$U_o = \frac{1}{\frac{1}{h_c} + \frac{D_o}{2k_m} \log_e \frac{D_o}{D_i} + \frac{D_o}{D_i} \frac{1}{h_\omega}} \qquad 12.3.2.$$

For given steam side conditions $h_c \approx$ constant for changes on the water side. Therefore the term $\left[\frac{1}{h_c} + \frac{D_o}{2k_m} \log_e \frac{D_o}{D_i}\right] \approx$ constant. h_ω is proportional to the water side velocity $\bar{V}_\omega$ raised to the 0.8 power. Therefore $\frac{D_o}{D_i} \cdot \frac{1}{h_\omega} \approx \frac{\text{constant}}{\bar{V}_\omega^{0.8}}$ it being assumed that the thermal properties controlling h_ω remain approximately constant with temperature. Therefore $\frac{1}{U_o} = \text{constant} + \frac{\text{constant}}{\bar{V}_\omega^{0.8}}$

U_o may be readily evaluated from measured data from equation (12.3.1.) and $\bar{V}_\omega$ can be accurately determined. Hence a plot of $\frac{1}{U_o}$ versus $\frac{1}{\bar{V}_\omega^{0.8}}$ on cartesian co-ordinates should yield a linear plot.

As $\bar{V}_\omega \to \infty$, $\frac{1}{U_o} \to \frac{1}{\frac{1}{h_c} + \frac{D_o}{2k_m} \log_e \frac{D_o}{D_i}}$ hence from the intercept on the $\frac{1}{U_o}$ axis h_c may be obtained from a knowledge of the thermal properties of the tube. This method suffers from the disadvantage that h_c is determined by extrapolation; to conditions when the water velocity is infinite. This method would therefore not be suitable for determining the small changes in h_c that could

occur with increasing intensity of vibration of the condenser tube. A further disadvantage of the method is the necessity to maintain conditions steady on the steam side for long periods while the water side velocity is varied. Obviously, the accuracy of the method depends on the obtaining of a large number of data points. The main advantage of the Wilson plot method has been its use on industrial equipment in the field where a minimum of instrumentation is a distinct advantage.

Another method of determining the condensation heat transfer coefficient is from a knowledge of the tube wall temperature. The total heat transfer Q can be accurately determined from water side measurements, if the vapour temperature or saturation pressure are known and the wall outside temperature is known then

$$h_c = \frac{Q}{A_o (\theta_v - \theta_{so})}$$

where θ_{so} is the mean temperature on the outside of the wall.

The usual method of determining wall temperature by laying thermocouples in filled grooves just under the surface of the tube cannot be used in condensation work. Jeffery (78) has found that even with the tube carefully lapped the presence of wires in the material causes strong local effects to occur in the condensation process. This effect was also noted by Hampson (79) in his study of filmwise and dropwise condensation on a short vertical surface.

Another method of measuring the average tube wall temperature is to use the metal tube as the sensing element in a resistance thermometer circuit. Accurate determinations of average temperature can be obtained from measurements of electrical resistance of the tube, a measurement that can be made with good precision with standard electrical equipment. From this average tube temperature the outside surface temperature can be determined.

In the next subsection the various methods available for the measurement of the electrical resistance of the tube wall and choice of the tube wall material will be discussed.

12.4. Methods of Determining the Electrical Resistance of the Condenser tube

(i) The d.c. Potentiometric Method - In this method the resistance tube is placed in series with a known standard resistance of low value and a limiting resistance, which keeps the d.c. current through the circuit at a practical level of between 10 - 30 A. The potential

drop across the test section of the tube and across the standard resistance are measured in quick succession. From these readings and the known value of the standard resistance the unknown resistance of the tube can be determined. The main precautions to be taken with the method are the elimination of the effects of thermal e.m.f. by reversing the polarity of the power circuit. The availability of a highly stable d.c. voltage source of high amp hour rating, and a highly stable micro-volt potentiometer are essential.

Accuracy of this method depends on the accuracy of the standard resistor and upon its stability, and that of the limiting current resistor. The stability of the potentiometer between successive readings is also essential.

2. The Kelvin Double Bridge Method for the measurement of low values of Resistance.

The Kelvin double bridge method has the advantage that at balance it is independent of fluctuations in the applied potential to the bridge circuit. The Kelvin double bridge is a d.c. bridge circuit, which, provided certain precautions are taken concerning the lead resistances connecting the unknown resistance to the bridge, gives a direct reading of the unknown resistance to a high degree of accuracy. The Kelvin double bridge is shown schematically in figure (12-2) below.

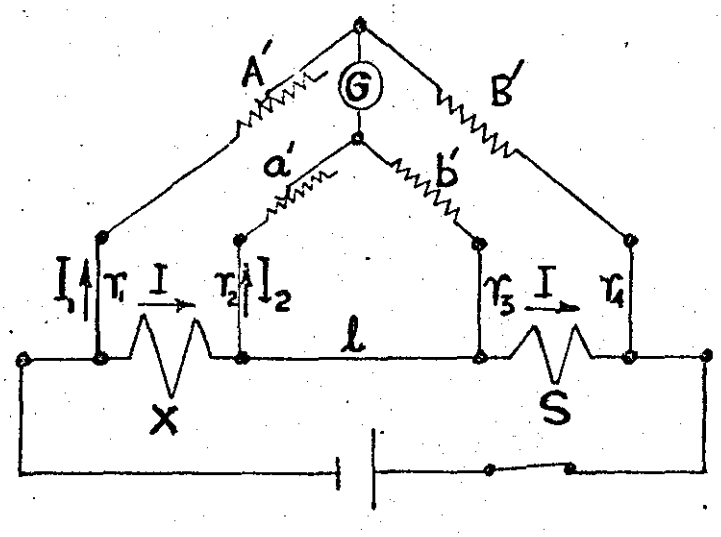

Fig. 12-2 Schematic Circuit Diagram of the Kelvin-Double Bridge

The unknown resistance x is determined in terms of the standard resistance S and the ratio arms A' and B'.

A, B, a and b are the total resistances in the designated bridge arms including the lead and contact resistance between the bridge arms and the junction points on the resistors. If the resistances between the galvanometer junction point and the resistance binding posts are A', B', a' and b' then

$$A = A' + r_1 \qquad B = B' + r_4$$

$$a = a' + r_2 \qquad b = b' + r_3$$

A' and a' are adjusted until the galvanometer G is balanced - i.e. zero current through the galvanometer. At balance the voltage drop across A is equal to the sum of the voltage drops across X and a, while that across B is equal to the sum of the voltage drops across b and S.

Therefore $I_1 A = IX + I_2 a$ 12.4.1.

and $I_1 B = IS + I_2 b$ 12.4.2.

also $(I - I_2)\ell = I_2(a + b)$ 12.4.3.

from (12.4.3) $I_2 = I \cdot \dfrac{\ell}{a + b + \ell}$ 12.4.4.

substituting for I_2 in (12.4.1.) and (12.4.2.)

$$I_1 A = I\left(X + \frac{a\ell}{a + b + \ell}\right) \qquad 12.4.5.$$

$$I_1 B = I\left(S + \frac{b\ell}{a + b + \ell}\right) \qquad 12.4.6.$$

Dividing (12.4.5.) by (12.4.6.) and rearranging

$$X = S.\frac{A}{B} + \frac{b\ell}{a + b + \ell}\left(\frac{A}{B} - \frac{a}{b}\right) \qquad 12.4.7.$$

By ganging the variable resistors so that $A'/B' = a'/b'$ for all settings, and making the values A'; a'; B'; b' large while ℓ is maintained at a low value.

$$X = S \cdot \frac{A}{B} \qquad 12.4.8.$$

$$= S\,\frac{A'}{B'}\,\frac{(1 + r_1/A')}{1 + r_4/B'} \qquad 12.4.9.$$

Since A' and B' are large i.e. of order 100 Ω and r_1 and r_4 are small, of order 0.1 Ω

$$X = S\,\frac{A'}{B'} \qquad 12.4.10$$

The Kelvin double bridge is also subjected to thermal e.m.f. problems; this effect is reduced by taking readings with reversed polarity of

the voltage source as for the potentiometric method.

Because of the advantages of the Kelvin bridge mentioned earlier, and the availability of such an instrument, it was decided to use this method for wall temperature measurement.

The instrument available was a Type K.W.1. bridge manufactured by the Croyden Precision Instruments Co. The bridge operated in conjunction with a Pye Scalamp Galvanometer and a Pye type 11330 Galvanometer preamplifier. This system was suitable for the detection of variations of resistance of 0.1 $\mu\Omega$. For the copper tube used the resistance will be of the order of 100 - 200 $\mu\Omega$. For the measurement of such values of resistance the 100 $\mu\Omega$ internal standard on the K.W.1. bridge was used i.e. S in figure (12-2). The values of the B' and b' resistances are 100 Ω. For the range 100 - 200 $\mu\Omega$ in the unknown resistance X; the variable resistances A' and a' vary between 100 and 200 Ω. From equation (12.4.7)

$$X = S\,\frac{A'}{B'}\left[\frac{1 + r_1/A'}{1 + r_4/B'}\right] + \frac{b\,l}{a + b + l}\left[\frac{A'}{B'}\left(\frac{1 + r_1/A'}{1 + r_4/B'}\right) - \frac{a'}{b'}\left(\frac{1 + r_2/a'}{1 + r_3/b'}\right)\right] \qquad 12.4.11.$$

Now $\frac{A'}{B'} = \frac{a'}{b'}$, and by using the internal standard $r_4/B' = r_3/b'$ since $r_4 = r_3$. By using identical potential leads on X so that $r_1 = r_2$, then $r_1/A' = r_2/a'$, and $\left[\frac{A'}{B'}\left(\frac{1 + r_1/A'}{1 + r_4/B'}\right) - \frac{a'}{b'}\left(\frac{1 + r_2/a'}{1 + r_3/b'}\right)\right] = 0$

Therefore $$X = S\,\frac{A'}{B'}\left[\frac{1 + r_1/A'}{1 + r_4/B'}\right] \qquad 12.4.12.$$

By the choice of $r_1 = r_2$ the effect of l has been eliminated completely. By using the internal standard, r_4 is very small compared to r_1 the potential lead resistance. If r_1 is suitably chosen it is very much less than A'. Then

$$X = S\,\frac{A'}{B'} \qquad 12.4.13.$$

$$= \frac{.0001\ A'}{100}$$

$$X = A' \times 10^{-6}\ \Omega \qquad 12.4.14.$$

12.5. Selection of tube material and dimensions

The tube material and dimensions are obviously important when the tube is to be used as a resistance thermometer element. A parameter that allows for the assessment of suitability of tube material and dimensions with regard to use as a resistance thermometer element is the sensitivity S. The sensitivity is defined as the change in temperature of the tube causing a micro-ohm change in its resistance. This is the inverse of $\frac{\rho L \alpha}{a}$, the resistance change of a tube of length L and wall cross-sectional area a for a degree centigrade change in temperature. The material of the tube has a specific resistance ρ and a temperature coefficient of resistance α. Therefore

$$S = \frac{a}{\rho L \alpha} \quad {}^{\circ}C/\mu\Omega \qquad 12.5.1.$$

If a length of 1 foot is considered - this corresponds closely to the length used in this application - and the tube O.D. and wall thickness taken to correspond to nominal $\frac{3}{4}$ in. diameter tube with 19 S.W.G. wall thickness, which is the B.S. specification 659 for light gauge copper tubing. This gives the actual diameter of the tube as 0.83 ins. and the wall thickness as 0.040 ins. The O.D. of the tube corresponds closely to that used in actual condenser applications. For these dimensions S can be evaluated for various materials.

This tabulation is shown below, the electrical properties being taken from Kaye and Laby (80);

Tube Material	$\rho \times 10^6 \Omega$cm at 20°C	α °C^{-1}	S °C/$\mu\Omega$
Aluminium	2.82	0.0036	2.07
Brass	6.60	0.0016	1.98
Copper	1.72	0.004	3.00
Nickel	7.24	0.0054	5.40
Stainless Steel	78.0	0.0010	0.270

From the tabulated information it would appear that stainless steel would be the obvious choice because of its high sensitivity. However other factors have to be taken into account. Some of these associated with the electrical characteristics of the tube and others associated with the ability to maintain filmwise condensation on the tube, this being a necessity for comparison with subsequent analysis.

The forming processes used in the manufacture of tubing cause it to work harden. In this condition the material is not stable and the electrical properties are known to vary over long periods of time. To reduce the effects of work hardening it is usual to anneal the material this results in better stability of the material properties. The effects of work hardening are most pronounced in alloy materials, but are also present to a much lesser extent in commercially pure materials, due to the presence of impurities.

In using the tube as a resistance thermometer, the generation of thermal e.m.f. due to the junction of differing materials at differing temperatures is to be avoided. This is particularly true in the fixing of potential and current leads to the tube wall, these should be made from the same material as the tube.

Finally the selection of a particular tube material could be influenced by the ability of the material to sustain filmwise condensation. It has been found by Blackman (81) that stainless steel would sustain prolonged filmwise condensation. Hampson (79) has found that suitably prepared copper surfaces would maintain filmwise condensation for periods up to 24 hours.

Finally the question of ready availability of the tube is of importance.

On the basis of these considerations, it was decided to use commercially available copper tubing of the dimensions specified earlier. The main advantages being, the ready availability of leads, tubing and copper strip for fabrication of the tube assembly. Fabrication itself could easily be carried out using soldering techniques. The tubing consists of 99.85% Copper; up to 0.04% maximum Phosphorous with the remaining percentage being impurities. The long term electrical stability of the annealed tubing was found to be very good. The temperature coefficient of resistance was consistant at $0.0026^{\circ}C^{-1}$ and the specific resistance at 20°C was 2.65×10^{-6} ohm cm. These changes in the values of α and ρ from those quoted earlier for pure copper are qualitatively in agreement with the observations of Powell (82) who found for a sample of commercial purity copper tested, that $\alpha = 0.0016^{\circ}C^{-1}$ and $\rho = 4.1 \times 10^{-6}$ ohm cm.

This means that the sensitivity S for the commercial copper tube used would be $3.04^{\circ}C/\mu\Omega$. Recalling that the Kelvin double bridge to be used is capable of detecting changes of $0.1\mu\Omega$. It is

found that with the system used here, temperature changes of the tube of about 0.30°C can be detected. It is interesting to note that the sensitivity has not differed from that of the high purity copper.

Having decided upon the tube material and dimensions it now becomes necessary to clear two points. The first being to show that I^2R heating effects of the tube are negligible compared with the condensation heat load, and therefore its effect on wall temperature will be negligible.

The second point concerns the resistance temperature calibration of the tube and its subsequent use to predict the tube temperature under conditions where condensation is present.

12.6. I^2R Heating Effects in the Copper Tube

For a maximum tube resistance of about 200 $\mu\Omega$ and a current through the tube of about 20A (the actual current drawn by the Kelvin bridge was somewhat less – 9.5A) the I^2R heating would be about 0.3 Btu/hr. the condensation heat load would be of the order of 10,000 Btu/hr which would be a fairly typical value. Hence the I^2R heating effect would be negligible.

12.7. The Tube Resistance under Condensation Conditions

In the calibration of the resistance tube, the method usually adopted consists of immersing the tube in a thermostatically controlled calibration tank filled with heated water or oil. Under these conditions the temperature resistance characteristics of the tube can be plotted in the form of a calibration curve. Under these conditions there is no temperature gradient across the tube wall, there is no variation of temperature around the circumference of the tube, and finally there is no variation of temperature along the tube length. However, when the tube is installed as a condenser tube under test conditions there will be a gradient in temperature across the wall of the tube because of the heat flow due to condensation, because of the variation in the condensate film thickness round the tube there will be a temperature variation around the tube and finally because of the cooling water flow through the tube there will be an axial gradient in temperature along the tube. It is proposed here to see what effects these variations have on the resistance of the tube, and to obtain corrections for these effects so that a correction may be applied to the calibrated resistance and hence the average outside tube surface temperature obtained.

Two studies of this problem have been made the first by Jeffrey (78) and the second by Watson and Clark (83).

In the study of the temperature gradient across the condenser wall Jeffrey assumed a linear temperature profile for a thin walled tube, whereas Watson and Clark did not. In the study here with a tube wall thickness of 0.040 ins. the assumption of a linear temperature profile would appear reasonable. This can be shown in a much simpler manner than that adopted by Jeffrey as follows. The heat conducted through a hollow cylinder is given by

$$Q = \frac{2\pi k L (\theta_o - \theta_i)}{\log_e r_o/r_i} \qquad 12.7.1.$$

where k is the thermal conductivity of the material, L is the tube length and θ_o and θ_i are the temperatures at radii r_o and r_i from the axis of the tube. At steady state conditions it is also known that

$$Q = \frac{2\pi k L (\theta - \theta_i)}{\log_e r/r_i} \qquad 12.7.2.$$

where θ is the temperature in the wall at radius r from the axis. Equating 12.7.1. and 12.7.2. and re-arranging

$$\frac{\theta - \theta_i}{\theta_o - \theta_i} = \frac{\log_e (r/r_i)}{\log_e (r_o/r_i)} \qquad 12.7.3.$$

Now $r_o = r_i + t$ and $r = r_i + y$ where t is the thickness of the tube wall and y is some distance into the wall from r_i but less than t. then

$$\frac{\theta - \theta_i}{\theta_o - \theta_i} = \frac{\log_e \left[1 + y/r_i\right]}{\log_e \left[1 + t/r_i\right]} \qquad 12.7.4.$$

using the fact that $\log_e(1 + x) = x - \frac{x^2}{2} + \frac{x^3}{3}$ ------ it can be seen that when t/r_i is small.

$$\frac{\theta - \theta_i}{\theta_o - \theta_i} = \frac{y}{t} \qquad 12.7.5.$$

In fact for the tube used in this study the second term of the $\log_e(1+x)$ expansion is about 6% of the value of the first term, so the assumption of a linear temperature profile across the tube wall is justified.

Using the assumption of a linear temperature profile Jeffrey

obtained

$$\frac{R}{R_m} = C \qquad 12.7.6.$$

where R is the resistance of the tube at θ with no temperature gradient across it, and R_m is the resistance of the tube under conditions of heat flow across the wall, its value being determined at θ_m, the mean of θ_o and θ_i.

Now
$$C = \frac{1}{\frac{2(r_o/r_i - 1)(1 + D)}{\alpha_m (\theta_o - \theta_i)(\frac{r_o}{r_i} + 1)} - D} \qquad 12.7.7.$$

and
$$D = \frac{\log_e \left[\frac{2 - \alpha_m (\theta_o - \theta_i)}{2 + \alpha_m (\theta_o - \theta_i)} \right]}{\alpha_m (\theta_o - \theta_i)} \qquad 12.7.8.$$

Jeffrey calculated the value of C for various values of $(\theta_o - \theta_i)$ and (r_o/r_i) making the erroneous assumption that $\alpha_m = 0.0023^{\circ}F^{-1}$ for all metals. However by chance the value of α_m chosen by Jeffrey is numerically close to the value of α obtained in the experiments discussed by the author on a commercial grade copper tube, and since $\alpha_m(\theta_o - \theta_i)$ appears in 12.7.7. and 12.7.8. and is a pure number, use of Jeffrey's results for C may be used with little error here. These results for $r_o/r_i \simeq 1.1$ are shown plotted in figure (12-3)

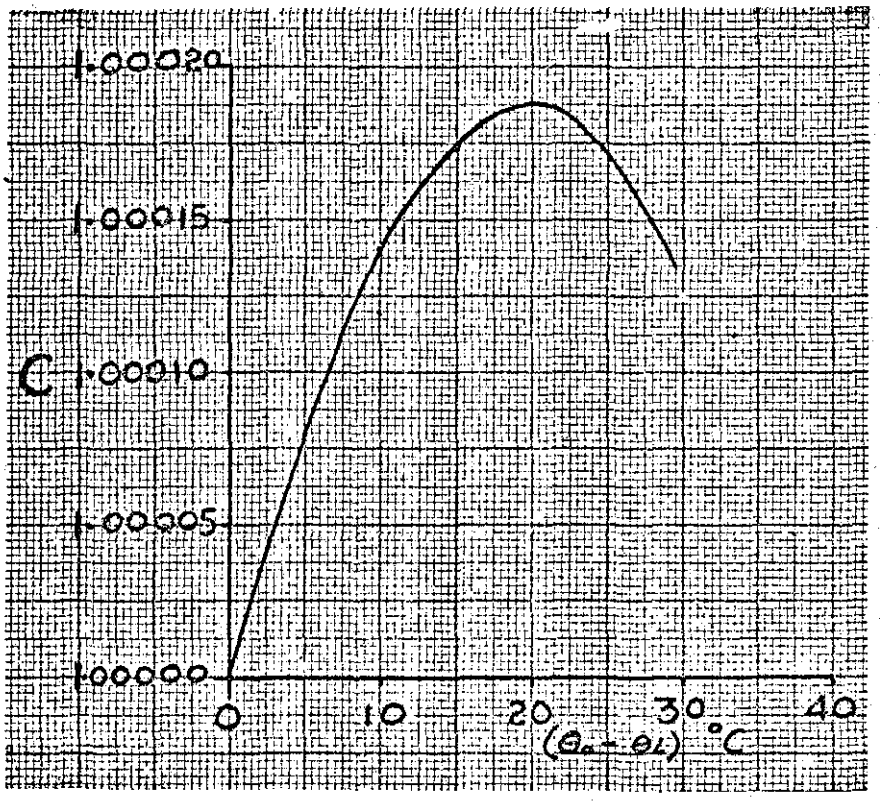

Fig. 12-3 The Ratio of tube Resistance under Isothermal Conditions to to Mean temperature conditions versus temperature difference across the tube after Jeffrey Ref. (78)

From figure (12- 3) it is clearly seen that the effect of temperature gradient across the tube wall is quite negligible. At high values of $(\theta_o - \theta_i)$ i.e. greater than 30°C, the value of C continues to decrease attaining values that are only very slightly smaller than unity.

Again in the case of temperature variation around the tube Jeffrey and Watson and Clark differ in their approach. Jeffrey working from experimental measurements of tube wall temperature variation, found that these could be suitably approximated by a cosine wave. On this basis Jeffrey found that there was a negligible correction for R required, the error resulting from neglecting the correction being of the order of 0.01%. Watson and Clark determined the temperature distribution around the circumference of the tube wall with the aid of Nusselts condensation theory for the horizontal tube, they found that a slight correction had to be made which effectively raised the temperature of the tube surface by about 1°C. However in the light of the earlier discussion on the Nusselt theory and its

tendency to underestimate the condensation heat transfer coefficient, it would appear that the correction would be smaller if not negligible if this fact were taken into account. Since the higher heat transfer coefficient would result in increased condenser tube surface temperature. Therefore Jeffrey's finding would appear more probable.

Finally Jeffrey shows that the measured resistance of the tube will be the average value for a given temperature variation along the tube.

From the foregoing discussion it can be concluded that when the resistance tube is operating in the condenser, its resistance will correspond to the mean wall temperature θ_m; this temperature can be readily obtained from the tank calibration curve of resistance versus temperature. The average outer surface temperature θ_o is obtained from

$$\theta_o = \theta_m + \frac{(\theta_o - \theta_i)}{2} \qquad 12.7.9.$$

where from equation (12.7.1.)

$$\theta_o - \theta_i = \frac{Q/A_o \cdot D_o \log_e \left[r_o/r_i\right]}{2k} \qquad 12.7.10$$

Q is obtained from the heat transfer on the waterside measurement, and k is computed from a knowledge of the electrical resistivity of the tube. Powell (82) obtained the following empirical relation relating the thermal conductivity to the resistivity.

$$k = 57.7 \left[2.39 \times 10^{-8} \frac{T}{\rho} + 0.075\right] \text{ Btu/hr ft } ^oF \qquad 12.7.11.$$

where T is in ^oK and ρ is in ohm cm.
For the value of $\rho = 2.65 \times 10^{-6}$ ohm cm. obtained by the author $k = 157$ Btu/hr ft ^oF this compares qualitatively with the value of 115 Btu/hr ft ^oF obtained by Powell.

Having discussed the two major points of how the horizontal tube is to be oscillated, and how the condensation heat transfer coefficient is to be determined, the next section will deal with the details of the experimental rig and some of the other instrumentation used.

13.0 DESIGN AND CALIBRATION OF THE EXPERIMENTAL RIG AND INSTRUMENTATION FOR THE STUDY OF CONDENSATION ON A HORIZONTAL TUBE IN A VERTICAL MODE OF OSCILLATION

13-1 The Condenser Shell

A condenser shell from a previous project was found to be available. This shell which is shown in a sectional view in figure 13-1 and in the photographs figure 13-2, consisted of a 6 in internal diameter cylindrical steel tube $\frac{1}{4}$" thick onto which was brazed a brass hood section of $\frac{1}{8}$" plate with a copper steam inlet pipe 3 ins. in diameter. (The reason for the brass hood section was that in the previous project the condenser was filled with a tube bundle, and deposits from a corroded hood on the tube bundle were to be avoided - hence the choice of brass). The holes in the steam delivery pipe were drilled at an angle to the vertical to avoid steam jets impinging directly onto the heat transfer surface. The brass hood contained three windows $3\frac{1}{2}$ x $2\frac{1}{2}$ ins.; two located at the centre of the condenser, on either side of the hood, and the third located to one side as shown in the figure. The cylindrical section contained six circular ports 1 in. diameter for instrumentation (or observation). The bottom of the cylinder had three flanged drainage pipes as shown in figure 13-1. The condenser shell was closed with steel end plates as shown in the photographs, the end plates carrying a single cylindrical opening pipe through which a rubber cooling water tube was fed.

This condenser shell appeared to be suitable for the study projected here, since the yoke assembly carrying the copper tube could be arranged to lie so that the tube was in view of the windows in the hood. The coupling link between the yoke and the vibrator could pass through a suitable bush located in the central drain in the condenser bottom. By suitably arranging a tray between the condenser tube and the T section of the yoke, the condensate could be drained from either of the other drains located in the bottom of the shell.

A simple Dexion frame could locate the condenser shell in a convenient position above the anti-vibration bed carrying the vibrator. In fact the shell frame could be fastened to the anti-vibration bed.

The above ideas were adopted, the anti-vibration bed consisted of a 4ft 6in. 6 in. by $\frac{3}{8}$ ins. thick I girder 16 in. deep placed on the concrete floor of the laboratory, the Dexion frame carrying the condenser shell being bolted to the I beam. This is shown in figure 13-3, where the position of the vibrator will also be noted.

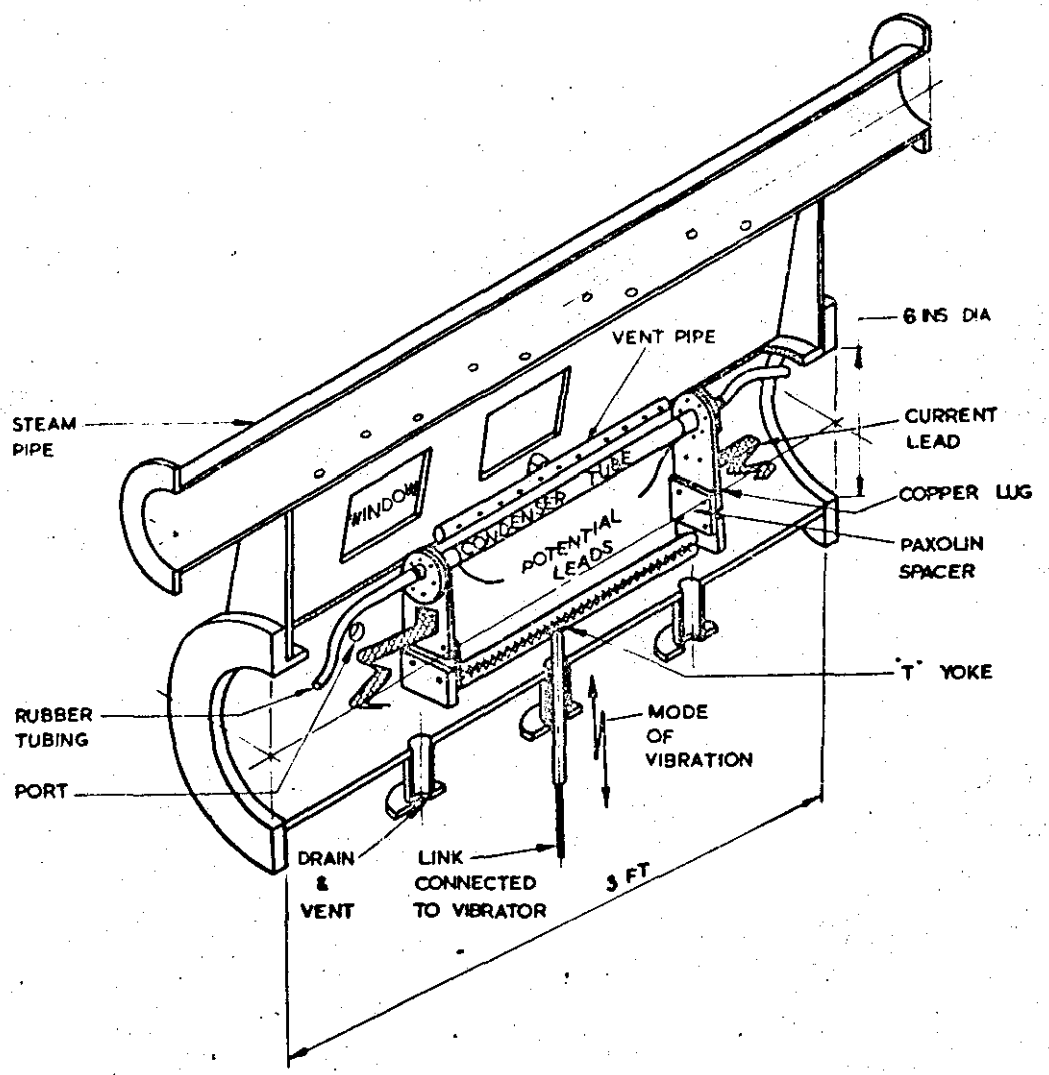

FIGURE 13.1. Sectional Drawing of Condenser Shell Showing Tube and Yoke in Position.

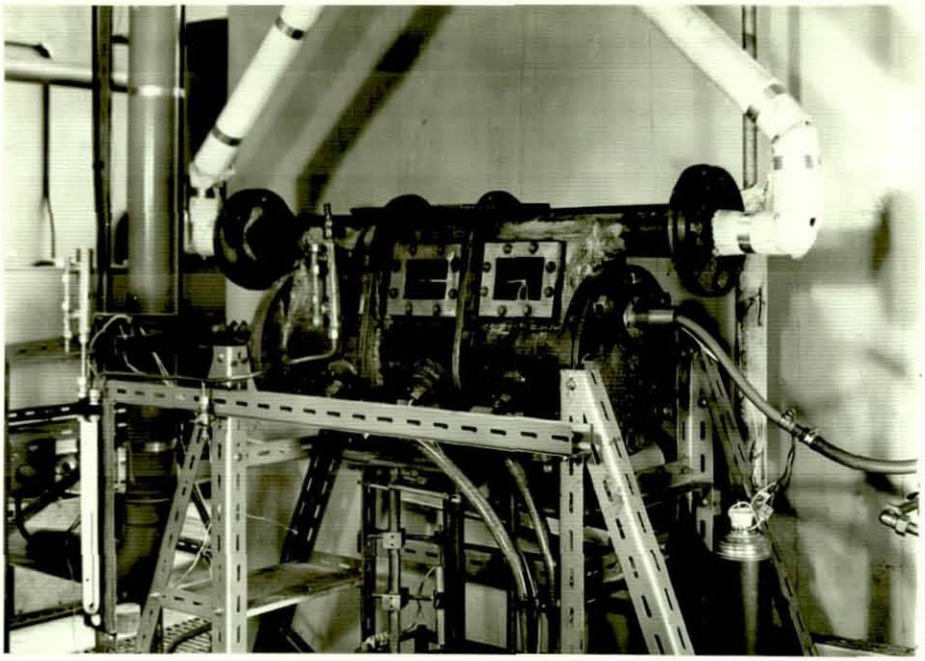

Fig. 13-2 (a) View of Condenser Shell Showing End Cover Plate in Place

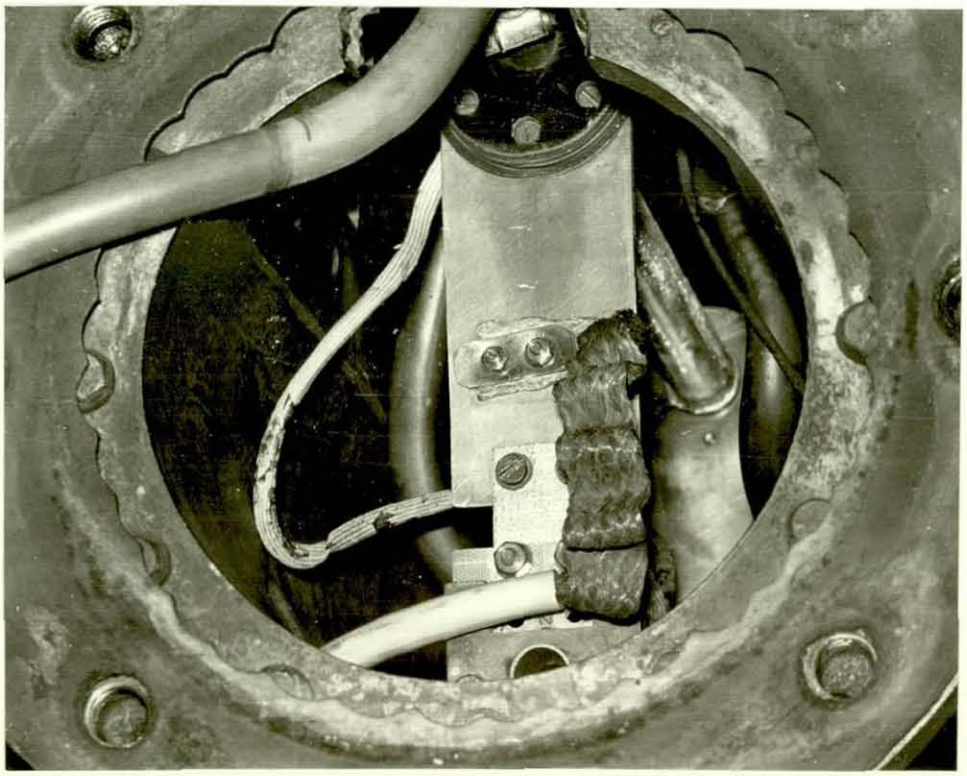

Fig. 13-2 (b) View into Condenser Shell with End Cover Plate Removed

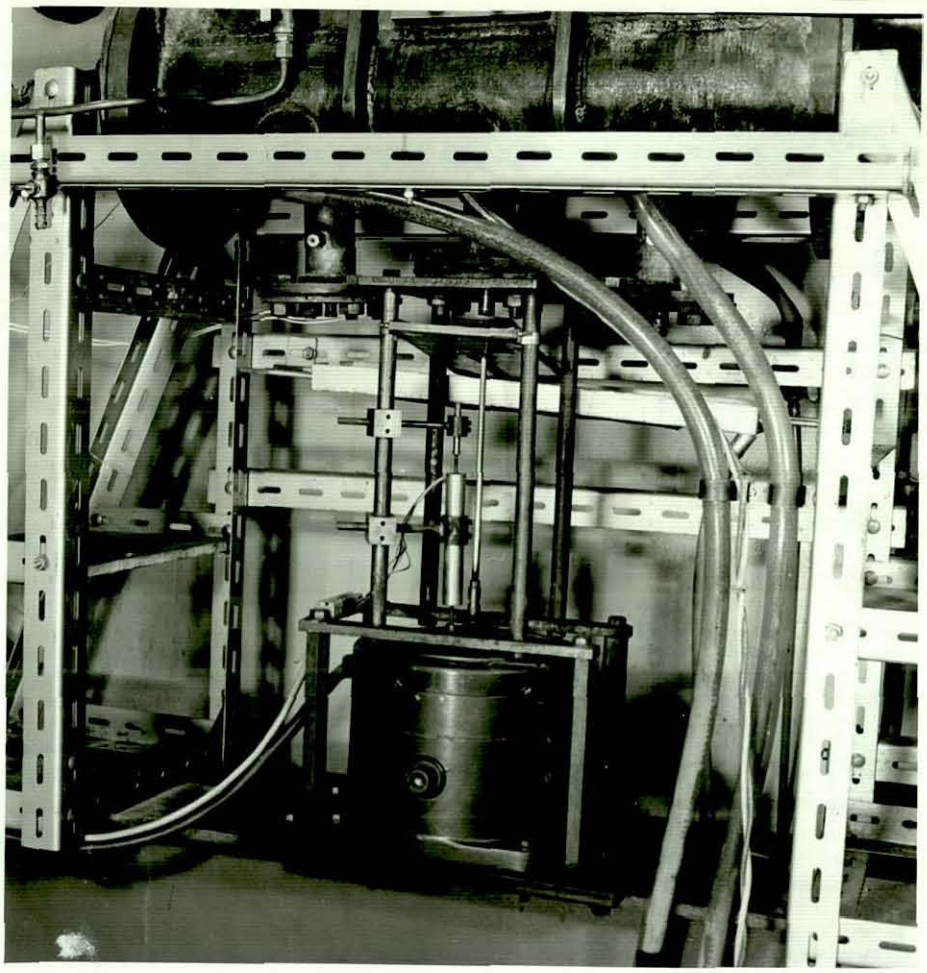

Fig. 13-3 Method of Mounting Condenser Shell on Anti-Vibration Bed

13.2. The Steam Supply

The steam supply to the Condenser shell through the copper steam inlet pipe was from a Stone Vapour Generator which was used for general project work in the laboratory. This boiler was capable of delivery up to 1000 lbm/hr of saturated steam at preset pressures from 40 to 150 p.s.i.g. The boiler was fully automatic and could maintain the delivery pressure to within $\pm$ 1 p.s.i.g. Because of the delivery of saturated steam from the boiler, the boiler was operated at pressures of between 80 - 100 p.s.i.g. the steam being throttled down through a safety value followed by a needle control valve in the line to a pressure which was about 1 to 2 inches of mercury above atmospheric pressure in the condenser shell.

Because the steam line to the condenser was unlagged the steam reached the condenser shell superheated by about 2^{o} - 3^{o}F. A steam strainer was fitted in the main steam line to trap foreign matter from the line. A blowdown system was incorporated in the steam line just ahead of the condenser inlet, this enabled condensed steam and corrosion accumulation in the line between experimental runs, to be cleared before testing was started.

The boiler could not operate on the fully automatic mode at loads below 100 lbm/hr; to overcome this difficulty a second condenser rig on the same line was run so that the minimum load could be achieved for automatic operation.

13.3. The Water Supply

Because of regulations made by the local Water Board, it was not possible to contemplate an experiment in which the cooling water was passed through the condenser tube, weighed and then discharged to waste.

In the system employed in this study the water was circulated by a pump through the condenser tube and then to the laboratory cooling tower, the pump inlet being connected to the cooling tower sump. Downstream of the condenser tube a two way cock was placed in the water line, this enabled a weigh tank to be brought into operation for calibration runs. The water flow was measured upstream of the condenser by means of a venturi tube in the $\frac{1}{2}$ in. bore water line, the venturi operated in conjunction with a compressed air manometer described later under instrumentation.

A line diagram showing the water and steam circuits to the condenser shell is shown in figure (13-4).

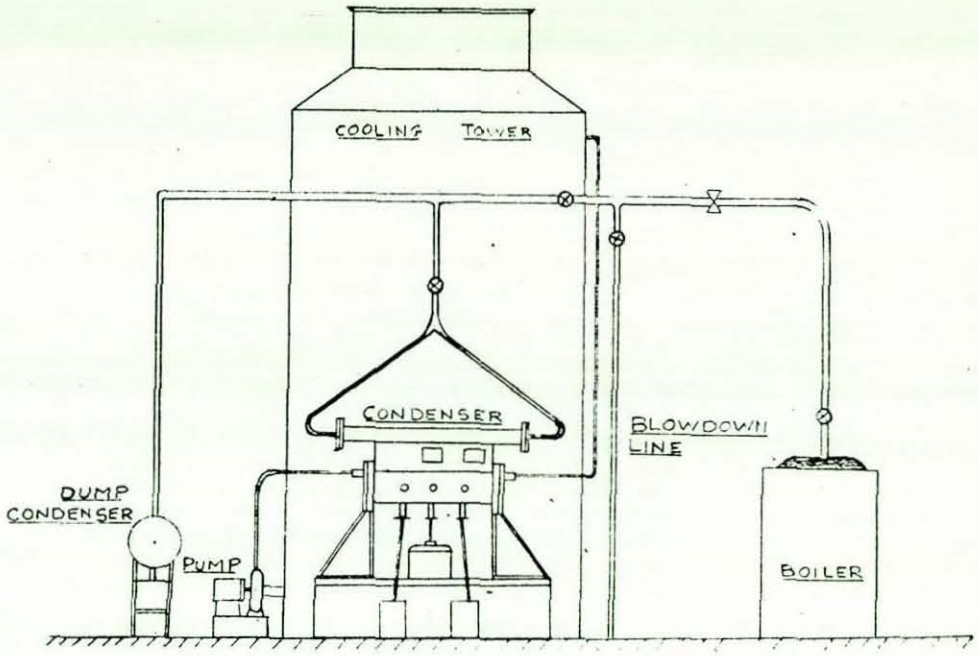

Fig. 13-4 Water and Steam Circuits to Condenser Rig.

13.4. The Condenser Tube and Yoke Assembly

As mentioned earlier, the condenser tube was of commercial copper 0.75 ins. I.D. and 0.83 ins. O.D. The copper tube was 13⅛ ins long and mounted between two copper end lugs as shown in figure 13-5. The two end lugs were to be connected to the current carrying leads by means of two 2 B.A. screws located near the bottom of the lug. The potential leads on the tube were located 12 ins. apart and were soldered onto the tube surface. These leads consisted of pure copper braid which when flattened had a rectangular section of ⅛ ins. x 1/16 ins., each lead was 8 ft long and had a resistance of 0.026 Ω

Each end of the tube was closed with a flange held to the end lug by six 4 B.A. screws. The end flanges carried ¼ ins. copper tube stubbs 2 in. long for inlet and outlet hose connections; the outlet water tube connection was set very close to the top of the condenser tube I.D. this ensured that the condenser tube would be full of water during operation.

The overall length of 13⅛ ins of the tube assembly left

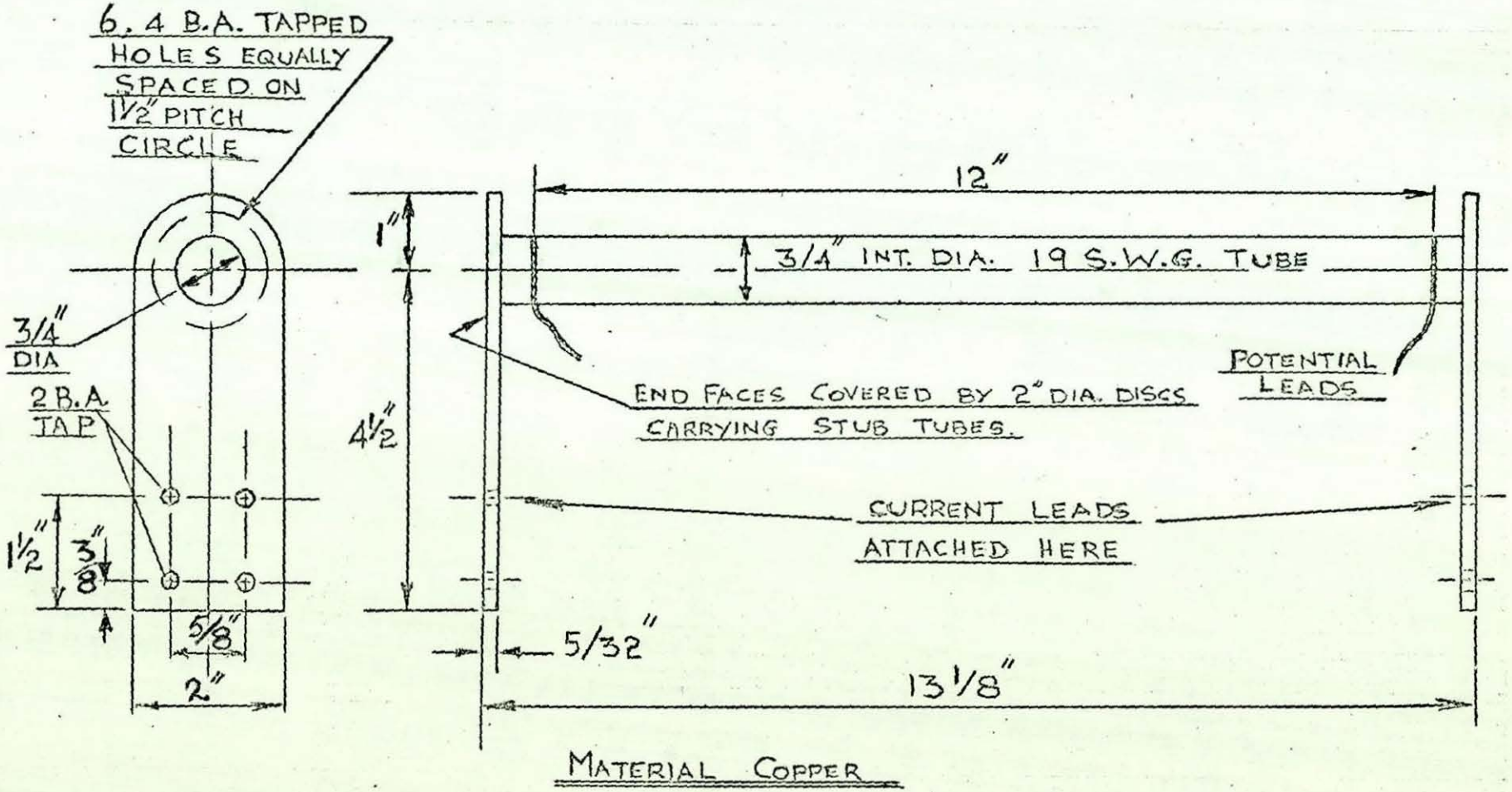

FIG 13-5. DETAIL OF CONDENSER TUBE

Fig. 13-5 Detail of Condenser Tube

Fig. 13-6 (a) Stainless Steel Yoke for tube Assembly

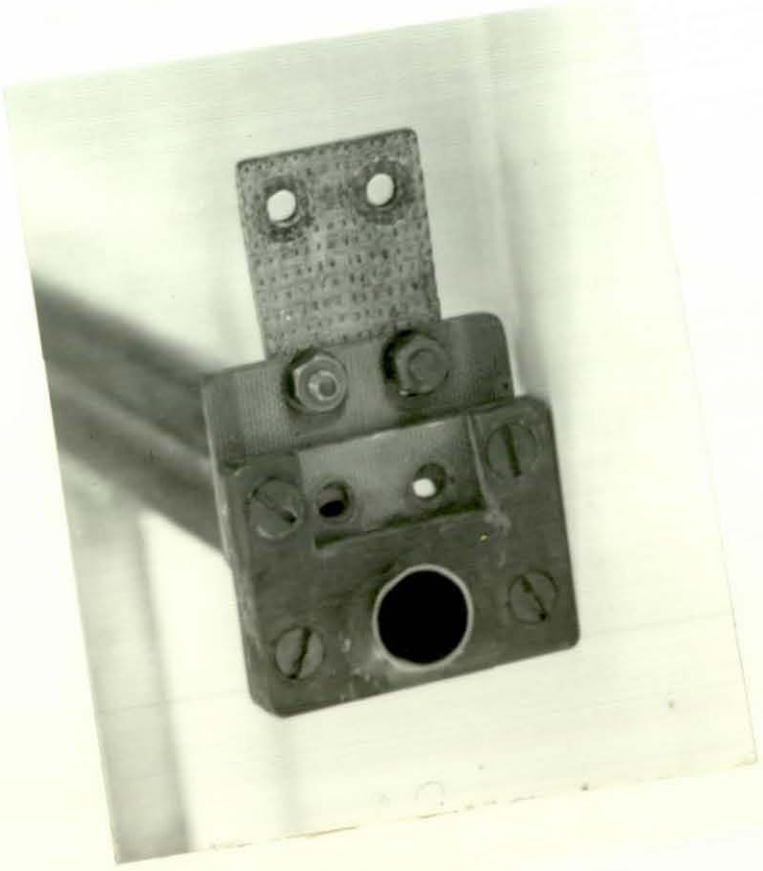

Fig. 13-6 (b) Detail of end fixing of Yoke for tube Assembly

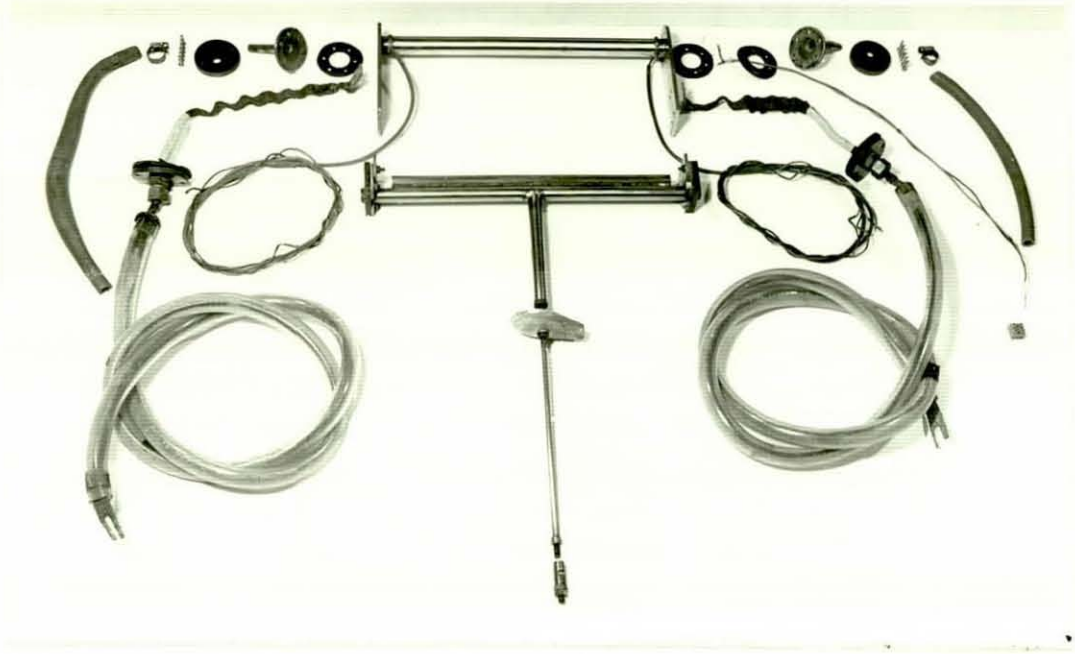

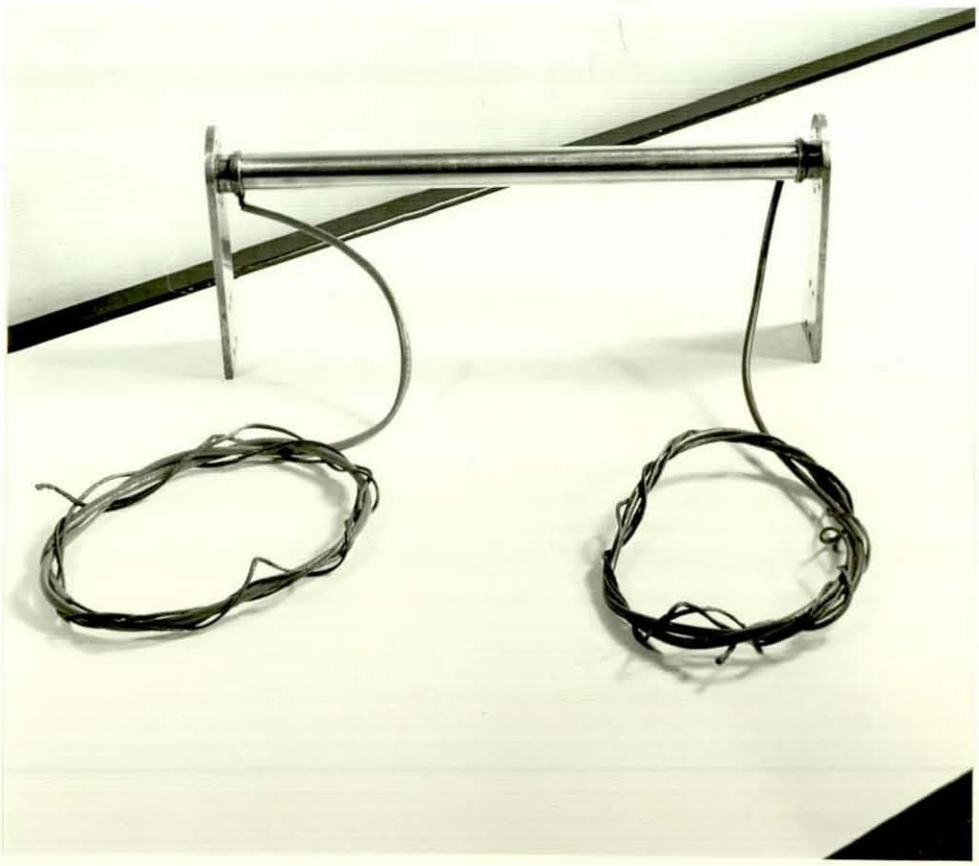

Fig. 13-7 Exploded Assembly of Copper tube and Yoke and Photograph of Condenser tube

approximately six inches on either end of the tube when it was in its assembled position in the shell, this gave good flexibility to the assembly and allowed adequate vibrational displacement of the tube, without severe stress on the rubber hose.

The yoke assembly is shown in figure 13-6. This was constructed from $\frac{5}{8}$ in. stainless steel tubing in the form of a T as shown. The steel end plates with Paxolin inner facings gave a dimension of $13\frac{1}{2}$ ins. between the inner facings, a further build up of $\frac{1}{8}$ in. of Paxolin sheet on either face followed by a further 1/16 ins. brought the dimension between the inner facings to $13\frac{1}{8}$ ins. which agreed with the dimension between the outsides of each copper lug. (The reason for the crude build up with successive layers of Paxolin was that originally it was thought that 3/16 in. Paxolin sheet would be available, however, this size was not available from stock). By using the Paxolin strips to connect the copper lugs on either end of the condenser tube to the T section, the tube assembly was electrically isolated from the rest of the yoke assembly.

A $\frac{1}{4}$ inch steel rod connected the bottom of the T section to the vibrator ; this rod carried an aluminium condensate catchpot and drain which ensured that condensate did not run down the connecting link onto the vibrator below.

A photograph of the full assembly is shown in figure 13-7. It should be pointed out here that the heavy current leads attached to the lugs were made from braded copper which when flattened was $\frac{3}{4}$ ins. x $\frac{1}{8}$ ins. these leads were each 7 ft long and had an electrical resistance of 0.0027Ω

The potential and current leads were encased in insulated sleeving and run through suitably sealed flanges covering the 1 inch openings in the condenser shell.

13.5. Measurements and Instrumentation

In this section the various measurements that need to be taken and the associated instrumentation will be discussed.

Temperature of Steam and Cooling water

The temperature of the steam and cooling water were measured by means of 26 S.W.G. Copper Constantan thermocouples. The Steam temperature measurements were taken with two independent thermocouples mounted in the shell in the vicinity of the condenser tube. The thermocouples were located at the end of an L shaped pocket made from $\frac{1}{8}$ in. O.D. copper tubing, the thermometer pockets were electrically

insulated from the condenser shell, and had an overall length of 6 ins. The cooling water inlet and outlet temperatures were each measured with a single thermocouple. The inlet thermocouple was wound in the form of a spring which fitted inside the rubber hose the hot junction end was located so that it was almost at the edge of the inlet water stub pipes. There was no possibility of the hot junction touching the copper stub pipe as it was turned into the spring see figure (13-8a)

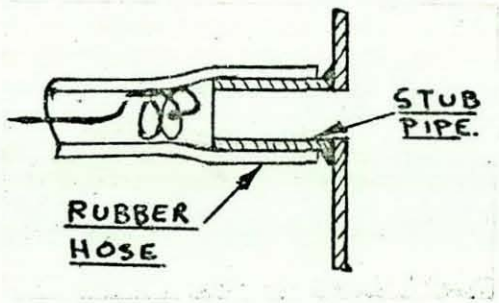

Fig. 13-8a Inlet water temperature thermocouple arrangement

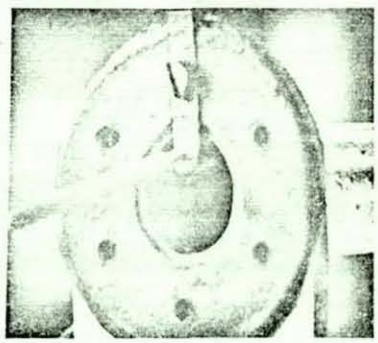

Fig. 13-8b Outlet water temperature thermocouple arrangement

The outlet water thermocouple was held by a stiff brass bracket so that the hot junction coincided with the outlet plane of the tube, this is shown in figure(13-8b) the thermocouple was thermally insulated from the bracket with Araldite. The thermocouple leads were taken out of the water line at points where the rubber hoses were connected with a copper jointing tube.

The thermocouples were all operated with their own cold junctions. These were sealed in individual glass tubes which were immersed in a thermos flask of ice.

Temperature measurements at steady state conditions were recorded on a Pye Precision Vernier Potentiometer operating in conjunction with a Pye Scalamp Galvanometer. This system was operated on a sensitivity scale which enabled e.m.f. changes down to 1μv to be determined. For the samples of copper-constantan used here the sensitivity in $^{o}C/mv$ was 22.8. Therefore the potentiometer system used here could detect changes of temperature of $0.0238^{o}C$ ($0.0428^{o}F$). To assist in determining the attainment of steady state conditions a multi channel Kent self balancing and recording potentiometer was used for the initial stages of each test run for recording steam and water side temperatures. When the chart record on the Kent indicated steady conditions, the thermocouple connections were transferred to the Pye Vernier potentiometer and final readings taken.

The thermocouples were calibrated in batches in a thermostatically controlled heated water bath, against N.P.L. calibrated thermometers graduated in 0.1°C increments. These calibrations were observed to be uniform for the whole batch of thermocouples, the e.m.f. versus temperature graph for the batch is shown in Appendix (VI) fig. 1.

Water Flow Measurement

This was carried out with a venturi tube fitted in the ½ ins. I.D. water line. The venturi tube had a throat to pipe I.D. ratio of 0.75 the diffuser angle on the venturi being 5° Undisturbed lengths of greater than 80 times the pipe I.D. were maintained upstream and downstream of the venturi. The pressure taps on the venturi tube were connected by polythene piping to a compressed air manometer. This simply consisted of two glass manometer tubes 36 ins. long by 5/16 ins. O.D., the lower end of each tube was connected to one of the pressure lines from the venturi tube. The upper ends of the two tubes were each connected to one branch of a Y connector made from copper tubing. These two branches of the Y terminated in a common leg which was brazed to a small air tight cylinder which had a bicycle tyre valve assembly attached to it.

Operation simply consisted in unscrewing the bicycle valve and lowering the manometer below the level of the water line - this was done by laying the manometer board horizontal. This caused the water from the line to flood through the system. The bicycle valve was screwed into place and air pumped into the system slowly. This forced the water down into the limbs of the manometer to a common height. Any pressure differential recorded with water flow through the venturi was simply recorded as a difference in head of water on the manometer. Precautions had to be taken to see that air bubbles were not left trapped in the polythene pressure lines after the pumping operation. The system is not sensitive to changes in ambient temperature or small air leakage from the system, since both these effects cause identical air pressure changes on each limb of the manometer.

The venturi was calibrated directly against a weigh tank this calibration being shown in Appendix (VI) fig. 2. From the calibration it can be seen that the water flow rate through the condenser tube can be determined with an accuracy of ± 3% at the outside, this allows for the possible error on the weigh scale which was calibrated itself with standard weights.

Amplitude and Frequency Measurement

The amplitude of oscillation was measured with a type 585 DT - 500 Differential Transformer in association with a type 592 - 300 Transducer Converter. This equipment is produced by the Sanborn Corp., Mass., U.S.A.

The transducer is of the linear differential transformer type, a schematic diagram of the transducer and converter being shown in figure (13-9).

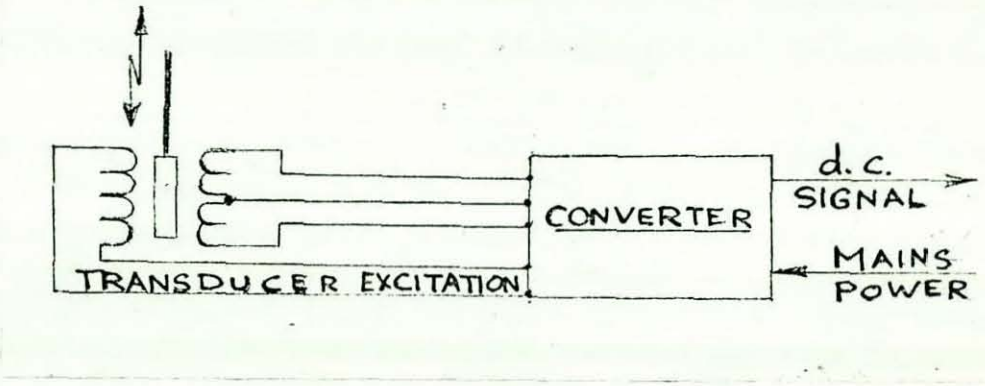

Fig. 13-9 Schematic Circuit Diagram of Sanborn Displacement Transducer

A cylindrical barrel with a central bore houses three windings. A primary coil which is fed from an external a-c exitation (the carrier wave generated in the converter unit) and two secondary coil windings which are connected series opposing. A soft iron core is free to move up and down in the central bore.

When the soft iron core is at the centre of the barrel equal voltages are induced in each secondary winding, hence there is zero output from the secondary circuit. When the soft iron core is moved away from the centre of the barrel a greater voltage is induced in one secondary compared with the other and there is an output voltage from the secondary, which represents the core displacement and its direction. The output from the secondary winding is fed back into the converter unit from which the output is a d.c. signal which is linearly dependent on the core displacement. The transducer was capable of measuring maximum displacements of $\pm$ 0.500 ins.; the

frequency response of the instrument being limited by the carrier wave frequency of 2.4 Kc/s.

The iron core had screwed into each of its ends a 3/32 in. dia. brass rod. The free end of one of these rods was screwed into the driving head of the vibrator adjacent to the driving link which oscillated the yoke assembly; the free end of the second rod was passed through a bush supported from a pillar on the vibrator. This enabled the core movement to correspond to that of the oscillating tube, while it was kept central in the bore of the transducer barrel. The transducer barrel was held in a clamp fixed to a pillar located on the vibrator. This enabled the barrel position to be adjusted for the zero reading, when there was no motion of the vibrator. See figure (13-10) which shows the transducer in position.

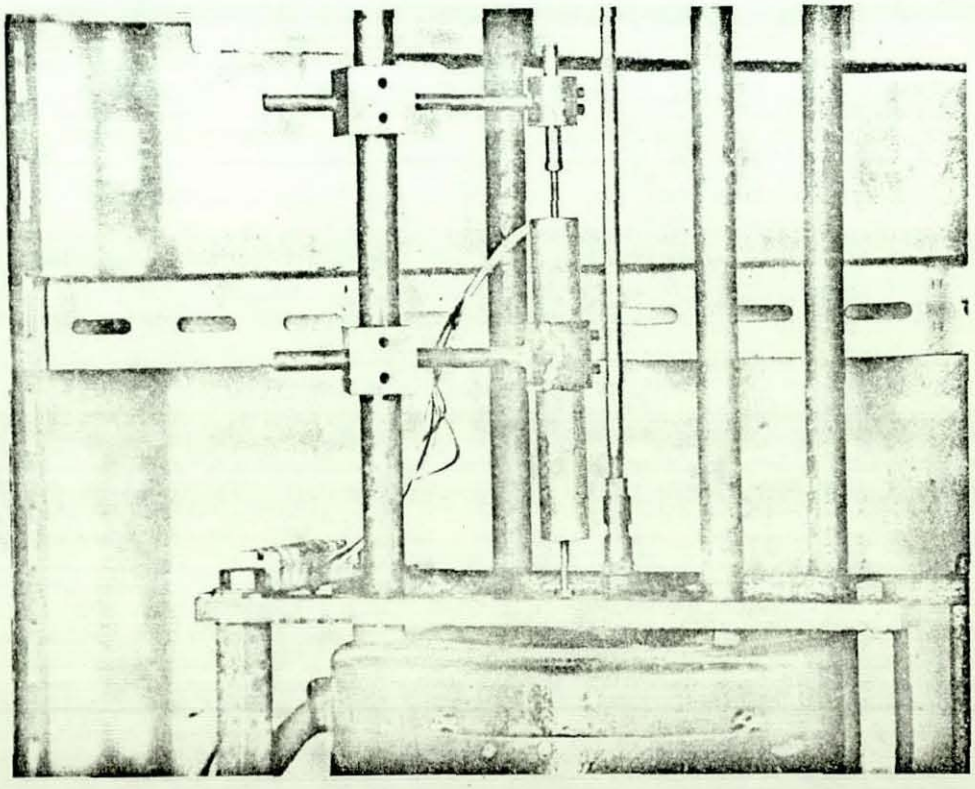

Fig. 13-10 Displacement Transducer Mounted on Vibrator

The d.c. output from the transducer was fed to an oscilloscope. A calibration had to be carried out to relate displacement of the scope trace with displacement of the core, this was simply done by unscrewing the rod on the driving head, adjusting the barrel for zero output, and then obtaining set displacements of the core with slip gauges placed between the driving head and the unscrewed rod, the corresponding displacement of the trace on the oscilloscope being noted. Before the calibration run the oscilloscope itself was calibrated against its own calibration waveform. The accuracy to which measurements of amplitude could be made was estimated at $\pm$ 0.002 ins. During test runs, the peak to peak value of the displacement waveforms were noted, half this value being used as the peak amplitude of oscillation. The voltage displacement characteristics of the transducer obtained with the oscilloscope are shown in Appendix VI figure (3).

Frequency of oscillation was noted directly from the frequency setting on the oscillator . This was found to agree with the frequency of the vibrator output in the range 20 - 100 c/s. This was verified by feeding a tapping from the output of the oscillator to the x plates of an oscilloscope, and feeding the transducer output to the Y plates. The results in all cases was a circular trace on the scope this according to Van Santen (84) is the path traced by a point common to two sinusoidal oscillations of identical frequency travelling at right angles to each other with a phase angle of 90° between them. This phase difference is to be expected, there is a negligible phase shift in the oscillation signal in its passage through the power amplifier and a 90° phase shift between the mechanical output from the vibrator and the input current. This effect is due to the characteristics of the electro-magnetic vibrator. This device produces a force F which is proportional to the input current i. The applied voltage e must then be proportional to dx /dt the velocity of vibration. This must be so since i·e must be equal to the mechanical power output from the system times an efficiency of conversion, therefore i·e is proportional to $F.\frac{dx}{dt}$. Now since e = constant $\frac{dx}{dt}$, then x the vibration displacement is $\int e.dt/\text{constant}$. For a sinusoidal variation of e with time it is seen that x is 90° out of phase with e because of the integration. Hence the output waveform from the transducer will be 90° out of phase with the oscillator output. The important fact here is that the frequency of vibrator output is consistent with that

indicated on the oscillator setting dial.

Trigger circuit for Flash Photography

It was decided that photographs of the condensate film could be informative, particularly when the oscillating tube was at points of maximum positive and negative displacement. To do this some form of trigger circuit appeared to be necessary to enable a camera flash gun to be fired when the oscillation amplitude was at a positive or negative peak. The technique adopted here was to black out the area around the condenser and use the camera with the shutter open, and use the trigger circuit to fire an electronic flash unit operated off the mains.

The trigger circuit was constructed in the following way. The incoming a.c. signal from the amplitude transducer was amplified and passed through a selector switch through a variable resistor to the grid of a Thyratron valve. The Thyratron valve is a gas filled Triode, and is a discharge tube. Positive potential, applied to the grid of the Thyratron causes rapid electrical breakdown and ionisation of the gas in the tube, this results in a heavy flow of electrons from the cathode to the anode, and a rapid increase in the anode current. The rapid increase in the anode current can be used to trigger a relay system thus firing the flash gun. The electron flow from cathode to anode is stopped by utilising a secondary relay circuit to break the anode circuit. A manual operation being necessary to reset the system. This system enables the positive peak amplitude to trigger the circuit, the negative peak amplitude is made to trigger the circuit by switching the selector so that the output from the first amplifier I passes through a second amplifier II and then to the variable resistor and Thyratron grid. The second amplifier simply acts as a sign changer so that the negative peak is now able to trigger the circuit. The above discussion is summarised in the schematic diagram shown in figure (13-11)

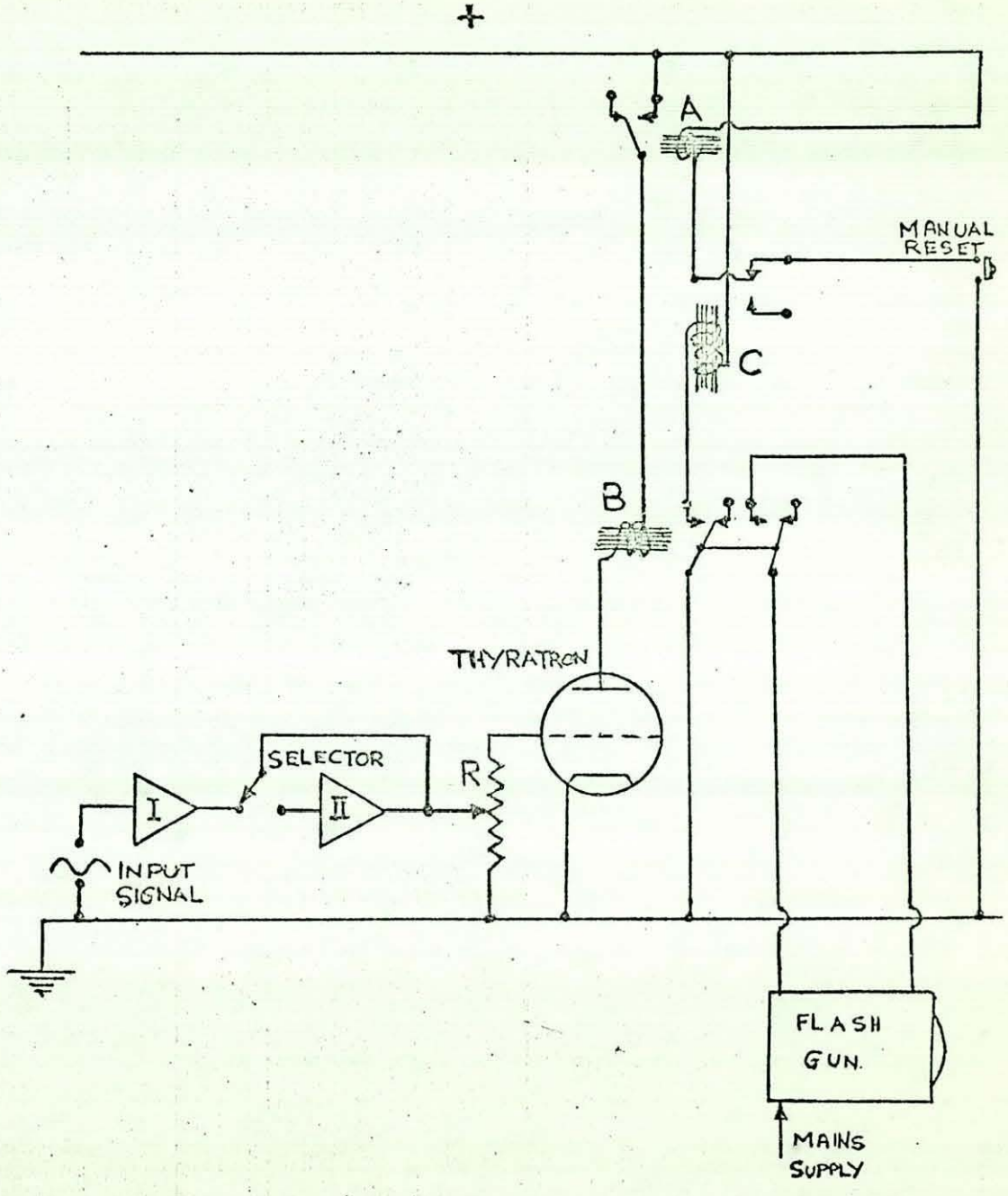

Fig. 13-11 Trigger Circuit for Flash Photography

At the commencement of operation the relays A; B and C are de-energised. Pressing the manual reset button causes A to be energised and the anode circuit closed. The system is now ready for operation. With the selector switch in the position shown the circuit will trigger from the positive (upward displacement of the tube). The amplified signal out of I passes through the variable resistor R to the grid of the Thyratron, a heavy current flows to the

anode energising B, this closes the flash gun circuit causing the gun to fire and also energisesrelay C which causes the anode circuit to open.

To synchronise the flash gun firing with the maximum displacement postions, a stroboscope was used to locate the maximum displacement positions in the oscillation cycle. The grid voltage to the Thyratron was altered by means of the variable resistor R, until the observed maximum position and the flash gun firing coincided.

Tube resistance measurement

This was discussed at some length earlier, here the emphasis will be placed on the calibration of the tube. With the low resistance potential and current leads used here, the effects of lead resistance will be completely negligible. The Kelvin double bridge was operated in conjunction with a reversing switch which enabled the polarity of the e.m.f. from the 2 volt cell to the bridge to be reversed. The tube with attached end lugs and the operational leads was calibrated in a heated thermostatically controlled water tank. The copper lugs being placed on Paxolin sheets to avoid shorting through the metal floor of the tank.

The calibration of the tube resistance with temperature is shown in Appendix (VI) figure 4.

Figures 13-12 and 13-13 show the condenser and associated measuring equipment.

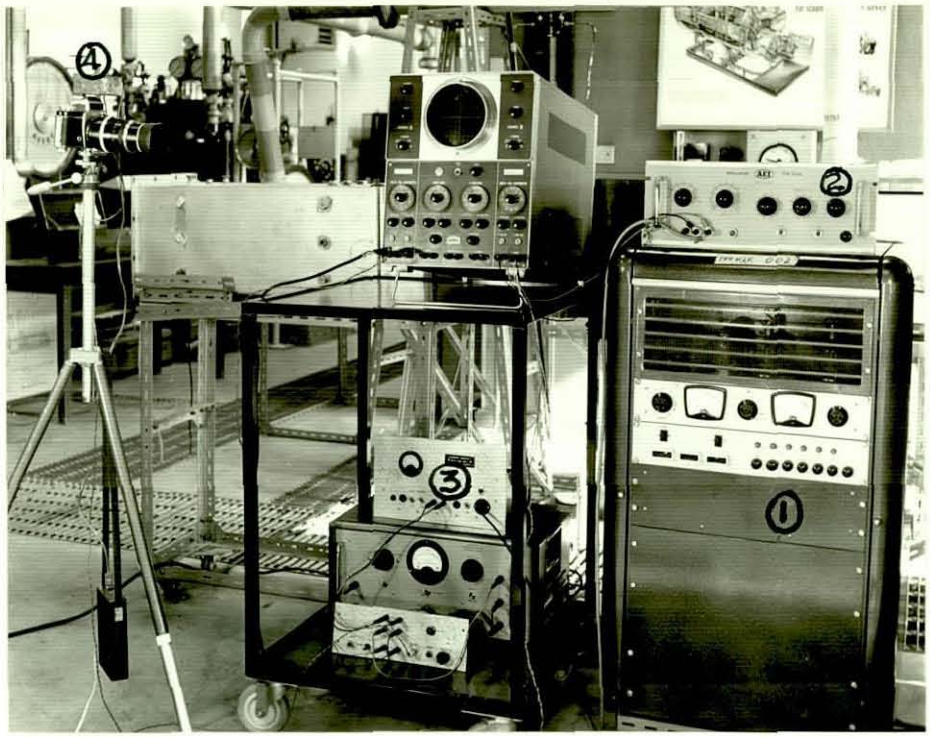

Fig. 13-12 Vibrator Power Amplifier (1) Oscillator (2) Trigger Circuit and Oscilloscope (3) and Flash Gun (4)

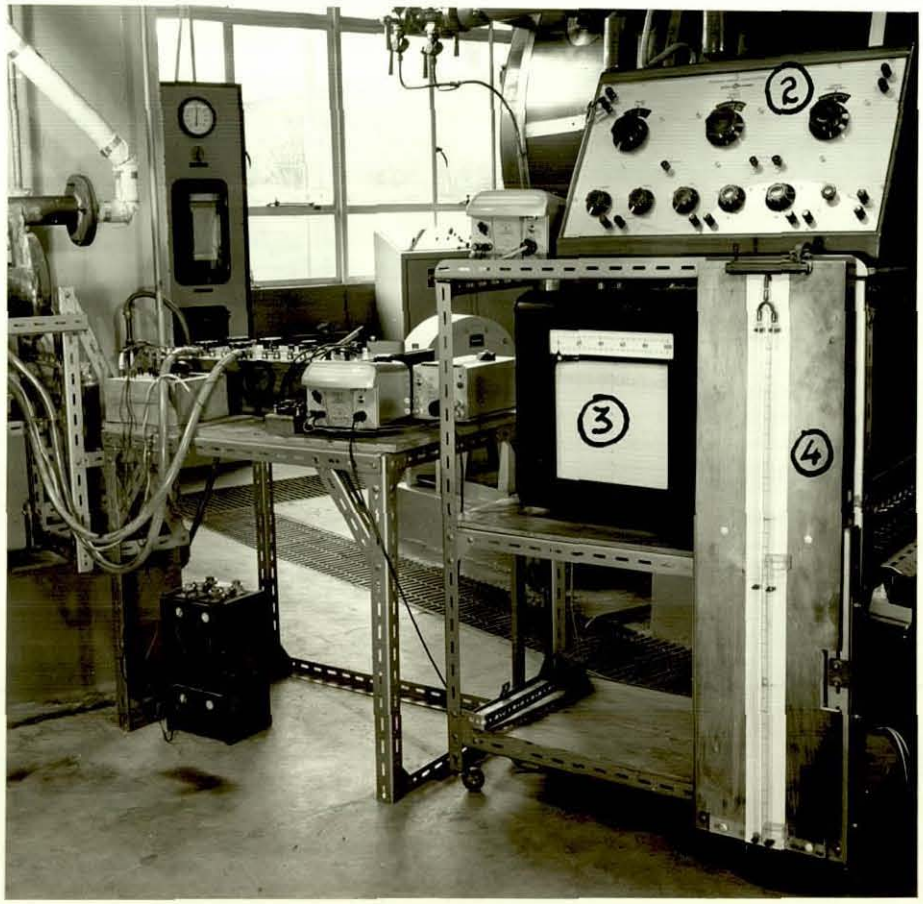

Fig. 13-13 Kelvin Double Bridge (1) Pye Vernier Potentiometer (2) Kent Multi-Channel Recorder (3) Compressed Air Manometer (4)

14.0 ASSESSMENT OF EFFECT OF POSSIBLE EXPERIMENTAL ERROR ON ACCURACY OF DETERMINATION OF CONDENSATION HEAT TRANSFER COEFFICIENT

14.1. Assessment of Overall Accuracy

The condensation heat transfer coefficient is to be computed from

$$h = \frac{Q}{A_o\ (\theta_v - \theta_{\not{s}o}\ )} \qquad 14.1.1.$$

where $Q = m_w,\ C_{pw}\ (\theta_{wo} - \theta_{wi})$

It has been shown that the capability of the temperature measuring system using the Pye Vernier Potentiometer could detect down to 0.043 °F. However the calibration standard could be read to the nearest 0.05°C (0.09°F). Hence ± 0.09 °F is the limit of accuracy of the recording on temperature. If the minimum temperature difference between outlet and inlet cooling water is to be about 4 °F, the maximum possible error in temperature difference would be 0.18 °F this would be approximately a 5% error on temperature difference. The maximum error in determining the water flow rate with weigh tank and stop watch has been found to be about 3%. The determination of surface area on the outside of the tube could be carried out with an accuracy of about 2%. The temperature difference $(\theta_v - \theta_{\not{s}o})$ will be controlled mainly by the error in determining $\theta_{\not{s}o}$ the temperature of the tube wall surface. The error in determining $\theta_{\not{s}o}$ was found to be about ± 0.6 °F. If temperature differences of the order of 15 °F are obtained the possible error in $(\theta_v - \theta_{\not{s}o})$ will be 4%.

To determine the effects of the individual errors on the error in the heat transfer coefficient use is made of the theory of errors. Schenck (85) shows that if R is a result which is some function of measured variables, say, W; X; Y and Z

then

$$R = f\ (W,X,Y,Z) \qquad 14.1.2.$$

If w;x;y;z; are the errors in the determination of the variables then

$$\begin{aligned} W &= W_c + w \\ X &= X_c + x \\ Y &= Y_c + y \\ Z &= Z_c + z \end{aligned} \qquad 14.1.3.$$

where W_c, X_c, Y_c, Z_c are the "correct" values of the variables. The error in the derived result is r; therefore $R = R_c + r$ and from equation (14.1.2.)

$$(R_c + r) = f\ (W_c + w,\ X_c + x,\ Y_c + y;\ Z_c + z) \qquad 14.1.4.$$

If f is asssumed to be continually differentiable, it can be expanded in a Taylor's series. Using the first two terms of the expansion and re-arranging results in

$$r = \left[\frac{\partial R}{\partial W_c}\right] \cdot w + \left[\frac{\partial R}{\partial X_c}\right] x + \left[\frac{\partial R}{\partial Y_c}\right] y + \left[\frac{\partial R}{\partial Z_c}\right] z \qquad 14.1.5.$$

Since the errors w, x, y, z can be +ve or −ve 14.1.5. is squared. The sum of the terms containing cross products will tend to zero since any cross product is as likely to be +ve as -ve.

Hence

$$r^2 = \left[\frac{\partial R}{\partial W_c}\right]^2 w^2 + \left[\frac{\partial R}{\partial X_c}\right]^2 x^2 + \left[\frac{\partial R}{\partial Y_c}\right]^2 y^2 + \left[\frac{\partial R}{\partial Z_c}\right]^2 z^2 \qquad 14.1.6.$$

The overall % error in the final result becomes

$$\frac{r}{R} \times 100 = \frac{100}{R}\left\{\left[\frac{\partial R}{\partial W_c}\right]^2 w^2 + \left[\frac{\partial R}{\partial X_c}\right]^2 x^2 + \left[\frac{\partial R}{\partial Y_c}\right]^2 y^2 + \left[\frac{\partial R}{\partial Z_c}\right]^2 z^2\right\}^{1/2} \qquad 14.1.7.$$

Applying (14.1.7.) to the problem under study using the errors in accuracy for the individual measurements obtained above, and the following "correct" measurements.

Water flow rate 1440 lbm/hr

Water side temperature rise 4°F

Tube outside surface area 0.232 ft^2

Difference between vapour and wall temperature 15°F

An overall error in the condensation heat transfer coefficient of approximately ± 7% is obtained. This error is of the order of normal expected error in experimental observations with condensation heat transfer. Here this represents an outer limit in experimental error, this is so because severe conditions on the water side and steam side temperature differences were used. Operating the condenser tube with a larger temperature rise in the cooling water and a larger vapour - wall temperature difference should help to keep the experimental error within the ± 7% limit quoted. This may appear to be a serious disadvantage, since at low intensities of oscillation the change in heat transfer coefficient with oscillation would be of the same order as the experimental error. To overcome this difficulty it is hoped that by grouping a large amount of data in the low intensity region

trends will be observed in the results. A further method of reducing the effects of experimental error is to utilise the ratio h_v/h_o in any comparison with theory; this will in general cause some cancellation of errors due to experimental method.

15.0 OPERATING PROCEDURE DURING TEST RUNS SPECIAL PROBLEMS ENCOUNTERED, AND THE METHOD OF EVALUATING THE TEST DATA

15.1. Start up and Attainment of Steady State Conditions

Prior to each test the condenser tube was thoroughly cleaned before installation in the condenser shell. This cleaning procedure was similar to that used by Hampson (79) to ensure filmwise condensation on copper surfaces. This was carried out in the following manner. The tube surface was given a light polishing with emery cloth, followed by a wash and soaking in Trichlorethylene to degrease the surface, the tube was then rinsed in water and rubbed with emery flour to remove any deposit from the trichlorethylene, the surface was finally given a thorough wash in water before immediate installation in the shell.

Prior to the commencement of each test run the instrumentation was given a check for normal function, and thermocouples tested for continuity and level of signal.

The water flow through the tube was set at the appropriate level; this was varied between about 22 and 24 lbm/min. with a few runs at flows up to about 28 lbm/min. to check the effect of water side flow velocity. In general it was found that with water flows between 22 and 24 lbm/min. a differential temperature of the water of between 6 and 8 ^{o}F could be maintained. The high water flow rates were not measured with the aid of the calibrated venturi, but directly in the weigh tank. Thermocouples function on the water side was checked by ensuring similar recordings for inlet and outlet temperature.

Having set the boiler pressure at 80 p.s.i.g. the steam line was "blown down", the load on the dump condenser was adjusted so that stable boiler operation was achieved, before the needle valve to the test condenser was opened. The steam pressure in the condenser shell was adjusted through use of the needle control valve at inlet so that it was 1.4" Hg. above atmospheric (a few tests were carried out with the shell pressure at 0.7" Hg because of a steam leak at the outlet carrying the current leads; however this was soon rectified.)

The system was allowed to reach a steady state before final readings were taken. In doing this a compromise had to be reached, the inlet water temperature was subjected to some fluctuations at times depending on the atmospheric conditions prevailing (as these affect the cooling tower performance). However it was found that after about an hour at a given set of conditions the readings were

quite steady. At steady state conditions readings of the inlet and outlet water temperatures were noted along with the steam temperature and the tube resistance along with measurements of water flow and shell pressure. A visual observation of the condenser tube was also carried out at each test point to check the condensate film for traces of breakdown to dropwise condensation.

In test runs with oscillation, the vibrator was set to give the appropriate frequency and amplitude of oscillation prior to the admission of steam to the condenser shell. The same general procedure was adopted for taking of readings and the period for the attainment of the steady state was as for the non oscillatory case.

In carrying out vibration runs two basic methods were used for obtaining data. In the first case the vibrator was operated at frequencies in the range 20 to 80 c/s going up in 10 c/s increments, the maximum current being supplied to the vibrator in each case (i.e. maximum amplitude of oscillation in each case). Whereas in the second case the vibrator was operated at a constant frequency and the amplitude of oscillation varied from zero to a maximum in three or four steps.

Because of the time taken to obtain steady state conditions it was found that test runs consisted of a set of three or four points per run.

15.2. Special Problems Encountered

Early in the test programme it was discovered that air in the system presented a problem; this was found because the values of heat transfer coefficient in the absence of oscillation were well below the value predicted by Nusselt's theory. To overcome this a pair of $\frac{1}{2}$" copper vent pipes drilled with a number of 1/16" holes were placed about $\frac{3}{4}$" away from the condenser tube and parallel to it. These pipes were connected to rubber hose which was led from the condenser shell through the 1" ports provided for instrumentation. This was found to cure the problem of air in the condenser; values of the heat transfer coefficient were observed to be greater than those predicted by Nusselt's theory based on the appropriate operating conditions.

It was found that no trouble was experienced from dropwise condensation initially. Readings were taken over a two week period with no sign of dropwise condensation. At this stage as a part of routine servicing in the laboratory the main steam valve in the steam

line was serviced and packed with graphite grease, this was not found out till much later, when persistant dropwise condensation over a period of about two months led to an exhaustive check on boiler water preparation and servicing of the plant. To counteract the effects of grease in the system the steam line and condenser shell was operated with quantities of a strong industrial detergent - Quadraline - being used in the boiler feed water. However, extended periods of filmwise condensation greater than about twenty four hours were never again attained.

At this point it would be appropriate to mention that thermocouples and the condenser tube were recalibrated at regular intervals between runs. The tube resistance did show an increase with time, as was to be expected from the metal removal during polishing and cleaning. However, the temperature coefficient was observed to be completely stable.

To improve the setting of the trigger circuit so that the flash gun could be fired with certainty at the peaks of the oscillation cycle, a simple pulse circuit was used, operating from a photoelectric cell, which was energised by the light flash. A double channel Tektronix storage oscilloscope was used to store the input wave form from the displacement transducer on one channel, and store the pulse mark on the other. This enabled a better adjustment of the sensitivity control on the trigger circuit than could be obtained using the stroboscope method, which relied heavily on personal accuracy.

15.3. The Evaluation of Test Data - a Sample Calculation

A sample calculation will be carried out in detail to indicate the method used for the evaluation of the test data. This calculation will be carried through for the case of a static tube condition so that comparison can be made with Nusselt's theory for a horizontal tube. Exactly the same procedure is utilised in the evaluation of the data for the oscillating tube case.

Test No. 1.

Static tube

Mass flow rate of water $\dot{m}_w$	= 26.7 lbm/min.
Inlet water temperature θ_{wi}	= 15.40°C
Outlet water temperature θ_{we}	= 22.80°C
Steam Condenser Shell Temperature	= 102.0°C
Steam Pressure in Condenser Shell above atmospheric Pressure	= 1.4 ins Hg

Tube wall resistance = 136 $\mu\Omega$.

Mean Tube wall temperature corresponding to 136 $\mu\Omega$, obtained from tank calibration θ_m = 77.20°C

Heat Load $\dot{Q} = \dot{m}_w \cdot C_{pw} (\theta_{we} - \theta_{wi})$ = 11,850 CHU/HR

Difference between outside and inside tube wall temperature is

$$\theta_o - \theta_i = \frac{Q/A_o \quad D_o \log_e D_o/D_i}{2k}$$

For $A_o = 0.232$ ft^2;

$D_o = 0.830$ ins.

$D_i = 0.750$ ins.

$k = 157$ CHU/hr ft °C.

$\theta_o - \theta_i = 1.164$ °C

$$\theta_o = \theta_m + \frac{(\theta_o - \theta_i)}{2}$$

$= 77.20 + 0.58$ °C

$= \underline{77.78°C}$

Saturation temperature θ_{sat} corresponding to a shell pressure 1.4" Hg above atmospheric pressure is 101.1 °C.

$\theta_{sat} - \theta_o = 23.32$ °C, Since 1 CHU/°C = 1 Btu/°F

$$h = \frac{Q}{A_o (\theta_{sat} - \theta_o)} = \underline{\underline{2190}} \ \underline{\text{Btu/hr ft}^2 \ °F}$$

Check against Nusselt's equation $h = 0.72 \left[\frac{\rho^2 g \, h_{fg} \, k^3}{\mu_D (\theta_v - \theta_s)} \right]^{\frac{1}{4}}$

For a film temperature of $\theta_o + \frac{(\theta_{sat} - \theta_o)}{2}$ = 90.2 °C

Now $(\theta_v - \theta_s) = (\theta_{sat} - \theta_o) = 23.32$ °C

Evaluating the properties in Nusselt's equation at the film temperature of 90.2 °C.

$h_{Nusselt} = \underline{\underline{1850}}$ Btu/hr ft^2 °F

Therefore $h_o \approx 1.20 \, h_{Nusselt}$ which is of the right order of difference between experiment and Nusselt's theory.

The complete set of data obtained in this investigation are shown in Table I of Appendix (VII).

16.0 A THEORETICAL ANALYSIS OF THE EFFECT OF MECHANICAL OSCILLATION OF A HORIZONTAL CONDENSER TUBE IN THE VERTICAL PLANE ON CONDENSATION HEAT TRANSFER COEFFICIENT

16.1. Proposed Method of Analysis

From the experimental results obtained as outlined in section 15.1 and presented in Table I of Appendix VII, it is seen that the effect of mechanical oscillation of the condenser tube, causes small increases in the average condensation heat transfer coefficient with increasing oscillation intensity. Because the increases in heat transfer coefficient are small, it would appear that a perturbation method of analysis would be appropriate. This method of analysis would give an indication of the initial effects of oscillation on condensation heat transfer.

16.2. The Perturbation Solution

Because of the small observed increases in the condensation heat transfer coefficient with oscillation the rate of condensate drainage from the tube must increase slightly, hence the average condensate film velocity at any azimuthal position on the tube must also increase by a small amount. Similarly because of the increased heat transfer there must be a slight decrease in the average condensate film thickness, this assumes that the predominant mode of heat transfer through the film is by conduction.

If it is assumed that at any azimuthal position the mean velocity of the film under conditions of oscillation $\bar{u}'$ is composed of the sum of the mean velocity due to gravitational forces $\bar{u}$ and a small perturbation $(\epsilon)\ \bar{u}_1$ velocity due to the averaged effects of oscillation of the tube surface.

Therefore

$$\bar{u}' = \bar{u} + (\epsilon)\ \bar{u}_1 \qquad (16.2.1.)$$

The mean velocity due to gravitational forces $\bar{u}_1$ for an assumed parabolic velocity profile according to Nusselt's theory (Figure 9.1 and equation 9.2.8.) is

$$\bar{u} = \frac{g \delta_v^2}{3\nu} \sin \phi \qquad (16.2.2.)$$

where δ_v is the local film thickness of the film under oscillatory conditions, $\bar{u}_1$ is the average velocity due to oscillation and is considered to be equal to $\frac{2}{\pi} \cdot (a_{max}\omega) \sin \phi$, $(2/\pi)a_{max}$ is the average amplitude of oscillation over a half cycle and ω is the circular frequency of oscillation. (ϵ) is the perturbation parameter which is considered to be small and dimensionless.

If the discussion on streaming from a horizontal cylinder undergoing transverse mechanical oscillations is recalled, it will be noted that a condition for analysis was that a_{max}/D should be small. If therefore the perturbation parameter (ϵ) is set equal to a_{max}/D then

$$(\epsilon)\ \bar{u}_1 = \frac{2}{\pi}\left(\frac{a^2_{max}\omega}{D}\right) \cdot \sin \phi \qquad 16.2.3.$$

$$\text{and } \bar{u}' = \left[\frac{g\delta_v^2}{3\nu} + \frac{2}{\pi} \cdot \left(\frac{a^2_{max}\omega}{D}\right)\right] \sin \phi \qquad 16.2.4.$$

The advantage of using the averaged effect of oscillation as carried out above is that the time dependence of u' is eliminated. This means that provided the heat transfer is predominantly by conduction, an analysis can be set up in which the resulting differential equations will be ordinary rather than partial, and therefore solution easier. This means that details of the velocity distribution across the film at any Ø cannot be determined as a function of time. However, the main interest here is to see whether the prediction of average heat transfer coefficient is consistent with experimental findings.

Because changes in the average heat transfer coefficient with oscillation are small it is reasonable to assume that at low intensities of oscillation, heat transfer across the condensate film will be primarily due to conduction. It is now possible to equate the heat release due to condensation at the vapour-liquid interface of the condensate film to the heat transfer by conduction through the film to the tube wall. This is similar to Nusselt's assumption.

From figure (9-1) it is seen that the heat conducted through the element of condensate r.dØ which is of unit length and thickness δ_v is $\frac{k\,r}{\delta_v} \cdot \left[\theta_v - \theta_s\right] \cdot d\,\phi$. This conduction heat transfer is equal to the heat release due to condensation, which from equation (9.2.9.) is $\rho h_{fg} \cdot d\left[\bar{u}' \cdot \delta_v \cdot 1\right]$

Therefore

$$\frac{k \cdot r}{\delta_v}\left[\theta_v - \theta_s\right] \cdot d\,\phi = \rho h_{fg} \cdot d\left[\bar{u}' \delta_v \cdot 1\right] \qquad 16.2.5.$$

Substituting from 16.2.4. for $\bar{u}'$ in 16.2.5. and re-arranging results in

$$\frac{3\nu k r}{g\rho h_{fg}}\left[\theta_v - \theta_s\right]\cdot d\phi = \delta_v\, d\left[\left\{\delta_v^2 + \frac{6}{\pi}\left(\frac{\nu}{g}\right)\left(\frac{a^2_{max}\omega}{D}\right)\right\}\sin\phi\,\delta_v\right]$$

16.2.6.

The right hand side of 16.2.6. when expanded is

$$\delta_v\left[3\delta_v^2 \sin\phi\,.\,d\delta_v + \delta_v^3.\cos\phi\,.\,d\phi + \frac{6}{\pi}\left(\frac{\nu}{g}\right)\left(\frac{a^2_{max}\omega}{D}\right)\left\{\sin\phi\, d\delta_v + \delta_v\cos\phi\,.\,d\phi\right\}\right] \qquad 16.2.7.$$

Putting $\frac{3\nu k r}{g\rho h_{fg}}\left[\theta_v - \theta_s\right]$ = B = Constant as for the Nusselt solution and putting $\frac{6}{\pi}\left(\frac{\nu}{g}\right)\left(\frac{a^2_{max}\omega}{D}\right) = \gamma$

Equation 16.2.6. with expansion 16.2.7. becomes

$$d\phi = \left[\frac{3\delta_v^3 + \gamma\delta_v}{B}\right].\sin\phi\; d\delta_v + \left[\frac{\delta_v^4 + \gamma\delta_v^2}{B}\right].\cos\phi\, d\phi$$

16.2.8.

Putting $M = \frac{1}{B}$ and $\frac{\gamma}{B} = N$, 16.2.8. becomes

$$(3\,.\,M\delta_v^3 + N\delta_v)\frac{d\delta_v}{d\phi} + (M\delta_v^4 + N\delta_v^2)\cot\phi = \operatorname{cosec}\phi \qquad 16.2.9.$$

Putting $\frac{3}{4}\,.\,M\delta_v^4 + \frac{N}{2}.\delta_v^2 = Z$

16.2.10.

then $\frac{dZ}{d\phi} = (3M\delta_v^3 + N\delta_v)\frac{d\delta_v}{d\phi}$

Now equation 16.2.9. can be written as

$$\frac{dZ}{d\phi} + \left[\frac{4}{3}.Z + \frac{N}{3}\delta_v^2\right]\cot\phi = \operatorname{cosec}\phi \qquad 16.2.11.$$

In the absence of oscillation N = 0 and Z = Z_o and 16.2.11. becomes

$$\frac{dZ_o}{d\phi} + \frac{4}{3}Z_o\cot\phi = \operatorname{cosec}\phi \qquad 16.2.12.$$

Subtracting 16.2.12. from 16.2.11.

$$\frac{d}{d\phi}\left[Z - Z_o\right] + \frac{4}{3}\left[Z - Z_o\right]\cot\phi + \frac{N}{3}\delta_v^2\cot\phi = 0 \qquad 16.2.13$$

Now $Z = Z_o + P$, where P is the perturbation to Z_o; therefore

$(Z - Z_o) = P$ and 16.2.13 becomes

$$\frac{dP}{d\phi} + \frac{4}{3}.P\cot\phi + \frac{N}{3}\delta_v^2\cot\phi = 0 \qquad 16.2.14.$$

Now P should be small if $\frac{N\delta_v^2}{3}$ is small.

From the discussion of Nusselts theory, the solution of equations of the type given by (16.2.14) was carried out in appendix III. Using the same method as in Appendix III the following expression is obtained for P.

$$P = \frac{1}{\sin^{4/3}\phi}\left[-\frac{N}{3}\int\delta_v^2\cos\phi\sin^{1/3}\phi\,d\phi + c_1\right] \qquad 16.2.15$$

By the same reasoning as for the Nusselt solution the constant $c_1 = 0$

Therefore $$P = -\frac{N/3}{\sin^{4/3}\phi}\int_o^\phi \delta_v^2\cos\phi\sin^{1/3}\phi\cdot d\phi \qquad 16.2.16.$$

and $$Z = Z_o - \frac{N/3}{\sin^{4/3}\phi}\int_o^\phi \delta_v^2\cos\phi\sin^{1/3}\phi\,d\phi \qquad 16.2.17.$$

The solution of (16.2.12.) according to the method of Appendix III gives

$$Z_o = \frac{1}{\sin^{4/3}\phi}\int_o^\phi \sin^{1/3}\phi\;d\phi \qquad 16.2.18.$$

but from Nusselt's theory (equation 9.2.13)

$$\frac{\delta^4}{B} = Y = \frac{4}{3}\,\frac{1}{\sin^{4/3}\phi}\int_o^\phi \sin^{1/3}\phi\,d\phi \qquad 16.2.19$$

Therefore $$Z_o = \frac{3}{4}.\frac{\delta^4}{B} = \frac{3}{4}.Y \qquad 16.2.20.$$

where δ is the condensate film thickness according to Nusselt.

Therefore $$Z = \frac{3}{4} \cdot Y - \frac{N/3}{\sin^{4/3}\phi} \int_o^{\phi} \delta_v^2 \cos\phi \sin^{1/3}\phi \, d\phi$$

16.2.21

To solve 16.2.21 for Z it is necessary to know δ_v as a function of ϕ. As this is not known, an iterative procedure is adopted to determine δ_v.

To start the iteration it is assumed that $\delta_v = \delta$; where from Nusselt's theory $\delta = (Y \cdot B)^{\frac{1}{4}}$. Therefore the first iteration gives Z_1, where

$$Z_1 = \frac{3}{4} Y - \frac{N/3 \sqrt{B}}{\sin^{4/3}\phi} \int_o^{\phi} Y^{\frac{1}{2}} \cdot \cos\phi \sin^{1/3}\phi \, d\phi \qquad 16.2.22$$

It is known from 16.2.10 that

$$Z = \frac{3}{4} \cdot M \delta_v^4 + \frac{N}{2} \delta_v^2 \qquad 16.2.23$$

Therefore $$\delta_v = \left[-\frac{N}{3M} + \sqrt{\left(\frac{N}{3M}\right)^2 + \frac{4}{3} \frac{Z}{M}} \right]^{\frac{1}{2}} \qquad 16.2.24$$

Hence using Z_1 from (16.2.22) a better approximation to δ_v is obtained from (16.2.24). This value of δ_v is then used in (16.2.21) to generate Z_2 which gives a better approximation to δ_v from (16.2.24). Because the difference between δ and δ_v is small convergence of the iteration is rapid. The computation outlined above was programmed for a digital computer, the computation flow diagram being shown below. The value of Y from Nusselt's theory was re-evaluated from (16.2.19), Simpsons rule was used for all the numerical itegration, results for Y and δ_v were calculated for 2^o intervals from 0^o to 174^o. In the computation of δ_v the value of B was taken as 4.35×10^{-16} ft^4 this value was a representative mean for the experiments reported here. The experimental value of B did not vary significantly because of the small variations in temperature difference between the vapour and the tube wall. This was a consequence of the small range in water velocities used for the experiments. $\frac{N}{3}$ was increased in steps of 1×10^6 from 1×10^6 to 10×10^6 ft^{-2}. With values of δ_v of the

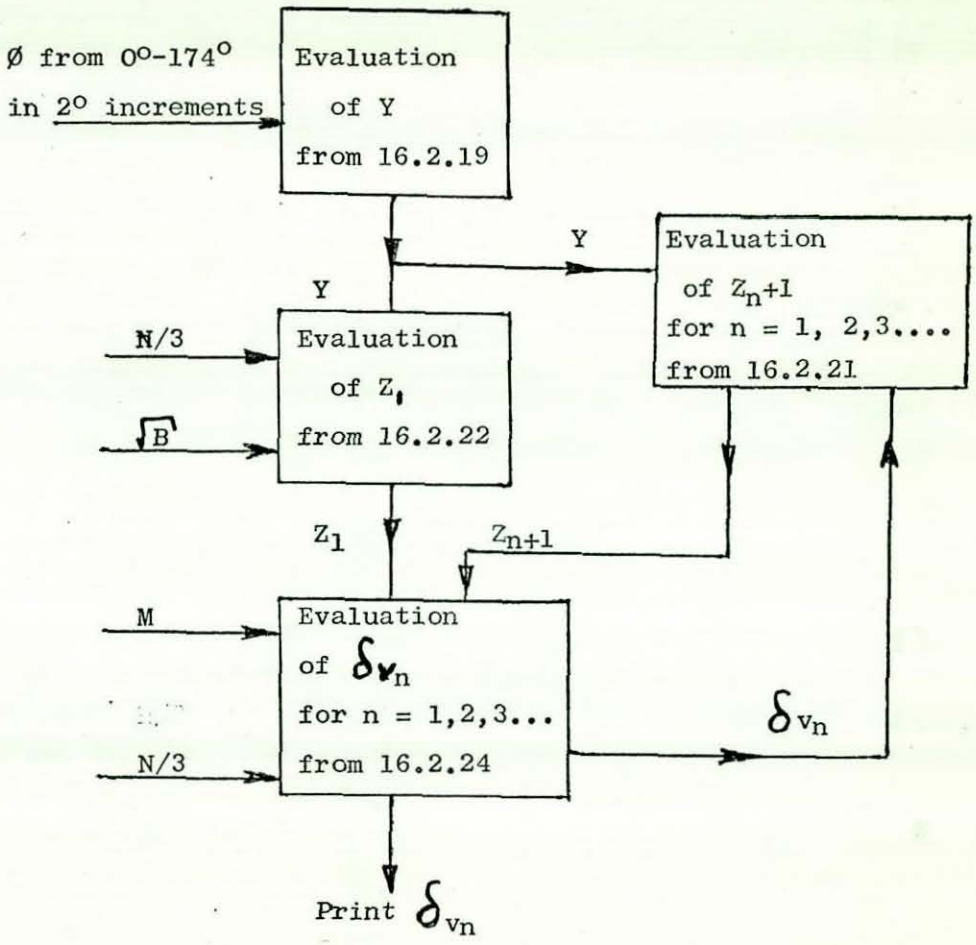

Computational Flow Diagram for Evaluation of δ_v

order of 2×10^{-4} ft. the value of $\frac{N}{3} \delta_v^2$ for $\frac{N}{3} = 10 \times 10^6$ will be 0.40. Z will be of the order of 2.76 from (16.2.10), but from (16.2.11.) it is seen that $\frac{N}{3} \delta_v^2$ must be small in comparison with $\frac{4}{3} \cdot Z$. For $\frac{N}{3} = 10 \times 10^6$, $\frac{N}{3} \delta_v^2$ is approximately 11% of $\frac{4}{3} Z$ this would represent an upper limit to the validity of the method presented here, since it is based on the assumption that the perturbations are small.

The average condensation heat transfer coefficient between any angle ϕ_1 and ϕ_2 is defined as

$$h = \frac{k}{\phi_2 - \phi_1} \int_{\phi_1}^{\phi_2} \cdot \frac{d\phi}{\delta} \qquad 16.2.25$$

hence from the computed values of δ_v the term $\frac{1}{\phi_2 - \phi_1} \int_{\phi_1}^{\phi_2} \frac{d\phi}{\delta}$ in 16.2.25 was evaluated between 0° and 174° for each value of $\frac{N}{3}$. For the case of the Nusselt solution the term $\frac{1}{\phi_2 - \phi_1} \int_{\phi_1}^{\phi_2} \cdot \frac{d\phi}{Y^{\frac{1}{4}}}$ was evaluated between 0° and 174°.

Therefore $$\frac{h_v}{h_o} = \frac{B^{\frac{1}{4}} \int_{\phi_1}^{\phi_2} \frac{d\phi}{\delta_v}}{\int_{\phi_1}^{\phi_2} \frac{d\phi}{Y^{\frac{1}{4}}}} \qquad 16.2.26.$$

The computed values of $\frac{h_v}{h_o}$ according to 16.2.26 between the limits 0° and 174° are shown plotted in figure 16-1 against $\frac{N}{3} D^2$. The

parameter $\frac{ND^2}{3}$ can be cast into a more meaningful form as shown below.

$$\frac{ND^2}{3} = \frac{D^2}{3} \frac{\left[\frac{6}{\pi}\left(\frac{\nu}{g}\right)\left(\frac{a_{max}}{D}\right)\left(a_{max}\,\omega\right)\right]}{\left[\frac{3\,\nu\,k\,.\,\frac{D}{2}\,.\,(\theta_v - \theta_s)}{g\,\rho\,h_{fg}}\right]} \qquad 16.2.27$$

Forming the Vibration Reynolds Number

$$Re_{vib.} = \frac{a_{max}\,\omega\,D}{\nu}$$

$$\frac{ND^2}{3} = \frac{\frac{4}{3\pi}\cdot\left(\frac{a_{max}}{D}\right) Re_{vib.}}{\left[\frac{k\,(\theta_v - \theta_s)}{\mathcal{M}\,h_{fg}}\right]} \qquad 16.2.28$$

With the exception of the ratio $\left(\frac{a_{max}}{D}\right)$ which is the perturbation parameter here, the parameters occurring in 16.2.28 are similar to those obtained in the discussion of the vertical tube subjected to transverse oscillation in the presence of condensation. It is seen that the ratio of the average heat transfer coefficients with and without oscillation is dependent on the ratio of perturbation oscillatory forces to momentum forces in the liquid film represented by the parameter $\left[\frac{k\,(\theta_v - \theta_s)}{\mathcal{M}\,h_{fg}}\right]$ obtained by Chen (63).

Experimental data points from Appendix VII are also shown in figure 16-1.

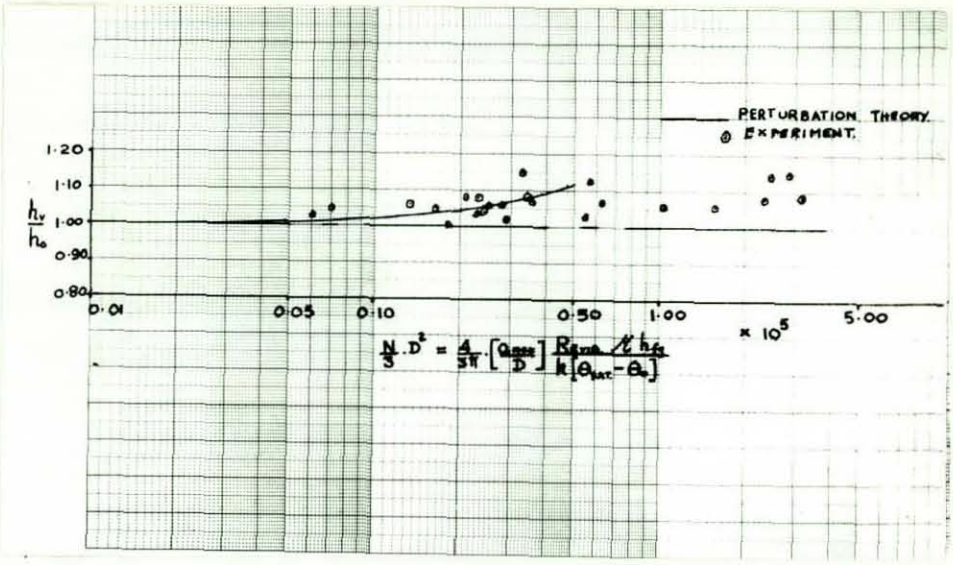

Fig. 16-1 Comparison between Perturbation Theory and Experiment for Condensation Heat Transfer on an Oscillating tube.

Computer read out of $Y^{\frac{1}{4}}$ is given in Tabe II of Appendix VII for a comparison with Nusselt's values tabulated in Appendix (IV).

Computer read out for values of the local condensate thickness δ_v under oscillatory conditions, have also been tabulated in Appendix VII, in Table III. These values have been taken from the final iteration of the computer solution and have been tabulated for values of $\frac{N}{3}$ of 1×10^6 4×10^6; 7×10^6 ft^{-2} and 10×10^6 only. It should be pointed out here that the final values of δ_v were obtained with two iterations for low values of $\frac{N}{3}$ but with three iterations for values of $\frac{N}{3}$ greater than 7

A comparison of the variation of local condensate film thickness according to Nusselt's theory and the Perturbation theory developed here is

shown in figure (16-2). A value of $B = 4.35 \times 10^{-16}$ ft^4 being used for both computations, while $\frac{N}{3} = 10 \times 10^6$ ft^{-2} was used for the perturbation solution.

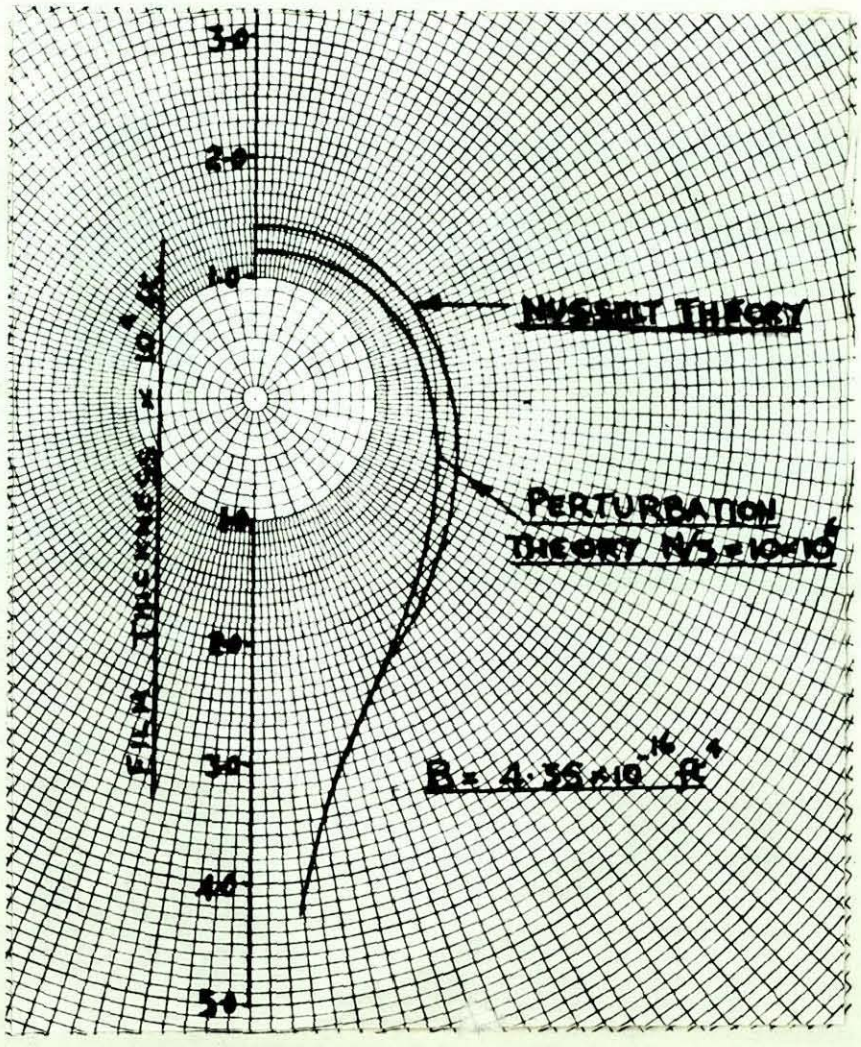

Fig. 16-2 Variation of film thickness of condensate according to Nusselt's Theory and Perturbation theory.

16.3. Discussion of Results and Conclusions

From figure 16-1 agreement between the Perturbation analysis and experiment is seen to exist. Both indicate initial increases of heat transfer of the same order with increasing oscillation intensity of the condenser tube. Despite the method of plotting the experimental data in the form h_v/h_o some scatter in the results is apparent, however, this scatter is well within the error tolerance specified in section (14.1)

and in accord with the scatter of results obtained by other workers in the field of condensation heat transfer.

At high intensities of oscillation i.e. $\frac{N}{3} > 10 \times 10^6$

$$\frac{4}{3\pi}\left(\frac{a_{max}}{D}\right)\frac{Re_{vib}\,\mathcal{K}\,h_{fg}}{k\,(\theta_{sat}-\theta_o)} > 0.5 \times 10^6$$

the perturbation analysis is not expected to hold. Beyond this point the experimental results show a continued gradual increase in heat transfer coefficient with increasing oscillation intensity. The probable reason for the very gradual increase in heat transfer coefficient with increasing high intensity oscillations is the movement of the condensate film back and forth due to the oscillation of the condenser tube. Figures 16-4 and 16-6 obtained with the aid of the flash gun trigger circuit described earlier show the effect of oscillation on the condensate film, when compared with the condensate film on the tube in the absence of oscillations as shown in figure (16-3). These photographs show that when the condenser tube was at its maximum positive (upward) displacement, the liquid in the condensate film accumulated on the bottom side of the tube. It can be assumed therefore that the condensate film thickness was reduced on the upper half of the cylinder. When the condenser tube was at its maximum negative (downward) displacement the photographs show the reduced accumulation on the lower side of the tube. Since the amount of condensate leaving the surface was not observed to increase very significantly over the oscillation free case it appears reasonable to conclude that at this lower position of tube displacement the condensate film is caused to "bunch up" towards the upper part of the tube, this results in a drop in the condensation heat transfer coefficient. The nett result is a small increase in the average coefficient of heat transfer for the whole surface, over a complete cycle of oscillation. It is interesting to note that at the highest intensities of oscillation studied here (f = 20 c/s a = 0.177 ins) there was no break up of the condensate film and "throwing off" of droplets from the surface, which might have been expected. In fact the behaviour of the film on the tube was very similar to that observed by Raben et al (73). For the intensities used here the ratios h_v/h_o are similar in value to those obtained by Raben et al for the same intensities of oscillation. Due to equipment

limitations it was not possible to observe the effect of higher intensities of oscillation, however it would appear from the photographic evidence provided here that the condensate film would remain intact and that the increase in heat transfer would continue but now a greater proportion of it would be due to convective mixing in condensate film. Very high intensities of oscillation would be required to rupture the liquid film.

From the practical standpoint there appears to be no advantage to be gained in utilising vibration of horizontal tubes to cause increases in heat transfer, the increases being too small to warrent additional cost due to tube fatigue failure and special design considerations.

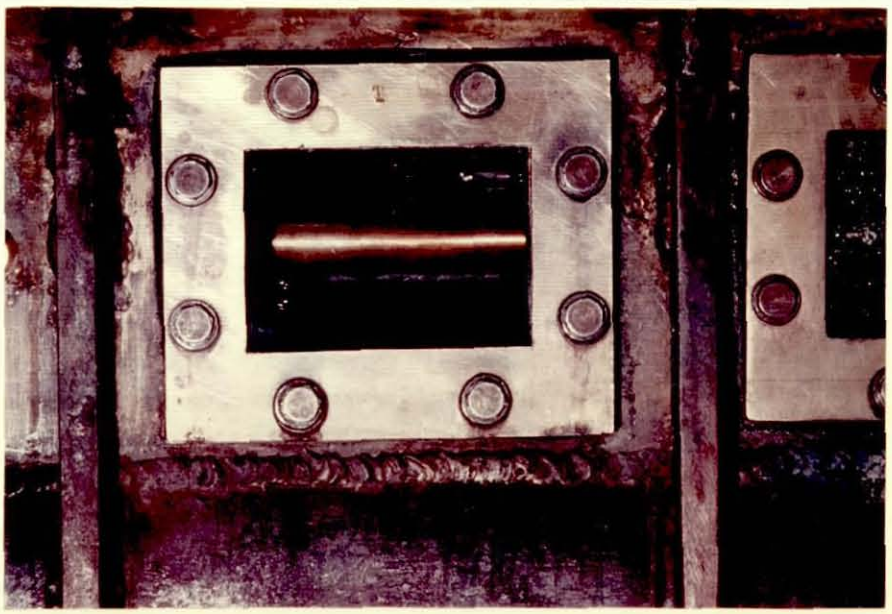

Fig. 16-3 Filmwise Condensation on a Horizontal Tube in the Absence of Oscillation

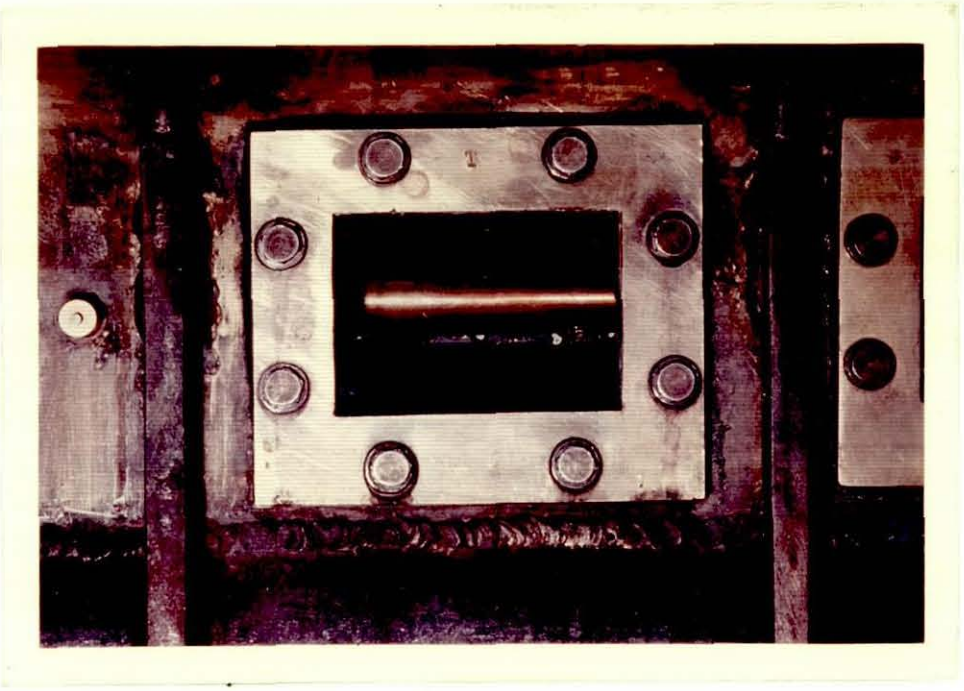

Fig. 16-4 Filmwise Condensation on a Horizontal Tube in the presence of Mechanical Oscillation (20 c/s, a = 0.17 ins) Tube at Maximum Positive Displacement

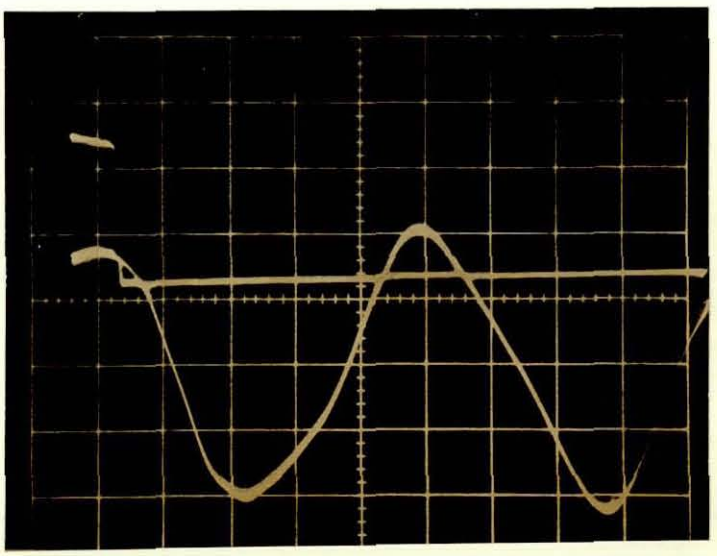

Fig. 16-5 Waveform from Displacement transducer and Pulse Mark for Conditions of Fig. (16-4)

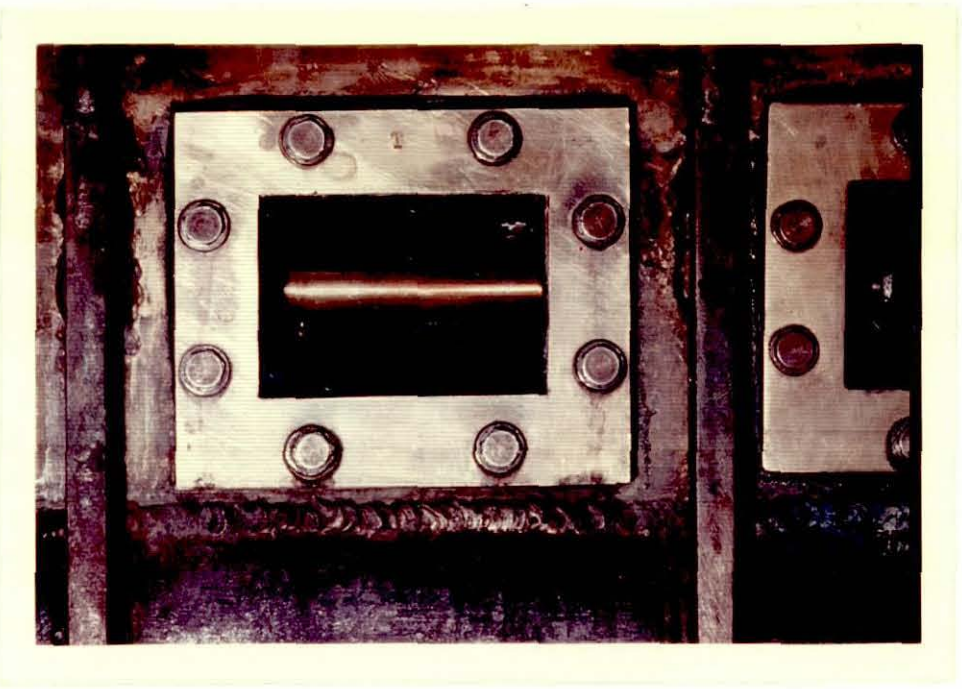

Fig. 16-6 Filmwise Condensation on a Horizontal Tube in the Presence of Mechanical Oscillation (20 c/s a = 0.17 ins) Tube at Maximum Negative Displacement

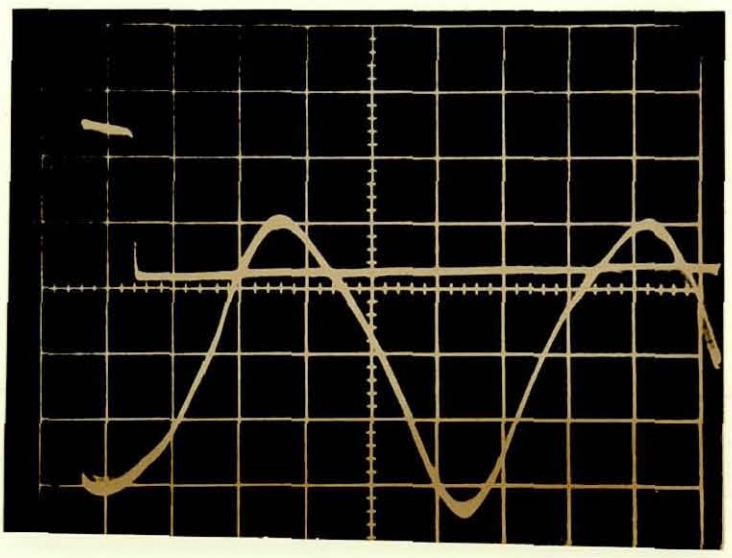

Fig. 16-7 Waveform from Displacement Transducer and Pulse Mark for Conditions of Fig. (16-6)

17.0 OVERALL CONCLUSIONS

Overall Conclusions

In this thesis, the Danckwerts-Mickley surface renewal concept has been extended to account for the enhanced mixing in forced convection, free convection and condensation over surfaces, in the presence of acoustic oscillation in the fluid medium or mechanical oscillations of the heat transfer surface.

Utilising the surface renewal concept, the ratio of the average heat transfer coefficient in the presence of oscillation to that in the absence of oscillation has been calculated and found to be in good agreement with experiment, in all cases, within the limits of the model and experimental error.

In the case of acoustic and mechanical oscillation effects on free convection from heated cylinders in air, it has been shown in this thesis that the method developed using the Danckwerts-Mickley model could be extended to the case of Grashof Number $\rightarrow 0$, and the results obtained for average Nusselt Number are in better agreement with experimental data than the asymptotic solutions of Richardson.

Finally, experiments carried out by the author on the effects of mechanical oscillation in a vertical plane, on condensation heat transfer on a horizontal tube show that the effects of oscillation on average heat transfer are small, and of no practical significance. The experimental findings are corroborated by a first order perturbation analysis around Nusselt's classical theory for laminar filmwise condensation on a horizontal cylinder.

18.0 PROPOSALS FOR FUTURE WORK

18.1. Future Work

In the course of the work carried out and reported in this thesis, a number of problems have come to light which need investigation.

In the combustion driven acoustic oscillation problem, work can be attempted to verify the hypothesis of Kline et al which was used by the present author to account for mixing in the boundary layer, viz. the superposition of the acoustic energy and the shear energy in the boundary layer. This would necessitate the direct measurement of shear stress in the wall region by means of the Preston tube technique (86), (87), (88) - this would appear to be the only technique which would be suitable under the arduous conditions of operation of a combustion chamber. The measurement of the acoustic pressure at the wall will have to be carried out at the same location as the Preston tube measurements, and would therefore necessitate a crystal pressure transducer suitable for operation at high working temperatures. As far as can be ascertained from the literature (86-88) the Preston tube technique has not been utilised under the type of conditions envisaged here. So, a very thorough investigation of this method of measurement under the conditions discussed here would be of great practical value.

Arising from the above work, an attempt could be made at defining a model to predict the pressure forces on the wall arising from the interaction of acoustic pressure and combustion heat release in the wall region.

In the free convective field, there appears to be scope for at least two investigations. The first involves the interaction between the convective plume above the cylinder and an acoustic field, because, it is this interaction which appears to cause instability in the wake region. There is a possibility that this problem could be related to the instability of fluid jets in acoustic fields, some work in this area has been carried out by Sato and Sakao (89).

Secondly, there is the problem of considering the effects of acoustic fields on free convection when free convective forces are large.

In the field of condensation, a worthwhile theoretical investigation would be to include Kapitza's wave motion equations in a study of pseudo-laminar condensate flow over short vertical surfaces and horizontal tubes, and to check for closer agreement with the observed data on condensation heat transfer coefficient in the absence of non-condensable gases.

In the area of more direct industrial application, there would appear to be possibilities in utilising oscillatory effects in heat transfer in the convective drying of fabric passing through oven driers.

In the process of fabric cleaning, the use of oscillation (flapping) of the fabric has been found to be advantageous to the cleaning process. The oscillation of the fabric sheet is achieved by using the fabric as an interface between jets of water and steam parallel to the surface of fabric, because of Helmholtz type instability (90) caused by the differing densities of the fluids, the fabric flaps, causing efficient cleaning of the fabric. A more thorough study of this process might be worthwhile.

----------oOo----------

BIBLIOGRAPHY AND REFERENCES

BIBLIOGRAPHY

1. Vibration and Sound.
   P.M. Morse.
   2nd ed. McGraw-Hill, New York (1948).

2. Principles of Modern Acoustics.
   G.W. Swenson
   Van Nostrand, New York (1953).

3. Osborn, J.R.
   Unstable Burning in Solid and Liquid Propellant Rocket Motors.
   Raketentechnit und Raumfahrtforschung, 2, 47 (1963).

4. Osborn, J.R. and Bonell, J.M.
   Importance of Combustion Chamber Geometry in High Frequency Oscillations in Rocket Motors.
   A.R.S. Jour, 31, 482 (1961).

5. Theory of Combustion Instability in Liquid Propellant Rocket Motors.
   L. Crocco and S.I. Cheng.
   Butterworths, London (1956).

6. Some Fundamentals of Combustion.
   D.B. Spalding.
   Butterworths, London (1955).

7. Mickley, H.S. and Fairbanks, D.F.
   Mechanism of Heat Transfer to Fluidized Beds.
   A.I. Ch. E. Jour, 1, 374 (1955).

8. Fluid Dynamics.
   J.W. Daily and D.R.F. Harlemann.
   Addison-Wesley, Reading, (1966).

9. Industrial Electronic Circuits and Applications.
   R.R. Benedict and N. Weiner.
   2nd ed. Prentice-Hall, Englewood Cliffs, (1965).

10. Electrical Measurements.

F.K. Harris

John Wiley, New York (1957).

11. Mathematics of Physics and Modern Engineering.

I.S. Sokolinikoff and R.M. Redheffer

McGraw-Hill, New York, (1958).

12. Non Linear Analysis

W.J. Cunningham

McGraw-Hill, New York (1958).

References

1. Anandha Rao, M.

   A survey Study of the Effects of Vibrations, Sound Fields and Pulsations on Heat and Mass Transfer, from Flat Plates, Cylinders and Ducts.

   ARL. 65 - 217 OCT. (1965) OHIO.

2. Jackson, T.W.; Harrison, W.B. and Boteler, W.C.

   Free Convection, Forced Convection and Acoustic Vibrations in a Constant Temperature Vertical tube.

   A.S.M.E. Jour. Heat Transfer; 81, 68, (1959).

3. Jackson, T.W.; Purdy, K.R. and Oliver, C.C.

   The Effects of Resonant Acoustic Vibrations on Nusselt Number for a Constant Temperature Horizontal Tube.

   International Developments in Heat Transfer (1961), P.483.

4. Purdy, K.R. Jackson, T.W. and Gorton, C.W.

   Viscous Fluid Flow under the Influence of a Resonant Acoustic Field.

   A.S.M.E. Jour. Heat Transfer, 86, 97 (1964).

5. Jackson, T.W. and Purdy, K.R.

   Resonant Pulsating Flow and Convective Heat Transfer.

   A.S.M.E. Jour. Heat Transfer 87, 507 (1965).

6. Lemlich, R. and Hwu C.K.

   The Effect of Vibration on Forced Convective Heat Transfer.

   A.I. Ch.E. Jour., 7, 102, (1961).

7. Pulsating Combustion - The Collected works of F.H. Reynst. Edited by M.W. Thring, Pergamon, Oxford (1961).

8. Male, T., Kerslake, W.R. and Tischler, A.O.

   Photographic Study of Rotary Screaming and Other Oscillations in a Rocket Engine.

   N.A.C.A. RM E 54 A29.

9. Kreig, H.C.

   The Tangential Mode of Combustion Instability. A.R.S. Propellants, Combustion and Liquid Rockets Conference, Florida (1961).

10. Zartman, W.N.

Heat Transfer from Acoustically Resonating Gas Flames in a Cylinderical Burner.

Ph.D. Thesis, University of Michigan (1961).

11. Boundary Layer Theory,

H. Schlichting,

Pergamon, Oxford (1955).

12. Convective Heat and Mass Transfer.

W.M. Kays.

Mc.Graw-Hill, New York (1966).

13. Danckwerts, P.V.

The Significance of Liquid-Film Coefficients in Gas Absorption.

Ind. Eng. Chem. 43, 1460 (1951).

14. Higbie, R.

The Rate of Absorption of a Pure Gas into a Still liquid during short periods of Exposure.

Trans. American Inst. of Chem. Engineers. 31, 365 (1935).

15. Mickley, H.S. and Fairbanks, D.F.

Mechanism of Heat Transfer to Fluidized Beds.

A.I.Ch.E. Jour., 1, 374 (1955).

16. Conduction Heat Transfer.

P.J. Schneider

Addison-Wesley, Reading (1955).

17. Tables of Integrals and other Mathematical Data.

H.B. Dwight.

4th. Ed. Macmillan, NEW YORK (1961).

18. Fage, A. and Townend, H.C.H.

An Examination of Turbulent Flow with an Ultramicroscope.

Proc. Roy. Soc. London 135 (A), 656 (1932).

19. Hanratty, T.J.

Study of Turbulence close to a Solid Wall.

The Physics of Fluids Supplement on Boundary Layers and Turbulence. S 126 (1967).

20. Bakewell, H.P. and Lurnley, J.L.

Viscous Sub layer and adjacent wall region in Turbulent Pipe Flow.

Physics of Fluids 10, 1880 (1967).

21. Sherwood, T.K., Smith K.A. and Fowles, P.E.

The Velocity and eddy Viscosity distribution in the wall region of Turbulent Pipe flow.

Chem. Eng. Sci. 23, 1225 (1968).

22. Kline, S.J., Reynolds, W.C., Schraub, P.W. and Runstadler, F.A.

The Structure of Turbulent Boundary Layers.

Jour. Fluid Mech. 30, 741 (1967).

23. Locke, G.S.H. and Trotter, F.J. de B.

Observations on the Structure of a Turbulent Free Convection Boundary Layer.

Int. J. Heat Mass Transfer. 11, 1225, (1968).

24. Ruckenstein, E.

A Note concerning Turbulent Exchange of Heat on Mass with a Boundary.

Chem. Eng. Sci. 7, 265 (1958).

25. Danckwerts, P.V.

Gas Absorption Accompanied by Chemical Reaction.

A.I.Ch.E. Jour. 1, 457 (1954).

26. Toor, H.L. and Marchello, J.M.

Film - Penetration Model for Mass and Heat Transfer.

A.I.Ch.E. Jour. 4, 97 (1958).

27. Heat Trasmission

W.H. Mc.Adams.

4th. Ed. Mc.Graw-Hill, New York (1954).

28. Staff of N.A.C.A. Lewis Laboratory.
A Summary of Preliminary Investigations into the Characteristics of Combustion Screech in Ducted Burners.
N.A.C.A. Report, 1384.

29. F.K. Bannister.
Pressure Waves in Gases in Pipes
Akroyd Stuart Memorial Lecture (1958), University of Nottingham.

30. Shine, A.J.
The Effects of Transverse Vibrations on Heat Transfer Rate from a Heated Vertical Plate in Free Convection.
A.S.M.E. Paper No. 59 - HT - 27.

31. Blankenship, V. and Clark, J.A.
Effects of Oscillation on Free Convection from a Vertical Finite Plate.
A.S.M.E. Jour. Heat Transfer. 86, 149 (1964).

32. Blankenship, V. and Clark, J.A.
Experimental Effects of Transverse Oscillations on Free Convection Of a Vertical, Finite Plate.
A.S.M.E. Jour. Heat Transfer. 86, 159 (1964).

33. Eckert, E.R.G. and Soehnghen, E.
Interferomatiic Studies on the Stability and Transition to Turbulence of a Free Convection Boundary Layer.
Gen. Discussion on Heat Transfer, (1951) P.321.

34. Szewczyk, A.A.
Stability and Transition of the Free Convection Layer Along a Vertical Flat Plate.
Int. J. Heat Mass Transfer. 5, 903, (1962).

35. Principles of Heat Transfer.
F. Kreith.
International, Scranton (1960).

36. Eckert, E.R.G.

Research During the Last Decade on Forced Convection Heat Transfer.

Invited Lecture, International Developments in Heat Transfer (1961).

37. Lowe, H.C.

Heat Transfer from a Vibrating Horizontal Tube to Air.

M.Sc. Thesis, London University (1965).

38. Hermann, R.

Heat Transfer by Free Convection from Horizontal Cylinders in Diatomic Gases.

N.A.C.A. TM 1366.

39. Westervelt, P.J.

The Theory of Steady Rotational Flow Generated by a Sound Field.

Jour. Acoust. Soc. Amer. 25, 60 (1953).

40. West, G.D.

Circulations Occuring in Acoustic Phenomena.

Proc. Phys. Soc. London, 64B 483 (1951).

41. Holtsmark, J., Johnson, I., Sikkeland, T. and Skavlem, S.

Boundary Layer Flow Near a Cylinderical Obstacle in an Oscillating Incompressible Fluid.

Jour. Acoust. Soc. Amer. 26, 102 (1954).

42. Raney, W.P., Corelli, J.C. and Westervelt, P.J.

Acoustic Streaming in the Vicinity of a Cylinder.

Jour. Acoust. Soc. Amer. 26, 1006 (1954).

43. Stuart, J.T.

Double Boundary Layers in Oscillatory Viscous Flow.

Jour. Fluid Mech. 24, 673 (1966).

44. The Work of P.N. Kubanskii is reported in:-

Fand, R.M. and Cheng, P.

The Influence of Sound on Heat Transfer from a Cylinder in Cross Flow.

Int. J. Heat Mass Transfer. 6, 571 (1963).

45. Fand, R.M. and Kaye, J.

The Influence of Sound on Free Convection from a Horizontal Cylinder

A.S.M.E. Jour. Heat Transfer, 83, 133 (1961).

46. Fand, R.M. and Kaye, J.

Acoustic Streaming Near a Heated Cylinder.

Jour. Acoust. Soc. Amer. 32, 579 (1960).

47. Fand, R.M., Roos, J., Cheng, R., and Kaye, J.

The Local Heat Transfer Coefficient Around a Heated Horizontal Cylinder in an Intense Sound Field.

A.S.M.E. Jour. Heat Transfer, 84, 245 (1962).

48. Fand, R.M. and Peebles, E.M.

A Comparison of the Influence of Mechanical and Acoustic Vibrations on Free Convection from a Horizontal Cylinder.

A.S.M.E. Jour. Heat Transfer 84, 268 (1962).

49. Fand, R.M. and Kaye, J.

The Influence of Vertical Vibrations on Heat Transfer by Free Convection from a Horizontal Cylinder.

International Developments in Heat Transfer 490, (1961).

50. Westervelt, P.J.

Effect of Sound Waves on Heat Transfer.

Jour. Acoust. Soc. Amer. 32, 337 (1960).

51. Richardson, P.D.

A Correlation of the Influence of Sound on Heat Transfer as Measured by Fand and Kaye.

A.S.M.E. Jour. Heat Transfer, 87, 314 (1965).

52. Lee, B.H., and Richardson, P.D.

Effect of Sound on Heat Transfer from a Horizontal Circular Cylinder at Large Wave lengths.

Jour. Mech. Eng. Sci. 7, 127 (1965).

53. Richardson, P.D.

Local Details of the Influence of a Vertical Sound Field on Heat Transfer from a Circular Cylinder.

Proc. 3rd International Heat Transfer Conference, P.71, (1966).

54. Richardson, P.D.

The Effect of Vibrations and Oscillations on Heat Transfer from a Circular Cylinder.

Brown University, Div. of Engineering Report, AF USAF Aerospace Res. Labs. ARL 66-0235 (1966).

55. Turbulence.

J.O. Hinze.

McGraw-Hill, New York (1959).

56. Heat and Mass Transfer.

E.R.G. Eckert and R.M. Drake.

McGraw-Hill, New York (1959).

57. Heat Transfer Vol. 1.

M. Jakob,

Wiley, New York (1949).

58. Bromley, L.A., Brodkey, R.S. and Fishman, N.

Heat Transfer in Condensation.

Ind. Eng. Chem. 44, 2962 (1952).

59. Peck. R.E. and Reddie, W.A.

Heat Transfer Coefficients for Vapours Condensing on Horizontal Tubes.

Ind. Eng. Chem. 43, 2926 (1951).

60. Bromley, L.A.

Effect of Heat Capacity of Condensate.

Ind. Eng. Chem. 44, 2966 (1952).

61. Sparrow, E.M. and Gregg, J.L.

A Boundary Layer Treatment of Laminar Film Condensation.

A.S.M.E. Jour. Heat Transfer 81, 13, (1959).

62. Koh, J.C.Y., Sparrow, E.M. and Hartnelt, J.P.

The Two Phase Boundary Layer in Laminar Film Condensation.

Int. J. Heat Mass Transfer, 2, 69 (1961).

63. Chen, M.M.

An Analytical Study of Laminar Film Condensation: Part I - Flat Plates

A.S.M.E. Jour. Heat Transfer, 83, 48, (1961).

64. Sparrow, E.M. and Gregg, J.L.
Laminar Condensation Heat Transfer on a Horizontal Cylinder.
A.S.M.E. Jour. Heat Transfer 81, 291 (1959).

65. Fundamentals of Heat Transfer.
H. Grober, S. Erk and U. Grigull.
McGraw-Hill, New York, (1961).

66. Dukler, A.E. and Bergelin, O.P.
Characteristics of Flow in Falling Liquid Films.
Chem. Eng. Prog. 48, 557 (1952).

67. Portalski, S.
The Mechanism of Flow in Wetted Wall Columns.
Ph.D. Thesis, London University (1960).
Portalski, S.

68. Eddy Formation in Film Flow Down a Vertical Plate.
Ind. and Eng. Chem. Fundamentals, 3, 49, (1964).

69. Portalski, S.
Studies of Falling Liquid Film Flow.
Chem. Eng. Sci. 18, 787. (1963).

70. Portalski, S.
Velocities in Film Flow of Liquids on Vertical Plates.
Chem. Eng. Sci. 19, 575, (1964).

71. Hampson, H.
The Condensation of Steam on a Tube with Film wise or Dropwise Condensation and in the Presence of a Non Condensable Gas.
International Developments in Heat Transfer (1961) P.310.

72. Fundamentals of Heat Transfer
S.S. Kutateladze.
2nd Ed. Edward Arnold, London (1963).

73. Raben I.A. Commerford, G. and Dietert, R.
An Investigation of the Use of Acoustic Vibrations to Improve Heat Transfer Rates and Reduce Sealing in Distillation Units Used for

Saline Water Conversion.

Office of Saline Water, Research Report No. 49.

U.S. Dept. of Commerce, Washington.

74. Haughey, D.P.

Heat Transfer During Condensation on a Vibration Tube.

Trans. Inst. Chem. Engineers, 43, 40 (1965).

75. Brooke-Benjamin, T.

Wave Formation in Laminar Flow Down on Inclined Plane.

Jour. Fluid Mech. 2, 554 (1957).

76. Atkinson, B. and Caruthers, P.A.

Velocity Profile Measurements in Liquid Films.

Trans. Inst. Chem. Engineers, 43, 33 (1965).

77. J.P. Den Hartog,

Mechanical Vibrations.

4th Ed. McGraw-Hill, New York, (1956).

78. Jeffrey, J.O.

A Precision Method for the Measurement of Condenser Tube Surface Temperatures for the Determination of Film Coefficients of Heat Transmission.

Cornell University Engineering Expt. Station.

Bulletin No. 21 (1936).

79. Hampson, H.

The Condensation of Steam on a Metal Surface.

General Discussion on Heat Transfer (1951) P.58.

80. Physical and Chemical Constants.

G.W.C. Kaye and T.H. Laby.

13th Ed. Longmans, London, 1966.

81. Blackman, L.C.F.

Dropwise Condensation of Steam.

Research 11, 394 (1958).

82. Powell, R.W.

Correlation of Metallic Thermal and Electrical Conductivities for Both Solid and Liquid Phases.

Int. J. Heat Mass Transfer. 8, 1033 (1965).

83. Watson, G.G. and Clark, R.D.

Determination of the Tube-Wall Temperature in a Heat Exchanger from the Tube Resistance.

National Engineering Laboratory Report 272 (1967) England.

84. Mechanical Vibrations.

G.W. Van Santen.

3rd Edition Philips Technical Library (1961).

85. Theories of Engineering Experimentation.

H. Schenk.

McGraw-Hill, New York (1961).

86. Preston, J.H.

The Determination of Turbulent Skin Friction by Means of Pitot Tubes.

Jour. R.Ae. Soc. 58, 109 (1954).

87. Rajaratnam, N.

A Theoretical Calibration Curve for the Preston Tube on Smooth Boundaries for Large Reynolds Numbers.

Jour. R.Ae. Soc. 69, 136 (1965).

88. Patel, V.C.

Calibration of the Preston Tube and limitations on its use in Pressure Gradients.

Jour. Fluid Mechanics. 23, 185 (1965).

89. Sato, H. and Sakas, F.

An Experimental Investigation of a Two Dimensional Jet at Low Reynolds Numbers.

Jour. Fluid Mech. 20, 337 (1964).

90. Birkhoff, G.

Helmholtz and Taylor Instability.

13th Symposium in Applied Mathematics.

American Mathematical Society (1962).

APPENDICES

Appendix I (a) and (b)

If an elementary parrallelpiped of fluid of side Δx, Δy and Δz is considered, through which an acoustic pressure pulsation is assumed to pass in the x direction only. The propagation speed of the disturbance will be the sonic velocity c in the fluid. If a sinusoidal pulsation in pressure is assumed then the instantaneous pressure P can be expressed in terms of a mean pressure P_o as.

$$P_x = P_o \; e^{i\omega(t - \frac{x}{c})} \qquad (1)$$

The force exerted on the plane through x of the parallelpiped by the pressure will be

$$P_x = \Delta y \cdot \Delta z \qquad (2)$$

The pressure on the plane through $x + \Delta x$, by use of Taylor's Theorem will be

$$P_x (x + \Delta x) \Delta y \Delta z = P_x \Delta y \Delta z + \frac{\partial P_x}{\partial x} \Delta x \Delta y \Delta z \qquad (3)$$

The mass of fluid in the parallelpiped is $\rho \Delta x \cdot \Delta y \cdot \Delta z$ and it will be accelerated by the pressure pulsation by $\frac{\partial v_x}{\partial t}$ in the x direction.

Equating Inertia forces and Nett pressure forces on the element Δx, Δy, Δz results in

$$\frac{\rho}{g_c} \frac{\partial v_x}{\partial t} = - \frac{\partial P_x}{\partial x} \qquad (4)$$

The velocity v_x will also vary in the manner

$$v_x = v_o \; e^{-i\omega(t - \frac{x}{c})} \qquad (5)$$

Now $$\frac{\partial v_x}{\partial t} = - i \cdot \omega \cdot v_x \qquad (6)$$

and $$- \frac{\partial p}{\partial x} = + i \frac{\omega}{c} \cdot P_x$$

Hence from (4) and (6)

$$v_x = \frac{P_x \cdot g_c}{\rho c} \qquad (7)$$

The sound itensity I of an acoustic wave is defined as the power transmitted per unit area in the direction of wave propagation.

Therefore $I_x = P_x v_x$

$$= \tfrac{1}{2} P_{max} v_{max} \qquad (8)$$

From (7) and (8)

$$\frac{I_x}{c} = \tfrac{1}{2} \rho \frac{v_{max}^2}{g_c} \qquad (9)$$

but $v_{max} = (a_{max} \omega)$

$$\frac{I_x}{c} = \tfrac{1}{2} \cdot \frac{\rho}{g_c} \cdot (a_{max} \omega)^2$$

or $$\frac{I_x}{c} = \frac{\rho}{g_c} (a_{rms} \omega)^2 \qquad (10) \quad \text{I (a)}$$

From (7)

$$(a_{rms} \omega) = \frac{P_{rms} \cdot g_c}{\rho\, c} \qquad (11) \quad \text{I (b)}$$

Appendix II

Zartman Data Run No. 20

Air Mass Velocity G_A	= 4810 lbm/hr ft^2
Combustion Gas Temperature θ_b	= 2350 ^oF
Chamber Wall Temperature θ	= 209 ^oF
Chamber Pressure	= 20 lbf/in^2
Equivalence Ratio ϕ	= 0.814
S.P.L.	= 150.5 db
f	= 4125 c/s
h_v/h_o	= 1.63

For Stoichiometric Combustion of Propane C_4H_{10}.

$$C_4H_{10} + 6.5\ O_2 + 6.5 \times 3.76\ N_2$$
$$5\ H_2O + 4\ CO_2 + 6.5 \times 3.76\ N_2$$

The equivalence ratio ϕ = $\dfrac{\text{Actual Propane Air ratio}}{\text{Stoichiometric Propane Air ratio}}$

Since $\phi < 1.0$ there is an excess of air in the products of combustion. The products of combustion are now.

$H_2O = 0.814 \times 5.0 = 4.070$

$CO_2 = 0.814 \times 4.0 = 3.256$

Free $O_2 = 6.5 - \dfrac{4.070}{2} - 3.256 = \underline{\underline{1.209}}$

Hence Moles of Products are:-

$$n_{H2O} + n_{CO_2} + n_{O_2} + n_{N_2} = n_{Total}$$

$$4.070 + 3.256 + 1.209 + 24.400 = \underline{\underline{32.955}}\ \underline{\underline{\text{Moles}}}$$

The absolute viscosity of the mixture can be obtained at the film temperature (Mean between gas and wall temperature) from

$$\mu_{\substack{mix \\ 1280\ ^oF}} = \frac{\sum_J n_J \sqrt{M_J}\,\mu_J}{\sum_J n_J \sqrt{M_J}}$$

where J is the J th component of the mixture and M is the molecular weight.

$$\mu_{\substack{mix \\ 1280\ ^oF}} = 2.767 \times 10^{-5}\ \text{lbm/ft sec.}$$

Now $R_{mix} = \sum_J x_J R_J$

where R_{mix} is the gas constant for the mixture and x_J and R_J the mole fraction and gas constant for the J th component respectively.

$$\text{Hence } \rho_{mix} = \frac{P}{R_{mix}\, T_{film}} = \underline{0.0292} \text{ lbm/ft}^3$$

$$\nu_{mix} = 9.46 \times 10^{-4} \text{ ft}^2/\text{sec.}$$

$$\text{(S.P.L.) db} = 20 \log_{10} \left[\frac{P}{P_o} \right]_{r.m.s.}$$

where $P_o = 0.0002$ dyne/cm^2 $= 0.418 \times 10^{-6}$ lbf/ft^2

$$\left[\frac{P}{P_o} \right]_{r.m.s.} = 10^{(S.P.L./20)} = 10^{7.525}$$

Hence $P_{r.m.s.} = \underline{14.1 \text{ lbf/ft}^2}$

$$\text{Now } (a_{rms}\omega) = \frac{P_{r.m.s.}\ g_c}{\rho\ C}$$

C at T_{film} = 2060 ft/sec.

Hence $(a_{rms}\omega)$ = 7.55 ft/sec.

Evaluation of v*:-

$$v^* = (0.0333)^{\frac{1}{2}}\ \bar{V}^{7/8} \left[\frac{\nu}{R} \right]^{\frac{1}{8}}$$

$$G = \left[\frac{4810}{3600} \right] = 1.339 \text{ lbm/sec.ft}^2$$

$$\rho_{mix} \text{ @ } T_{bulk} = .0292 \times \frac{1740}{2810} = \underline{.0181} \text{ lbm/ft}^3$$

$$\bar{V} = \frac{G}{\bar{\rho}} = 74 \text{ ft/sec.}$$

$$v^* = (.0333)^{\frac{1}{2}} \cdot (74)^{7/8} \cdot \left[\frac{9.46 \times 24}{10^4 \times 5} \right]^{\frac{1}{8}}$$

$$= 4.05 \text{ ft/sec.}$$

Now $$\frac{h_v}{h_o} = \left[1 + \frac{(a_{r.m.s.}\omega)^2}{v^*}\right]^{\frac{1}{4}}$$

$$= \left[1 + \left(\frac{7.55}{4.05}\right)^2\right]^{\frac{1}{4}}$$

$$= \underline{1.48}$$

This is 10% less than the value of $\frac{h_v}{h_o}$ obtained experimentally.

Appendix III

The solution of Nusselts equation.

$$\frac{dY}{d\phi} \sin\phi + \frac{4}{3} Y \cos\phi - \frac{4}{3} = 0 \qquad (1)$$

which is a linear first order differential equation was carried out by multiplying (1) by a factor $F(Y,\phi)$ and then determining the form which F had to take to make (1) an Exact Differential Equation.
(1) can be written as

$$\sin\phi \cdot dY + \frac{4}{3} Y \cos\phi - 1 \; d\phi = 0 \qquad (2)$$

On multiplying through by F, the resulting equation will be exact if

$$\frac{\partial}{\partial\phi}\left[F \sin\phi\right] = \frac{\partial}{\partial Y}\left[F \cdot \frac{4}{3} (\cos\phi - 1)\right] \qquad (3)$$

Therefore

$$F\cos\phi + \sin\phi \frac{\partial F}{\partial\phi} = F.\frac{4}{3}.\cos\phi + \frac{4}{3}(\cos\phi - 1)\frac{\partial F}{\partial Y} \qquad (4)$$

If it is assumed that $F = F(\phi)$
then

$$\sin\phi \frac{\partial F}{\partial\phi} = \frac{F}{3}\cos\phi \qquad (5)$$

Solution of (5) results in

$$F = \sin^{1/3}\phi \qquad (6)$$

Therefore Equation (2) multiplied through by $F = \sin^{1/3}\phi$ is

$$\sin^{4/3}\phi \; dY + \frac{4}{3}\left[Y\cos\phi - 1\right]\sin^{1/3}\phi \; d\phi = 0 \qquad (7)$$

The above differential equation is exact and may be written as
$du = 0$, or $u =$ constant c.
Since (7) is exact, then

$$\left[\frac{\partial u}{\partial Y}\right] = \left[\frac{\partial u}{\partial\phi}\right] \qquad (8)$$

$$\text{and } du = 0 = \left[\frac{\partial u}{\partial Y}\right] dY + \left[\frac{\partial u}{\partial\phi}\right] d\phi \qquad (9)$$

$$\text{Therefore } \left[\frac{\partial u}{\partial Y}\right] = \sin^{4/3}\phi \qquad (10)$$

and $\left[\frac{\partial u}{\partial \phi}\right] = \frac{4}{3}\left[\, Y \cos \phi - 1 \,\right] \sin^{1/3} \phi$ (11)

From (10) $u = Y \sin^{4/3} \phi + f(\phi)$ (12)

where $f(\phi)$ is a function of ϕ

Therefore $\frac{\partial}{\partial \phi}\left[\, Y \sin^{4/3} \phi + f(\phi) \,\right] = \frac{4}{3}\left[\, Y \cos \phi - 1 \,\right] \sin^{1/3} \phi$ (13)

and $\frac{4}{3} Y \sin^{1/3} \phi \cos \phi + \frac{\partial f(\phi)}{\partial \phi} = \frac{4}{3} Y \cos \phi \sin^{1/3} \phi - \frac{4}{3} \sin^{1/3} \phi$

hence $\frac{\partial f(\phi)}{\partial \phi} = -\frac{4}{3} \sin^{1/3} \phi$

and $f(\phi) = -\frac{4}{3} \int \sin^{1/3} \phi \cdot d\phi$ (14)

$$u = Y \sin^{4/3} \phi - \frac{4}{3} \int \sin^{1/3} \phi \, d\phi = c \text{ (constant)}$$

Therefore $Y = \frac{1}{\sin^{4/3} \phi}\left[\, \frac{4}{3} \int \sin^{1/3} \phi \, d\phi + C \,\right]$ (15)

Appendix IV

Results of Numerical Integration of Equation (9.2.16) according to Nusselt - Jakob (57).

ϕ°	$Y = \left(\frac{\delta}{B}\right)^4$	$Y^{\frac{1}{4}}$
0	1.000	1.000
5	0.963	0.991
10	0.991	0.998
20	1.013	1.003
30	1.049	1.012
40	1.097	1.023
50	1.156	1.037
60	1.247	1.057
70	1.359	1.080
80	1.513	1.109
90	1.714	1.144
100	1.985	1.187
110	2.365	1.240
120	2.905	1.306
130	3.733	1.390
140	5.081	1.501
150	7.588	1.660
160	13.317	1.910
170	34.385	2.422
175	87.733	3.061
180	∞	∞

Appendix V

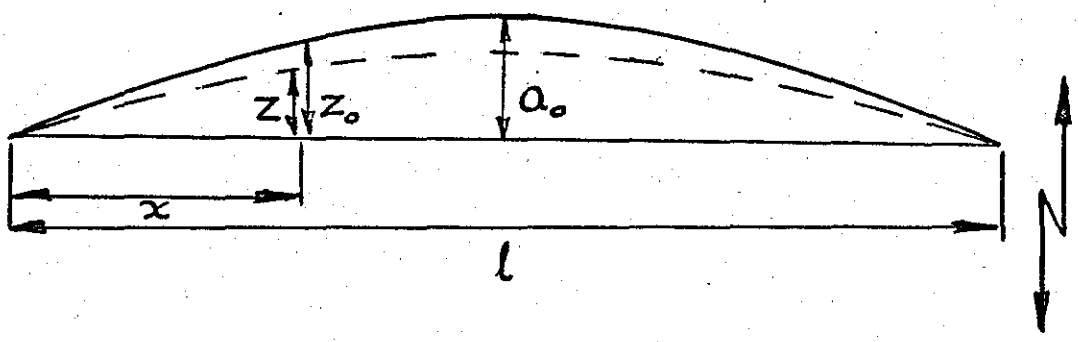

$z = z_o \sin \omega t$

and $z_o = a_o \sin \pi \frac{x}{l}$

K.E. of vibration at x for deflection of z at time t is

$$= \tfrac{1}{2} g_c (\omega z)^2$$

Using the r.m.s. value of z at x

K.E. of vibration is $\frac{1}{4g_c} \cdot (\omega z_o)^2$

The mean deflection of the Beam at maximum amplitude is

$$\bar{z}_o = \frac{a_o}{l} \int_o^l \sin \pi \frac{x}{l} \, dx = \frac{2 a_o}{\pi}$$

Therefore K.E. for mean deflection of the beam is

$$\text{K.E.} = \frac{1}{g_c} \left[\frac{a_o \omega}{\pi} \right]^2$$

APPENDIX VI

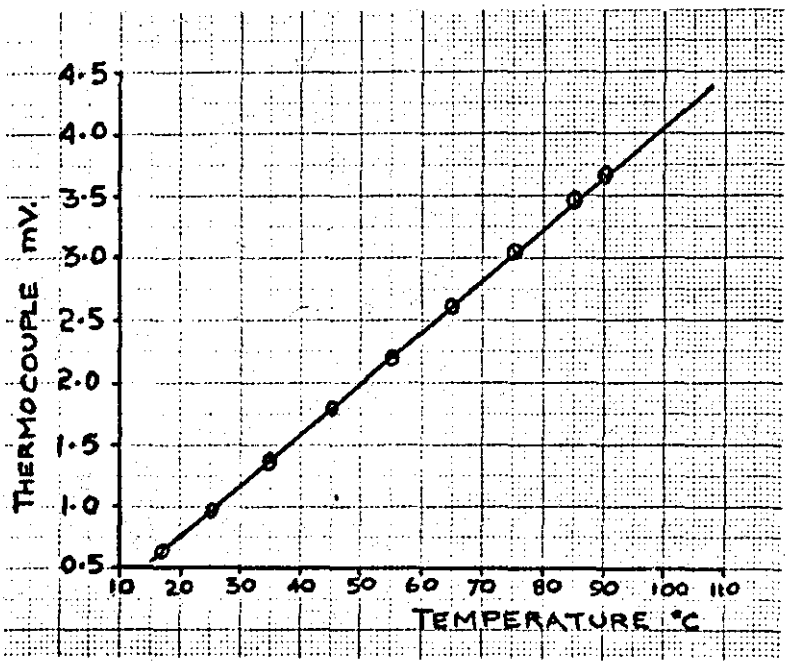

Fig. 1 Specimen Calibration of Copper Constantan Thermocouples

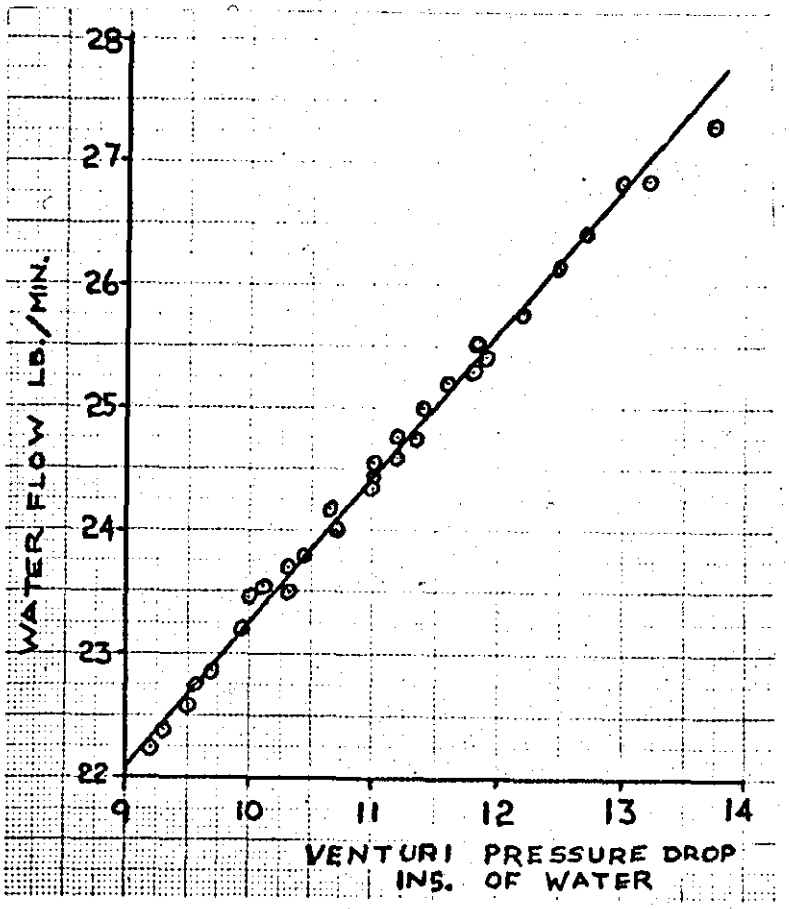

Fig. 2 Calibration of Venturi Tube for Water Flow Measurement

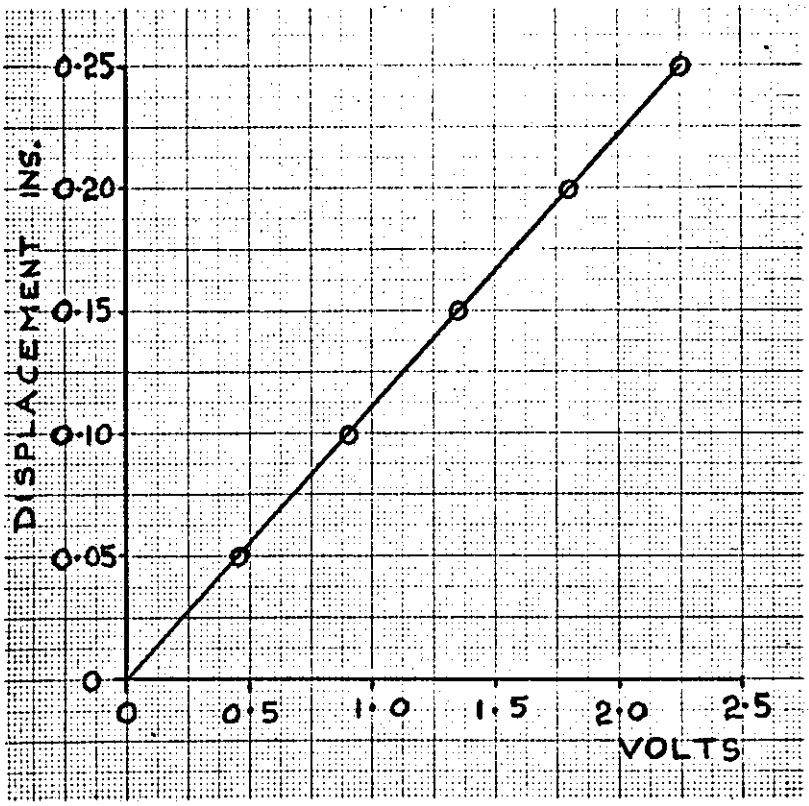

Fig. 3 Sanborn Displacement Transducer Calibration

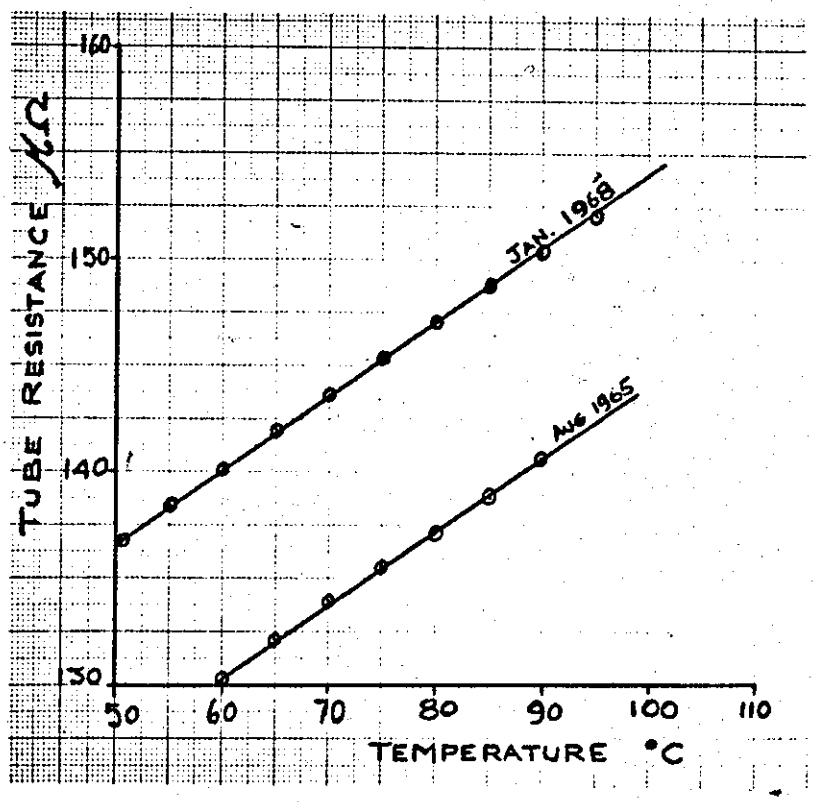

Fig. 4 Specimen Calibration of Resistance of the Copper Condenser Tube

Appendix VII Table I

	m_w lbm/min	θ_{wi} °C	θ_{we} °C	Q chu/hr	θ_m °C	$\frac{\theta_o-\theta_i}{2}$ °C	θ_o °C	$\theta_{sat}-\theta_v$ °C	h Btu/hr ft^2°F	f c/s	a ins	$\frac{k(\theta_{sat}-\theta_o)}{h_{fg}}$	Re_v	$\frac{N}{3}\frac{D^2}{4}\frac{a}{3\pi D}\frac{Re_v\mu h_{fg}}{k(\theta_{sat}-\theta_o)}$ =	$h_{Nusselt}$ Btu/hr ft^2 °F	$\frac{h_v}{h_o}$
(1)	26.7	15.40	22.80	11,850	77.2	0.58	77.78	23.32	2190	-	-	-	-	-	1850	-
(2)	24.6	15.5	22.5	10,310	78.6	0.51	79.11	22.0	2020	-	-	-	-	-	1870	-
(3)	24.6	14.2	21.8	11,200	78.4	0.55	78.95	22.15	2180	20	0.165	12.3×10^{-3}	33,700	2.32×10^5	-	1.08
(4)	24.4	14.3	21.8	11,000	78.4	0.54	78.94	22.16	2140	20	0.110	12.3×10^{-3}	22,450	1.03×10^5	-	1.06
(5)	24.4	14.3	21.8	10,000	78.4	0.54	78.94	22.16	2140	20	0.055	12.3×10^{-3}	11,225	0.2575×10^5	-	1.06
(6)	22.2	18.0	27.75	12,950	82.79	0.68	83.47	17.63	3160	-	-	-	-	-	2300	-
(7)	23.1	18.2	27.30	12,500	83.50	0.59	84.01	16.09	3360	80	0.025	9.6×10^{-3}	20,840	0.279×10^5	-	1.062
(8)	22.75	18.75	28.8	13,700	84.19	0.67	84.86	16.24	3640	20	0.155	9.0×10^{-3}	32,400	2.86×10^5	-	1.150
(9)	22.95	19.1	27.5	11,550	81.00	0.57	81.57	19.53	2550	-	-	-	-	-	2240	-
(10)	22.88	20.1	29.0	12,200	82.50	0.65	83.15	17.95	2930	60	0.032	10×10^{-3}	20,100	0.329×10^5	-	1.150
(11)	23.33	19.0	27.8	12,330	81.00	0.61	81.61	19.49	2720	-	-	-	-	-	2240	-
(12)	23.2	20.48	29.49	12,500	82.00	0.62	82.62	18.48	2920	40	0.055	10×10^{-3}	22,800	0.621×10^5	-	1.070
(13)	23.2	21.0	29.8	12,280	81.50	0.59	82.09	19.01	2780	40	0.038	10×10^{-3}	15,710	0.288×10^5	-	1.020
(14)	22.65	15.5	23.0	10,200	82.60	0.500	83.10	18.0	2440	-	-	-	-	-	2180	-
(15)	23.9	16.5	23.2	9,625	79.6	0.47	80.07	21.03	1970	-	-	-	-	-	1890	-
(16)	23.9	16.5	24.2	11,030	79.4	0.54	79.94	21.16	2260	20	0.166	11.8×10^{-3}	34,200	2.45×10^5	-	1.148
(17)	23.9	17.0	24.4	10,600	78.6	0.52	79.12	21.98	2080	30	0.110	12.2×10^{-3}	33,600	1.55×10^5	-	1.058
(18)	22.1	15.1	23.0	10,490	80.2	0.52	80.72	20.38	2220	40	0.055	11.3×10^{-3}	22,600	0.561×10^5	-	1.128
(19)	22.1	15.1	23.4	10,350	79.4	0.51	79.91	21.19	2110	50	0.040	11.8×10^{-3}	20,500	0.355×10^5	-	1.070
(20)	22.1	15.9	23.9	10,600	79.2	0.52	79.72	21.38	2140	60	0.028	11.9×10^{-3}	17,200	0.208×10^5	-	1.085

$\theta_{sat} = 101.1$ °C

Appendix VII Table I continued

	m_v lbm/min.	θ_{w_i} °C	θ_{w_e} °C	Q chu/hr	θ_m °C	$\frac{\theta_o-\theta_i}{2}$ °C	θ_o °C	$\theta_{sat}-\theta_v$ °C	h Btu/hr ft^2°F	f c/s	a ins	$\frac{k(\theta_{sat}-\theta_o)}{h_{fg}}$	Re_v	$N_u \cdot D^2 \frac{4}{3\pi}\frac{a}{D}\frac{Re_v \mu h_{fg}}{k(\theta_{sat}-\theta_o)}$	$h_{Nusselt}$ Btu/hr ft^2 °F	$\frac{h_v}{h_o}$
(21)	28.6	17.8	24.4	11,310	76.4	0.56	76.96	24.14	2020	-	-	-	-	-	1820	-
(22)	28.6	17.6	24.2	11,310	77.0	0.56	77.56	23.54	2080	20	.028	13×10^{-3}	5550	0.060×10^5	-	1.03
(23)	28.6	18.5	25.2	11,500	77.0	0.57	77.57	23.53	2115	20	.055	13×10^{-3}	11,100	0.240×10^5	-	1.045
(24)	28.2	18.6	25.3	11,320	77.0	0.56	77.56	23.54	2080	20	.083	13×10^{-3}	16,650	0.541×10^5	-	1.03
(25)	23.8	15.9	23.7	11,120	78.0	0.55	78.55	21.95	2190	-	-	-	-	-	1875	-
(26)	23.8	15.9	23.9	11,410	78.0	0.56	78.56	21.94	2250	40	.045	12.1×10^{-3}	11,890	0.163×10^5	-	1.05
(27)	29	19.6	26.0	11,150	76.6	0.55	77.15	23.95	2010	-	-	-	-	-	1830	-
(28)	27.9	20.5	27.1	11,050	77.5	0.54	78.04	23.06	2090	50	.038	12.8×10^{-3}	19,500	0.229×10^5	-	1.04
(29)	27.9	20.5	27.2	11,200	76.6	0.55	77.15	23.95	2010	60	.028	13.3×10^{-3}	17,200	0.182×10^5	-	1.00
(30)	22.65	16.3	24.8	11,500	81.8	0.56	82.36	18.74	2640	-	-	-	-	-	2040	-
(31)	22.85	17.0	25.25	11,300	83.0	0.56	83.56	17.54	2775	20	.025	9.9×10^{-3}	5,230	0.069×10^5	-	1.05
(32)	22.63	17.25	25.38	11,050	83.9	0.55	84.45	16.65	2860	30	.045	9.3×10^{-3}	14,150	0.352×10^5	-	1.082
(33)	22.88	17.0	25.3	11,400	83.0	0.57	83.57	17.53	2800	40	.025	4.8×10^{-3}	10,500	0.133×10^5	-	1.06
(34)	22.68	16.8	25.3	11,550	83.0	0.57	83.57	17.53	2850	80	.023	9.8×10^{-3}	19,050	0.230×10^5	-	1.08

$\theta_{sat} = 101.1$ °C

Appendix VII

Table II

ϕ°	$Y^{\frac{1}{4}}$	ϕ°	$Y^{\frac{1}{4}}$
0.0	1.0000	88.0	1.1377
2.0	0.9036	90.0	1.1453
4.0	0.9639	92.0	1.1532
6.0	0.9795	94.0	1.1614
8.0	0.9867	96.0	1.1700
10.0	0.9909	98.0	1.1789
12.0	0.9938	100.0	1.1882
14.0	0.9962	102.0	1.1979
16.0	0.9982	104.0	1.2080
18.0	1.0001	106.0	1.2185
20.0	1.0019	108.0	1.2295
22.0	1.0037	110.0	1.2410
24.0	1.0055	112.0	1.2530
26.0	1.0074	114.0	1.2655
28.0	1.0094	116.0	1.2786
30.0	1.0114	118.0	1.2924
32.0	1.0136	120.0	1.3069
34.0	1.0158	122.0	1.3220
36.0	1.0182	124.0	1.3380
38.0	1.0207	126.0	1.3548
40.0	1.0234	128.0	1.3725
42.0	1.0261	130.0	1.3912
44.0	1.0290	132.0	1.4110
46.0	1.0321	134.0	1.4319
48.0	1.0353	136.0	1.4542
50.0	1.0386	138.0	1.4779
52.0	1.0421	140.0	1.5032
54.0	1.0458	142.0	1.5303
56.0	1.0496	144.0	1.5594
58.0	1.0536	146.0	1.5908
60.0	1.0577	148.0	1.6248
62.0	1.0621	150.0	1.6617
64.0	1.0666	152.0	1.7021
66.0	1.0713	154.0	1.7465
68.0	1.0762	156.0	1.7956
70.0	1.0813	158.0	1.8506
72.0	1.0866	160.0	1.9125
74.0	1.0922	162.0	1.9832
76.0	1.0979	164.0	2.0652
78.0	1.1039	166.0	2.1619
80.0	1.1102	168.0	2.2787
82.0	1.1166	170.0	2.4245
84.0	1.1234	172.0	2.6150
86.0	1.1304	174.0	2.8817

Appendix VII

Table III $\frac{N}{3} = 1 \times 10^6 \text{ ft}^{-2}$

ϕ^o	δ_v ft	ϕ^o	δ_v ft
0.0	0.0001422	88.0	0.0001625
2.0	0.0001283	90.0	0.0001636
4.0	0.0001370	92.0	0.0001647
6.0	0.0001393	94.0	0.0001659
8.0	0.0001403	96.0	0.0001672
10.0	0.0001409	98.0	0.0001685
12.0	0.0001413	100.0	0.0001699
14.0	0.0001417	102.0	0.0001713
16.0	0.0001420	104.0	0.0001728
18.0	0.0001422	106.0	0.0001743
20.0	0.0001425	108.0	0.0001759
22.0	0.0001428	110.0	0.0001776
24.0	0.0001430	112.0	0.0001794
26.0	0.0001433	114.0	0.0001812
28.0	0.0001436	116.0	0.0001831
30.0	0.0001439	118.0	0.0001852
32.0	0.0001442	120.0	0.0001873
34.0	0.0001445	122.0	0.0001895
36.0	0.0001449	124.0	0.0001918
38.0	0.0001453	126.0	0.0001943
40.0	0.0001456	128.0	0.0001969
42.0	0.0001460	130.0	0.0001996
44.0	0.0001465	132.0	0.0002025
46.0	0.0001469	134.0	0.0002056
48.0	0.0001474	136.0	0.0002088
50.0	0.0001479	138.0	0.0002123
52.0	0.0001484	140.0	0.0002160
54.0	0.0001489	142.0	0.0002200
56.0	0.0001495	144.0	0.0002242
58.0	0.0001501	146.0	0.0002288
60.0	0.0001507	148.0	0.0002338
62.0	0.0001513	150.0	0.0002391
64.0	0.0001520	152.0	0.0002450
66.0	0.0001527	154.0	0.0002515
68.0	0.0001534	156.0	0.0002587
70.0	0.0001542	158.0	0.0002667
72.0	0.0001550	160.0	0.0002757
74.0	0.0001558	162.0	0.0002860
76.0	0.0001566	164.0	0.0002979
78.0	0.0001575	166.0	0.0003120
80.0	0.0001584	168.0	0.0003290
82.0	0.0001594	170.0	0.0003502
84.0	0.0001604	172.0	0.0003779
86.0	0.0001614	174.0	0.0004167

Appendix VII

Table III $\frac{N}{3} = 1.4 \times 10^6 \text{ ft}^{-2}$

ϕ°	δ_v ft	ϕ°	δ_v ft
0.0	0.0001357	88.0	0.0001571
2.0	0.0001219	90.0	0.0001583
4.0	0.0001308	92.0	0.0001595
6.0	0.0001330	94.0	0.0001607
8.0	0.0001340	96.0	0.0001621
10.0	0.0001345	98.0	0.0001634
12.0	0.0001350	100.0	0.0001649
14.0	0.0001353	102.0	0.0001664
16.0	0.0001356	104.0	0.0001679
18.0	0.0001358	106.0	0.0001695
20.0	0.0001361	108.0	0.0001712
22.0	0.0001364	110.0	0.0001730
24.0	0.0001367	112.0	0.0001748
26.0	0.0001369	114.0	0.0001767
28.0	0.0001372	116.0	0.0001787
30.0	0.0001376	118.0	0.0001808
32.0	0.0001379	120.0	0.0001830
34.0	0.0001382	122.0	0.0001853
36.0	0.0001386	124.0	0.0001878
38.0	0.0001390	126.0	0.0001903
40.0	0.0001394	128.0	0.0001930
42.0	0.0001398	130.0	0.0001959
44.0	0.0001403	132.0	0.0001989
46.0	0.0001407	134.0	0.0002020
48.0	0.0001412	136.0	0.0002054
50.0	0.0001418	138.0	0.0002090
52.0	0.0001423	140.0	0.0002128
54.0	0.0001429	142.0	0.0002169
56.0	0.0001435	144.0	0.0002213
58.0	0.0001441	146.0	0.0002261
60.0	0.0001447	148.0	0.0002312
62.0	0.0001454	150.0	0.0002367
64.0	0.0001461	152.0	0.0002428
66.0	0.0001468	154.0	0.0002495
68.0	0.0001476	156.0	0.0002568
70.0	0.0001484	158.0	0.0002651
72.0	0.0001492	160.0	0.0002743
74.0	0.0001501	162.0	0.0002849
76.0	0.0001509	164.0	0.0002971
78.0	0.0001519	166.0	0.0003115
80.0	0.0001528	168.0	0.0003289
82.0	0.0001538	170.0	0.0003506
84.0	0.0001549	172.0	0.0003788
86.0	0.0001560	174.0	0.0004183

Appendix VII

Table III $\frac{N}{3} = 7 \times 10^6 \text{ ft}^{-2}$

ϕ°	δ_v ft	ϕ°	δ_v ft
0.0	0.0001295	88.0	0.0001520
2.0	0.0001160	90.0	0.0001532
4.0	0.0001249	92.0	0.0001545
6.0	0.0001270	94.0	0.0001558
8.0	0.0001280	96.0	0.0001572
10.0	0.0001285	98.0	0.0001586
12.0	0.0001289	100.0	0.0001601
14.0	0.0001293	102.0	0.0001616
16.0	0.0001295	104.0	0.0001633
18.0	0.0001298	106.0	0.0001649
20.0	0.0001301	108.0	0.0001667
22.0	0.0001304	110.0	0.0001685
24.0	0.0001306	112.0	0.0001704
26.0	0.0001309	114.0	0.0001724
28.0	0.0001312	116.0	0.0001745
30.0	0.0001316	118.0	0.0001767
32.0	0.0001319	120.0	0.0001790
34.0	0.0001323	122.0	0.0001814
36.0	0.0001327	124.0	0.0001839
38.0	0.0001331	126.0	0.0001865
40.0	0.0001335	128.0	0.0001893
42.0	0.0001339	130.0	0.0001923
44.0	0.0001344	132.0	0.0001954
46.0	0.0001349	134.0	0.0001987
48.0	0.0001354	136.0	0.0002022
50.0	0.0001360	138.0	0.0002059
52.0	0.0001365	140.0	0.0002098
54.0	0.0001371	142.0	0.0002140
56.0	0.0001377	144.0	0.0002186
58.0	0.0001384	146.0	0.0002234
60.0	0.0001391	148.0	0.0002287
62.0	0.0001398	150.0	0.0002344
64.0	0.0001405	152.0	0.0002407
66.0	0.0001413	154.0	0.0002475
68.0	0.0001421	156.0	0.0002551
70.0	0.0001429	158.0	0.0002635
72.0	0.0001437	160.0	0.0002730
74.0	0.0001446	162.0	0.0002839
76.0	0.0001456	164.0	0.0002964
78.0	0.0001465	166.0	0.0003111
80.0	0.0001475	168.0	0.0003289
82.0	0.0001486	170.0	0.0003510
84.0	0.0001497	172.0	0.0003798
86.0	0.0001508	174.0	0.0004200

Appendix VII

Table III $\frac{N}{3} = 10 \times 10^6 \text{ ft}^{-2}$

ϕ^o	δ_v ft	ϕ^o	δ_v ft
0.0	0.0001238	88.0	0.0001471
2.0	0.0001104	90.0	0.0001484
4.0	0.0001193	92.0	0.0001497
6.0	0.0001214	94.0	0.0001511
8.0	0.0001223	96.0	0.0001525
10.0	0.0001229	98.0	0.0001540
12.0	0.0001233	100.0	0.0001555
14.0	0.0001236	102.0	0.0001571
16.0	0.0001239	104.0	0.0001588
18.0	0.0001241	106.0	0.0001606
20.0	0.0001244	108.0	0.0001624
22.0	0.0001247	110.0	0.0001643
24.0	0.0001250	112.0	0.0001663
26.0	0.0001253	114.0	0.0001683
28.0	0.0001256	116.0	0.0001705
30.0	0.0001259	118.0	0.0001727
32.0	0.0001263	120.0	0.0001751
34.0	0.0001267	122.0	0.0001776
36.0	0.0001271	124.0	0.0001802
38.0	0.0001275	126.0	0.0001829
40.0	0.0001279	128.0	0.0001858
42.0	0.0001284	130.0	0.0001888
44.0	0.0001289	132.0	0.0001920
46.0	0.0001294	134.0	0.0001954
48.0	0.0001299	136.0	0.0001990
50.0	0.0001305	138.0	0.0002029
52.0	0.0001311	140.0	0.0002069
54.0	0.0001317	142.0	0.0002113
56.0	0.0001323	144.0	0.0002159
58.0	0.0001330	146.0	0.0002210
60.0	0.0001337	148.0	0.0002264
62.0	0.0001344	150.0	0.0002322
64.0	0.0001352	152.0	0.0002387
66.0	0.0001360	154.0	0.0002457
68.0	0.0001368	156.0	0.0002534
70.0	0.0001377	158.0	0.0002621
72.0	0.0001386	160.0	0.0002718
74.0	0.0001395	162.0	0.0002829
76.0	0.0001405	164.0	0.0002957
78.0	0.0001415	166.0	0.0003108
80.0	0.0001425	168.0	0.0003289
82.0	0.0001436	170.0	0.0003514
84.0	0.0001447	172.0	0.0003808
86.0	0.0001459	174.0	0.0004217

APPENDIX VIII

PUBLICATIONS OF THE AUTHOR

(1) The Calculation of Heat Transfer Coefficient for Combustion Driven Transverse Oscillations in a Gas-Air Burner.
A. I. Ch. E. Jour. 13, 1114 (1967)

(2) Heat Transfer from a Vertical Transversely Vibrating Plane Surface to Air by Free Convection.
Int. Jour. Heat and Mass Transfer. 11, 605 (1968)

(3) The Effect of Vibration on Condensation Heat Transfer to a Horizontal Tube.
Proc. I. Mech. E. (In Press)

(4) The Calculation of Heat Transfer Coefficient for Condensation of Steam on a Vibrating Vertical Tube.

(5) The Effect of Acoustic and Mechanical Oscillation on Free Convection from Heated Cylinders in Air.
Chem. Eng. Science. (In Press)

THE CALCULATION OF HEAT TRANSFER COEFFICIENT FOR COMBUSTION DRIVEN TRANSVERSE OSCILLATIONS IN A GAS-AIR BURNER

KEY WORDS

Gas-Air (1); Acoustic Energy (1); Burner (10); Convection (2); Forced (0); Increased (0); Boilers (4); Boundary Layer (8),(9); Turbulent (0); Acoustics (8).

J. C. Dent,
Department of Mechanical Engineering,
Loughborough University of Technology,
Leicestershire,
England.

SUMMARY

In this paper a method is presented for the computation of the heat transfer coefficient in a Gas-Air burner in the presence of combustion driven transverse mode oscillations.

By considering the oscillations in pressure within the chamber to be small compared with the mean chamber pressure, and to be known, methods of acoustics may be used to determine the average energy density of the acoustic waves at the wall. Considering this acoustic energy to create greater mixing in the boundary layer enables the heat transfer problem to be considered by the Dankwerts-Mickley Model for turbulent heat exchange. With suitable definition of a friction velocity in terms of the friction velocity v^* for fully developed turbulent pipe flow and the root mean square particle velocity of the acoustic wave ($a_{r.m.s.}\omega$), it is found that agreement exists between the computed ratio of heat transfer coefficients, with and without combustion driven oscillations and the experiments of Zartman[10], which appear to be the only experimental data for transverse oscillations in a gas-air burner.

THE CALCULATION OF HEAT TRANSFER COEFFICIENT FOR COMBUSTION DRIVEN TRANSVERSE OSCILLATIONS IN A GAS-AIR BURNER

J. C. Dent
Department of Mechanical Engineering,
Loughborough University of Technology,
Loughborough,
Leicestershire,
England.

The occurrence of oscillations in combustion systems under certain conditions of operation was observed as far back as 1777,[1] but with the advent of jet and rocket propulsion systems a systematic study of this phenomenon has been undertaken.

The types of oscillation to be considered here are those associated with the aerothermochemistry and acoustics of the combustion system, in which the frequency of the oscillation corresponds to one or more of the resonant acoustic modes pertinent to the geometry of the combustion chamber.

The acoustic modes in their pure form for a cylindrical geometry are:-

(1) Longitudinal
(11) Transverse
(111) Radial.

The transverse mode can be of either a "Sloshing " or a "Spinning" form.

The above designation describes the motion of the fluid in the chamber. Figure (1) illustrates the various forms of oscillation in the absence of bulk flow of gas through the chamber.

In rocket motors [2],[7] where high energy fuels are used at high combustion chamber pressures, combustion driven oscillations are possible. These oscillations result in large fluctuations of pressure and velocity and increased heat transfer to the chamber walls, which, can destroy the chamber in a very short period of time. However, Reynst[3], Francis et al [4] and others [1] working with commercial hydrocarbons and pulverised solid fuels and air, at moderate combustion chamber pressures, have endeavoured to investigate controlled combustion driven oscillations with the view to their application in reducing the size of industrial boiler plant.

The theoretical and experimental work reported in the unclassified literature [1],[5],[6],[7],[8] has been associated in the main with rocket, jet afterburners and ramjet systems, where the main concern has been the suppression of combustion driven oscillations of all types. Therefore, the aim of much of this work has been in determining the Chemical, Geometric and Aerodynamic factors giving rise to combustion oscillation, and to set up

suitable limits within which stable operation of the system is possible. Since the transverse modes of oscillation have been found to give the largest increases in heat transfer, it is this mode which will receive attention here.

Any attempt at calculating the convective heat transfer coefficient between the combustion gases and the chamber wall by a consideration of the detailed fluid motion within the chamber would be extremely difficult. Therefore, a semi-empirical approach to the problem would appear more probable.

The frequency of fluctuations in pressure and velocity during combustion driven oscillations can be readily calculated from acoustic theory, and the results have been found to be in good agreement with experiment.[2], [5], [10] However, the magnitude of the pressure and velocity fluctuations cannot be predicted, because in the case of the rocket motor; the wave phenomena caused by the coupling of the combustion heat release and the acoustic waves in the chamber are outside the scope of acoustics, which is based on the assumption of small perturbations. In rocket motors the transverse mode is usually of the "Spinning" variety, whereas for the lower combustion intensity afterburner and ramjet the mode is likely to be of the "Sloshing" type. One can therefore think of the "spinning" mode as an overdriven "sloshing" mode.

In the combustion chamber studied by Zartman[10] using a Propane-Air mixture at moderate combustion chamber pressure, the level of the combustion driven oscillations were such that acoustic theory would be applicable. Before the magnitude of the pressure fluctuations in the combustion chamber can be calculated by acoustic methods, the phasing of heat release to the acoustic disturbances in the chamber due to flow and geometric considerations must be known. This type of information is not generally available, and can only be obtained from experimental data. Zartman[10] did not obtain data of this type, but measured the pressure fluctuations at the wall. If it is assumed then that from semi-empirical data the fluctuations in pressure at the chamber wall are known for a given geometry, fuel and flow condition, this paper presents a method by which the computation of the convective heat transfer coefficient from the hot gases to the chamber wall may be carried out. The results obtained by the method of this paper are compared with the experimental data of Zartman[10] who was concerned solely with the measurement of heat transfer coefficients during combustion driven oscillations.

HEORY

In the study of interphase mass transfer Dankwerts(11), (12) put forward the enetration model for the process. This model was later incorporated into a more eneral discussion by Toor and Marchello,(13) who applied it to the case of heat or ass transfer in turbulent pipe flow. In essence the heat exchange model of ref. 13) considers the laminar sub layer adjacent to the pipe wall to be penetrated by lumps" of fluid from the turbulent core and to exchange heat with the wall in a ransient manner before being displaced into the core by fresh fluid lumps from that egion; the whole process taking place randomly and at high frequency. A similar odel was put forward by Mickley and Fairbanks(14) for the transfer of heat in luidised beds. Here aggregates of particles are considered to randomly move to he containing wall, exchange heat with it in a transient manner and then be replaced y fresh aggregates from the core of the bed. These models have been put forward or complex mixing processes because detailed mathematical description of the fluid otion is not possible.

Male et al (2) from a photographic study of the "Spinning" mode of transverse scillations in a rocket motor conclude that it is possible that the high rates of eat transfer were due to turbulence, which caused macroscopic transfer of the gas o the chamber wall. Similar gas motion was observed in the photographic studies of rieg (15) on a rocket motor in which the "Spinning" transverse mode was present. t is reasonable to assume that a similar gas motion would be observed with the Sloshing" transverse mode of gas oscillations; but with the absence of the ravelling detonation front, which is present in high intensity combustion rocket ystems which are in a "Spinning" transverse mode of oscillation.

If one considers the effect of combustion driven oscillations in the transverse loshing mode to promote high frequency mixing in the laminar sub layer at the wall, hen it is possible to apply the Dankwerts- Mickley model to the calculation of the eat transfer coefficient between the gas and chamber wall.

From the Dankwerts-Mickley Model the heat transfer coefficient between the fluid edium and the containing wall is given by.

$$h = \sqrt{k \rho C_p S} \qquad (1)$$

he details of the derivation of equation (1) are to be found in references (13) and 14). The important quantity in equation (1) is the mixing coefficient S, which is ontrolled by the fluid dynamics and geometry of the particular situation.

Toor and Marchello [13] show that for turbulent pipe flow S_o is proportional to

$$\frac{\bar{V}}{D} N_{Re}^{0.8}.$$

In the theory of turbulent boundary layers [16] the friction velocity v^* is used as a measure of turbulent eddying, and of the transfer of momentum due to these eddies, and it is known [16] that v^* is proportional to $\bar{V}$, therefore if S_o is set proportional to $\frac{v^*}{D} N_{Re}^{0.8}$ then

$$h_o = \sqrt{k \rho C_p \beta \frac{v^*}{D} N_{Re}^{0.8}} \qquad (2)$$

It is shown in the Appendix that the value of h_o computed from equation (2) with the selection of a suitable value of the proportionality constant β, will be in substantial agreement with the value of h_o computed from the McAdam Correlation [17] $N_{Nu.} = 0.023 N_{Re}^{0.8} N_{Pr}^{0.4}$ with $N_{Pr} = 0.73$

and $10{,}000 \leq N_{Re} \leq 120{,}000$

The next step is to set up a form for the mixing coefficient S_v when a turbulent bulk flow with simultaneous transverse acoustic gas oscillations exists,

Now
$$\frac{\rho v^{*2}}{g_c} = \tau_{w_o} \qquad (3)$$

Due to the gas oscillation the average energy density [18] in the acoustic wave is.

$$\frac{I}{C} = \frac{\rho u_{max.}^2}{2 g_c}$$

$$= \frac{\rho u_{r.m.s.}^2}{g_c} \quad \text{for a wave of sinusoidal form}$$

$$= \frac{\rho}{g_c} \left[a_{r.m.s.} \omega \right]^2 \qquad (4)$$

If one considers that because of acoustic oscillations which are superimposed on the bulk flow, the average energy density of the acoustic wave at the wall supplements the frictional energy $\frac{\rho v^{*2}}{g_c}$, then the wall shearing stress τ_{w_o} is modified to τ_{wv} where

$$\tau_{wv} = \frac{\rho}{g_c} \left[v^{*2} + \left(a_{r.m.s.} \omega \right)^2 \right] \qquad (5)$$

If a friction velocity v^{**} is defined, and the mixing coefficient S_v is set proportional to $\frac{v^{**} N_{Re}^{0.8}}{D}$ where $v^{**} = \sqrt{v^{*2} + (a_{r.m.s.}\omega)^2}$ then:-

$$h_v = \sqrt{k \rho C_p \beta \frac{v^{**} N_{Re}^{0.8}}{D}} \qquad (6)$$

The proportionality constant must remain as β ; if this were not so, then with $(a_{r.m.s}\,\omega) = 0$; $\frac{h_v}{h_o} \neq 1$.

$$\therefore \quad \frac{h_v}{h_o} = \sqrt{\frac{v^{**}}{v^*}} = \left[1 + \left(\frac{a_{r.m.s}\,\omega}{v^*}\right)^2\right]^{1/4} \qquad (7)$$

Comparison with Experimental Data

For fully developed pipe flow[16] $\tau_{wo} = \frac{0.0333 \rho \bar{V}^{7/4}}{g_c} \left[\frac{\nu}{R}\right]^{1/4}$

Substituting for τ_{wo} in equation (3) and rearranging

$$v^* = (0.0333)^{1/2} \bar{V}^{7/8} \left[\frac{\nu}{R}\right]^{1/8} \qquad (8)$$

where ν in equation (8) is evaluated on a molal average basis at the mean of the gas and wall temperatures.

In the evaluation of $(a_{r.m.s.}\omega)$ from the measured acoustic intensity, the following assumption was made. The measured Sound Pressure Level at a point just upstream of the flameholder is the same as that at the point at which heat transfer measurements were made. This assumption appears reasonable in the light of experimental evidence[18] on a burner with flameholder in which a small peak pressure was observed just downstream of the flameholder; but over the remainder of the downstream length and part of the length upstream from the flameholder the pressure amplitude level was approximately constant. The following conversions were used in determing $(a_{r.m.s.}\omega)$ from the measured sound intensity in decibels[20]

Sound Pressure Level (S.P.L.) db = $20 \log_{10} \left[\frac{P}{P_o} \right]_{r.m.s.}$

where P_o = Reference Pressure Level = .0002 dynes/cm^2

$$(a_{r.m.s.}\,\omega) = \frac{P_{r.m.s.}\, g_c}{\rho c}$$

Only transverse oscillation data for the 17½ inch burning length were taken from reference (10), all property values being evaluated on an average molal basis at the average of gas and wall temperature. The reasons for using the 17½ inch data were (1) the effects of the combustion reaction at the point at which the heat transfer measurements were being made would be minimal, (2) the flow at that point corresponded closely to the fully developed condition on which the method presented in this paper is based.

Equation (7) is plotted in Figure (2), with the experimental data of reference (10) shown. A least squares plot of the data assuming a slope of ¼ for a linear law is also shown. The standard deviation between the experimental data points and equation (7) is 0.11.

A method has been presented by which the heat transfer coefficient between the gases and the wall of a combustion chamber may be computed, when the gases are in a transverse mode of oscillation in which the pressure fluctuations are small compared to the mean pressure in the chamber, and provided that the pressure fluctuations at the wall are known. The method indicates a continuous change in the heat transfer coefficient with intensity of oscillation, whereas Zartman observed increases in heat transfer occurred, only when the S.P.L. exceeded 130 db. However, at 130 db the increase predicted by the method here would fall within the range of normal experimental error for heat transfer during oscillation free combustion. At the high intensities, greater than 140 db., agreement exists between the method presented here and experiment. However, further experiments are required to completely verify the method put forward here. Experiments are also required to attempt to obtain a relation between burner geometry, operating conditions and Air-fuel Ratio, with S.P.L. within the chamber. If this can be done; then all the information necessary for predicting the performance of complete burners employing combustion driven transverse oscillations will be available.

APPENDIX

$$h_o = \sqrt{k \rho C_p S_o}$$

For fully developed turbuclent flow in a pipe

S_o proportional to $\frac{v^* N_{Re}^{0.8}}{D}$

$$\therefore \quad h_o = \sqrt{k \rho C_p \left[\frac{\beta v^* N_{Re}^{0.8}}{D}\right]}$$

where β = constant of proportionality

$$h_o \sqrt{\frac{D}{k \rho C_p}} = \sqrt{\beta} \sqrt{v^*} N_{Re}^{0.4}$$

For fully developed turbulent pipe flow from reference (16)

$$v^{*2} = \frac{0.0396 \bar{V}^{7/4} \nu^{1/4}}{D^{1/4}}$$

$$\therefore h_o \sqrt{\frac{D}{k \rho C_p}} = C_1 N_{Re}^{0.4} \frac{\bar{V}^{1/2}}{N_{Re}^{1/16}} \quad \text{where} \quad C_1 = \sqrt{\beta} (0.0396)^{1/4}$$

$$\therefore \frac{h_o D}{k} = C_1 N_{Re}^{0.838} N_{Pr}^{0.5} \qquad \text{(A1)}$$

McAdam Correlation reference (17)

$$\frac{h_o D}{k} = 0.023 N_{Re}^{0.8} N_{Pr}^{0.4} \qquad \text{(A2)}$$

valid in range $10{,}000 \leq N_{Re} \leq 120{,}000$

$0.7 \leq N_{Pr} \leq 120$

The results from (A1) and (A2) agree to within 6% when $C_1 = 0.0162$ and $N_{Pr} = 0.73$ for the range $10{,}000 \leq N_{Re} \leq 120{,}000$, a slight divergence in results occurs with increasing N_{Re}

NOTATION

a	Particle Amplitude	(L)
C	Sonic Velocity	(L/t)
C_1	A Constant	(Dimensionless)
C_p	Constant Pressure Thermal Capacity	(L^2/t^2T)
D	Combustion Chamber Inner Diameter	(L)
f	Frequency of oscillation	($1/t$)
g_c	Gravitational Constant	(Dimensionless)
h	Convective heat transfer coefficient	(M/t^3T)
I	Intensity of Acoustic Wave	($M/L\ t^2$)
k	Thermal Conductivity	(ML/t^3T)
N_{Nu}	Nusselt Number	(Dimensionless)
N_{Re}	Reynolds Number	(")
N_{Pr}	Prandtl Number	(")
P	Pressure	(M/t^2L)
R	Inner Radius of Combustion Chamber	(L)
S	Mixing Coefficient	($1/t$)
u	Particle velocity	(L/t)
v^*; v^{**}	Friction velocities	(L/t)
$\bar{V}$	Mean Free Stream velocity	(L/t)
β	A Constant	(Dimensionless)
ν	Kinematic Viscosity	(L^2/t)
ρ	Density	(M/L^3)
τ_w	Shear Stress at wall	(M/Lt^2)
ω	Circular Frequency = $2\pi f$	($1/t$)

Subscripts

- o Conditions of fully developed pipe flow and no oscillations
- v Conditions of fully developed pipe flow with oscillations present.

Other subscripts defined in text.

REFERENCES

1. Non Steady Flame Propagation Edited by G. H. Markstein
Pergamon Press, (1964).

2. T. Male, W. R. Kerslake & A. O. Tischler
N.A.C.A. RM E 54 A 29

3. Pulsating Combustion - Collected Works of F. H. Reynst.
Edited by M. W. Thring. Pergamon Press, (1961)

4. W. E. Francis, M. L. Hoggarth & D. Reay
Inst. Gas. Eng. Jour. June 1963 Vol. 3 No. 6 p.p. 301

5. J. R. Osborn
Raketentechnik Und Raumfahrtforschung. April - June (1963) p.p. 47

6. J. R. Osborn & J. M. Bonnell
A.R.S. Journal April 1961 Vol. 31 No. 4. p.p.482

7. J. R. Osborn & J. M. Bonnell
Rep. No. 1-60-1
Jet. Prop. Centre. Purdue University

8. Theory of Combustion Instability in Liquid Propellant Rocket Motors.
L. Crocco & S. I. Cheng
Butterworths Scientific Publications (1956).

9. W. N. Zartman & S. W. Churchill
A.I.Ch.E. Jour. (1961) Vol. 7, p.p. 588

10. W. N. Zartman; Ph.D. thesis Univ. of Mich.
Ann Arbor, Mich. (1960)

11. P. V. Dankwerts
Ind. Eng. Chem. (1951) Vol. 43 p.p. 1460

12. P. V. Dankwerts
A.I.Ch.E. Jour. (1955) Vol. 1 p.p. 456

13. H. L. Toor & J. M. Marchello
A.I.Ch.E. Jour. (1958) Vol. 4 p.p. 97

14. H. S. Mickley & D. F. Fairbanks
A.I.Ch.E. Jour. (1955) Vol. 1. p.p. 374

15. H.C. Krieg JR. The Tangential Mode of Combustion Instability.
ARS. Propellants Combustion & Liquid Rockets Conference. Florida 1961

16. Boundary Layer Theory H. Schlicting.
Pergamon Press, (1955)

17. Heat Transmission W. H. McAdams
McGraw Hill, (3rd Edition) (1954)

18. Introduction to Mechanics, Matter & Waves
U. Ingard & W. L. Kraushaar
Addison Wesley (1960)

19. N.A.C.A. Lewis Laboratory Staff
N.A.C.A. Report 1384 (1954)

20. Vibration & Sound P. M. Morse
Mc Graw Hill, (2nd Ed. 1948) 2nd Edition) 1948

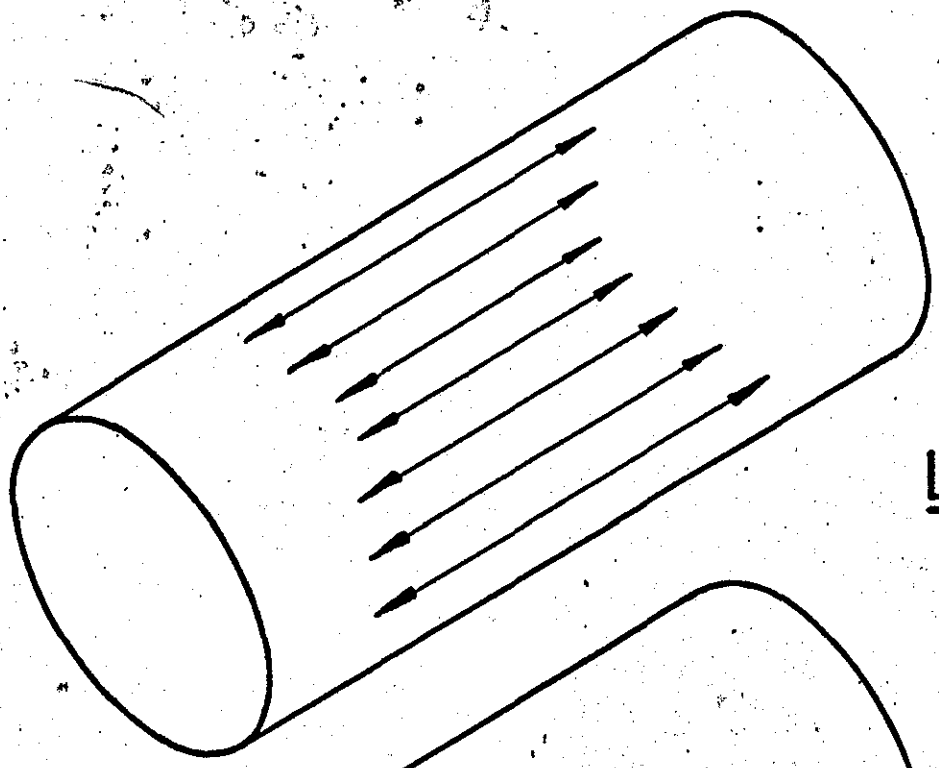

LONGITUDINAL

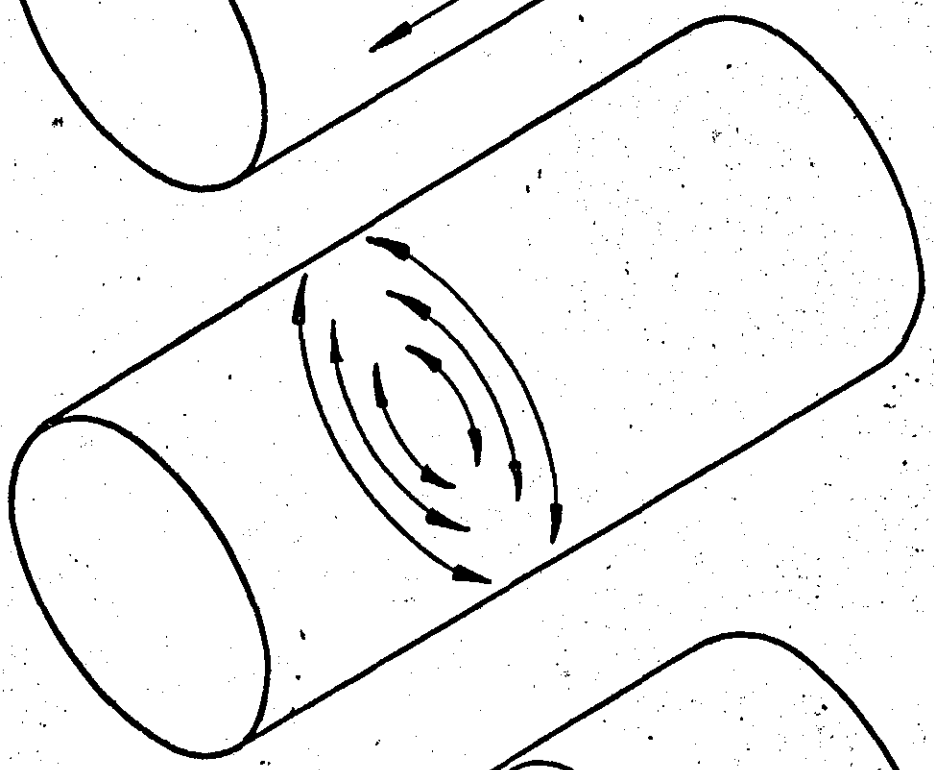

TRANSVERSE
SLOSHING

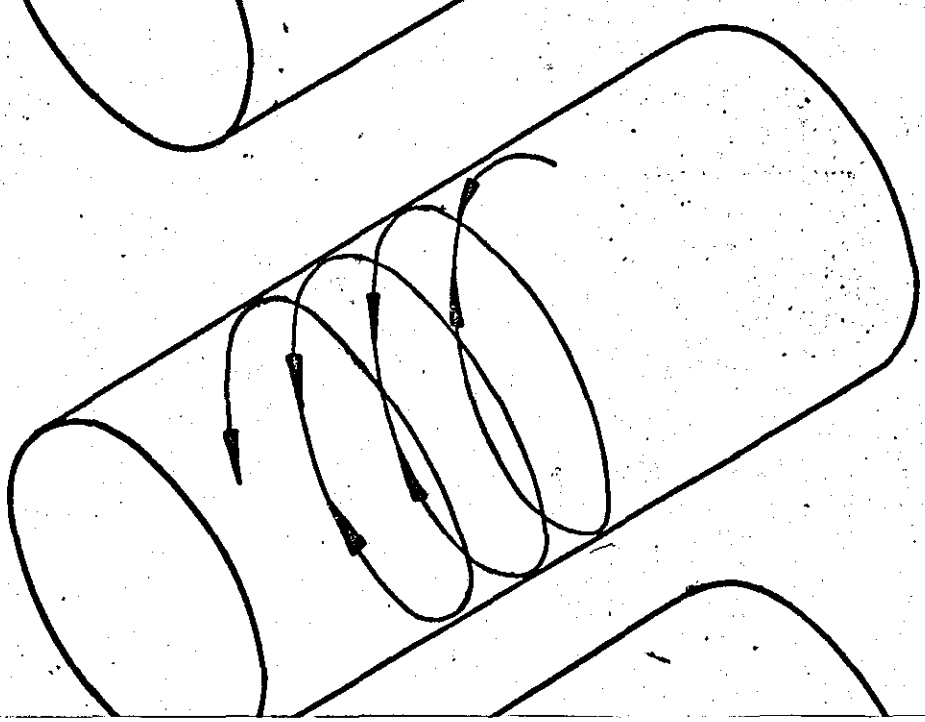

TRANSVERSE
SPINNING

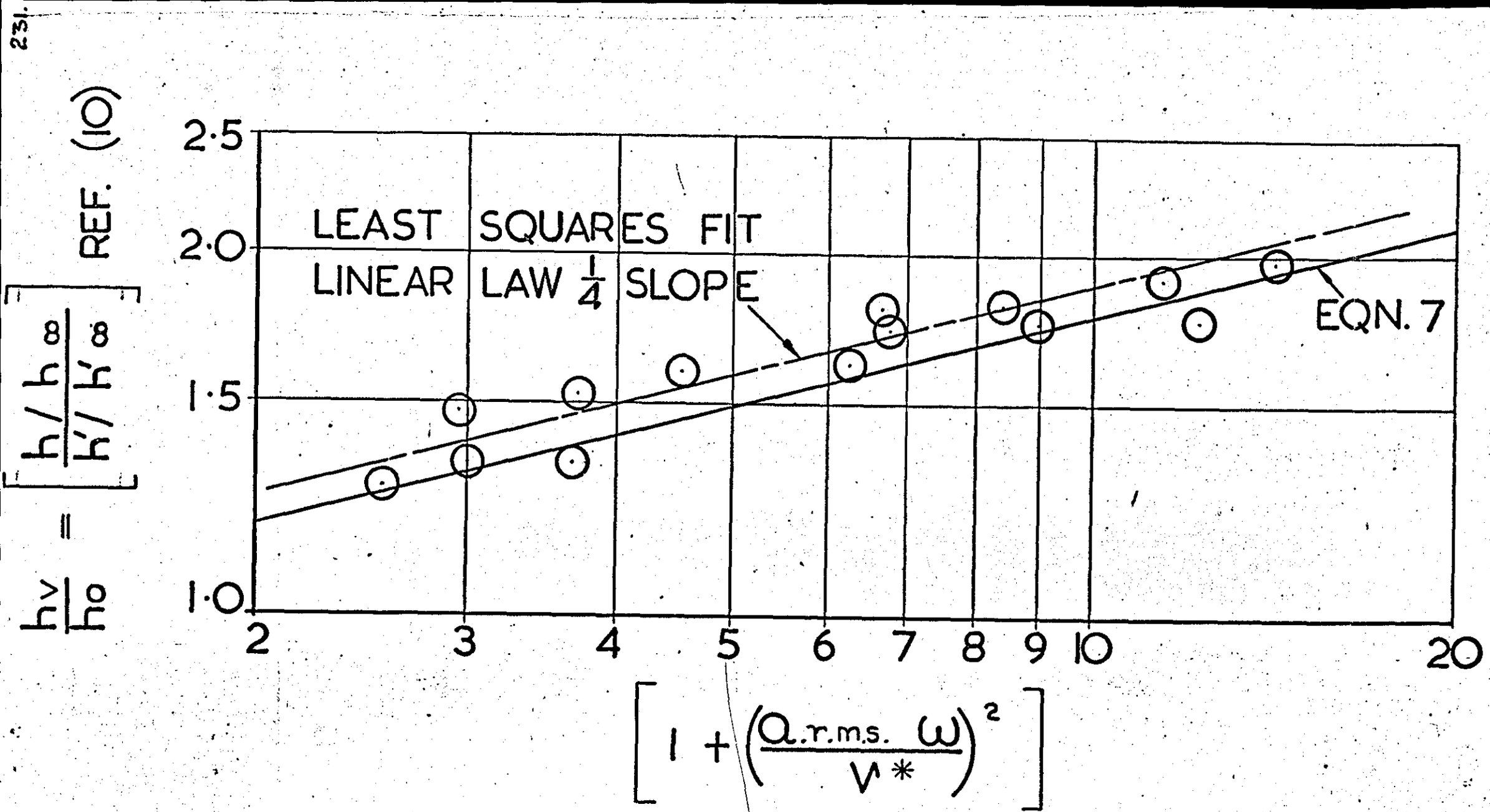

FIG 2. EFFECT OF ACOUSTIC OSCILLATION ON ON FORCED CONVECTIVE HEAT TRANSFER

HEAT TRANSFER FROM A VERTICAL TRANSVERSELY VIBRATING PLANE SURFACE TO AIR BY FREE CONVECTION

J. C. Dent,
Department of Mechanical Engineering,
Loughborough University of Technology.

NOTATION

Primary Dimensions

Mass (M), Length (L), Time (t), Temperature (θ)

a Amplitude of vibration (L)

C_p Constant Pressure Thermal Capacity ($L^2/t^2\ \theta$)

f Vibration frequency ($1/t$)

G_R Grashof Number based on Length of Plate (Dimensionless)

$\bar{h}$ Average Convective Heat Transfer Coefficient ($M/t^3\ \theta$)

k Thermal Conductivity ($ML/t^3\ \theta$)

L Length of Vertical Plate or plane surface (L)

n Dimensionless Constant

Re_{vib} Vibration Reynolds Number (Dimensionless) = $\dfrac{a_{RMS}\,\omega\,L}{\nu}$

S Mixing Coefficient ($1/t$)

$\bar{V}$ Fluid Velocity (L/t)

ν Kinematic Viscosity (L^2/t)

ρ Density (M/L^3)

ω Circular frequency ($1/t$)

SUBSCRIPTS

V Pertaining to conditions with oscillation present

Vo Pertaining to conditions at the critical vibration intensity

O Pertaining to conditions in absence of oscillation

R.M.S. Root Mean Square

Other subscripts defined in text

A E R E : INTERNAL MEMORANDUM

36/13660

FROM	Phone	Division / Branch	Bldg.	File No.
TO				

SUBJECT ..... Date .....

Heat Transfer From a Vertical Transversely Vibrating Plane Surface to Air by Free Convection

J. C. Dent,
Department of Mechanical Engineering,
Loughborough University of Technology.

The object of this communication is to show how the Danckwerts-Mickley Model for turbulent exchange may be applied to the above problem under conditions of transition to turbulence in the boundary layer.

Experiments [1], [2] with 6 and 8 inch plates respectively, showed that at low intensities of vibration (intensity = af) there are small decreases in heat transfer coefficient compared with the stationary plate, the boundary layer was observed to remain laminar. With increasing intensity a critical condition was observed at which transition occurred at the top of the plate, the turbulence being generated in the outer region of the boundary layer and propagating towards the surface. Intensities above the critical produced large increases in the heat transfer coefficient.

Experiments [3], [4] on transition in free convective boundary layers on stationary plates, showed that turbulence originated in the region of the point of inflexion in the laminar velocity profile, and propagated towards the surface. The fluid velocity at this point being 0.683 $\bar{V}_{max.}$ for air; $\bar{V}_{max.}$ being the maximum velocity in the laminar boundary layer at the point of transition.

From the Danckwerts-Mickley Model [5] for the turbulent heat exchange between a forced fluid flow and a stationary surface.

$$\bar{h} = \sqrt{k \rho C_p S} \qquad (1)$$

The mixing coefficient S depends on a characteristic velocity and length of the system and the Reynolds number. For the problem under discussion here, with intensity greater than the critical, S will depend on a characteristic velocity $\bar{V}_v$ the length of the surface and the Grashof number. It has been found [6] for the case of superimposed acoustic vibration on turbulent flow, that S could be defined when the acoustic energy supplements the kinetic energy due to turbulence. Here it may be assumed that the vibration kinetic energy supplements the kinetic energy of the fluid in the critical layer so that

$$\bar{V}_v^2 = \left[(0.683 \bar{V}_{max})^2 + (a_{RMS} \omega)^2 \right] \qquad (2)$$

In a manner similar to [5] but replacing the Reynolds number with Grashof number.

$$S \propto \frac{\bar{V}_v}{L}\left[G_{R_v}\right]^n \qquad (3)$$

If it is assumed that at the point of transition vibration does not supplement the energy of the boundary layer, then $0.683\ \bar{V}_{max.}$ is substituted for $\bar{V}_v$ in (3). Also, at transition we know that $\bar{h}_{v_0} \simeq \bar{h}_o$; hence from (1), (2) and (3) and the foregoing argument

$$\frac{\bar{h}_v}{\bar{h}_o} = \left[1 + 2.14\left(\frac{a_{RMS}\,\omega}{\bar{V}_{max.}}\right)^2\right]^{1/4} \qquad (4)$$

If $\bar{V}_{max.}$ is expressed in terms of the Grashof number [7] and transition is considered to take plate at x = L then

$$\underset{x=L}{\bar{V}_{max}} = 0.55\,\frac{G_{R_v}^{1/2}\,\nu}{L} \qquad (5)$$

In the derivation of the foregoing equations it has been assumed that $\Delta\theta_v = \Delta\theta_o$, for comparison with experimental data [1] ; [2] obtained at constant heat flux, it is necessary to correct for this.

Substituting (5) in (4); correcting for temperature and defining a Vibration Reynolds Number we have

$$\frac{\bar{h}_v}{\bar{h}_o} = \left[1 + \frac{7.09\,R_{e_{VIB}}^2}{G_{R_v}}\right]^{1/4}\left[\frac{G_{R_v}}{G_{R_o}}\right]^{1/4} \qquad (6)$$

Equation (6) with experimental data [1] , [2] are shown in figure (1). The critical Vibration Reynolds number will depend on the Grashof number for the static plate; the variation of $\left[\frac{R_{e_{VIB}}^2}{G_{R_o}}\right]_{CRITICAL}$ with G_{R_o} from data [1]; [2] is shown in figure (2). This gives the lower limit of validity of (6).

The upper limit of validity of (6) would occur when vibration forced convection controls; this can be said to occur when the heat transfer coefficient for free convection at the centre of the plate is 10% of that due to vibration.

For free convection the local coefficient at the centre of the plate $h_{L/2}$, [8] is

$$h_{L/2} \propto 0.214\,G_{R_o}^{1/4} \qquad (7)$$

For vibration forced convection, assuming laminar flow conditions, h_s at stagnation point at centre of plate, [9] is

$$h_s \propto \left[\frac{a\omega L}{\nu}\right]^{1/2} \tag{8}$$

Hence $$\frac{Re^2_{VIB}}{G_{R_o}} \simeq 11 \tag{9}$$

The range of data in [1] and [2] did not permit verification of (9). However, using arguments similar to above but modifying the equations for geometry [10], the data of [11] for free convection from horizontal cylinders executing large amplitude transverse vibrations gave an average value of $\left[\frac{Re^2_{VIB}}{G_{R_o}}\right]_{FORCED} \simeq 80$ whereas prediction gave approximately 120, the discrepancy is to be expected because of the simplifying assumptions made including neglect of turbulence. This indicates that the right hand side of (9) should be approximately 7. The method discussed here would not be applicable for $G_{R_o} \geq 1.5 \times 10^8$ as a turbulent boundary layer would exist on the stationary plate.

Using the Danckwerts-Mickley Model for turbulent heat exchange a method has been developed for the calculation of heat transfer from a transversely vibrating plane surface to air by free convection, under conditions of early transition to turbulence caused by the vibration. Agreement has been shown between prediction and available experimental data, and a tentative upper limit of $\left[\frac{Re^2_{VIB}}{G_{R_o}}\right] \simeq 7$ has been set above which the convective process is vibration forced.

REFERENCES

1. V. D. Blankenship and J. A. Clark
Experimental Effects of Transverse Oscillations On Free Convection of a Vertical, Finite Plate.
J. Heat Transfer 86, 159 (1964)

2. A. J. Shine
The Effect of Transverse Vibrations on the Heat Transfer Rate from a Heated Vertical Plate in Free Convection.
A.S.M.E. Paper Number 59-HT-27

3. E. R. G. Eckert and E. Soehnghen
Interferometric Studies on the Stability and Transition to Turbulence of a Free Convection Boundary Layer.
Proc. General Discussion on Heat Transfer, 321 (1951)

4. A. A. Szewczyk
Stability and Transition of the Free Convection Layer Along a Vertical Flat Plate.
Int. J. Heat Mass Transfer 5, 903 (1962).

5. H. L. Toor and J. M. Marchello
Film Penetration Model for Mass and Heat Transfer
A.I.Ch.E.J. 4, 97 (1958)

6. J. C. Dent
The Calculation of Heat Transfer Coefficient for Combustion Driven Transverse Oscillations in a Gas-Air Burner
To appear in A.I.Ch.E.J.

7. H. Schlichting,
Boundary Layer Theory 4th Edition, P. 333
McGraw Hill (1960)

8. F. Kreith
Principles of Heat Transfer, 1st Edition, P.308
International Textbook (1958)

9. E. R. G. Eckert
Research During the Last Decade of Forced Convection Heat Transfer (Lecture)
2nd International Heat Transfer Conference, Boulder (1961)

10. R. Hermann
Heat Transfer By Free Convection From Horizontal Cylinders in Diatomic Gases.
N.A.C.A. TM 1366 (1954)

11. H. C. Lowe,
Heat Transfer From a Vibrating Horizontal Tube To Air
M.Sc. Thesis London (1965).

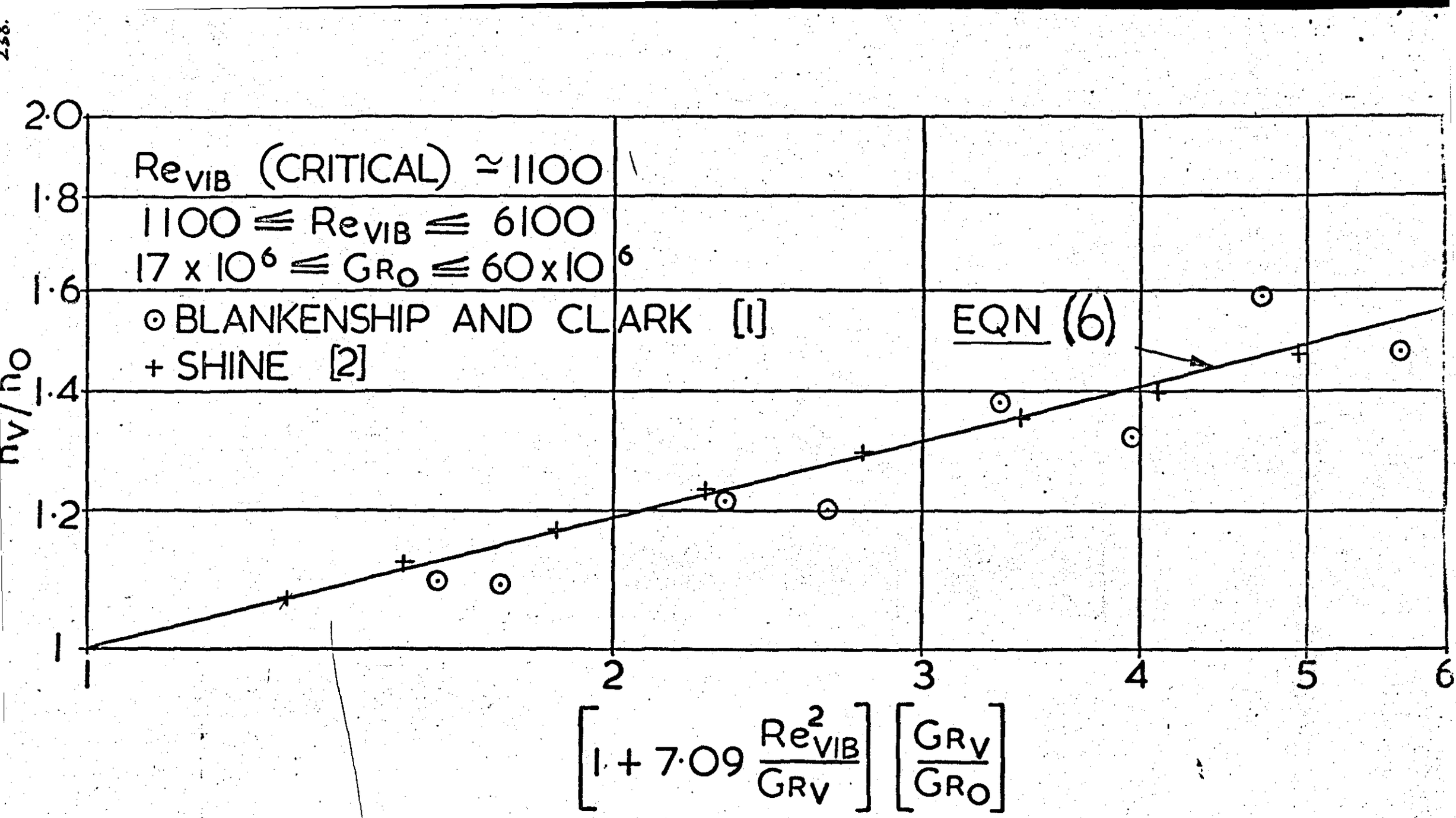

FIG 1 HEAT TRANSFER COEFFICIENT FOR A VERTICAL TRANSVERSELY

FIG. 2.
LOWER LIMIT OF $\frac{Re^2_{VIB}}{Gr_O}$

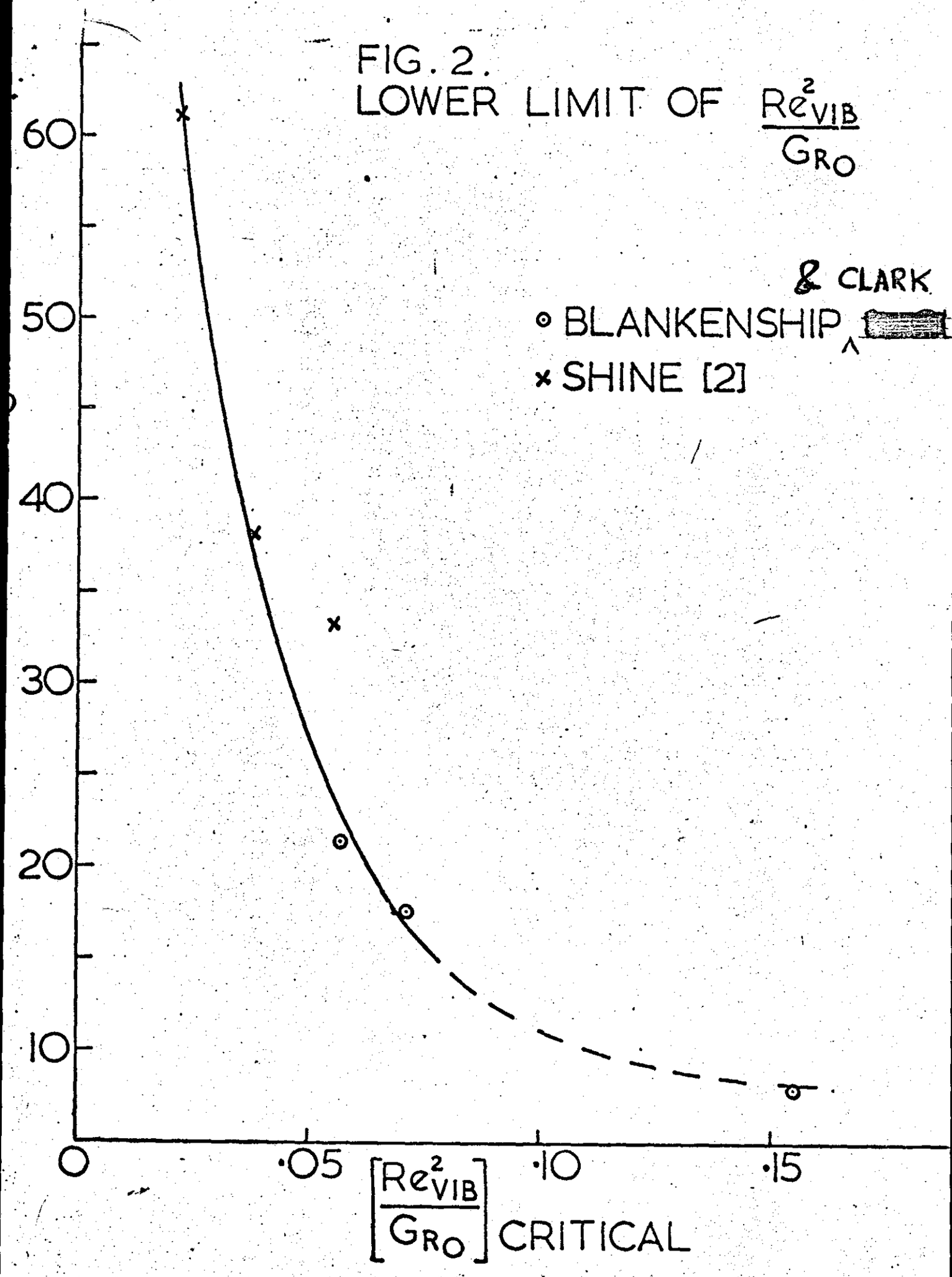

THE EFFECT OF VIBRATION ON CONDENSATION HEAT TRANSFER TO A HORIZONTAL TUBE

By

J. C. Dent

Loughborough University of Technology

Department of Mechanical Engineering

Summary

An exploratory study was carried out on the condensation of air free steam at a pressure slightly above atmospheric, on a horizontal condenser tube vibrating in the plane of the gravitational field.

Experiments conducted in the frequency range 20 - 80 c/s with maximum amplitudes up to 0.17 ins, showed that the condensation heat transfer coefficient increased with increasing intensity (a·f) of vibration, up to a maximum of about 15%, above the vibration free value. A perturbation analysis verified the experimental findings.

Because of the small observed increases in heat transfer, it can be concluded that tube vibration effects on condensation heat transfer in Power Plant condensers will be negligible.

Notation

Fundamental Dimensions M, L, T, t

a	Amplitude (L)
A	Outside Surface Area of Condenser tube $(L)^2$
C_p	Thermal Capacity $(L^2/t^2\ T)$
D	Outside Diameter of tube (L)
f	Vibration frequencey (1/t)
g	Acceleration due to gravity (L/t^2)
h	Condensation heat transfer coefficient $(M/t^2\ T)$
hf_g	Enthalpy of Vapourisation (L^2/t^2)
k	Thermal Conductivity (ML/t^3T)
$\dot{m}$	Water mass flow rate (M/t)
r	Condenser tube radius (L)
u	Velocity of Condensate film (L/t)
y	Co-ordinate Normal to Surface of tube (L)
δ	Local Condensate film thickness (L)
ϵ	Perturbation Parameter (Dimensionless)
ϕ	Angular Position on tube (^{o} or radian)
μ	Absolute Viscosity (M/L t)
ν	Kinematic Viscosity (L^2/t)
ρ	Density (M/L^3)
θ	Temperature (T)
ω	Circular frequency (rads/t)

Suffices

o	in absence of vibration
v	in presence of vibration
w_o	water outlet
w_i	water inlet
sat.	Pertaining to conditions at saturated vapour state
sur	Pertaining to surface

Other notation and suffices defined in text.

The Effect of Vibration on Condensation Heat Transfer to a Horizontal Tube

It is known that a certain amount of tube vibration in the plane of the gravitational force is present in the normal underslung power plant condenser. It is possible that the forces due to vibration acting on the condensate film will supplement the forces due to gravity and cause increased drainage of the condensate from the tube surface. The purpose of this paper is to describe an exploratory experimental and theoretical study of this problem.

Raben et al (1) carried out experiments with steam condensing at atmospheric pressure on a transversely vibrating vertical tube of 1 in. diameter and approximately 3 ft in length. The authors found that the condensation heat transfer coefficient increased with increasing vibration intensity, - where intensity is defined as the product of vibration amplitude and frequency - increases up to 50% were observed in the frequency range 38 to 98 c/s. with amplitudes of the order of 0.1 to 0.5 ins. The authors also found that the increases in heat transfer with vibration were reduced when air was introduced into the steam supply line to the condenser chamber.

Haughey (2) conducted an experimental investigation into the condensation of ethanol vapour on a 0.905 dia. horizontal tube, in the presence of longitudinal oscillation of the tube along its axis. The author observed increases of the condensation heat transfer coefficient with oscillation intensity up to 20% above that for the oscillation free case. The frequency of oscillation was varied between 0 and 140 c/s and the maximum amplitude of oscillation was 0.059 ins.

The papers of Raben et al (1) and Haughey (2) appear to be the only works discussing the effects of tube vibration on condensation heat transfer. No work appears to have been conducted with vibration of a horizontal tube in the same plane as the gravitational force.

Experimental Study

Because it is easier and less expensive to conduct condensation experiments at pressures that are above atmospheric pressure rather than below it, and because of the exploratory nature of the study, experiments were carried out with steam at a pressure of 1.5 ins. of mercury above atmospheric in the condenser shell.

The condenser shell was made from 6 in. dia. steel piping onto which was welded a hood and steam delivery pipe. The shell was provide. with a number of instrument ports and three $3\frac{1}{2}$ in. x $2\frac{1}{2}$ in. observation ports. Care was taken to see that steam from the delivery pipe did not impinge on the condenser tube.

Condensate was drained from the bottom of the condenser shell. A central port in the bottom of the condenser shell carried a Phosphor Bronze bush through which the leg of a stainless steel tube T assembly passed. The leg of the T was connected to a 40 lbf thrust electro-magnetic vibrator mounted on an anti vibration bed. The condenser shell was also mounted on the anti-vibration bed by means of a Dexion frame.

The condenser tube was made from 99.85% pure annealed copper tubing of 0.83 in. O.D. and 0.04 ins. wall. The tube was $13\frac{1}{8}$ ins. long and was attached to the T assembly by copper lugs. Paxolin spacers ensured electrical isolation of the tube from the T and the rest of the condenser. The ends of the condenser tube were closed with copper flanges carrying hose connectors for $\frac{1}{2}$ in. rubber tubing used for the water supply.

A Drawing of the condenser and of the tube and T assembly is shown in figure 1

Steam supply was from a small automatically controlled boiler on which delivery pressure could be preset in the range 20 to 150 p.s.i.g. Water supply to the condenser tube was from a centrifugal pump, flow measurement being achieved by means of a calibrated venturi.

Evaluation of Condensation Heat Transfer Coefficient

The method selected for the evaluation of condensation heat transfer coefficient necessitated the accurate measurement of outside surface temperature of the tube. Use of thermocouples located at the surface of the tube were not considered, because of the strong local effects on the condensation process observed by Hampson (3). The method used was that proposed by Jeffrey (4) and further discussed by Watson and Clark (5). This method used the tube as the unknown resistance in an electrical bridge circuit, A Kelvin double bridge with a preamplifier and galvanometer was used here for the determination of tube temperature, the effect of lead wires on the measurements were reduced to a negligible level by methods discussed by Harris (6). The long term electrical stability of the tube was very good. Frequent resistance - temperature calibration in a temperature controlled water bath overcame the difficulty of increased resistance due to cleaning and polishing.

The condensation heat flux was determined from the product of water flow and its temperature rise. Water inlet and outlet temperatures being measured with 26 s.w.g. Copper-Constantan thermocouples located in the plane of the inlet and outlet water flanges by means of brackets. The thermocouple wire was taken from the condenser along the inside of the rubber water pipes. Thermocouple e.m.f. was measured on a Vernier Potentiometer capable of determining changes in temperature of about 0.05°C. The heat transfer coefficient was determined from

$$h = \frac{\dot{m}\ C_p\ (\theta_{w_o} - \theta_{w_i})}{A\ (\theta_{sat} - \theta_{sur})} \qquad (1)$$

$\dot{m}$ could be determined with an accuracy of 3%. For expected values of $(\theta_{w_o} - \theta_{w_i})$ and $(\theta_{sat} - \theta_{sur})$ of about 5°C and 15°C respectively the expected accuracy of measurements are 1% and 2.5%. A was determined with an estimated accuracy of 2%. From the theory of errors (7) the estimated error in h would be about 5%.

Measurement of amplitude and frequency

Vibration amplitude was measured with a linear transformer displacement transducer. The moveable core of the transformer being suitably linked to the driving head of the vibrator. The output from the transformer was displayed on an oscilloscope. The electromagnetic vibrator was fed with a preset frequency signal from an oscillator through a power amplifier. The set frequency of the oscillator and that from the transducer were found to agree in the range $20 \leq f \leq 100$ c/s. The amplitude of vibration was controlled through the power amplifier.

Experimental Procedure and Precautions

Before steam was admitted to the condenser all instruments and transducers were checked for level of signal with cold water circulating through the tube.

The steam line was blown down before steam was admitted to the condenser, through a strainer and throttling valve. Boiler pressure was set to ensure 1° to 2°C of superheat of vapour in the condenser. The system was allowed to stabilise for about an hour before final readings were taken.

A static run was carried out before each set of vibration runs and the results compared with Nusselt's theory for filmwise condensation on a horizontal tube (8) which gives

$$h_o = 0.72 \left[\frac{\rho^2 g h_{fg} k^3}{\mu D (\theta_{SAT.} - \theta_{SUR})} \right]^{\frac{1}{4}} \qquad (2)$$

If the value of h_o determined experimentally was between 10 - 20% greater than that predicted by equation (2), the test was continued, this is in accord with McAdam (9). An increase much greater than 20% indicating dropwise condensation while a decrease indicated the presence of air in the condenser.

To ensure filmwise condensation the tube was cleaned in accordance with the method of Hampson (3). To ensure adequate removal of air from the vicinity of the tube, two ½ in perforated copper pipes running parallel along the length of the tube and at a distance of about ¾ ins. from it

were connected through rubber tubing to a vent pipe. The condenser was operated with an estimated Air/Steam mass ratio of 0.008 at entry, and a mass ratio of steam vented to entering steam of about 0.70.

Experiments were conducted with a water flow rate through the tube of between 22 and 29 lbm/hr., at these flow rates the effect of tube vibration was confined to the condensation process, Raben et al[(1)]. The mean bulk temperature of the water varied between about 70 to 80°F, whereas the condensation heat flux varied between 7.5×10^4 and 10×10^4 Btu/hr. ft.^{2}. Vibration frequency was varied in the range $20 \leq f \leq 80$ C/s with maximum amplitudes up to 0.17 ins.

Discussion of Results

The experiments showed that the effect of tube vibration caused small increases (up to a maximum of 15%) of the condensation heat transfer coefficient with vibration intensity.

A photographic study of the condensate film at points of maximum upward and downward displacement of the tube were made. This was achieved with a relay circuit actuated through a Thyratron, the circuit enabled the selection of either a positive or negative voltage peak (from the displacement transducer) to trigger a mains operated camera flash gun. To obtain good contrast, colour photography was used. Because of the inability to reproduce these photographs here sketches of the condensate film with and without vibration are shown in figure (2).

The rate of condensate drainage did not increase significantly with vibration, as one might have expected the vibration to throw condensate off the tube surface. The photographs from which the diagrams in figure (2) were sketched indicate that the condensate film during the upward displacement of the tube is forced towards the lower part of the tube, because of high surface tension forces the liquid film in this region becomes distended rather than rupturing. On the downward displacement of the tube the reverse process takes place, but because the inertia forces due to vibration and the gravitational forces are in opposition, the film shows a tendency to move back to the undisturbed condition, i.e. there is no significant disturbance of the film observed at the top of the tube. No ripple formation of the condensate was observed on the sides of the tube.

During the upward displacement of the tube with condensate moving towards the lower part of the tube, the condensate film thickness on the upper parts of the tube are reduced and therefore better heat conduction occurs.

It is interesting to note that Raben et al (1) also observed that very little condensate was thrown off the vibrating tube, instead it was seen to accumulate at the two stagnation points of the vibrating tube.

Because the orientation of the gravitational forces and inertia forces at these two points were the same, the areas of condensate accumulation were the same at each point.

Theoretical Analysis

From the foregoing discussion it is seen that increases in condensation heat transfer coefficient with increasing vibration intensity are small. To verify that these increases are of the right order a simple analysis will be carried out as a check.

Because of the small observed increases in the average condensation heat transfer coefficient with vibration intensity, the rate of condensation and hence the average condensate velocity at any angular position Ø must increase by a small amount.

If at any Ø the mean velocity of the condensate film under vibration conditions is $\bar{u}'$, which is composed of the sum of the mean velocity due to gravitational forces $\bar{u}$ and a small perturbation velocity. $\epsilon(\bar{u}_1)$ due to the averaged effect of oscillation of the tube surface.

Then $u' = \bar{u} + \epsilon(\bar{u}_1)$ (3)

The mean velocity due to gravitational forces $\bar{u}$ for an assumed parabolic velocity distribution according to Nusselt theory (8) is

$$\bar{u} = \frac{g \delta_v^2}{3\nu} \sin \emptyset \qquad (4)$$

δ_v is the local film thickness under vibratory conditions. $\bar{u}_1$ is the average velocity due to vibration and for sinusoidal oscillation is considered to be $\frac{2}{\pi}(a_{max}\omega) \sin \emptyset$. In the discussion of problems on convection and acoustic streaming about a horizontal vibrating cylinder (10) the assumption is made that (a_{max}/D) is small. The perturbation parameter ϵ is considered to be small and dimensionless. If therefore we put $\epsilon = (a_{max}/D)$

$$\text{Then} \quad \bar{u}' = \left[\frac{g \delta_v^2}{3\nu} + \frac{2}{\pi}\left(\frac{a^2_{max}\omega}{D}\right)\right] \sin \emptyset \qquad (5)$$

If it is assumed with Nusselt that the heat release due to condensation, is equal to the heat conducted through the film then from figure (3)

$$\frac{k r}{\delta_v}\left[\theta_{sat.} - \theta_{sur.}\right] d\emptyset = \rho h_{fg} \; d\left[\bar{u}' . \delta_v . 1\right] \qquad (6)$$

Substituting for $\bar{u}'$ from (5) in (6) re-arranging and noting that

$$B = \frac{3\nu k r}{g \rho h_{fg}}\left[\theta_{sat.} - \theta_{sur.}\right]$$

$$C = \frac{6}{\pi}\left(\frac{\nu}{g}\right)\left(\frac{a^2_{max}\,\omega}{D}\right)$$

$$M = \frac{1}{B}$$

$$N = \frac{C}{B}$$

Then $$\left[3M\,\delta_v^3 + N\delta_v\right]\frac{d\delta_v}{d\phi} + \left[M\delta_v^4 + N\delta_v^2\right]\cot\phi = \operatorname{cosec}\phi \qquad (7)$$

Putting $Z = \frac{3}{4}M\delta_v^4 + \frac{N}{2}\delta_v^2$

(7) becomes

$$\frac{dZ}{d\phi} + \left[\frac{4}{3}Z + \frac{N}{3}\delta_v^2\right]\cot\phi = \operatorname{cosec}\phi \qquad (8)$$

In the absence of oscillation $N = 0$ and $Z = Z_o$ and (8) becomes

$$\frac{dZ_o}{d\phi} + \frac{4}{3}Z_o\cot\phi = \operatorname{cosec}\phi \qquad (9)$$

Subtracting equation (9) from (8) and putting $Z = Z_o + P$ where P is the perturbation to Z_o, gives

$$\frac{dP}{d\phi} + \frac{4}{3}P\cot\phi + \frac{N}{3}\delta_v^2\cot\phi = 0 \qquad (10)$$

Provided $\frac{N\delta_v^2}{3}$ is small P is small

The solution to (10) is carried out in the Appendix and is

$$P = -\frac{N/3}{\sin^{4/3}\phi}\int_o^\phi \delta_v^2\cos\phi\sin^{1/3}\phi\,d\phi \qquad (11)$$

The solution of equation (9) according to the method mentioned in the Appendix is

$$Z_o = \frac{1}{\sin^{4/3}\phi}\int_o^\phi \sin^{1/3}\phi\,d\phi \qquad (12)$$

Therefore $$Z = \frac{1}{\sin^{4/3}\phi}\int_o^\phi \sin^{1/3}\phi\,d\phi - \frac{N/3}{\sin^{4/3}\phi}\int_o^\phi \delta_v^2\cos\phi\,\sin^{1/3}\phi\,d\phi \qquad (13)$$

According to Nusselt's theory of filmwise condensation on a horizontal tube (8)

$$\frac{\delta^4}{B} = \frac{4/3}{\sin^{4/3}\phi} \int_0^{\phi} \sin^{1/3} \phi \, d\phi \qquad (14)$$

where δ is the local condensate film thickness in the absence of oscillation.

Hence $$Z_o = \frac{3}{4} \frac{\delta^4}{B} \qquad (15)$$

The solution of (13) requires the knowledge of δ_v as a function of ϕ. As this is not known, an iterative process is used to obtain δ_v.

To start the iteration it is assumed that $\delta_v = \delta$ where δ is obtained from evaluating (14). The first iteration gives Z_1 from equation (13). But from the definition of Z

$$Z_1 = \frac{3}{4} M \delta_{v_1}^2 + \frac{N}{2} \delta_{v_1}^2$$

therefore $$\delta_{v1} = \left[- \frac{N}{3M} + \sqrt{\left(\frac{N}{3M}\right)^2 + \frac{4Z_1}{M}} \right]^{\frac{1}{4}} \qquad (16)$$

The value of δ_{v_1} from (16) is substituted in (13) and the value of Z_2 computed and hence δ_{v2} obtained from the definition of Z. Because the difference between δ and δ_v is small the convergence of the iteration is rapid.

The computation was programmed for a digital computer, results being evaluated for 2° intervals between 0° and 174°. In the computation B was taken as 4.35×10^{-16} ft^4 this value being a representative average for the experiments. $\frac{N}{3}$ was increased in steps of 1×10^6 from 1×10^6 to 10×10^6 ft^{-2}.

With values of δ_v of the order of 2×10^{-4} ft the value of $\frac{N}{3} \delta_v^2$ for $\frac{N}{3} = 10 \times 10^6$ ft^{-2} will be 0.40. Therefore $\frac{N}{3} \delta_v^2$ is approximately 11% of $\frac{4}{3}$ Z. This would represent an upper limit to the validity of the analysis, since from equation (8), $\frac{N}{3} \delta_v^2$ must be small compared with $\frac{4}{3}$ Z.

The average condensation heat transfer coefficient between any angles ϕ_1 and ϕ_2 is defined as

$$h_v = \frac{k}{\phi_2 - \phi_1} \int_{\phi_1}^{\phi_2} \frac{d\phi}{\delta_v} \qquad (17)$$

Therefore $$\frac{h_v}{h_o} = \frac{\int_{\phi_1}^{\phi_2} d\phi / \delta_v}{\int_{\phi_1}^{\phi_2} d\phi / \delta} \qquad (18)$$

The computed values of $\frac{h_v}{h_o}$ according to (18) between the limits 0^o and 174^o are shown plotted against $\frac{N}{3} \cdot D^2$ in figure (4) (5). The experimental data points are also shown on this figure.

The parameter $\frac{N}{3}.D^2$ can be put into a more meaningful form, if a vibration Reynolds number $Re_{vib} = \frac{a_{max}\,\omega\, D}{\nu}$ is defined, then.

$$\frac{ND^2}{3} = \frac{\frac{4}{3\pi}\left(\frac{a_{max}}{D}\right) Re_{vib}}{\frac{k\,(\theta_{sat.} - \theta_{sur.})}{\mathcal{H}\, h_{fg}}} \qquad (19)$$

The parameter $\frac{k\,(\theta_{sat} - \theta_{sur})}{\mathcal{H}\, h_{fg}}$ represents the momentum forces in the liquid film due to gravity forces and was obtained by Chen (11) in the study of filmwise condensation. Therefore ND^2 represents the ratio of perturbation forces due to oscillation to momentum forces due to gravity.

Discussion and Conclusions

The foregoing experimental and analytical investigation are in substantial agreement, both showing that the effect of vibration of a horizontal condenser tube in the plane of the gravitational force causes the condensation heat transfer and therefore the condensation rate to increase slightly. The assumption of increased heat transfer being due to better conduction through the reduced film thickness brought about by vibration, appears valid within the limits of the analysis.

From a practical standpoint there is no advantage whatsoever in attempting to exploit tube vibration to enhance condensation heat transfer, the presence of non condensable gases in power plant condensers operating at sub atmospheric pressures would reduce the very small increases observed with vibration.

References

1. Raben, I.A., Commeford, G. and Dietert, R.
An Investigation of the Use of Acoustic Vibrations to Improve Heat Transfer Rates and Reduce Scaling in Distillation Units used for Saline Water Conversion.
Office of Saline Water, Research Rep. No. 49. U.S. Dept. of Commerce, Washington D.C.

2. Haughey, D.P.
Heat Transfer During Condensation on a Vibrating Tube.
Trans. Inst. Chem. Eng. 43, 40 (1965)

3. Hampson, H.
The Condensation of Steam on a Metal Surface.
I.Mech.E. - A.S.M.E. General Discussion on Heat Transfer (1951) P.58.

4. Jeffrey, J. O.
A precision Method for the Measurement of Condenser Tube Surface Temperatures for the Determination of Film Coefficients of Heat Transmission.
Cornell Univ. Eng.Expt. Station
Bulletin No. 21 (1936).

5. Watson, G.G. and Clark, R.D.
Determination of Tube Wall Temperature in a Heat Exchanger from the Tube Resistance.
National Eng. Lab. Rep. 272 (1967).

6. Electrical Measurements
F.K. Harris
John Wiley, New York, (1957)

7. H. Schenck
Theories of Engineering Experimentation
McGraw-Hill, New York (1961)

8. M. Jakob
Heat Transfer Vol. I
John Wiley, New York (1949)

9. W. H. McAdams
Heat Transmission
4th ed. McGraw-Hill, New York (1954)

10. H. Schlichting
Boundary Layer Theory
Pergamon, Oxford (1955)

11. Chen, M. M.
An Analytical Study of Laminar Film Condensation
A.S.M.E. Jour. Heat Transfer. 83, 48, (1961).

12. I. S. Sokolnikoff and R. M. Redheffer
Mathematics of Physics and Modern Engineering
McGraw-Hill, New York, (1958)

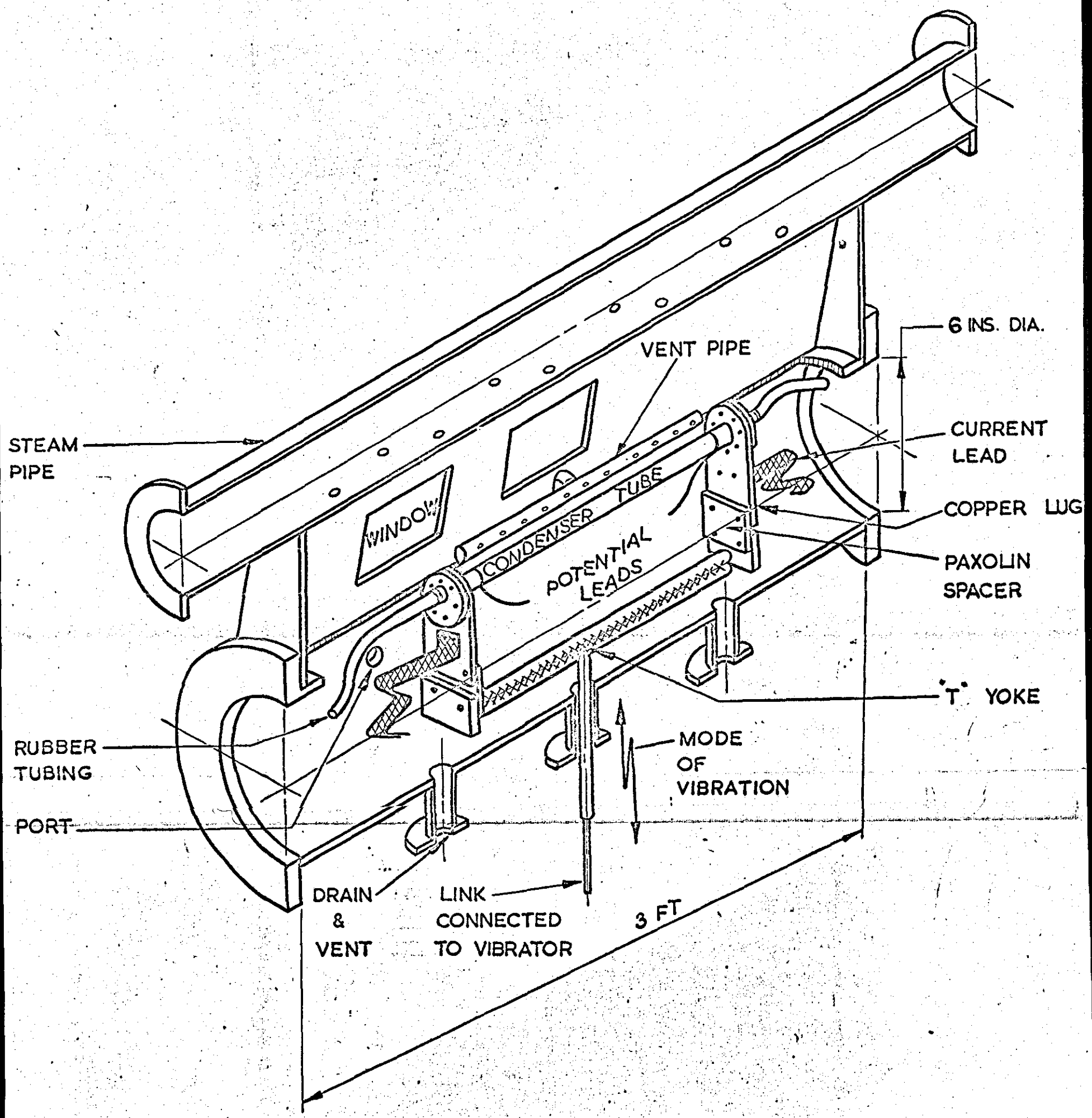

FIG. 1 CONDENSER & TUBE ASSEMBLY.

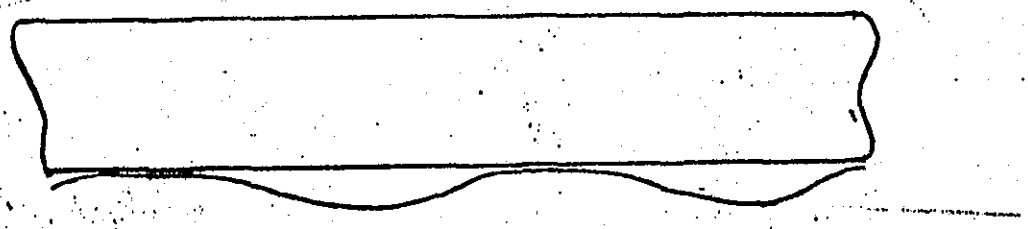

Fig. 2a Filmwise Condensation in absence of vibration of tube

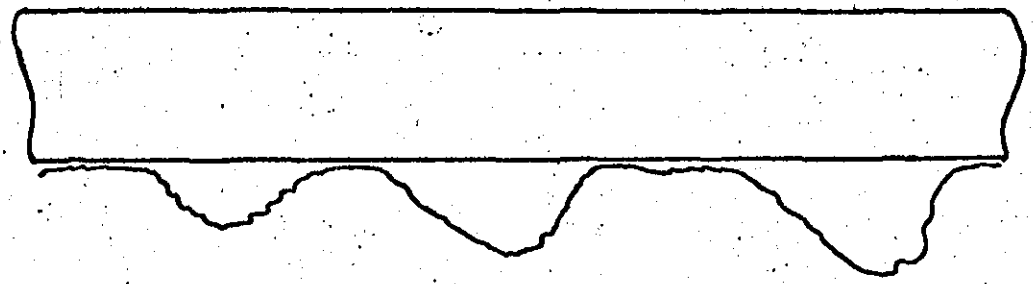

Fig. 2b Filmwise Condensation in the presence of tube vibration (20 c/s, a_{max} = 0.17 ins). Tube at maximum upward-displacement

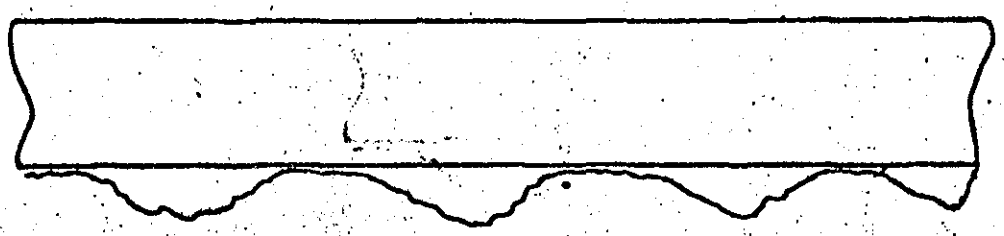

Fig. 2c Filmwise Condensation in the presence of tube vibration (20 c/s a_{max} = 0.17 ins). Tube at maximum downward displacement

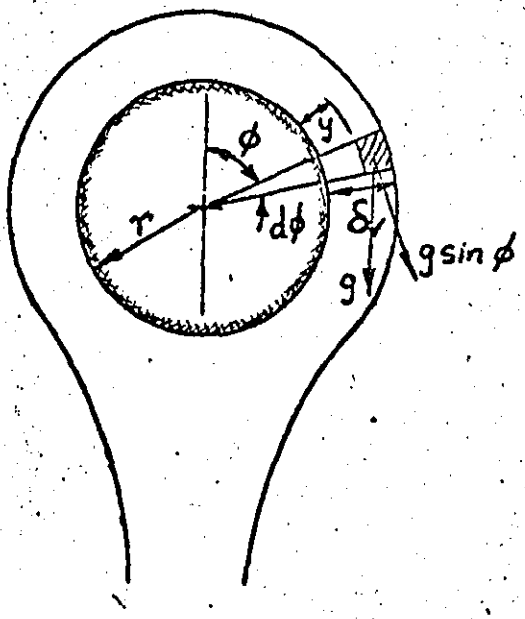

Fig. 3. Model of Condensate Film

T.P. 6.

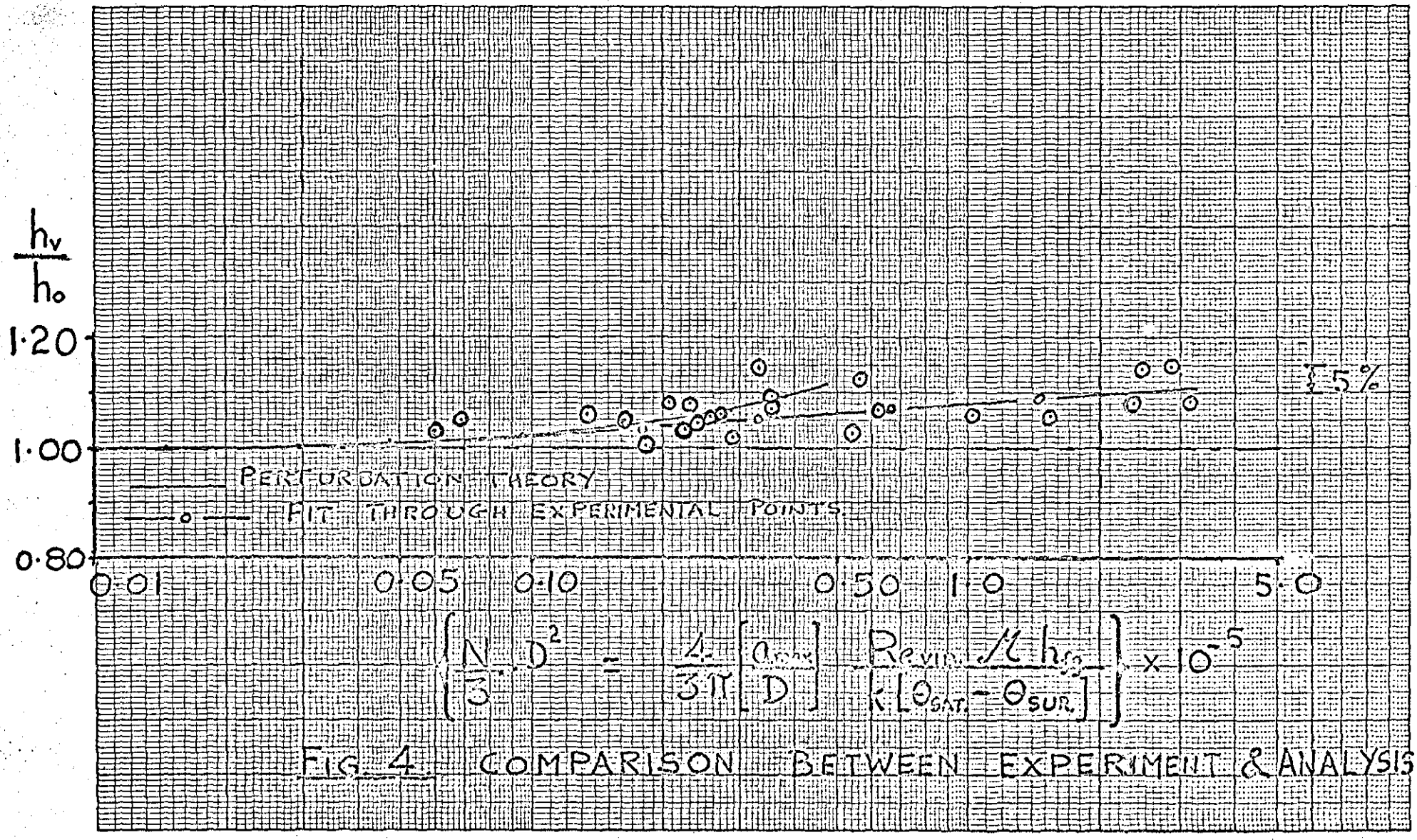

FIG. 4 COMPARISON BETWEEN EXPERIMENT & ANALYSIS

Appendix

$$\frac{dP}{d\phi} \sin\phi + \frac{4}{3} P \cos\phi + \frac{N}{3} \delta_v^2 \cos\phi = 0 \qquad \text{I}$$

Equation I is a first order equation linear in P and can be solved (Ref 12). by multiplying through by a factor F (P, Ø) and then determining the form F (P, Ø) has to take to make I exact.

The resulting equation will be exact if

$$\frac{\partial}{\partial\phi}\left[F \sin\phi \right] = \frac{\partial}{\partial P}\left[F \cos\phi \left(\frac{4}{3} P + \frac{N}{3} \delta_v^2 \right) \right] \qquad \text{II}$$

Therefore

$$F \cos\phi + \sin\phi \frac{\partial F}{\partial\phi} = F \frac{4}{3} \cos\phi + \left[\frac{4}{3} P + \frac{N}{3} \delta_v^2 \right] \cos\phi \cdot \frac{\partial F}{\partial P} \qquad \text{III}$$

If it is assumed that F = F (Ø) only, then

$$\sin\phi \frac{dF}{d\phi} = \frac{F}{3} \cos\phi \qquad \text{IV}$$

Solution of IV results in

$$F = \sin^{1/3}\phi \qquad \text{V}$$

I Multiplied through by V and re-arranged yields

$$\sin^{4/3}\phi \, dP + \left[\frac{4}{3} P + \frac{N}{3} \delta_v^2 \right] \cos\phi \sin^{1/3}\phi \cdot d\phi = 0 \qquad \text{VI}$$

VI is exact and may be written as

$$dY = 0 = \left[\frac{\partial Y}{\partial P} \right] \cdot dP + \left[\frac{\partial Y}{\partial \phi} \right] \cdot d\phi$$

$$\text{or } Y = \text{constant } C_1 \qquad \text{VII}$$

for exactness $\left[\frac{\partial Y}{\partial P} \right] = \left[\frac{\partial Y}{\partial \phi} \right]$

Therefore from VI & VII

$$\left[\frac{\partial Y}{\partial P} \right] = \sin^{4/3}\phi \qquad \text{VIII}$$

and $$\left[\frac{\partial Y}{\partial \phi} \right] = \frac{4}{3} \left[P + \frac{N}{4} \delta_v^2 \right] \cos\phi \sin^{1/3}\phi \qquad \text{IX}$$

Integrating VIII $Y = P \sin^{4/3} \phi + f(\phi)$ X

where $f(\phi)$ = function of ϕ

From IX and X

$$\frac{\partial}{\partial \phi}\left[P \sin^{4/3}\phi + f(\phi)\right] = \frac{4}{3}\left[P + \frac{N}{4}\delta_v^2\right]\cos\phi \sin^{1/3}\phi \quad \text{XI}$$

On expansion of XI and re-arrangement

$$\frac{d f(\phi)}{d\phi} = \frac{N}{3}\delta_v^2 \cos\phi \sin^{1/3}\phi \quad \text{XII}$$

Therefore $f(\phi) = \frac{N}{3}\int \delta_v^2 . \cos\phi \sin^{1/3}\phi \, d\phi$ XIII

From VII; X and XIII

$$P = \frac{1}{\sin^{4/3}\phi}\left[C_1 - \frac{N}{3}\int \delta_v^2 . \cos\phi \sin^{1/3}\phi . d\phi\right] \quad \text{XIV}$$

Because of symmetry of the condensate film

$$\frac{d P}{d \phi} = 0 \text{ at } \phi = 0$$

from I, at $\phi = 0$

$$P = -\frac{N}{4}\delta_v^2 \quad \text{XV}$$

Using the fact that at small values of ϕ, $\sin\phi \approx \phi$ and also the fact that as $\phi \to 0$, δ_v will tend to a constant value since $\frac{dP}{d\phi} = 0$. Integration of XIV under these cnnditions yields

$$P = \frac{C_1}{\phi^{4/3}} - \frac{N\delta_v^2}{4} \quad \text{XVI}$$

from XV and XVI $C_1 = 0$

Therefore

$$P = -\frac{N}{3\sin^{4/3}\phi}\int_0^{\phi} \delta_v^2 \cos\phi \sin^{1/3}\phi \, d\phi \quad \text{XVII}$$

THE CALCULATION OF HEAT TRANSFER COEFFICIENT FOR CONDENSATION OF STEAM ON A VIBRATING VERTICAL TUBE

J.C. Dent
Mechanical Engineering Department,
Loughborough University of Technology,
Leicestershire

Summary

Using the Danckwerts-Mickley model for turbulent exchange, a method has been developed in this paper for the calculation of heat transfer coefficient for filmwise condensation on a vertical tube, in a transverse mode of vibration.

Provided the amplitude of vibration $a_o \leq 0.35$ ins. agreement has been shown to within $\pm$ 7%, when comparison has been made with the experimental data of Raben et al[1] which were ~~conducted~~ obtained with $22.5 \leq f \leq 98$ c/s and $0.05 \leq a_o \leq 0.5$ ins., with condensation head load in the range $22,000 \leq Q \leq 55,000$ Btu/hr.

Notation

a_o Amplitude of vibration (L)

C_p Constant Pressure Thermal Capacity (L^2/t^2T)

f Vibration frequency ($^1/_t$)

G Mass flow rate of Condensate per unit perimeter or length (M/tL)

g Acceleration due to Gravity (L/t^2)

g_c Gravitational Constant (Dimensionless)

h Heat Transfer Coefficient ($M/_t{}^3T$)

h_{f_g} Enthalpy of vapourisation (L^2/t^2)

k Thermal Conductivity (ML/t^3T)

λ Characteristic length (L)

R_{e_f} Film Reynolds Number (Dimensionless) = $\frac{4G}{\mu}$

Q Condensation Heat Load (ML^2/t^3)

S Mixing Coefficient ($1/_t$)

u Velocity in liquid film ($L/_t$)

V_v Characteristic velocity ($L/_t$)

x Distance down tube length (L)

y Local position in liquid film measured from tube wall (L)

δ Thickness of liquid film (L)

μ Absolute Viscosity (M/Lt)

ν Kinematic Viscosity (L^2/t)

ρ Density of Condensate (M/L^3)

θ Temperature (T)

ω Circular frequency (1/t)

Subscripts

o	Conditions in absence of vibrations
v	Conditions in presence of vibrations
sat	Saturated vapour conditions
w	tube wall conditions

Other notation defined in text and Appendix,

The Calculation of Heat Transfer Coefficient for Condensation of Steam on a Vibrating Vertical Tube

The problem of condensation on a vertical tube in a transverse mode of vibration was studied experimentally by Raben et al[1], who were investigating the feasibility of using tube vibration to enhance evaporator performance in saline water conversion systems. These experiments were carried out using a 1 in. diameter condenser tube 41 ins. long. The tube was mounted in a 3 in. dia. Pyrex pipe 38 ins. long, with a central T section. The condenser tube was held by end cover plates fitted with '0' ring seals, so that it could vibrate in the transverse mode as a pivot ended beam. The tube was maintained in vibration through a yoke assembly attached to it, which was connected to an electromagnetic vibrator by a driving rod passing through the central T section of the Pyrex condenser shell.

Experimental data were obtained with the tube static and with it vibrating at frequencies in the range 22.5 to 98 c/s with amplitudes up to 0.5 ins. at the resonant frequency of 38 c/s. Data were obtained at heat loads of approximately 22,000; 38,000 and 55,000 Btu/hr this being achieved by control of the inlet water temperature to the condenser tube. Steam was condensed at approximately atmospheric pressure, care being taken to ensure that non-condensable gases were not present in the shell. The vapour velocity over the condenser surface was low.

These experiments showed that beyond a critical condition, (below which the effect of vibration was negligible) the condensation heat transfer coefficient increased continually with vibration intensity - (defined as the product of vibration amplitude and frequency) - to about 55% above the vibration free value, at a frequency of 73 c/s and an amplitude of 0.2 ins. The heat transfer coefficient for the static tube was found to be 10% greater than that predicted by Nusselt's theory[2]. Observation of the

condensate film on the tube showed that the water was not thrown off the tube during vibration as might have been expected, but was moved from side to side to form accumulations at the points on the tube as shown in figure (1). This movement of the condensate contributes to greater mixing in the film and therefore improved heat transfer. The mixing mechanism would result from an interaction of the vibratory motion of the tube and the motion of the liquid film down it under the action of gravity.

Ideally one would seek a solution to the problem under study by attempting to specify the local conditions of flow, mixing and heat transfer mathematically, and on solution of the resulting equations with appropriate boundary conditions obtain the average effects of mixing on heat transfer for the whole surface. However, because the process involving the interaction of large amplitude vibrations of the heat transfer surface, and the motion of the liquid film under the action of gravity is complex, a semi-empirical approach to the solution of the problem appears reasonable.

In the study of complex mixing processes associated with stirred chemical reactors, fluidised beds etc., the surface renewal concept of Danckwerts[3] and Mickley[4] has found successful application.

The surface renewal concept has been extended to turbulent heat and mass transfer at a solid fluid interface by Hanratty[5], and Toor and Marchello[6]. It has also been applied in the calculation of mass transfer rates at a gas-liquid interface, for the gravitational flow of a rippled two dimensional liquid film over a plane vertical surface[7].

In the Danckwerts - Mickley surface renewal model for the turbulent exchange of heat between a fluid and a solid surface, it is assumed that macroscopic "lumps" of fluid from the bulk region, move randomly to contact the boundary surface, exchange heat with it in a transient manner before being displaced by fresh "lumps"

from the bulk region. The renewal process is assumed to take place randomly and at high frequency, the distribution of "ages" of lumps in contact with the surface decreasing exponentially with age - at small values of time surface is covered predominantly by fresh "lumps", at large values of time, little of surface is covered by "old" fluid lumps.

It can be shown[3] ; [6] that the average heat transfer coefficient at the fluid-solid surface is given by

$$h = \left[k \rho C_p S \right]^{\frac{1}{2}} \qquad (1)$$

where $S = \frac{1}{A} \int_A S_x^{\frac{1}{2}} \cdot dx$, is the average rate of renewal of fluid lumps at the surface. The renewal rate S (or mixing coefficient) is constant for lumps of all ages at the surface, and is controlled by the geometry and fluid mechanics of the problem - there is no preferential renewal of any particular age group at the surface.

The concept of surface renewal is in accord with observations of turbulent forced convective flows carried out by Fage and Townend[8], Hanratty and his co-workers[9], Bakewell and Lumley[10] and Sherwood et al[11]. Observation of the turbulent free convective boundary layer fluctuations by Locke and Trotter[12], gives further support to a surface renewal model for the exchange process at the wall.

Toor and Marchello[6] show that the surface renewal or mixing coefficient is proportional to $\frac{V}{D}$ for fully developed turbulent pipe flow, where V is the average flow velocity in the pipe and D the pipe diameter. For turbulent pipe flow the scale of the turbulent mixing is of the order of the pipe diameter.

In the problem under study here where the mixing motion is due to the combined action of gravity on the liquid film, and the lateral movement of the film due to tube vibration, the mixing coefficient S_v under these conditions might be expected to be

proportional to $\frac{V_v}{\lambda}$, where V_v is a representative velocity of the liquid film under vibratory conditions and λ is a scale of mixing which is of the order of the condensate film thickness.

From previous work by the author[13];[14] on convective heat transfer in the presence of oscillation, and the work of Brooke-Benjamin[15] on the stability of liquid films, V_v is assumed to be of the form $\left[\left(\frac{a_o \omega}{\pi}\right)^2 + u_{max}^2\right]^{\frac{1}{2}}$, where $\left(\frac{a_o \omega}{\pi}\right)^2$ is proportional to the mean kinetic energy of the vibrating tube (See Appendix).

Under critical conditions of vibration, when the heat transfer coefficient for the tube is just beginning to increase, the mixing coefficient will be proportional to $\frac{V_{CRITICAL}}{\lambda}$; there being no change in the order of magnitude of the scale of mixing.

Therefore
$$\frac{h_v}{h_{CRITICAL}} = \left[\frac{V_v}{V_{CRITICAL}}\right]^{\frac{1}{2}} \qquad (2)$$

In the problem under study here, there is transition of flow from laminar to a pseudo-turbulent mode under vibration free conditions. With vibration present the condensate film is moved between the stagnation points of the vibrating tube, in addition to its movement under the action of gravity down the tube. Under these conditions the motion of the film is not easily described mathematically, therefore the average mixing coefficient for the whole surface cannot be obtained from the integration of a number of point values along the surface. An alternate procedure is to consider the observed behaviour of the condensate film under vibratory and non-vibratory conditions and from this postulate a mixing model based on a representative flow velocity at a single point on the tube surface, and test the result of this in equation (2), against experimental data for the ratio $\frac{h_v}{h_o}$, it being noted that numerically $h_o \approx h_{CRITICAL}$

In the present study no definitive information concerning instability of the condensate film, and its transition to turbulence is given by Raben et al[1]. It is therefore assumed that turbulent instability first occurs at the point of transition to pseudo-turbulent flow, when the film Reynolds number $R_{e_f} = 400$ Portalski[16], [17]. Hence the representative fluid velocity u_{max} for the condensate film will be evaluated at this point.

The Nusselt theory[2] will be used for the calculation of u_{max}, as this has been found by Kutateladze[18] to give a reasonable approximation of filmwise condensation behaviour upto $R_{e_f} \lesssim 400$ for the condensation of steam.

At the critical condition when vibration first causes an increase in heat transfer coefficient, it is assumed that vibration does not supplement mixing, so that under these conditions $V_{CRITICAL} = u_{max}$ and

$$\frac{h_v}{h_{CRITICAL}} = \left[1 + \left(\frac{a_o \omega}{\pi u_{max}}\right)^2\right]^{\frac{1}{4}} \qquad (3)$$

For the parabolic velocity distribution in the condensate film which is valid to the point of transition to pseudo-turbulent flow[17], Nusselt theory[2] yields

$$u_{max} = \frac{\rho g \delta^2}{2\mu} \qquad (4)$$

and

$$\delta = \left[\frac{4 \mu k x (\theta_{SAT} - \theta_\omega)}{g \rho^2 h_{f_g}}\right]^{\frac{1}{4}} \qquad (5)$$

Therefore

$$u_{max}^2 = \frac{g k x (\theta_{SAT} - \theta_\omega)}{\mu h_{f_g}} \qquad (6)$$

From equations (3) and (6)

$$\frac{h_v}{h_{CRITICAL}} = \left[1 + \frac{\left(\frac{a_o \omega}{\pi}\right)^2}{\frac{g k x (\theta_{SAT} - \theta_{\omega_w})}{\mu h_{f_g}}} \right]^{\frac{1}{4}} \quad (7)$$

$$\text{Now } G = \int_o^{\delta} \rho . u . dy \quad (8)$$

From Nusselt's theory

$$u = \frac{g \delta^2}{\nu} \left[\left(\frac{y}{\delta}\right) - \frac{1}{2} \left(\frac{y}{\delta}\right)^2 \right] \quad (9)$$

$$\text{Therefore } G = \frac{\rho^2 . g . \delta^3}{3\mu} \quad (10)$$

From (5) and (10) R_{e_f} can be written as

$$R_{e_f} = \frac{4}{3} \left[\frac{4 k x (\theta_{SAT} - \theta_\omega) \rho^{\frac{2}{3}} . g^{\frac{1}{3}}}{\mu^{5/3} . h_{f_g}} \right]^{\frac{3}{4}} \quad (11)$$

Comparison with Experiment

For each test run tabulated in reference (1) the value of x for which $R_{e_f} = 400$ was evaluated from equation (11), all physical properties of the condensate being evaluated at the film temperature with the exception of enthalpy of vapourisation, which was evaluated at the saturation temperature. The value of x obtained in this way was used in equation (7). The comparison between $\frac{h_v}{h_{CRITICAL}}$ from equation (7) and the values of $\frac{h_v}{h_o}$ obtained experimentally in reference (1) are shown in figure (2).

Remembering that the static tube tests of reference (1) resulted in heat transfer coefficients which were about 10% in excess of those predicted by Nusselt's theory [2],

it is estimated that the error introduced by use of Nusselt's theory in equation (7), for calculation of u_{max} will result in an error of about 5% in comparison with experimental data for $\left[h_v/h_o \right]$

In the comparison of experimental data from reference (1) with equation (7), it was found that data for the resonant mode vibration at 38 c/s with amplitude greater than 0.35 ins., were not in as close agreement with equation (7) as the other data. The reasons for this are thought to be:

1) The mixing model put forward considered only the energy associated with the tube vibration and the liquid film kinetic energy to characterise the mixing process. At large amplitudes of vibration, adhesion forces in the liquid film will be of greater significance in inhibiting the lateral motion of the liquid film, thus the simple model would overpredict mixing and heat transfer in these situations.

2) The possibility exists that at large amplitudes of vibration ($a_o \gtrsim 0.3$ ins) there is a departure from the assumption of the tube behaving as a pivot ended beam, and the tendency to vibrate as a built in beam. This will reduce the tube vibration energy for a given amplitude and frequency. Again the specified mixing model would cause an over prediction of the heat transfer coefficient.

For most situations that might possibly arise in engineering practice a_o is likely to be less than about 0.3 ins. because of failure due to metal fatigue in the condenser tubes. Therefore the method discussed here for computing condensation heat transfer coefficient in the presence of transverse vibration of vertical condenser tubes would appear adequate.

Acknowledgement

The author would like to express his thanks to the U.S. Department of the Interior, Office of Saline Water Research and Development for the provision of R & D Report No. 49 (ref. 1).

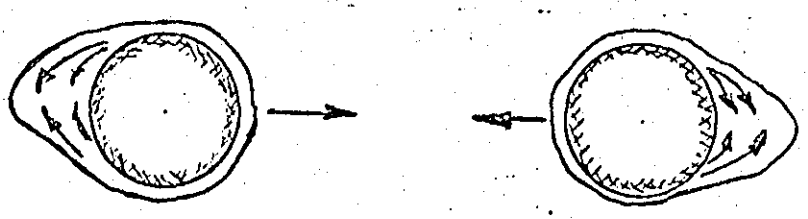

Fig. 1. Movement of Condensate film due to lateral vibration of vertical tube (reference 1)

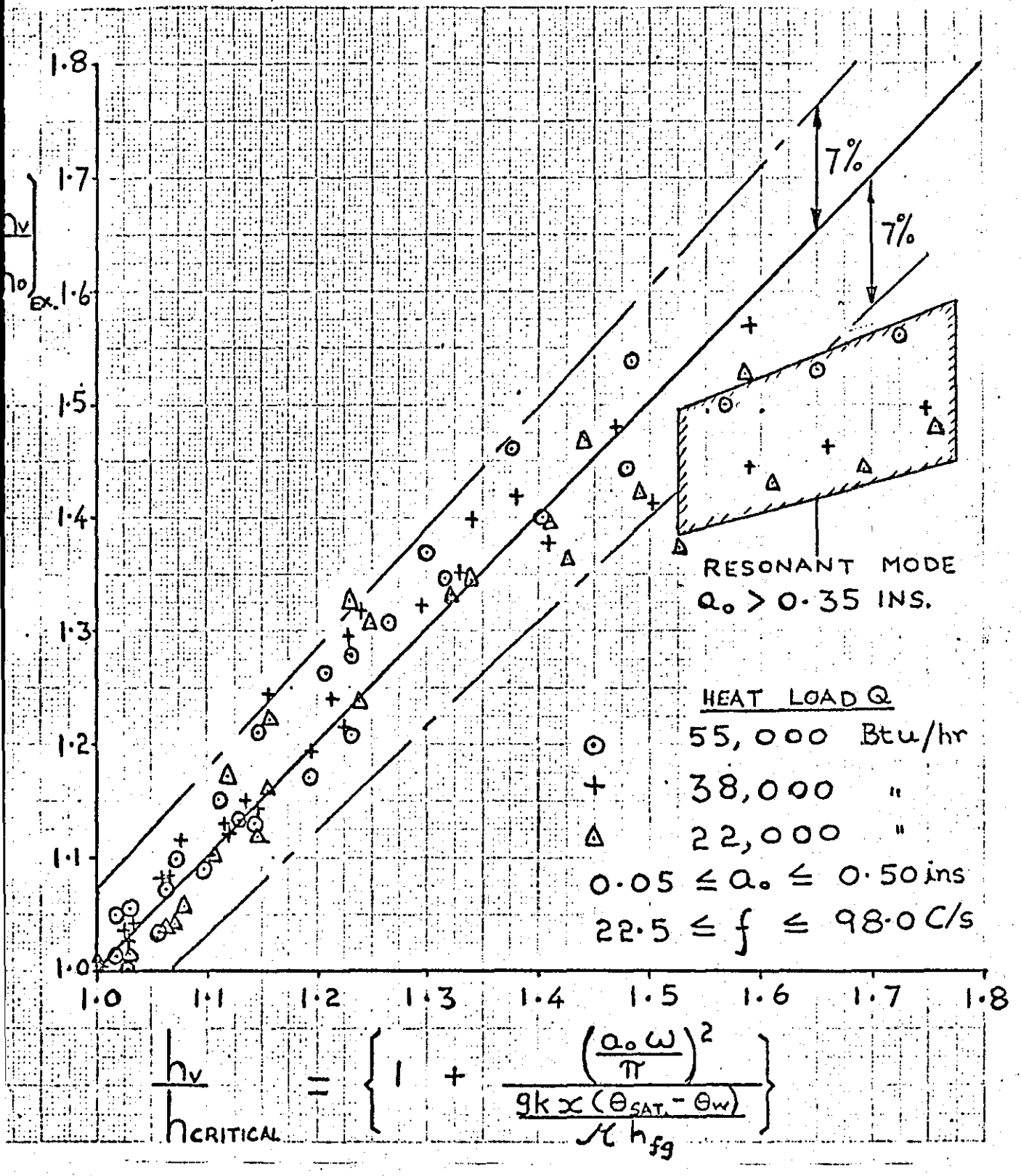

Fig. 2. Comparison between equation (7) and experimental data of reference (1)

REFERENCES

1. Raben, I.A., Commerford, G. and Dietert, R.
U.S. Dept. of Interior, Office of Saline Water Research and Development, Rep. No. 49.

2. Heat Transfer Vol. 1.
M. Jakob.
Wiley, New York (1949)

3. Danckwerts, P.V.
The significance of liquid-film coefficients in gas absorption.
Ind. Eng. Chem., 43, 1460 (1951)

4. Mickley, H.S. and Fairbanks, D.F.
Mechanism of heat transfer to fluidised beds.
A.I.Ch. E.J. 1, 374 (1955)

5. Hanratty, T.J.
Turbulent exchange of mass and momentum with a boundary.
Ibid. 2, 359 (1956)

6. Toor, H.L. and Marchello, J.M.
Film penetration model for mass and heat transfer.
Ibid. 4, 97, (1958)

7. Howard, D.W. and Lightfoot, E.N.
Mass transfer to falling films Part 1. Application of the surface stretch model to uniform wave motion.
Ibid. 14, 458 (1968)

8. Fage, A. and Townend, H.C.H.

An examination of turbulent flow with an ultra microscope.

Proc.Roy.Soc. London 135A, 656 (1932)

9. Hanratty, T.J.

Study of turbulence close to a solid wall.

The Physics of Fluids Supplement on Boundary Layers and Turbulence.

S 126 (1967)

10. Bakewell, H.P. and Lumley, J.L.

Viscous sublayer and adjacent wall region in turbulent pipe flow.

Physics of Fluids 10, 1880, (1967)

11. Sherwood, T.K., Smith, K.A., and Fowles, P.E.

The velocity and eddy viscosity distribution in the wall region of turbulent pipe flow.

Chem.Eng.Sci. 23, 1225 (1968)

12. Locke, G.S.H., and Trotter, F.J. de B.

Observations on the structure of a turbulent free convection boundary layer.

Int. J. Heat Mass Transfer 11, 1225 (1968)

13. Dent, J.C.

The calculation of heat transfer coefficient for combustion driven transverse oscillations in a gas-air burner.

A.I.Ch. E.J. 13, 1114, (1967)

14. Dent, J.C.

Heat transfer from a vertical transversely vibrating plane surface to air by free convection.

Int. J. Heat Mass Transfer. 11, 605 (1968)

15. Brooke-Benjamin, T.

Wave formation in laminar flow down an inclined plane.

J. Fluid Mech. 2, 554 (1957)

16. Portalski, S.

Studies of falling liquid film flow.

Chem. Eng. Sci. 18, 787 (1963)

17. ----------

Velocities in film flow of liquids on vertical plates.

ibid ------- 19, 575 (1964)

18. Fundamentals of Heat Transfer.

S.S. Kutateladze.

2nd Ed. Edward Arnold, London (1963)

Appendix

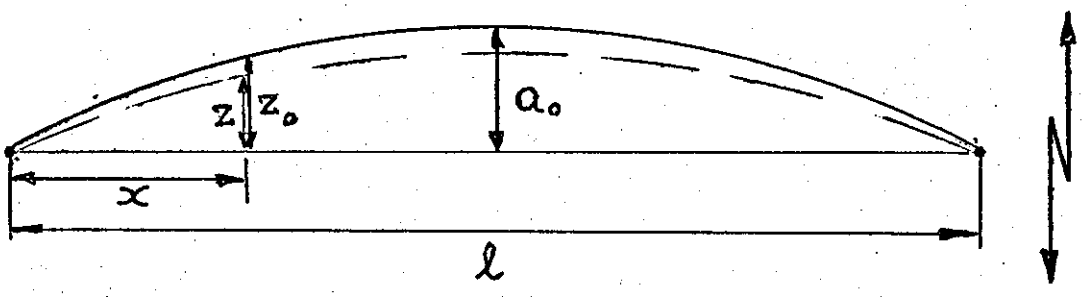

$$z = z_o \sin \omega t$$

and $$z_o = a_o \sin \pi \frac{x}{\ell}$$

K.E. of vibration at x for deflection of z at time t is

$$= \tfrac{1}{2} g_c (\omega z)^2$$

Using the r.m.s. value of z at x

K.E. of vibration is $\frac{1}{4g_c} \cdot \cdot (\omega z_o)^2$

The mean deflection of the Beam at maximum amplitude is

$$\bar{z}_o = \frac{a_o}{\ell} \int_o^{\ell} \sin \pi \frac{x}{\ell} \, dx = \frac{2 a_o}{\pi}$$

Therefore K.E. for mean deflection of the beam is

$$\text{K.E.} = \frac{1}{g_c} \left[\frac{a_o \omega}{\pi}\right]^2$$

The Effect of Acoustic and Mechanical Oscillation on Free Convection from Heated Cylinders in Air

J. C. DENT
Mechanical Engineering Dept.,
University of Technology,
Loughborough,
Leicestershire.

NOTATION

FUNDAMENTAL UNITS, MASS [M], LENGTH [L], TIME [t] AND TEMPERATURE [T]

a	Amplitude of oscillation	[L]
C_p	Thermal Capacity of Air	$[L^2/t^2T]$
D	Diameter of Cylinder or pipe	[L]
f	Oscillation Frequency	[1/t]
g_c	Gravitational Constant	[DIMENSIONLESS]
G_R	Grashof Number based on Cylinder Diameter	[DIMENSIONLESS]
h	Average heat transfer Coefficient	$[M/t^3T]$
k	Thermal Conductivity of Air	$[ML/t^3T]$
L	Characteristic Length	[L]
m	A Constant	[DIMENSIONLESS]
n	A Constant	[DIMENSIONLESS]
Re_s	Streaming Reynolds Number = $\left[\frac{a^2\omega}{\upsilon}\right]$	[DIMENSIONLESS]
S	Mixing Coefficient	[L/t]
t	Time	[t]
U	Velocity	[L/t]
V	Velocity	[L/t]
Γ	Scale of turbulence or mixing	[L]
λ	Wavelength of Acoustic Oscillation	[L]

υ	Kinematic Viscosity of Air	$[L^2/t]$
ρ	Density of Air	$[M/L^3]$
θ	Temperature	$[T]$
ω	Circular Frequency	$[1/t]$

SUBSCRIPTS

o	In absence of oscillations
s	Pertaining to Streaming flow conditions
v	Pertaining to Oscillation conditions

Other Notation defined in text.

Summary

A method based on the Danckwerts Mickley Model for turbulent mixing has been presented for the calculation of average heat transfer coefficient from heated horizontal cylinders in air, placed in a plane stationary sound field with $\frac{\lambda}{2D} \geq 6.0$, or subjected to mechanical oscillations in a transverse plane with $\frac{a}{D} < 1$.

Agreement with published experimental data is good provided $\Delta\theta \leq 50^{\circ}F$ and $\frac{Re_s^2}{G_R} \lesssim 10$.

The effects of Acoustic and Mechanical oscillations on Free convection from heated cylinders in air

The transverse oscillation of a circular unheated cylinder in still air, or maintaining the cylinder in a transverse acoustic field, causes a steady isothermal streaming motion of the fluid to be set up around the cylinder.

This streaming motion results from the interaction between the viscous forces, and those resulting from the Reynolds stresses set up by the oscillation in the fluid medium.

In free convection from a stationary heated cylinder to a quiescent fluid medium, the convective flow is dependent on the interaction of the buoyancy and viscous forces within the fluid.

The problem under study here would therefore involve an interaction between the forces resulting from isothermal streaming and those associated with free convection.

The object of this paper is to present a method for the calculation of the average heat transfer coefficient for heated horizontal cylinders in air, which are held in a plane stationary sound field, or are subjected to transverse mechanical oscillations in still air. Only those cases of mechanical oscillation for which the ratio $\frac{a}{D} < 1$ will be discussed.

A survey of the experimental work carried out in this field can be conveniently tabulated in the following way.

Conditions of Oscillation	Experimental Variables	Cylinder Diameter ins.	Reference
1) Horizontal Sound Field, perpendicular to cylinder axis	$645 \leq f \leq 6100$ C/s. $0 \leq \Delta\theta \leq 250^{\circ}F$ $0 \leq$ S.P.L. ≤ 151 db	$\frac{3}{4}$	1 - 4
2) Mechanical Oscillations of the cylinder in a horizontal plane	$27 \leq f \leq 104$ C/s. $20 \leq \Delta\theta \leq 200^{\circ}F$ $0 < a/D < 1$	$\frac{5}{8}$, $\frac{7}{8}$	5, 6
3) Vertical Sound Field Perpendicular to cylinder axis.	$709 \leq f \leq 1476$ C/s. $\Delta\theta \simeq 140^{\circ}F$ $125 \leq$ S.P.L. ≤ 140 db	1.83	7
4) Mechanical Oscillation of the cylinder in the vertical plane	$29 \leq f \leq 225$ C/s. $25 \leq \Delta\theta \leq 200^{\circ}F$ $0 < a/D < 1$	$\frac{5}{8}$, $\frac{7}{8}$	5, 8

Observations made in the course of the above listed experiments show that certain features of the flow and average heat transfer are common for a given plane of oscillation, irrespective of whether the oscillations are acoustic or mechanical.

Fand and Peebles[6] showed that provided the ratio $\frac{\lambda}{2D} \geq 6.0$ for acoustic oscillation, the average heat transfer coefficient in the presence of acoustic oscillation is the same as that for mechanical oscillation for the same intensity (af) of oscillation. It was found[1], [6] that at low intensities of oscillation the effect of oscillation on the average heat transfer coefficient was negligible. At a critical intensity (S.P.L.$\simeq$ 140 db; af $\simeq$0.3ft/sec) the average heat transfer coefficient began to increase, and continued to do so with increasing oscillation intensity.

Flow visualisation[2];[5];[6] showed that at the critical intensity a streaming motion began to develop in the upper two quadrants above the cylinder.

At a higher intensity (S.P.L. ≃ 146 db; af ≃ 0.7 ft/sec), this streaming motion established itself, and consisted of the periodic growth and collapse of two vortices centred in the two quadrants above the cylinder. The growth and collapse of the vortices alternated between each quadrant. Further increases in intensity of oscillation caused the vortices to increase in size, but the basic character of the flow remained unaltered. It was found[2] that with $\frac{\lambda}{2D}$ >6.0 the development and size of the vortices were independent of frequency of oscillation.

Measurements of local heat transfer coefficient[3] showed increases on both upper and lower surfaces of the cylinder, the former being about four times greater than the latter in magnitude. The increase of the heat transfer coefficient on the upper surfaces being attributed to vortex growth and collapse in the region causing greater fluid mixing, while the increases on the lower surfaces were attributed to unsteadiness in the laminar boundary layer induced by oscillation. Richardson[7] using Schlieren techniques observed the boundary layer behaviour around a heated cylinder in a standing vertical sound field. He found that at 139 db S.P.L. the boundary layer between the lower stagnation point and 45° from it was distended and unsteady, with the possibility of two standing vortices being formed along the length of the cylinder and centred on the 45° points. With acoustic intensity of 140 db, the fluid from the bottom of the cylinder began to "bubble" up through the boundary layer and pass into the wake, first on one side of the cylinder and then the other. With further increase in the intensity of oscillation, the frequency of the "bubble"

shedding increased. The initial thickening of the boundary layer caused a decrease in the average heat transfer coefficient of between 3 and 20%. Richardson concluded that the flow field was qualitatively consistent with a superposition of the acoustic streaming and convective flow fields.

Lowe[5] carried out a flow visualisation study, (using smoke) of the effects of vertical mechanical oscillation on free convection about a heated cylinder. He observed that instability occured at the top of the cylinder at the critical intensity (when the average heat transfer coefficient is just increasing), and that this instability developed to turbulence which moved upstream towards the lower stagnation point with increasing intensity of oscillation. Just below the critical intensity a decrease of about 4% in the average heat transfer coefficient was noted. Lowe also noted that the difference between average coefficients of heat transfer for oscillations in the vertical and horizontal plane were small.

A smoke study by Fand and Kaye[8] for vertical mechanical oscillations also revealed a turbulent flow field about the cylinder, though no observations were discussed concerning the onset of the instability.

From the foregoing survey it is clear that horizontal acoustic and mechanical oscillation have the same effect on the average heat transfer coefficient from the cylinder, and give rise to the same flow mechanism provided oscillation intensity is above the critical and $\frac{\lambda}{2D} > 6.0$.

The literature dealing with acoustic and mechanical oscillation in the vertical plane show that beyond the critical intensity of oscillation, a transition type of instability from laminar to turbulent flow in the wake and on the upper surface of the cylinder exists.

For both horizontal and vertical oscillations it is the increase in mixing on the upper surfaces of the cylinder that are causing the large increases in heat transfer coefficient. Because instability and mixing are initiated on the upper surfaces of the cylinder for both horizontal and vertical modes of oscillation, and because Lowes' results[5] show that the plane of oscillation has little effect on the average heat transfer coefficient, the possibility exists of setting up a common method to calculate the average heat transfer coefficient for either plane of oscillation. Further support to this is given by the flow visualisation of Lee and Richardson[4] and Richardson[7] these authors conclude that for horizontal and vertical modes of acoustic oscillation, the flow field is qualitatively consistent with a superposition of the streaming and convective flows about the cylinder.

In attempting a common method of calculating the heat transfer coefficient, an analysis cannot be made by specifying local conditions of flow, and integrating these obtain an averaged effect. This is so because local conditions are different for each plane of oscillation. However, a semi-empirical approach can be adopted whereby from observed data, variables can be chosen which characterise the flow and mixing behaviour in the boundary layer. A mixing mechanism can be postulated to account for increased mixing in the boundaty layer due to oscillation, and from this the average heat transfer coefficient calculated and checked against experiment.

The Mixing Model

In the study of the effects of acoustic and mechanical oscillations on convective and condensation heat transfer Dent [9 - 11] has found that a suitable model for the averaged effects of mixing in the boundary layer could be developed from the Danckwerts - Mickley [12], [13] model for mass or heat transfer in the presence of a high degree of mixing such as in stirred reactors and fluidised beds. In the application of the Danckwerts - Mickley Model to the turbulent heat transfer from a fluid to a wall surface, it is considered that "lumps" of fluid from the bulk region move randomly and at high frequency to the wall, exchange heat with it in a transient manner before being displaced by fresh fluid "lumps" into the bulk region.

Locke and Trotter [14] have found from their experiments on turbulent structure in a free convective boundary layer, that the concept of a passive laminar sublayer was not strictly valid. Therefore the use of the Danckwerts - Mickley exchange model in the problem under study here would appear to be justified.

According to the Danckwerts - Mickley Model the average heat transfer coefficient between the fluid and the wall is given by [12][13]

$$h = \left[k \rho C_p S \right]^{\frac{1}{2}} \qquad (1)$$

where S is the average mixing or renewal coefficient over the surface, and is controlled by the fluid mechanics and geometry of the particular situation.

Toor and Marchello[15] have shown that for turbulent pipe flow

$$S \propto \frac{U}{D} \cdot Re^{0.8} \qquad (2)$$

Because the scale of turbulence (Γ) in pipe flow is proportional to pipe diameter equation (2) can be written as

$$S \propto \frac{U}{\Gamma} \cdot R_e^{0.8} \qquad (3)$$

In the absence of oscillation the turbulent free convective flow over a body of characteristic length L which is not large in comparison with the scale of turbulence or mixing, might reasonably be expected to have a mixing coefficient of the form

$$S \propto \frac{V}{\Gamma} \cdot G_R^{n} \qquad (4)$$

where V is a representative velocity in the boundary layer.

In the problem under study here the mixing is induced by the streaming flow interacting with the laminar free convective flow field to produce a transition to turbulence. In the study of transition of laminar free convective flows to turbulence,[16-18] it has been found that the instability originates in the region of the outer point of inflexion in the laminar velocity profile. It would therefore appear reasonable to expect the intereaction between the streaming and laminar free convective flows to occur in this region. It was pointed out earlier that the greater part of the increased mixing and heat transfer due to oscillation occurs on the upper surface of the cylinder. From Hermann's analysis[19] of the laminar free convective flow of gases over a horizontal cylinder, it is known that decceleration of the flow commences at a point approximately 135^{o} from the lower stagnation point on the cylinder. The tendency to separation and vortex formation in a deccelerating flow over a cylinder, and the instability condition discussed above, make the choice of the point of interaction between

the streaming and free convective flow, at the outer inflexion point in the laminar velocity profile, 135^{o} from the lower stagnation point, appear quite reasonable.

From previous work[9 - 11] it is assumed that the characteristic velocity V_v, for free convection in the presence of oscillation, which is to be used in the expression for the mixing coefficient S_v, can be established by considering the energy of the flow in the critical region of the laminar velocity profile at 135^{o}, to be supplemented by the energy of the streaming flow at the same point.

Hence

$$\frac{V_v^2}{2g_c} = \frac{1}{2g_c}\left[V^2_{INFLEXION} + V^2_{STREAMING}\right]_{@135^{o}} \quad (5)$$

But from Herman[19] $V_{\substack{INFLEXION \\ @\ 135^{o}}} = \dfrac{0.345\upsilon\, G_R^{\frac{1}{2}}}{D}$

and from Schlichting[20] $V_{\substack{STREAMING \\ @\ 135^{o}}} = \pm\, 3\left(\dfrac{a^2\omega}{D}\right)$, the positive sign indicating direction of fluid motion for a horizontal mode of oscillation and the negative sign, fluid motion for a vertical oscillation mode.

Making the appropriate substitutions in (5)

$$V_v = \left[0.119\left(\frac{G_R^{\frac{1}{2}}\upsilon}{D}\right)^2 + 9\left(\frac{a^2\omega}{D}\right)^2\right]^{\frac{1}{2}} \quad (6)$$

In the presence of oscillation and free convection, where there has been a transition to vortex growth and collapse, or turbulence in the fluid

flow, the mixing coefficient S_v might be expected to have the form.

$$S_v \alpha \frac{V_v}{\Gamma} \quad G_R^m \qquad (7)$$

or $$S_v \alpha \left[0.119 \left(\frac{G_R^{\frac{1}{2}} \upsilon}{D}\right)^2 + 9\left(\frac{a^2 \omega}{D}\right)^2\right]^{\frac{1}{2}} \cdot \left(\frac{G_R}{\Gamma}\right)^m$$

Therefore $$h_v \alpha \left[\frac{k \rho C_p G_R^m}{\Gamma}\right]^{\frac{1}{2}} \left[0.119 \left(\frac{G_R^{\frac{1}{2}} \upsilon}{D}\right)^2 + 9\left(\frac{a^2 \omega}{D}\right)^2\right]^{\frac{1}{4}} \qquad (8)$$

At the critical intensity of oscillation, when the average heat transfer coefficient is just beginning to increase, the effect of the streaming flow on the mixing coefficient and therefore on average heat transfer coefficient is negligible, therefore

$$S_{CRITICAL} \alpha \frac{G_R^m}{\Gamma_{CRITICAL}} \cdot \left[0.119 \left(\frac{G_R^{\frac{1}{2}} \upsilon}{D}\right)^2\right]^{\frac{1}{2}} \qquad (9)$$

Hence

$$\frac{h_v}{h_{CRITICAL}} = \left[\frac{\Gamma_{CRITICAL}}{\Gamma}\right]^{\frac{1}{2}} \cdot \left[1 + \frac{75.5\, R_{es}^2}{G_R}\right]^{\frac{1}{4}} \qquad (10)$$

In the study of unsteady laminar boundary layers[20] the boundary layer thickness over which unsteady effects are of importance, is found to be equal to $\left[\frac{\upsilon}{\omega}\right]^{\frac{1}{2}}$. In the study of turbulence[21] $\left[\frac{\upsilon}{\omega}\right]^{\frac{1}{2}}$ is found to be proportional to the scale of turbulence. Therefore putting $\Gamma \alpha \left[\frac{\upsilon}{\omega}\right]^{\frac{1}{2}}$ relates the scale of the mixing motion due to the oscillation with the

frequency.

In the case of mechanical oscillation of the heated cylinder (frequencies < acoustic frequencies), in which the intensity of oscillation is such that a fully developed vortex system or turbulent mixing is created about the cylinder, it is expected that an increase in the scale of the mixing process will be present when compared with acoustic oscillations for which $\frac{\lambda}{2D} \geq 6.0$. If it is assumed that at the critical condition for mechanical and acoustic oscillation the scale of mixing is the same (provided $\frac{\lambda}{2D} \geq 6.0$), then, evaluation of $\Gamma_{CRITICAL}$ at $\frac{\lambda}{2D} = 6.0$ for an ambient temperature of $70^{o}F$ and $D = \frac{3}{4}$ in. yeilds $\Gamma_{CRITICAL} \alpha \left[\frac{\upsilon}{1496}\right]^{\frac{1}{2}}$

Therefore $$\left[\frac{\Gamma_{CRITICAL}}{\Gamma}\right]^{\frac{1}{2}} = \left[\frac{f}{1496}\right]^{\frac{1}{4}}$$

For acoustic oscillation for which $\frac{\lambda}{2D} \geq 6.0$, the effect of frequency on vortex size was negligible (Fand and Kaye[2]) therefore the effect of scale of mixing on $\frac{h_v}{h_{CRITICAL}}$ will be negligible, hence for acoustic oscillation.

$$\frac{h_v}{h_{CRITICAL}} = \left[1 + \frac{75.5\ R_{es}^{\ 2}}{G_R}\right]^{\frac{1}{4}} \qquad (11)$$

For mechanical oscillation where scale of mixing is of importance

$$\frac{h_v}{h_{CRITICAL}} = \left[\frac{f}{1496}\right]^{\frac{1}{4}} \left[1 + \frac{75.5\ R_{es}^{\ 2}}{G_R}\right]^{\frac{1}{4}} \qquad (12)$$

Numerically $h_{CRITICAL} \approx h_o$ the heat transfer coefficient in the absence of oscillation. Therefore $\frac{h_v}{h_{CRITICAL}}$ from equation (11) and (12)

above may be plotted against $\frac{h_v}{h_o}$ from experiment.

Before a comparison between equations (11) and (12) and experiment is carried out, it would be desirable to establish the conditions of validity of these two equations. The method put forward here considers a superposition of the energy in the streaming motion with that of the critical layer in the laminar boundary layer, to give increased mixing and heat transfer in the boundary layer. The destabilising effect of the hot wall surface[20] cannot be accounted for. It is expected therefore that the method developed here would be valid for cases of low $\Delta\theta$, therefore comparison with the experimental data of references (1); (5); and (6) and (8) have been considered at the lowest $\Delta\theta$ at which heat transfer data were obtained.

From Lowe's experimental data[5] it is clear that an upper limit to the validity of equations (11) and (12) occurs when oscillation induced forced convection prevails. This occurs when $\frac{R_{es}^2}{G_R} \gtrsim 10$. The lower limit of validity would be at conditions of oscillation which first produce a fully developed condition of turbulence or vortex growth and collapse. From the data of references (1); (5) and (8) this has been established in figure (1)

Comparison with Experiment

A plot of $\frac{\bar{h}_v}{h_o}$ from the experimental data of references (1); (5); (6) and (8) is shown in figure (2) against $\frac{h_v}{h_{CRITICAL}}$ from equations (11) and (12).

It will be seen from figure (2) that the results calculated from equations(11) and (12) for the increase in heat transfer coefficient due to oscillation, are in good agreement with the measured values of h_v/h_o provided $\Delta\theta \leq 50^oF$ and $R_{es}^2/G_R \lesssim 10$.

A method based on the Danckwerts - Mickley Model for turbulent mixing has been presented for the calculation of average heat transfer coefficient from heated horizontal cylinders in air placed in a plane stationary sound field with $\frac{\lambda}{2D} \geq 6.0$, or subjected to mechanical oscillations in a transverse plane. Agreement with experiment is good provided $\Delta\theta \leq 50^oF$ and $\frac{R_{es}^2}{G_R} \lesssim 10$.

Acknowledgement

The author would like to express his thanks to Mr. H. C. Lowe for providing a copy of his thesis from which some of the data in figures (1) and (2) were obtained.

REFERENCES

(1) Fand, R. M. and Kaye, J., Jour. Heat Transfer, 83, 133 (1961)

(2) ———
Jour. Acoust. Soc. Amer. 32, 579 (1960)

(3) Fand, R. M., Roos, J. Cheng, R., and Kaye, J.,
Jour. Heat Transfer, 84, 245 (1962)

(4) Lee, B. H and Richardson, P. D.
Jour. Mech. Eng. Sci. 7, 127 (1965)

(5) Lowe, H. C.
M.Sc. Thesis, LONDON UNIVERSITY (1965)

(6) Fand, R. M. and Peebles E. M.
Jour. Heat Transfer, 84, 268 (1962)

(7) Richardson, P. D.
Proc. 3rd International Heat Transfer Conference 71 (1966)

(8) Fand, R. M. and Kaye, J.
Int. Development in Heat Transfer, Boulder, Colorado 490 (1961)

(9) Dent, J. C.
A.I.Ch.E. Jour. 13, 1114 (1967)

(10) ———
Int. J. Heat Mass Transfer 11, 605 (1968)

(11) ———
ibid in Press

(12) Danckwerts, P. V.
Ind. Eng. Chem. 43, 1460, (1951)

(13) Mickley, H. S. and Fairbanks, D. F.
A.I.Ch.E. Jour, I, 374 (1955)

(14) Locke, G. S. H. and Trotter, F. J. de B.
Int. J. Heat Mass Transfer 11, 1225 (1968)

(15) Toor, H. L. and Marchello, J. M.
A.I.Ch.E. Jour. 4, 97 (1958)

(16) Eckert, E. R. G. and Soehnghen, E.
Proc. General Discussion on Heat Transfer, I. Mech. E.
London 321, (1951)

(17) Szewczyk, A. A.
Int. J. Heat Mass Transfer 5, 903, (1962)

(18) Blankenship, V and Clark, J. A.
Jour. Heat Transfer 86, 159 (1964)

(19) Hermann, R.
N.A.C.A. T.M. 1366 Trans. from VDI Forsch. No. 379, (1936)

(20) Schlichting, H.
Boundary Layer Theory, 6th Ed. McGraw Hill, New York (1968)

(21) Hinze, J. O.
Turbulence, McGraw Hill, New York (1959)

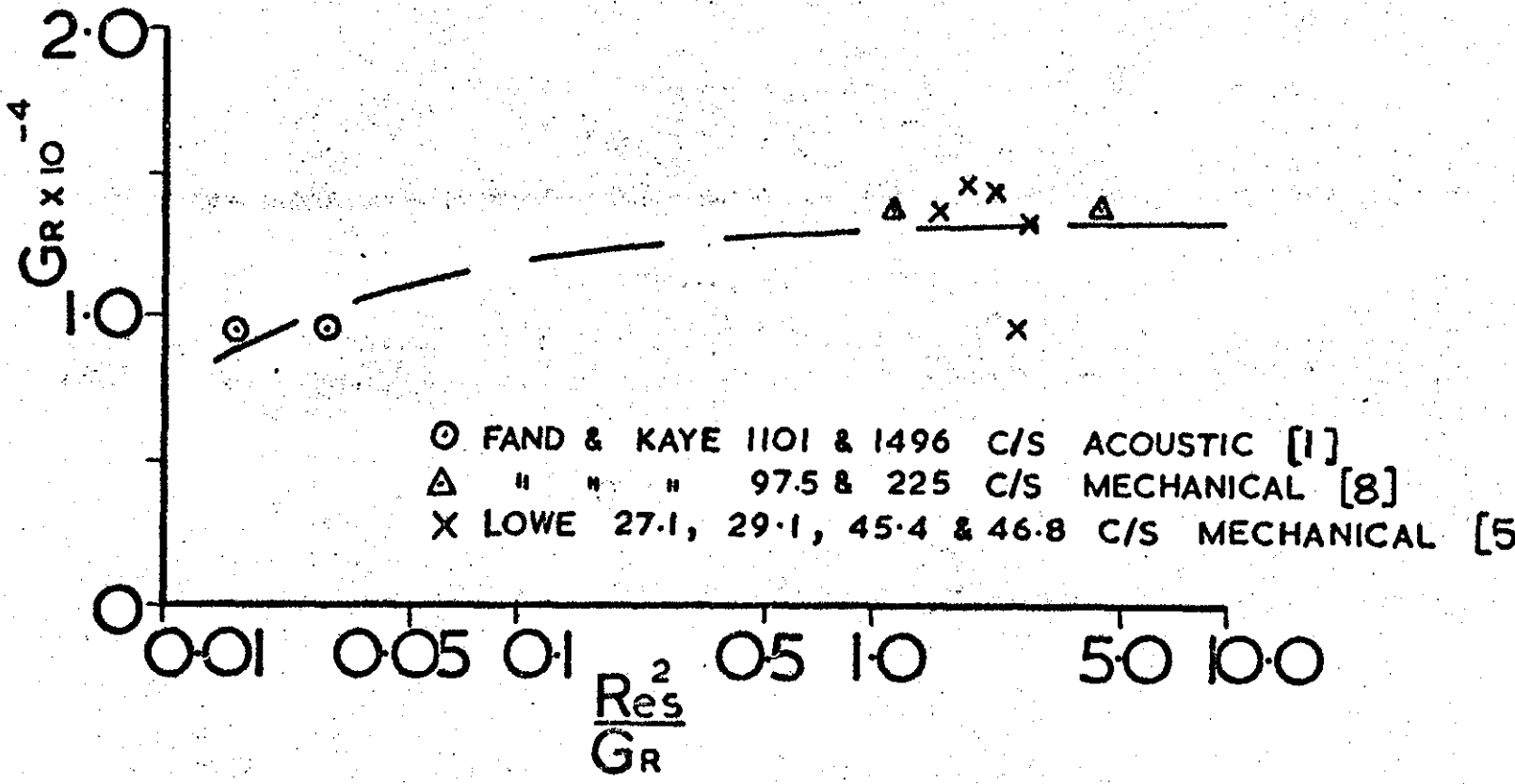

FIG. 1 CONDITIONS FOR FULLY DEVELOPED VORTEX FLOW OR TURBULENCE.

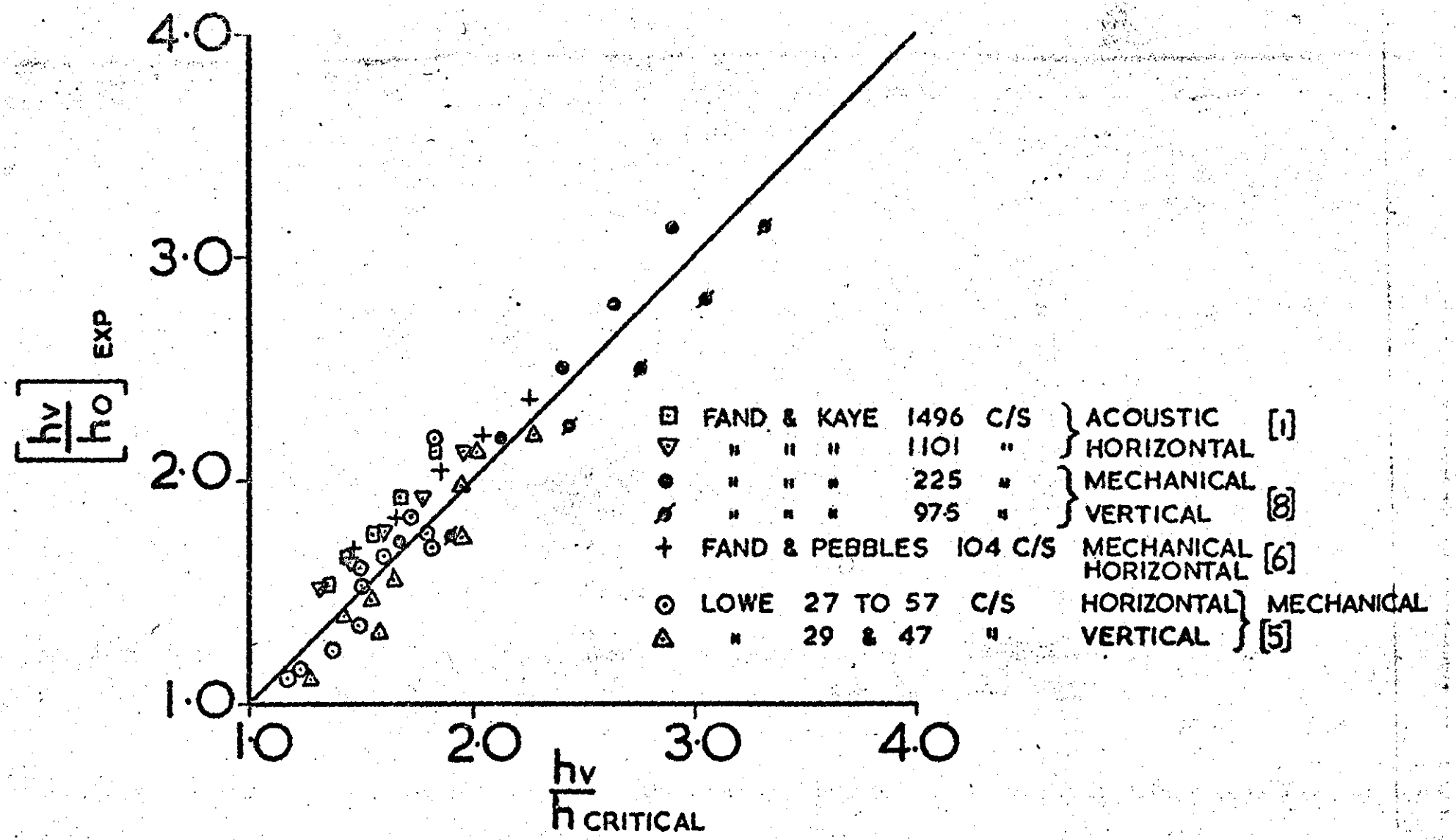

FIG. 2 COMPARISON BETWEEN EXPERIMENT AND EQUATIONS (11) AND (12)